FAKULTNÍ NEMOCNICE OSTRAVA

SBORNÍK VYBRANÝCH IMPAKTOVANÝCH PRACÍ ZA ROK 2015

Sborník vybraných impaktovaných prací za rok 2015
Vydavatel: Fakultní nemocnice Ostrava
Periodicita: roční
Počet výtisků: 100 ks

ISBN 978-80-906002-9-4 (print)
ISBN 978-80-88159-00-1 (on-line)

Obsah / Content

Úvodní slovo

Vážené kolegyně, vážení kolegové,

dostává se Vám do rukou třetí číslo sborníku nejlepších vědeckých prací Fakultní nemocnice Ostrava, publikovaných v impaktovaných časopisech v roce 2015. Nový sborník je souhrnem 20 prací, které v roce 2015 získaly nejvyšší impakt faktor. Představují přehled vynikajících autorských prací a výsledky klinického výzkumu, který již má své významné postavení vedle kvalitní lékařské péče a výuky studentů.

Autorské publikace jsou odrazem vědecké práce, která je nedílnou součástí poskytované zdravotní péče. Stoupající počet výzkumných projektů vlastního i kolaborativního výzkumu a počtů impaktovaných publikací je důkazem vynikající odborné úrovně napříč lékařskými obory. Fakultní nemocnice Ostrava je žádaným partnerem pro spolupráci, zejména v aplikovaném klinickém výzkumu pro transfer nových technologií. Rozrůstá se spolupráce nejen mezi vědeckými institucemi a výzkumnými organizacemi, ale i spolupráce s komerčními subjekty v rámci Moravskoslezského regionu i zahraničními institucemi.

Fakultní nemocnice, jako výzkumná organizace, vykazuje již několik let tuto stoupající úroveň a řadí se tak mezi kvalitní vědecké instituce, které jsou registrovány a hodnoceny v rámci RIV. Naším dlouhodobým cílem je zvyšovat úroveň vědecké práce a sborník nejlepších impaktovaných prací tak přináší zajímavý náhled na hloubku a rozsah aktuální vědecké práce v naší nemocnici.

Přeji Vám hodně úspěchů ve Vaší vědecké a publikační činnosti, kterou Fakultní nemocnice Ostrava bude vždy podporovat.

MUDr. Václav Procházka, Ph.D., MSc.
Náměstek ředitele FNO pro vědu a výzkum

Foreword

Dear Colleagues

You are holding in your hands already the third edition of the Collection of the best scientific works of the University Hospital Ostrava, published in various journals with an impact factor in 2015. The new Collection is a summary of twenty publications, which obtained the highest impact factor in 2015. They represent an overview of excellent author works and outcomes of clinical research, an activity, which has acquired an important position at our hospital, besides providing medical care and teaching of students.

Author publications are a reflection of scientific work, which is an integral part of the provided medical care. The rising number of research projects of own and collaborative research, and the number of publications in high-impact journals are a proof of the excellent expert level across various medical specialities. University Hospital Ostrava is a desired partner for cooperation, especially in applied clinical research for transfer of technologies. The cooperation is growing not only with scientific institutions and research organizations but also with commercial partners in the Moravian-Silesian Region, as well as institutions from abroad.

University Hospital Ostrava, as a research organization, has been manifesting this rising trend, and thus belongs among high-quality research institutions, which are registered and evaluated within the RIV system. Our long-term aim is to improve the level of scientific cooperation; Collection of the best impacted publications brings an interesting preview on the depth and extent of the current scientific work in our hospital.

I wish you much success in your further scientific and publication activities, which will be always supported by the University Hospital Ostrava.

Václav Procházka, MD, PhD, MSc
Deputy director for Science and Research

1. Randomized clinical trial comparing neurological outcomes after carotid endarterectomy or stenting

Kuliha M, Roubec M, Procházka V, Jonszta T, Hrbáč T, Havelka J, Goldírová A, Langová K, Herzig R, Školoudík D

Originally published in British Journal of Surgery, 2015, vol. 102, no. 3, p. 194-201.

Randomized clinical trial

Randomized clinical trial comparing neurological outcomes after carotid endarterectomy or stenting

M. Kuliha[1], M. Roubec[1], V. Procházka[2], T. Jonszta[2], T. Hrbáč[3], J. Havelka[2], A. Goldírová[1,4], K. Langová[5], R. Herzig[6] and D. Školoudík[1,4]

Departments of [1]Neurology, [2]Radiology and [3]Neurosurgery, Comprehensive Stroke Centre, University Hospital Ostrava, Ostrava, [4]Department of Nursing, Faculty of Health Sciences, Palacký University, and [5]Department of Biophysics, Faculty of Medicine and Dentistry, Institute of Molecular and Translational Medicine, Palacký University, Olomouc, and [6]Department of Neurosurgery, Comprehensive Stroke Centre, Military University Hospital, Prague, Czech Republic

Correspondence to: Professor D. Školoudík, Department of Neurology, Comprehensive Stroke Centre, University Hospital Ostrava, CZ-708 52 Ostrava-Poruba, Czech Republic (e-mail: skoloudik@hotmail.com)

Background: **Silent infarction in the brain can be detected in around 34 per cent of patients after carotid endarterectomy (CEA) and 54 per cent after carotid angioplasty and stenting (CAS). This study compared the risk of new infarctions in the brain in patients undergoing CEA or CAS.**

Methods: **Consecutive patients with internal carotid artery (ICA) stenosis exceeding 70 per cent were screened for inclusion in this prospective study. Patients with indications for intervention, and eligible for both methods, were allocated randomly to CEA or CAS. Neurological examination, cognitive function tests and MRI of the brain were undertaken before and 24 h after intervention.**

Results: **Of 150 randomized patients, 73 (47 men; mean age 64·9(7·1) years) underwent CEA and 77 (58 men; 66·4(7·5) years) had CAS. New infarctions on MRI were found more frequently after CAS (49 *versus* 25 per cent; $P = 0·002$). Lesion volume was also significantly greater after CAS ($P = 0·010$). Multiple logistic regression analyses identified intervention in the right ICA as the only independent predictor of brain infarction (odds ratio 2·10, 95 per cent c.i. 1·03 to 4·25; $P = 0·040$). Stroke or transient ischaemic attack occurred in one patient after CEA and in two after CAS. No significant differences were found in cognitive test results between the groups.**

Conclusion: **These data confirm a higher risk of silent infarction in the brain on MRI after CAS in comparison with CEA, but without measurable change in cognitive function. Registration number: NCT01591005 (http://www.clinicaltrials.gov).**

Pilot study results were presented to the 65th Annual Meeting of the American Academy of Neurology, San Diego, California, USA, March 2013

Paper accepted 19 September 2014

Published online 16 December 2014 in Wiley Online Library (www.bjs.co.uk). **DOI:** 10.1002/bjs.9677

Introduction

Carotid artery stenosis causes 20–25 per cent of strokes[1]; the risk increases with the severity of stenosis[2]. In the 1990s, a series of randomized clinical trials established the superiority of carotid endarterectomy (CEA) plus aspirin over aspirin alone in preventing stroke[1,3,4]. CEA remains the standard of care for severe internal carotid artery (ICA) stenosis[5]. In the past decade, carotid angioplasty and stenting (CAS) has become an alternative treatment for carotid stenosis because general anaesthesia and surgical incisions can be avoided. These features have reduced the incidence of postoperative wound problems and cranial nerve injury compared with surgery[4,6–10].

The safety and effectiveness of CEA and CAS have been investigated in many studies; subsequent meta-analyses have produced conflicting results regarding the comparative safety, effectiveness and changes in cognitive function[6–10]. Appraisal of the trials and meta-analyses, particularly the Carotid Revascularization Endarterectomy *Versus* Stenting Trial (CREST)[10], suggested that CEA and CAS have similar rates of postoperative death and disabling stroke, but that CAS is associated with a higher 30-day risk of any stroke, especially for patients aged over 70 years[6–10]. Moreover, silent infarctions in the brain can be detected more often after CAS (54 per cent *versus* 34 per cent after CEA)[11–15]. The effect of CAS and

CEA on cognitive function remains controversial; a recent systematic review[16] did not give a definite conclusion.

The aim of this prospective randomized study was to compare the risk of asymptomatic and symptomatic brain infarction, and their influence on cognitive function, in patients with symptomatic and asymptomatic severe ICA stenosis undergoing elective CEA or CAS.

Methods

The study was conducted in accordance with the Helsinki Declaration of 1975 (as revised in 2004 and 2008). It was approved by the local ethics committee (MZ10-FNO). All patients provided written informed consent before enrolment. The study has been registered at http://www.clinicaltrials.gov (NCT01591005).

Patients

The inclusion criteria were: ICA stenosis exceeding 70 per cent (symptomatic or asymptomatic) detected by duplex ultrasonography and confirmed using CT angiography (CTA); indication for carotid intervention (CEA or CAS) according to criteria set by the American Heart Association[5]; age 40–80 years; functionally independent (modified Rankin score 0–2 points); and no contraindication to MRI, CTA or digital subtraction angiography. Consecutive patients were enrolled between 4 September 2011 and 18 December 2013. Randomization was computer-generated; patients were assigned equally to CEA or CAS.

Carotid endarterectomy

Surgery was undertaken according to standard protocols using general anaesthesia. The centre has undertaken over 400 CEAs during the past 5 years. A carotid shunt was used according to protocol (only in 3 patients). All patients continued long-term aspirin therapy (100 mg/day) in the perioperative phase. A dose of 100 units per kg bodyweight unfractionated heparin was administered before flow arrest in the carotid artery. Protamine was given 5 min after flow restoration in the ICA. Clopidogrel (75 mg) was administered for 5 days after surgery.

Carotid artery stenting

All procedures were carried out via the femoral approach following a Seldinger technique. This centre has undertaken more than 500 CAS procedures in the past 5 years. All patients were on long-term aspirin (100 mg/day) and were given a 525-mg loading dose of clopidogrel. A dose of 10 000 units unfractionated heparin was administered at the beginning of the intervention. A cerebral protection device (FilterWire EZ™; Boston Scientific, Natick, Massachusetts, USA) was used in all but three patients, in whom it was not possible to navigate the device into proper position owing to difficult anatomy. The type of covered stent and other specific intervention strategies were left to the discretion of the interventional radiologists. All patients had diagnostic angiography for verification of the characteristics of the ICA stenosis. Four-vessel angiography was used only in patients with multiple stenoses detected on CTA. After predilatation of the stenosis (if needed), an appropriate stent for each stenosis was implanted and then dilated using a balloon catheter. Angiography was used to evaluate the position of the implanted stent, as well the intracranial circulation.

MRI

MRI was conducted before, and 24 h after intervention using a 1·5-T Avanto system (Siemens, Erlangen, Germany). Sequences were applied at an identical level, with the same slice thickness and identical cut number. Slice thickness comprised the cut thickness (5 mm) plus gap (10 per cent). The standard number of slices was 25.

In accordance with previous studies[11–14], new ischaemic lesions in the brain were defined as hyperintense lesions on postintervention diffusion-weighted (DW) imaging that were not present on pretreatment MRI. Ischaemic lesions in the brain (number and total volume of hyperintense lesions on DW imaging) were evaluated by a radiologist and neurologist, both blinded to the study protocol, and disagreements were resolved by consensus. Images acquired before and after intervention were evaluated to assess the presence, number, manually measured volume and location of new ipsilateral ischaemic lesions in the brain after the carotid procedure. Ischaemic lesions with a diameter smaller than 0·5 cm^3 and those with diameter of 0·5 cm^3 or more were evaluated separately in subanalyses. Enlargement of a previously present DW-MRI lesion by at least 50 per cent or at least 0·5 cm^3 was evaluated separately.

Clinical examination

Physical and neurological examination was carried out by a blinded neurologist before, and 24 h and 30 days after intervention. This included evaluation of neurological deficit using the National Institutes of Health Stroke Scale, dependency (assessed using a modified version of the Rankin scale), and cognitive function.

Cognitive function testing

The following cognitive tests were included. Mini Mental State Examination (MMSE) was used to assess orientation, registration (immediate memory), short-term memory and language functioning. This test is composed of 30 questions; 1 point is given for every correct answer (result evaluation 0–30 points). Second was a clock-drawing test for a brief cognitive task testing executive functioning (memory, concentration, initiation, energy, mental clarity and indecision). Errors in clock-drawing are classified as omissions, perseverations, rotations, misplacements, distortions, substitutions and additions. The Shulman scoring system (0–5 points) was used for test result evaluation. Third, verbal fluency tests were used to test executive functioning and linguistic skills. Participants had to say as many words beginning with the letter 'p' as possible from a given category within 60 s. This was scored from 0 to 7 points: 0–1 word, 0 points; 2–3 words, 1 point; 4–5 words, 2 points; 6–7 words, 3 points; 8–10 words, 4 points; 11–13 words, 5 points; 14–17 words, 6 points; and more than 17 words, 7 points. All cognitive tests were performed by a blinded investigator.

Endpoints for study analyses

The primary endpoint was the incidence of new ischaemic lesions (larger than 0·5 cm^3) on brain DW-MRI performed 24 h after intervention. Secondary endpoints were: changes in cognitive tests after 24 h and 30 days; incidence of postoperative stroke or transient ischaemic attack (TIA) at 30 days; and death, any stroke or myocardial infarction (greater than twofold increase in cardiac troponin T level or electrocardiographic evidence of ischaemia) within 30 days[17].

Statistical analysis

The sample size of the study was calculated based on an expected 80 per cent difference in new ischaemic lesions on DW-MRI between CEA (estimated prevalence 30 per cent) and CAS (54 per cent), and a 1·5-point difference in follow-up cognitive test results. Calculations suggested that a minimum of 73 patients in each group were needed to reach a significant difference with an α value of 0·05 (two-tailed) and a β value of 0·8, assuming that 15 per cent of subjects would be lost to follow-up.

The normality of data distribution was checked using the Shapiro–Wilk test. Data with a normal distribution (age, delay between symptoms and intervention) are reported as mean(s.d.). Variables not fitting a normal distribution (degree of ICA stenosis, volume of ischaemic lesions, results of cognitive tests) are presented as mean and median (i.q.r.). Continuous variables were compared by Student's *t* test if normally distributed; otherwise, the Mann–Whitney *U* test was used. Categorical variables were compared by Fisher's exact test. Multiple logistic regression analyses were used to determine possible predictors of a new brain infarction. The following variables were included in univariable and multiple logistic regression analyses: age, sex, arterial hypertension, diabetes mellitus, hyperlipidaemia, statin dose, coronary heart disease, atrial fibrillation, smoking, alcohol abuse, side, severity, preoperative symptoms, delay from symptoms to intervention, severity of contralateral ICA stenosis and type of intervention. Spearman correlation coefficient and intraclass correlation coefficient were calculated for the evaluation of interobserver and intraobserver agreements of brain infarction volume measurement. All tests were carried out at an α-level of significance of 0·05. The data were analysed using SPSS® version 17.0 (IBM, Armonk, New York, USA).

Results

In total, 150 of 307 screened patients fulfilled the inclusion criteria (*Fig. 1*). Seventy-three patients (47 men; mean age 64·9(7·1) years) were randomized to CEA and 77 (58 men; 66·4(7·5) years) to CAS. No patient was lost to 30-day follow-up. The proportion of patients with symptomatic stenoses, and the delay from symptom onset to intervention was similar in the two groups (*Table 1*). Clinical and procedural variables were well matched between the groups, except for diabetes mellitus, which occurred significantly more frequently in the CAS group ($P = 0·014$).

MRI outcomes

New infarctions in the brain on DW-MRI were found in 18 patients (25 per cent) after CEA and in 38 (49 per cent) after CAS group ($P = 0·002$). The volume of new brain infarction was also significantly higher following CAS ($P = 0·010$) (*Table 2*). Enlargement of a previously present DW-MRI lesion was not detected in any patient. There was no correlation between statin dose (15 patients used 20 mg simvastatin, 26 patients 10 mg; 57 patients used 20 mg atorvastatin, 7 patients 40 mg) and volume of brain infarction ($r = –0·008$, $P = 0·929$).

The Spearman correlation coefficient for interobserver agreement of brain infarction volume measurements was 0·98, and the intraclass correlation coefficient for intraobserver agreement was 0·99 (both $P < 0·001$).

Bilateral infarctions were detected in 15 patients (19 per cent) after CAS, but none after CEA ($P < 0·001$) (*Table 2*).

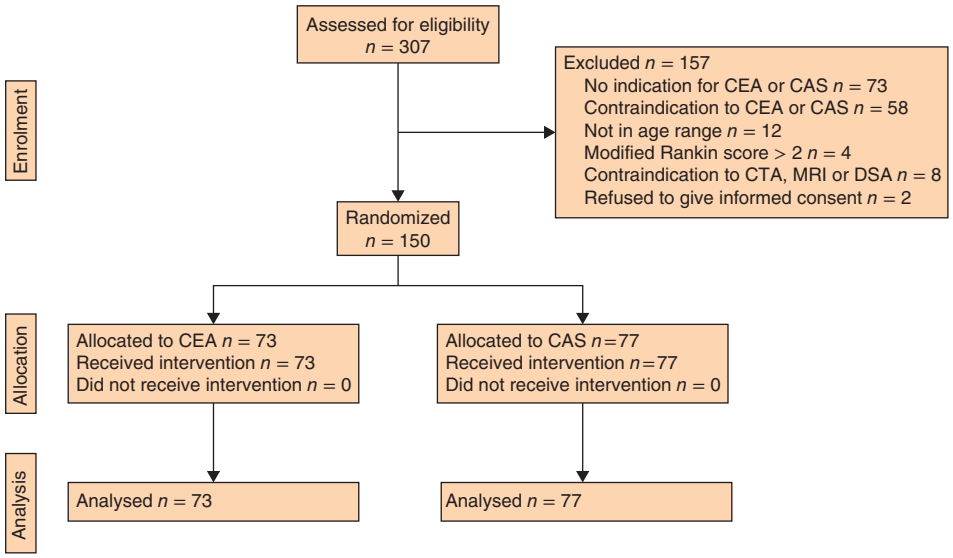

Fig. 1 CONSORT diagram for the study. CEA, carotid endarterectomy; CAS, carotid angioplasty and stenting; CTA, CT angiography; DSA, digital subtraction angiography

Table 1 Demographic and clinical data

	Carotid endarterectomy ($n = 73$)	Carotid angioplasty and stenting ($n = 77$)	P‡
Age (years)*	64·9(7·1)	66·4(7·5)	0·210§
Sex ratio (M : F)	47 : 26	58 : 19	0·158
Right-sided stenosis	38 (52)	37 (48)	0·744
Severity of stenosis (%)†	81·3; 80 (70–90)	81·8; 80 (70–90)	0·700¶
Symptomatic stenosis	48 (66)	39 (51)	0·070
Delay between symptoms and intervention (days)*	41·3(28·9)	41·5(41·4)	0·893§
Contralateral stenosis > 50%	26 (36)	39 (51)	0·074
Arterial hypertension	61 (84)	70 (91)	0·222
Diabetes mellitus	24 (33)	41 (53)	0·014
Hyperlipidaemia	52 (71)	54 (70)	1·000
Ischaemic heart disease	24 (33)	33 (43)	0·241
Atrial fibrillation	4 (5)	9 (12)	0·247
Smoking	22 (30)	16 (21)	0·196
Alcohol abuse	2 (3)	5 (6)	0·443
Statin use	52 (71)	54 (70)	1·000
Antithrombotics	71 (97)	77 (100)	0·212
Antiplatelets	59	73	
Anticoagulation	12	4	

Values in parentheses are percentages unless indicated otherwise; *values are mean(s.d.) and †mean; median (i.q.r.). ‡Fisher's exact test, except §Student's t test and ¶Mann–Whitney U test.

Table 2 MRI outcomes after carotid intervention

	Carotid endarterectomy ($n = 73$)	Carotid angioplasty and stenting ($n = 77$)	P†
Ipsilateral new brain infarctions	18 (25)	38 (49)	0·002
Volume of ischaemic lesion (cm^3)*	0 (0–0·025)	0 (0–0·250)	0·010‡
New brain infarctions > 0·5 cm^3	9 (12)	10 (13)	1·000
New brain infarctions in both hemispheres	0 (0)	15 (19)	< 0·001

Values in parentheses are percentages unless indicated otherwise; *values are median (i.q.r.). †Fisher's exact test, except ‡Mann–Whitney U test.

Table 3 Changes in cognitive test results after carotid endarterectomy and carotid artery stenting (adjusted for diabetes mellitus)

	Changes after 24 h			Changes after 30 days		
	CEA	CAS	*P**	CEA	CAS	*P**
MMSE	−0·58; 0 (−1 to 0)	−0·47; 0 (−1 to 1)	0·560	−0·73; 0 (−1 to 0)	−0·82; 0 (−1 to 0)	0·525
Clock-drawing test	−0·35; 0 (0 to 0)	−0·37; 0 (0 to 0)	0·678	−0·71; 0 (0 to 0)	−0·75; 0 (−2 to 0)	0·138
Verbal fluency test	0·32; 0 (−1·5 to 2)	−0·28; 0 (−2 to 1)	0·231	−2·93; −2 (−6 to 0)	−3·11; −2 (−7 to 1)	0·752

Values are mean; median (i.q.r.). CEA, carotid endarterectomy; CAS, carotid angioplasty and stenting; MMSE, Mini Mental State Examination. *Mann–Whitney *U* test.

Table 4 Changes in cognitive test results in patients with and without a new brain infarction

	Changes after 24 h			Changes after 30 days		
	New infarction	No new infarction	*P**	New infarction	No new infarction	*P**
MMSE	−1·14; 0 (−1 to 0)	−0·15; 0 (−1 to 0)	0·046	−1·21; 0 (−1 to 0)	−0·58; 0 (−1 to 0)	0·921
Clock-drawing test	−0·63; 0 (−1 to 0)	−0·16; 0 (0 to 0)	0·029	−0·77; 0 (−1 to 0)	−0·72; 0 (−1 to 0)	0·730
Verbal fluency test	−0·94; 0 (−2 to 1)	0·13; 0 (−1 to 2)	0·048	−3·80; −2 (−6 to 0)	−2·71, −2 (−6 to 0)	0·253

Values are mean; median (i.q.r.). MMSE, Mini Mental State Examination. *Mann–Whitney *U* test.

Four of 15 patients with bilateral infarctions underwent four-vessel brain angiography before CAS. Three had contralateral ICA occlusion, four had atrial fibrillation and one patient had a combination of all three risk factors. The remaining three patients with bilateral infarctions underwent CAS of the right ICA.

Stepwise multiple logistic regression analyses revealed intervention in the right ICA to be the only independent predictor of brain infarction, with an odds ratio (OR) of 2·10 (95 per cent c.i. 1·03 to 4·25; $P = 0·040$) for all procedures. After stratification for treatment, the OR for CEA was 4·72 (1·37 to 16·22; $P = 0·014$), whereas the side of intervention was not significant after CAS. Atrial fibrillation was the only independent predictor of bilateral brain infarction, with an OR of 14·67 (2·21 to 97·56; $P = 0·005$). After stratification for treatment, the OR for CAS was 5·14 (1·10 to 23·91; $P = 0·037$); no bilateral brain infarction was detected after CEA.

Clinical outcomes

Postoperative stroke or TIA occurred in only one patient after CEA and in two after CAS. No patient in either group died or had a myocardial infarction. Other complications, including peripheral nerve palsy, vocal cord palsy or pseudoaneurysm, were more common after CEA (15 *versus* 1; $P < 0·001$).

Cognitive function tests

A significant worsening of the MMSE score 24 h after CEA ($P = 0·013$), and in the clock-drawing test after CAS ($P = 0·025$), were noted, but overall no significant differences were observed in cognitive test results between CEA and CAS either 24 h or 30 days after intervention (*Table 3*). Patients with new ischaemic lesions had a significantly greater decrease in cognitive test scores 24 h after intervention, with a non-significant trend persisting after 30 days (*Table 4*). Unrest or mild delirium lasting for a few hours was noted after the procedure in 26 per cent of patients with new ischaemic lesions compared with 16 per cent of those without DW-MRI lesions ($P = 0·122$).

Discussion

This prospective randomized trial evaluated both the rate of new ischaemic lesions on MRI and changes in cognitive function after CAS and CEA. A previous report from the International Carotid Stenting Study–Magnetic Resonance Imaging Substudy[18] undertook a similar analysis, but the follow-up cognitive tests were done in only a limited number of subjects[19]. Only four other small prospective randomized studies evaluated cognitive function after CAS and CEA, without evaluation of new cerebral lesions[16].

The present study demonstrated a twofold increase in new ischaemic lesions in the brain, with significantly larger lesion volume, after CAS compared with CEA. These data accord with previous findings[11–14]. Flach and colleagues[11] found new ischaemic lesions in 43 per cent of patients after CAS with a mean lesion volume of 2·52 cm^3, compared with 9 per cent of patients after CEA and a mean lesion volume of 1·74 cm^3. Similarly, Lacroix and co-workers[12] reported new ischaemic lesions in 42·6 per cent of patients after CAS and in only 11·7 per cent after CEA. Bonati *et al.*[13] detected new ischaemic lesions in 50 per cent of subjects after CAS compared with 17 per cent after CEA.

Meta-analyses[14] of six studies confirmed a significantly higher risk of a new lesion on DW-MRI after CAS (37 per cent) than CEA (10 per cent), with an OR of 6·1.

In the present study, 19 per cent of patients also had new lesions in the contralateral hemisphere on DW-MRI after CAS. Similar results have been reported before[11–14]. Only atrial fibrillation was found to be an independent risk factor for new ischaemic lesions outside the treated vascular territory after CAS in the present analysis.

DW-MRI is being used increasingly to detect markers of subclinical stroke[20,21]. It is sufficiently sensitive to detect small infarctions in the brain within the first 24 h after CEA or CAS[22–25]. The reported higher prevalence of new DW-MRI lesions after CAS is related primarily to manipulation with catheters, guidewires and sheaths in the supra-aortic vasculature before angioplasty and stenting; it may also be a consequence of diagnostic angiography, which is usually carried out before CAS[14,26]. Moreover, detection of lesions using DW-MRI is dependent on the duration of scanning[27]. Variations in the reported rates of brain infarction after carotid interventions in particular studies may be the result of differences in the timing of follow-up MRI. In the present study, this examination was performed 24 h after intervention in order to detect procedure-related changes only.

Despite developments and improvements in the method of carotid stenting, the proportion of new ischaemic lesions on DW-MRI remains similar to that reported in older studies[13,14,28]. New ischaemic lesions after CAS might be reduced by use of cerebral protection devices, closed-cell stents and optimal medical treatment[14,29–31]. Some studies suggested no beneficial effect of filter-type protection devices[18,32,33], but two small recent studies[29,30] showed that proximal embolic protection reduces the rate of microembolic signals during CAS more effectively than filter protection. A high loading dose of clopidogrel (600 mg) with a high dose of atorvastatin reduced the risk of cerebral lesions, stroke or TIA during the following 30 days in one study[32]. Nevertheless, a second study[34] failed to show the superiority of a high loading dose of clopidogrel (600 mg) in comparison with a standard dose (300 mg).

The impact of side of the treated stenosis and associated previous symptoms on the risk of new ischaemic brain lesions is also uncertain. In the present study, intervention in the right ICA was the only independent risk factor for brain infarction, although only after CEA. This is difficult to explain, but could be accounted for if surgeons were more careful when performing the procedure in the left ICA in order to avoid neurological deficit in the dominant hemisphere. The same result was reported by Wimmer and colleagues[35] after CAS. Conversely, intervention in the left ICA was a risk factor for perioperative stroke or death in the North American Symptomatic Carotid Endarterectomy Trial (NASCET)[36] and the Endarterectomy *Versus* Angioplasty in Patients with Symptomatic Severe Carotid Stenosis (EVA-3S) trial[37]. Stingele and colleagues[38] did not find the side of the stenosis to be a risk factor in CAS or CEA groups. The risk of perioperative stroke is usually higher in patients with a symptomatic stenosis, but neither meta-analyses[14] of six studies comparing CAS with CEA directly, nor the present study, showed a higher rate of new DW-MRI lesions in patients with a symptomatic stenosis. Moreover, delay before intervention was not identified as a risk factor for new brain infarction in the present study.

Cognitive changes are also important signs of ischaemic lesions in the brain after CEA or CAS. The present study showed a worsening trend in all cognitive tests after both CAS and CEA. The biggest difference between the groups was found in the verbal fluency test 24 h after intervention, with a mean decrease of 0·6 points more in the CAS than in the CEA group. A study of around 400 patients per group would be needed to prove statistical significance of this observation. Patients with a new infarction had a significantly greater short-term decrease in all cognitive test results than those without new MRI lesions, and there was also a trend towards increased unrest or mild delirium after the procedure in these patients. By 30 days there were no significant differences in cognitive function between the groups.

The present study had some limitations. The small size did not allow significant differences in the rates of perioperative stroke and death to be ascertained. Serial follow-up MRI was not done to compare the progression or persistence of detected ischaemic lesions. A software package for mapping of brain infarction volume was not used. This was a single-centre investigation with mandatory use of brain protection devices during CAS and shunts during CEA.

Acknowledgements

This work was supported by grants from the Internal Grant Agency of the Ministry of Health of the Czech Republic (NT/11386-5/2010, NT/13498-4/2012, NT/11046-6/2010), an internal grant from University Hospital Ostrava (MH CZ-DRO-FNOs/2012), and a grant from the Ministry of Education, Youth and Sports of the Czech Republic (CZ.1.05/2.1.00/010030).
Disclosure: The authors declare no conflict of interest.

References

1 Cina CS, Clase CM, Haynes RB. Carotid endarterectomy for symptomatic carotid stenosis. *Cochrane Database Syst Rev*

2000; (2)CD001081. Update in *Cochrane Database Syst Rev* 2011; (4)CD001081.
2 Grotta JC, Bigelow RH, Hu H, Hankins L, Fields WS. The significance of carotid stenosis or ulceration. *Neurology* 1984; **34**: 437–442.
3 Chambers BR, Donnan GA. Carotid endarterectomy for asymptomatic carotid stenosis. *Cochrane Database Syst Rev* 2005; (4)CD001923.
4 Ferguson GG, Eliasziw M, Barr HW, Clagett GP, Barnes RW, Wallace MC *et al.* The North American Symptomatic Carotid Endarterectomy Trial: surgical results in 1415 patients. *Stroke* 1999; **30**: 1751–1758.
5 Brott TG, Halperin JL, Abbara S, Bacharach JM, Barr JD, Bush RL *et al.*; American College of Cardiology Foundation/American Heart Association Task Force on Practice Guidelines; American Stroke Association; American Association of Neuroscience Nurses; American Association of Neurological Surgeons; American College of Radiology; American Society of Neuroradiology; Congress of Neurological Surgeons; Society of Atherosclerosis Imaging and Prevention; Society for Cardiovascular Angiography and Interventions; Society of Interventional Radiology; Society of NeuroInterventional Surgery; Society for Vascular Medicine; Society for Vascular Surgery; American Academy of Neurology and Society of Cardiovascular Computed Tomography. 2011 ASA/ACCF/AHA/AANN/AANS/ACR/ASNR/CNS/SAIP/SCAI/SIR/SNIS/SVM/SVS guideline on the management of patients with extracranial carotid and vertebral artery disease: executive summary. *Stroke* 2011; **42**: e420–e463.
6 Yavin D, Roberts DJ, Tso M, Sutherland GR, Eliasziw M, Wong JH. Carotid endarterectomy *versus* stenting: a meta-analysis of randomized trials. *Can J Neurol Sci* 2011; **38**: 230–235.
7 Economopoulos KP, Sergentanis TN, Tsivgoulis G, Mariolis AD, Stefanadis C. Carotid artery stenting *versus* carotid endarterectomy: a comprehensive meta-analysis of short-term and long-term outcomes. *Stroke* 2011; **42**: 687–692.
8 Murad MH, Shahrour A, Shah ND, Montori VM, Ricotta JJ. A systematic review and meta-analysis of randomized trials of carotid endarterectomy *vs* stenting. *J Vasc Surg* 2011; **53**: 792–797.
9 Eckstein HH, Ringleb P, Allenberg JR, Berger J, Fraedrich G, Hacke W *et al.* Results of the Stent-Protected Angioplasty *versus* Carotid Endarterectomy (SPACE) study to treat symptomatic stenoses at 2 years: a multinational, prospective, randomised trial. *Lancet Neurol* 2008; **7**: 893–902.
10 Brott TG, Hobson RW II, Howard G, Roubin GS, Clark WM, Brooks W *et al.*; CREST Investigators. Stenting *versus* endarterectomy for treatment of carotid-artery stenosis. *N Engl J Med* 2010; **363**: 11–23.
11 Flach HZ, Ouhlous M, Hendriks JM, Van Sambeek MR, Veenland JF, Koudstaal PJ *et al.* Cerebral ischemia after carotid intervention. *J Endovasc Ther* 2004; **11**: 251–257.
12 Lacroix V, Hammer F, Astarci P, Duprez T, Grandin C, Cosnard G *et al.* Ischemic cerebral lesions after carotid surgery and carotid stenting. *Eur J Vasc Endovasc Surg* 2007; **33**: 430–435.
13 Bonati LH, Jongen LM, Haller S, Flach HZ, Dobson J, Nederkoorn PJ *et al.*; ICSS-MRI study group. New ischaemic brain lesions on MRI after stenting or endarterectomy for symptomatic carotid stenosis: a substudy of the International Carotid Stenting Study (ICSS). *Lancet Neurol* 2010; **9**: 353–362.
14 Schnaudigel S, Gröschel K, Pilgram SM, Kastrup A. New brain lesions after carotid stenting *versus* carotid endarterectomy: a systematic review of the literature. *Stroke* 2008; **39**: 1911–1919.
15 Müller M, Reiche W, Langenscheidt P, Hassfeld J, Hagen T. Ischemia after carotid endarterectomy: comparison between transcranial Doppler sonography and diffusion-weighted MR imaging. *AJNR Am J Neuroradiol* 2000; **21**: 47–54.
16 Paraskevas KI, Lazaridis C, Andrews CM, Veith FJ, Giannoukas AD. Comparison of cognitive function after carotid artery stenting *versus* carotid endarterectomy. *Eur J Vasc Endovasc Surg* 2014; **47**: 221–231.
17 Tehrani DM, Seto AH. Third universal definition of myocardial infarction: update, caveats, differential diagnoses. *Cleve Clin J Med* 2013; **80**: 777–786.
18 Gensicke H, Zumbrunn T, Jongen LM, Nederkoorn PJ, Macdonald S, Gaines PA *et al.*; ICSS-MRI Substudy Investigators. Characteristics of ischemic brain lesions after stenting or endarterectomy for symptomatic carotid artery stenosis: results from the International Carotid Stenting Study–Magnetic Resonance Imaging Substudy. *Stroke* 2013; **44**: 80–86.
19 Altinbas A, van Zandvoort MJ, van den Berg E, Jongen LM, Algra A, Moll FL *et al.* Cognition after carotid endarterectomy or stenting: a randomized comparison. *Neurology* 2011; **77**: 1084–1090.
20 Bendszus M, Stoll G. Silent cerebral ischaemia: hidden fingerprints of invasive medical procedures. *Lancet Neurol* 2006; **5**: 364–372.
21 Ringleb PA, Bruckmann H, Eckstein HH, Fraedrich G, Hartmann M, Hennerici M *et al.*; SPACE Collaborative Group. 30 day results from the SPACE trial of stent-protected angioplasty *versus* carotid endarterectomy in symptomatic patients: a randomised non-inferiority trial. *Lancet* 2006; **368**: 1239–1247.
22 Hammer FD, Lacroix V, Duprez T, Grandin C, Verhelst R, Peeters A *et al.* Cerebral microembolization after protected carotid artery stenting in surgical high-risk patients: results of a 2-year prospective study. *J Vasc Surg* 2005; **42**: 847–853.
23 Roh HG, Byun HS, Ryoo JW, Na DG, Moon WJ, Lee BB *et al.* Prospective analysis of cerebral infarction after carotid endarterectomy and carotid artery stent placement by using diffusion-weighted imaging. *AJNR Am J Neuroradiol* 2005; **26**: 376–384.

24 Poppert H, Wolf O, Resch M, Theiss W, Schmidt-Thieme T, Graefin von Einsiedel H *et al.* Differences in number, size and location of intracranial microembolic lesions after surgical *versus* endovascular treatment without protection device of carotid artery stenosis. *J Neurol* 2004; **251**: 1198–1203.
25 Feiwell RJ, Besmertis L, Sarkar R, Saloner DA, Rapp JH. Detection of clinically silent infarcts after carotid endarterectomy by use of diffusion-weighted imaging. *AJNR Am J Neuroradiol* 2001; **22**: 646–649.
26 Bendszus M, Koltzenburg M, Burger R, Warmuth-Metz M, Hofmann E, Solymosi L. Silent embolism in diagnostic cerebral angiography and neurointerventional procedures: a prospective study. *Lancet* 1999; **354**: 1594–1597.
27 Rapp JH, Wakil L, Sawhney R, Pan XM, Yenari MA, Glastonbury C *et al.* Subclinical embolization after carotid artery stenting: new lesions on diffusion-weighted magnetic resonance imaging occur postprocedure. *J Vasc Surg* 2007; **45**: 867–872.
28 Gossetti B, Gattuso R, Irace L, Faccenna F, Venosi S, Bozzao L *et al.* Embolism to the brain during carotid stenting and surgery. *Acta Chir Belg* 2007; **107**: 151–154.
29 Bijuklic K, Wandler A, Hazizi F, Schofer J. The PROFI study (Prevention of Cerebral Embolization by Proximal Balloon Occlusion Compared to Filter Protection During Carotid Artery Stenting): a prospective randomized trial. *J Am Coll Cardiol* 2012; **59**: 1383–1389.
30 Montorsi P, Caputi L, Galli S, Ciceri E, Ballerini G, Agrifoglio M *et al.* Microembolization during carotid artery stenting in patients with high-risk, lipid-rich plaque. A randomized trial of proximal *versus* distal cerebral protection. *J Am Coll Cardiol* 2011; **58**: 1656–1663.
31 Patti G, Tomai F, Melfi R, Ricottini E, Macrì M, Sedati P *et al.* Strategies of clopidogrel load and atorvastatin reload to prevent ischemic cerebral events in patients undergoing protected carotid stenting. Results of the randomized ARMYDA-9 CAROTID (Clopidogrel and Atorvastatin Treatment During Carotid Artery Stenting) study. *J Am Coll Cardiol* 2013; **61**: 1379–1387.
32 Barbato JE, Dillavou E, Horowitz MB, Jovin TG, Kanal E, David S *et al.* A randomized trial of carotid artery stenting with and without cerebral protection. *J Vasc Surg* 2008; **47**: 760–765.
33 Macdonald S, Evans DH, Griffiths PD, McKevitt FM, Venables GS, Cleveland TJ *et al.* Filter-protected *versus* unprotected carotid artery stenting: a randomised trial. *Cerebrovasc Dis* 2010; **29**: 282–289.
34 Van Der Heyden J, Van Werkum J, Hackeng CM, Kelder JC, Breet NJ, Deneer VH *et al.* High *versus* standard clopidogrel loading in patients undergoing carotid artery stenting prior to cardiac surgery to assess the number of microemboli detected with transcranial Doppler: results of the randomized IMPACT trial. *J Cardiovasc Surg* 2013; **54**: 337–347.
35 Wimmer NJ, Yeh RW, Cutlip DE, Mauri L. Risk prediction for adverse events after carotid artery stenting in higher surgical risk patients. *Stroke* 2012; **43**: 3218–3224.
36 Barnett HJ, Taylor DW, Eliasziw M, Fox AJ, Ferguson GG, Haynes RB *et al.* Benefit of carotid endarterectomy in patients with symptomatic moderate or severe stenosis. North American Symptomatic Carotid Endarterectomy Trial Collaborators. *N Engl J Med* 1998; **339**: 1415–1425.
37 Naggara O, Touzé E, Beyssen B, Trinquart L, Chatellier G, Meder JF *et al.*; EVA-3S Investigators. Anatomical and technical factors associated with stroke or death during carotid angioplasty and stenting: results from the Endarterectomy *Versus* Angioplasty in Patients with Symptomatic Severe Carotid Stenosis (EVA-3S) trial and systematic review. *Stroke* 2011; **42**: 380–388.
38 Stingele R, Berger J, Alfke K, Eckstein HH, Fraedrich G, Allenberg J *et al.* Clinical and angiographic risk factors for stroke and death within 30 days after carotid endarterectomy and stent-protected angioplasty: a subanalysis of the SPACE study. *Lancet Neurol* 2008; **7**: 216–222.

2.

Gender differences in the treatment of first-episode schizophrenia: Results from the European First Episode Schizophrenia Trial

Češková E, Přikryl R, Libiger J, Švancara J, Jarkovský J

Originally published in Schizophrenia Research, 2015, vol. 169, no. 1-3, p. 303-307.

Schizophrenia Research 169 (2015) 303–307

Contents lists available at ScienceDirect

Schizophrenia Research

journal homepage: www.elsevier.com/locate/schres

Gender differences in the treatment of first-episode schizophrenia: Results from the European First Episode Schizophrenia Trial

Eva Ceskova [a,b,c,d,*], Radovan Prikryl [a,b], Jan Libiger [e], Jan Svancara [f], Jiri Jarkovsky [f]

[a] Department of Psychiatry, Faculty Hospital Brno, Czech Republic
[b] Central European Institute of Technology, Masaryk University (CEITEC MU), Brno, Czech Republic
[c] Department of Clinical Studies Medical Faculty, University Ostrava, Czech Republic
[d] Department of Psychiatry, Faculty Hospital Ostrava, Czech Republic
[e] Department of Psychiatry, University Hospital Hradec Kralove, Czech Republic
[f] Institute of Biostatistics and Analyses, Faculty of Medicine, Masaryk University, Brno, Czech Republic

ARTICLE INFO

Article history:
Received 22 August 2015
Received in revised form 2 October 2015
Accepted 6 October 2015
Available online 3 November 2015

Keywords:
First-episode schizophrenia
Treatment response
Antipsychotics
Gender differences

ABSTRACT

Gender differences in the response to antipsychotic treatment have been detected in the past, but not studied in great detail. The results of the European First-Episode Schizophrenia Trial (EUFEST) were analyzed with a focus on gender differences in the response to randomized treatment of first-episode schizophrenia. A total of 498 patients (298 men and 200 women) were randomly assigned by a web-based online system to open-label treatment with haloperidol, amisulpride, olanzapine, quetiapine, and ziprasidone. Treatment response was evaluated using the positive and negative syndrome scale (PANSS). Data were collected at baseline and then prospectively for one year. Baseline characteristics (age and proportion of patients assigned to individual antipsychotics) were the same between the male and female patients with the exception of ziprasidone: significantly fewer men, proportionately, were prescribed ziprasidone. There was no significant difference between genders between the initial total PANSS and subscale scores. A significant interaction between time and gender was found, with more robust PPANSS and TPANSS score improvement in women during the course of treatment. Of all of the antipsychotics used, only olanzapine led to significantly greater improvement in the total PANSS score in women during the follow-up period. Gender differences should be given more attention in research and clinical practice. Their causes require clarification, and future strategies for dealing with them may be considered in early intervention programs and guidelines.

1. Introduction

Gender differences in psychotic disorders have been observed in terms of illness onset and course. Clinical studies that examine outcomes separately for men and women can help determine whether treatment has differential effectiveness or distinct side effects according to gender. The issue of gender-specific responses to medication interventions addresses an understudied area. For many years, researchers omitted women from clinical trials to avoid the difficulty of assessing the potentially interfering effects of female hormones and the bias menstrual cycles might mean for study results.

Many studies have tried to determine the role of gender in schizophrenia, but mainly in terms of epidemiology, clinical symptoms, and course of illness. Gender differences in antipsychotic responses have been less systematically pursued. However, gender-related effects may play a role in antipsychotic treatment (Seeman, 2004). It has been hypothesized that estrogen, with effects on both neurodevelopment and neurotransmission, may play a protective role in women with schizophrenia and account for some of the gender differences observed in the disorder (Canuso and Pandini, 2007; Groleger and Novak-Grubic, 2010). Gender differences in response to individual antipsychotics have been observed (Usall et al., 2007; Raedler et al., 2006; Segarra et al., 2011; Xiang et al., 2010; Müller et al., 2006).

Fifty sites in 14 countries, including three Czech centers, participated in the European First-Episode Schizophrenia Trial (EUFEST), a one-year pragmatic, multicenter, randomized trial focused on the prospective evaluation of treatment effectiveness under circumstances similar to routine clinical practice (Kahn et al., 2008). The aim of this paper is to use the EUFEST data to evaluate gender differences in schizophrenia in response to typical (low dose of haloperidol) and atypical antipsychotics. We hypothesized that there would be gender differences in the response to individual antipsychotics and between typical and atypical antipsychotics. We expected greater improvement of psychopathology in women than in men.

* Corresponding author at: Department of Psychiatry, Faculty Hospital Brno, Jihlavska 102, Brno-Bohunice 625 00, Czech Republic.
E-mail address: eva.ceskova@gmail.com (E. Ceskova).

http://dx.doi.org/10.1016/j.schres.2015.10.013
0920-9964/

2. Methods

2.1. Study design

Data from EUFEST were used for the present study. The EUFEST rationale, design, and methods were published elsewhere (Fleischhacker et al., 2005; Kahn et al., 2008). The subjects were 18–40 years of age, met the Diagnostic and Statistical Manual of Mental Disorders fourth edition (DSM IV) criteria for schizophrenia, schizophreniform disorder, or schizoaffective disorder. The first episode of schizophrenia in a partially antipsychotic-naive study population must not have lasted more than two years since the first onset of symptoms. The use of any antipsychotic drug had to be shorter than two weeks in the previous year and must not have exceeded six weeks cumulatively. All participants, or their legal representatives, provided written informed consent. The trial complied with the Declaration of Helsinki and was approved by the ethics committees at the participating centers. The study is registered as an International Standard Randomized Controlled Trial, number ISRCTN68736636.

2.2. Treatment

Patients were randomly assigned by a dedicated web-based online system to a daily regimen of haloperidol (1–4 mg), amisulpride (200–800 mg), olanzapine (5–20 mg), quetiapine (200–750 mg), or ziprasidone (40–160 mg). Patients and their treating physicians were not blinded to the assigned treatment. All study drugs were given orally, within the above dose ranges, at the treating psychiatrist's discretion. The use of mood stabilizers, benzodiazepines, antidepressants, and anticholinergic drugs was allowed, and documented (Kahn et al., 2008).

2.3. Assessment

To evaluate gender differences in response to antipsychotics, positive and negative syndrome scale (PANSS, Kay et al., 1987) scores were applied. For a more detailed analysis, the total PANSS and all subscales (positive PPANSS, negative NPANSS, and general GPANSS) scores were used.

2.4. Data analysis

Demographic, clinical, and treatment-related data were collected at baseline and then prospectively for 12 months. We analyzed the baseline data and data collected after 1, 3, 6, 9, and 12 months. We compared the men and women in terms of mean PANSS total and all subscales scores.

Standard descriptive statistics were applied in the analysis: absolute and relative frequencies for categorical variables and mean supplemented by a 95% confidence interval for continuous variables and scores.

The statistical significance of differences between men and women was tested using Fisher's exact test for categorical variables and an unpaired t-test for continuous variables and scores. The statistical significance of gender, treatment, and their overall interaction was computed using generalized estimating equations (GEE) with time as a within-subject variable. Bonferroni correction was applied for multiple testing; $\alpha = 0.05$ was taken as the level of statistical significance in all analyses. Statistical analysis was computed using SPSS 22 (IBM Corporation, 2013).

3. Results

3.1. Demographic data

Descriptive data for patients in the EUFEST trial have been published. The data can be summarized as follows: The study was performed at 50 sites in 14 countries. A total of 498 patients (298 men and 200 women) were randomly assigned by a web-based online system to haloperidol (1–4 mg per day, n 103: 64 men, 39 women), amisulpride (200–800 mg per day, n 104: 58 men, 46 women), olanzapine (5–20 mg per day, n 105: 67 men, 38 women), quetiapine (200–750 mg per day, n 104. 68 men, 36 women), or ziprasidone (40–160 mg per day, n 82: 41 men, 41 women); follow-up visits were continued for one year (Kahn et al., 2008).

3.2. Baseline characteristics — comparison between men and women

Baseline characteristics (age and proportion of patients assigned to individual antipsychotics) were the same between men and women with the exception of ziprasidone: significantly fewer men, proportionately, were randomly assigned to ziprasidone. The initial total PANSS and all PANSS subscales scores did not differ between groups (Table 1).

3.3. Psychopathology change — comparison between men and women

After three months of treatment, a significantly greater improvement in the total PANSS and all PANSS subscales scores, was seen in women. However, after Bonferroni correction was applied, only PPANS and total PANSS score remained significant. After six months, the women had improved significantly more in the total PANSS and the PPANSS subscale, but only in the PPANSS subscale after Bonferroni correction. After nine months, significantly more pronounced improvement was seen in women in the total PANSS and all the PANSS subscale scores, with the exception of the NPANSS. After Bonferroni correction only PPANSS subscale and the total PANSS scores in women was significant— see Table 2.

Using GEE, a significant interaction between time and gender was found, with a more robust PPANSS and TPANSS score improvement in women over the course of treatment — see Table 4, model 1, and Table 2.

3.4. Psychopathology change — comparison between men and women in response to all given antipsychotics

Among all antipsychotics randomized to EUFEST participants at the admission to the trial, only olanzapine led to significantly greater improvement in all domains of psychopathology, e.g. the total PANSS

Table 1
Comparison of male and female baseline characteristics.

Results	Whole sample N = 498	Men N = 298	Women N = 200	P value
Age in years at study entry (95% CI)	26.0 (25.5–26.5)	25.6 (25.0–26.2)	26.5 (25.7–27.3)	0.069
Antipsychotic randomized at study entry				
Haloperidol	103 (20.7%)	64 (21.5%)	39 (19.5%)	0.652
Amisulpride	104 (20.9%)	58 (19.5%)	46 (23.0%)	0.369
Olanzapine	105 (21.1%)	67 (22.5%)	38 (19.0%)	0.372
Quetiapine	104 (20.9%)	68 (22.8%)	36 (18.0%)	0.217
Ziprasidone	82 (16.5%)	41 (13.8%)	41 (20.5%)	**0.050**
Psychopathology (PANSS)				
PPANSS	23.1 (22.6–23.7)	22.9 (22.2–23.6)	23.5 (22.6–24.3)	0.346
NPANSS	21.2 (20.6–21.9)	21.3 (20.4–22.2)	21.2 (20.1–22.2)	0.870
GPANSS	44.1 (43.2–45.1)	43.6 (42.4–44.8)	44.9 (43.4–46.5)	0.179
TPANSS	88.5 (86.7–90.4)	87.8 (85.4–90.2)	89.6 (86.7–92.5)	0.344
GAF score	40.0 (38.8–41.2)	40.1 (38.5–41.7)	40.0 (38.2–41.8)	0.941

PPANSS: positive PANSS subscale score; NPANSS: negative PANSS subscale score; GPANSS: general PANSS: subscale score; TPANSS: total PANSS score; CI: confidence interval; significant results are shown in bold.

Table 2
PANSS score changes from baseline (95% CI) — comparison of men and women.

Results	All subjects N = 498	Men N = 298	Women N = 200	P value	P value Bonferroni corr.
After one month	N = 452	N = 267	N = 185		
PPANSS	−7.2 (−7.8; −6.6)	−6.9 (−7.6; −6.1)	−7.7 (−8.6; −6.8)	0.136	0.680
NPANSS	−3.1 (−3.6; −2.5)	−2.7 (−3.4; −2.0)	−3.6 (−4.5; −2.7)	0.120	0.600
GPANSS	−9.3 (−10.2; −8.3)	−8.6 (−9.7; −7.5)	−10.2 (−11.7; −8.6)	0.109	0.545
TPANSS	−19.5 (−21.2; −17.7)	−18.2 (−20.3; −16.0)	−21.3 (−24.2; −18.4)	0.084	0.420
After three months	N = 406	N = 234	N = 172		
PPANSS	−11.1 (−11.8; −10.5)	−10.3 (−11.2; −9.5)	−12.2 (−13.2; −11.3)	**0.003**	**0.015**
NPANSS	−5.4 (−6.1; −4.8)	−4.8 (−5.7; −3.9)	−6.3 (−7.3; −5.2)	**0.042**	0.210
GPANSS	−15.2 (−16.3; −14.1)	−14.1 (−15.6; −12.6)	−16.7 (−18.3; −15.2)	**0.020**	0.100
TPANSS	−31.8 (−33.9; −29.7)	−29.3 (−32.1; −26.4)	−35.2 (−38.1; −32.3)	**0.004**	**0.020**
After six months	N = 363	N = 209	N = 154		
PPANS	−12.0 (−12.7; −11.3)	−11.2 (−12.2; −10.3)	−13.1 (−14.1; −12.1)	**0.007**	**0.035**
NPANSS	−6.1 (−6.8; −5.3)	−5.6 (−6.6; −4.7)	−6.6 (−7.7; −5.5)	0.211	0.995
GPANSS	−16.9 (−18.2; −15.7)	−16.1 (−17.8; −14.4)	−18.0 (−19.8; −16.3)	0.130	0.650
TPANSS	−35.1 (−37.4; −32.8)	−33.0 (−36.2; −29.9)	−37.9 (−41.1; −34.6)	**0.038**	0.190
After nine months	N = 340	N = 194	N = 146		
PPANSS	−12.8 (−13.5; −12.0)	−11.9 (−13.0; −10.9)	−13.9 (−14.9; −12.9)	**0.008**	**0.040**
NPANSS	−6.7 (−7.5; −5.8)	−6.0 (−7.1; −4.9)	−7.5 (−8.8; −6.2)	0.085	0425
GPANSS	−17.9 (−19.2; −16.6)	−16.6 (−18.4; −14.8)	−19.6 (−21.4; −17.7)	**0.026**	**0.131**
TPANSS	−37.3 (−39.8; −34.9)	−34.6 (−38.0; −31.2)	−40.9 (−44.4; −37.5)	**0.011**	0.055
After one year	N = 341	N = 194	N = 147		
PPANSS	−13.1 (−13.9; −12.3)	−12.6 (−13.6; −11.6)	−13.7 (−14.9; −12.6)	0.159	0.795
NPANSS	−7.1 (−7.9; −6.2)	−6.7 (−7.8; −5.5)	−7.6 (−8.9; −6.4)	0.275	0.995
GPANSS	−19.0 (−20.4; −17.7)	−18.3 (−20.1; −16.5)	−20.1 (−21.9; −18.2)	0.182	0.910
TPANSS	−39.3 (−41.9; −36.8)	−37.7 (−41.2; −34.2)	−41.6 (−45.2; −38.0)	0.130	0.650

PPANSS: positive PANSS subscale score; NPANSS: negative PANSS subscale score; GPANSS: general PANSS subscale score; TPANSS: total PANSS score; significant results are shown in bold.

and all the PANSS subscale scores in women. However, only an improvement in the total PANSS remained significant after Bonferroni correction — see Table 3.

Based on the GEE analysis, no significant interaction between treatment and gender was found — see Table 4, model 2.

4. Discussion

The primary outcome measure of the EUFEST was all-cause treatment discontinuation, which was substantially lower in patients on second-generation antipsychotic drugs than in those taking haloperidol. The differences between the treatment groups and the interaction between treatment and time were not significant. Further, there were no significant differences between the treatment groups for the depression score and adherence (Kahn et al., 2008). However the proportion of response and remission was higher for most second-generation antipsychotics than for haloperidol (Boter et al., 2009). Subgroup analysis for gender did not show statistically significant differences in all-cause treatment discontinuation between patients on haloperidol and those taking second-generation antipsychotic drugs (Kahn et al., 2008).

In the present study, we evaluated gender differences in the treatment response to first (haloperidol) and second-generation antipsychotics (amisulpride, olanzapine, quetiapine, ziprasidone). We found that the change of psychopathology, especially positive and total symptoms from baseline, was significantly higher in women than in men during the follow-up visits. This may suggest a faster and more robust response to antipsychotics in women. These findings correspond to the literature reporting a generally better treatment response in women (Abel et al., 2010; Cotton et al., 2009).

On the basis of a simple comparative analysis, we found a better response to treatment in women than in men after olanzapine, one of the five randomized antipsychotics in EUFEST. GEE analysis revealed no significant interaction between treatment and gender was found, but gender differences in response to specific treatments should be much more vigorously studied. Gender may be a predictor of clinical response to antipsychotic treatment, but its influence is not the same for all antipsychotics.

Data dealing with gender differences in the treatment response to risperidone, a second-generation antipsychotic, are somewhat contradictory, scarce, or insufficient (Segarra et al., 2011; Raedler et al., 2006; Ceskova and Prikryl, 2012).

Concerning amisulpride, except for higher dose-related plasma amisulpride levels in women, an explorative study found no clinically relevant gender-specific aspects in relation to prescribed dose, effectiveness, or side effects (Müller et al., 2006).

The SOHO (Schizophrenia Outpatient Health Outcomes) study was a three-year, prospective, observational study of health outcomes associated with antipsychotic treatment in 10 European countries. The study

Table 3
PANSS score changes after 12 months from baseline (mean) — comparison of men and women in response to individual antipsychotics.

	Amisulpride		Haloperidol		Olanzapine		Quetiapine		Ziprasidone	
	M N = 37	W N = 33	M N = 41	W N = 26	M N = 49	W N = 34	M N = 43	W N = 27	M N = 24	W N = 28
PPANSS[a]	−13.1 (6.2)	−14.2 (6.5)	−12.6 (6.6)	−9.8 (7.6)	−11.4 (8.0)	−15.4 (6.7)	−13.3 (8.1)	−13.2 (7.9)	−13.2 (5.4)	−15.1 (6.2)
NPANSS[a]	−7.2 (7.7)	−7.3 (8.2)	−6.6 (8.4)	−4.6 (6.7)	−5.4 (7.3)	−9.1 (7.2)	−6.6 (9.9)	−9.1 (7.3)	−8.6 (8.8)	−7.6 (9.7)
GPANSS[a]	−18.1 (10.6)	−20.1 (10.8)	−19.5 (12.7)	−15.4 (12.4)	−16.0 (13.9)	−22.5 (10.9)	−19.6 (14.4)	−20.3 (9.6)	−18.7 (11.5)	−21.0 (12.9)
TPANSS[a]	−38.4 (20.6)	−41.6 (20.3)	−38.7 (24.5)	−30.5 (24.5)	−32.9 (26.0)	**−47.0 (20.0)**[b]	−40.0 (28.1)	−42.3 (21.0)	−40.5 (22.3)	−43.8 (24.1)

[a] Mean (standard deviation).
[b] Change significantly higher on level alpha = 0.05 (Bonferroni corrected); significant results are shown in bold.

Table 4
Sources of variability of PANSS score.

Variability source[a]	PPANS	P	NPANSS	P	GPANSS	P	TPANSS	P
	% expl. var		% expl. var		% expl. var		% expl. var	
Model 1								
Gender	0.3%	**0.028**	1.8%	**0.013**	0.1%	0.232	0.3%	**0.036**
Time	99.0%	<**0.001**	96.6%	<**0.001**	99.0%	<**0.001**	98.8%	<**0.001**
Gender * Time	0.7%	**0.033**	1.6%	0.331	0.9%	0.084	0.9%	**0.037**
Model 2								
Gender	0.2%	**0.049**	1.7%	**0.013**	0.1%	0.276	0.3%	**0.045**
Time	98.6%	<**0.001**	92.9%	<**0.001**	98.0%	<**0.001**	97.9%	<**0.001**
Gender * Time	0.8%	**0.030**	1.6%	0.307	0.9%	0.077	0.9%	**0.033**
Treatment	0.4%	0.209	1.5%	0.230	0.5%	0.233	0.5%	0.120
Gender * Treatment	0.1%	0.795	2.3%	0.077	0.4%	0.360	0.4%	0.304

[a] Analysis based on generalized estimating equations with time as a within-subject variable; significant results are shown in bold.

found gender to be a significant predictor of response as measured by the Clinical Global Impression Scale. Women in the study had greater clinical improvement. The highest gender differences were found in the outcomes of treatment with typical antipsychotics and clozapine. Olanzapine-related gender differences were reported in quality of life; no treatment outcome differences were found for risperidone (Usall et al., 2007).

A tentative explanation for our findings may be the pharmacokinetics of olanzapine. The gender-related differences in drug metabolism are well documented (Damoiseaux et al., 2014). Apparently, there are no gender-related polymorphisms in the genes of cytochrome P450 enzymes in humans, since most abundant CYP enzymes are encoded by the genes on autosomal chromosomes (Zanger and Schwab, 2013). The differences in the rate of drugs metabolism could be therefore caused by other factors, such as differences in body weight, gastric emptying, body fat content or influence of the sex hormones on metabolic activity of CYP enzymes, which are also well documented (Zhang et al., 2006).

Differences in olanzapine exposure related to gender and smoking may account for some of the variability in response to olanzapine. Smokers clear olanzapine faster than non/past smokers. Polyaromatic hydrocarbons in cigarette smoke are known to induce the liver enzyme cytochrome P450 1A2. CYP1A2 is the major enzyme responsible for metabolizing olanzapine. Estrogen is a known inhibitor of CYP1A2, which could explain the slower olanzapine clearance found in women (Bigos et al., 2008). Therefore, it is possible that higher levels of olanzapine are reached with the standard olanzapine dose, as reported by Citrome et al. (2009). This is in accordance with SPC information, where lower metabolic capacity for olanzapine is reported in females with suggestion of decreasing the doses in subjects with 2 or more factors decreasing the rate olanzapine metabolism (females, non-smokers, elderly) (SPC Zyprexa/Infopharm). The question is, if the differences in pharmacokinetics of olanzapine would persist even in the case the dose would be adjusted to the body weight.

Unfortunately, the antipsychotic plasma levels are not available for the EUFEST patients. Their smoking status was recorded, but not available for this analysis.

Generally, men present fewer depressive symptoms than women, which may explain their worse treatment results according to a range of outcome measures (Abel et al., 2010). This may partially account for the better efficacy of olanzapine among women in our study. However, we did not find any differences in the PANSS subscale scores between men and women at the beginning of the study. Further, Kahn did not report differences between treatment effects in depression scores with antipsychotic drugs (Kahn et al., 2008). A re-analysis of the EUFEST by Rybakowski et al. (2012) did not demonstrate a differential effect of the antipsychotic studied on depressive symptomatology.

Co-medication, especially antidepressants, could be partially responsible for the differences in efficacy. Kahn (Kahn et al., 2008) reported that a higher proportion of patients on olanzapine used antidepressants. We have analyzed the differences in co-medication between both sexes post-hoc. Only patients with co-medication were taken into consideration. Women more frequently received adjunctive treatment with specific serotonin reuptake inhibitors (42/221, 19% vs. 45/146, 30.8%, $p = 0.012$). However, no significant differences between men and women were detected in the use of antidepressants in the groups on different randomized antipsychotics in the study, including olanzapine.

Our results are subject to the limitations related to the original protocol. The EUFEST study was a pragmatic study, powered and aimed at the measurement of effectiveness, and it did not focus on the detection of gender differences. Further, there was not a reliable measurement of adherence (i.e., plasma levels monitoring) only the self-report compliance scale.

5. Conclusion

The findings support the assumption of gender differences in the decrease of psychopathology in response to treatment with different antipsychotic drugs in first-episode schizophrenia. The gender differences should be further researched. No treatment guidelines refer to gender as a potentially important factor in the choice of antipsychotics. This analysis supports the notion that they should be taken into consideration. Sensitivity to gender differences can serve specific needs of patients and perhaps improve treatment outcomes.

Role of funding source

EUFEST was funded by the European Group for Research in Schizophrenia (EGRIS) with grants from Astra Zeneca, Pfizer, and Sanofi-Aventis. As to the present study, neither EGRIS nor any sponsor had any further role in the data analysis and interpretation, in the writing of the report, or in the decision to submit the paper for publication.

Contributors

All authors participated in the conception and design of the study and in the critical revision of the manuscript, and all authors gave their final approval for publication. Ceskova analyzed and interpreted the data and drafted the manuscript. Svancara and Jarkovsky performed the statistical analysis.

Conflict of interest

EC received a speaker's honoraria from Janssen-Cilag and Angelini CR and fees for the advisory board from Janssen-Cilag, CR.

RP, JL, JS and JJ report no conflicts of interest.

Acknowledgments

This study was supported by the project CEITEC — Central European Institute of Technology (CZ.1.05/1.1.00/02.0068) from the European Regional Development Fund. The project had no role in the study design, in the data collection, in the writing of the paper, or in the decision to submit the paper.

We are grateful to Wolfgang Fleischhacker and René Kahn for providing all the EUFEST data and for their inspiring remarks.

References

Abel, K.M., Drake, R., Goldstein, J.M., 2010. Sex differences in schizophrenia. Int. Rev. Psychiatry 22, 417–428.

Bigos, K.L., Pollock, B.G., Coley, K.C., Miller Del, D., Marder, R.S., Aravagiri, M., et al., 2008. Sex, race, and smoking impact olanzapine exposure. J. Clin. Pharmacol. 48, 157–165.

Boter, H., Peuskens, J., Libiger, J., Fleischhacker, W.W., Davidson, M., Galderisi, S., Kahn, R.S., 2009. Effectiveness of antipsychotics in first-episode schizophrenia and schizophreniform disorder on response and remission: an open randomized clinical trial (EUFEST). Schizophr. Res. 115, 97–103.

Canuso, C.M., Pandini, G., 2007. Gender and schizophrenia. Psychopharmacol. Bull. 40, 178–190.

Ceskova, E., Prikryl, R., 2012. Importance of gender in the treatment of schizophrenia. Prim. Care Companion CNS Disord. 14. http://dx.doi.org/10.4088/PCC.12m01407.

Citrome, L., Stauffer, V.L., Chen, L., Kinon, B.J., Kurtz, D.L., Jacobson, J.G., Bergstrom, R.F., 2009. Olanzapine plasma concentrations after treatment with 10, 20, and 40 mg/d in patients with schizophrenia: an analysis of correlations with efficacy, weight gain, and prolactin concentration. J. Clin. Psychopharmacol. 29, 278–283.

Cotton, S.M., Lambert, M., Schimmelmann, B.G., Poley, D.L., Morley, K.I., McGorry, P.D., Conus, P., 2009. Gender differences in premorbid, entry, treatment, and outcome characteristics in a treated epidemiological sample of 661 patients with first episode psychosis. Schizophr. Res. 114, 17–24.

Damoiseaux, V.A., Proost, J.H., Jiawan, V.C., Melgert, B.N., 2014. Sex differences in the pharmacokinetics of antidepressants: influence of female sex hormones and oral contraceptives. Clin. Pharmacokinet. 53, 509–519.

Fleischhacker, W.W., Keet, I.P., Kahn, R.S., EUFEST Steering Committee, 2005. The European First Episode Schizophrenia Trial (EUFEST): rationale and design of the trial. Schizophr. Res. 78, 146–156.

Groleger, U., Novak-Grubic, V., 2010. Gender, psychosis and psychotropic drugs: differences and similarities. Psychiatr. Danub. 22, 338–342.

Kahn, R.S., Fleischhacker, W.W., Boter, H., Davidson, M., Vergowe, Y., Keet, I.P.M., et al., for the Eufest study group, 2008. Effectiveness of antipsychotic drugs in first-episode schizophrenia and schizophreniform disorder: an open randomised clinical trial. Lancet 371, 1085–1097.

Kay, S., Fiszbein, A., Opler, L.A., 1987. The positive and negative syndrome scale for schizophrenia. Schizophr. Bull. 13, 261–278.

Müller, M.J., Regenbogen, B., Sachse, J., Eich, F.X., Härtter, S., Hiemke, C., 2006. Gender aspects in the clinical treatment of schizophrenic inpatients with amisulpride: a therapeutic drug monitoring study. Pharmacopsychiatry 39, 41–46.

Raedler, T.J., Schreiner, A., Naber, D., Wiedermann, K., 2006. Gender-specific effects in the treatment of acute schizophrenia with risperidone. Pharmacopsychiatry 39, 171–174.

Rybakowski, J.K., Vansteelandt, K., Szafranski, T., Thys, E., Jarema, M., Fleischhacker, W., Kahn, R.S., Peuskens, J., EUFEST Study Group, 2012. Treatment of depression in first episode of schizophrenia: results from EUFEST. J. Eur. Neuropsychopharmacol. 22, 875–882.

Seeman, M.V., 2004. Gender differences in the prescribing of antipsychotic drugs. Am. J. Psychiatry 161, 1324–1333.

Segarra, R., Ojeda, N., Zabala, A., Garcia, J., Catalán, A., Eguiluz, J.I., Gutiérrez, M., 2011. Similarities in early course among men and women with a first episode of schizophrenia and schizophreniform disorder. Eur. Arch. Psychiatry Clin. Neurosci. 262, 95–105.

Usall, J., Suarez, D., Haro, J.M., SOHO Study Group, 2007. Gender differences in response to antipsychotic treatment in outpatients with schizophrenia. Psychiatry Res. 153, 225–231.

Xiang, Y.T., Wang, C.Y., Weng, Y.Z., Bo, Q.J., Chiu, H.F., Zhao, J.P., et al., 2010. Sex differences in patients with schizophrenia: a prospective, multi-center study. Psychiatry Res. 177, 294–298.

Zanger, U.M., Schwab, M., 2013. Cytochrome P450 enzymes in drug metabolism: regulation of gene expression, enzyme activities, and impact of genetic variation. Pharmacol. Ther. 138, 103–141.

Zhang, Y., Kim, M.J., Bertino Jr., J.S., Nafziger, A.N., Sellers, E.M., 2006. Use of omeprazole as a CYP3A probe drug: effect of sex and menstrual cycle phase on CYP3A activity in healthy Caucasian adults. J. Clin. Pharmacol. 46, 345–352.

3. Retroperitoneoscopic adrenalectomy in obese patients: is it suitable?

Zonča P, Bužga M, Ihnát P, Martínek L

Originally published in Obesity Surgery, 2015, vol. 25, no. 7, p. 1203-1208.

OBES SURG (2015) 25:1203–1208
DOI 10.1007/s11695-014-1475-8

ORIGINAL CONTRIBUTIONS

Retroperitoneoscopic Adrenalectomy in Obese Patients: Is It Suitable?

Pavel Zonča · Marek Bužga · Peter Ihnát · Lubomír Martínek

Published online: 15 November 2014

Abstract
Background The aim of this study was to evaluate the suitability of posterior retroperitoneoscopic adrenalectomy for patients with morbid obesity.
Methods This retrospective clinical cohort study included patients who underwent elective posterior retroperitoneoscopic adrenalectomy. Intraoperative (operative time, blood loss, intraoperative complications, conversion rate) and postoperative (hospital stay, morbidity, mortality) parameters were compared between the two study subgroups: obese (body mass index [BMI] ≥30 kg/m^2) and non-obese patients (BMI <30 kg/m^2).
Results A total of 137 subsequent patients were enrolled in the study (41 obese and 96 non-obese patients). Mean tumour size was 5.2±2.2 cm; aldosteronism and incidentaloma were the most frequent indications. Operative time was significantly longer (87 vs. 65 min; P=0.0006) in obese patients. There was no difference in operative blood loss. One conversion was necessary. Overall, the 30-day postoperative morbidity was significantly higher in obese patients (26.8 vs. 11.5 %; P=0.025). The hospital stay was significantly longer in obese patients (3.1 vs. 2.5 days; P=0.003).
Conclusions Dorsal retroperitoneoscopic adrenalectomy can be safely performed in morbidly obese patients, maintaining the advantages of minimally invasive surgery. Avoiding an abdominal approach is beneficial for patients. There is a more favourable postoperative course, shorter hospital stay, better cosmetic outcome and quicker recovery with dorsal retroperitoneoscopic adrenalectomy. The prolonged operative time, longer hospital stay and higher risk of postoperative complications that occurred in obese patients were acceptable in light of the generally higher risk associated with surgeries performed in obese patients.

Keywords Retroperitoneoscopic adrenalectomy · Obesity · Minimally invasive surgery · Postoperative morbidity

P. Zonča (✉) · P. Ihnát · L. Martínek
Department of Surgical Studies, Faculty of Medicine, University of Ostrava, Syllabova 19, Ostrava 703 00, Czech Republic
e-mail: pavel.zonca@fno.cz

P. Zonča · P. Ihnát · L. Martínek
Department of Surgery, University Hospital Ostrava, 17.listopadu 1790, Ostrava 70852, Czech Republic

M. Bužga
Department of Physiology and Pathophysiology, Faculty of Medicine, University of Ostrava, Syllabova 19, Ostrava 703 00, Czech Republic
e-mail: marek.buzga@osu.cz

Introduction

Laparoscopic adrenalectomy was first presented by Snow in 1991 [1], and subsequent elaboration of the technique was carried out by Gagner in 1992 [2]. Shortly after the introduction of laparoscopic adrenalectomy, the minimally invasive approach replaced traditional (open) adrenalectomy in the treatment of small benign lesions of the adrenal glands. The laparoscopic approach offers a more favourable postoperative course, shorter hospital stay, better cosmetic outcome, quicker recovery and lower costs [3, 4]. Retroperitoneoscopic adrenalectomy was proposed as an alternative to transabdominal laparoscopic adrenalectomy by Gaur [5], Mercan [6] and Mandressi [7] very shortly after Gagner's work. The technique of retroperitoneoscopic adrenalectomy, which was modified by Walz in 1995 [8], allows for an even more advantageous postoperative course by minimizing blood loss, shortening the hospital stay, facilitating the avoidance of intraperitoneal abdominal organs and enabling bilateral adrenalectomy without the necessity of changing a patient's position [9–11].

A characteristic feature of the present world population is a progressive increase in the number of obese individuals,

which is associated with many negative consequences, including a significantly higher risk of perioperative and postoperative complications [12]. Simultaneously, the development and more frequent use of imaging technology have led to an increase in the number of incidental adrenal tumours [13]. Therefore, an increased number of obese patients requiring adrenalectomy can realistically be expected.

The evaluation of treatment risks and the selection of optimal operative techniques for adrenalectomy in obese patients have become problematic in recent years [14–17]. The benefits of laparoscopic transabdominal adrenalectomy over an open approach have been unquestionably proven in obese patients; less blood loss, a more favourable postoperative course and a shorter hospital stay have been reported [15]. However, the place of retroperitoneoscopic adrenalectomy as performed in obese patients is currently ambiguous. Some authors consider obesity to be a relative contraindication to the retroperitoneoscopic dorsal approach [18, 19]. However, retroperitoneoscopic adrenalectomy is a safe procedure in patients with a body mass index (BMI) below 30 kg/m^2; with advanced technical experience, there is the potential to apply this approach in obese patients who may benefit from it. Thus, the aim of this study was to evaluate the treatment outcomes of posterior retroperitoneoscopic adrenalectomy in morbidly obese patients.

Materials and Methods

Patients and Study Design

This retrospective clinical study was performed at two institutions, the Department of Visceral and Minimally Invasive Surgery in Wesseling (Germany) and the Department of Surgery at University Hospital in Ostrava (Czech Republic). Our cohort consisted of all patients who underwent posterior retroperitoneoscopic adrenalectomy over a 5-year period.

Indications for surgery were as follows: benign, hormonally active adrenal gland tumours; hormonally inactive tumours with a diameter of more than 5 cm or with signs of progressive growth; hormonally inactive tumours with a diameter of less than 5 cm and suspicious imaging characteristics; and solitary secondary tumours of the adrenal gland. Contraindications to a posterior retroperitoneoscopic approach were tumours greater than 12 cm in diameter, tumours invading their surroundings and lesions with a pronounced risk of high malignancy according to preoperative imaging modalities. Patients with incomplete data were excluded from the study.

The following data were collected and analysed retrospectively: demographic data (age, sex), clinical data (American Society of Anaesthesiologists [ASA] classification, BMI), tumour histopathology, perioperative outcomes (operative time, complications during surgery, blood loss, conversions) and postoperative outcomes (morbidity, mortality). Postoperative complications were defined as any complications occurring within the first 30 days after surgery. Complications were assessed according to the Clavien–Dindo classification.

Two study subgroups were established: obese patients (BMI ≥30) and non-obese patients (BMI <30); all of the previously mentioned data categories were compared between the subgroups. The cut-off BMI of 30 was established in accordance with the literature [15, 17]. The primary goal of the study was the comparison of postoperative outcomes between obese and non-obese patients; the secondary goal was the comparison of perioperative characteristics.

Surgery

All patients underwent standard preparation for surgery in cooperation with endocrinologists. Surgery was performed under general anaesthesia. The technique for posterior retroperitoneoscopic adrenalectomy described by Walz [20] was employed in all operations. Patients were placed in a prone (jackknife) position (Fig. 1), with hips flexed at a 90° angle (this position allows maximization of the space between the ribs and iliac crests). A transverse incision (approximately 2 cm long) was made in the scapular line; the retroperitoneal space was reached, and a working space was prepared with the fingers. A 10-mm trocar for the camera was introduced, and a capno-retroperitoneum (up to 24 mmHg) was established. Working trocars were inserted—a 12-mm trocar from the lateral side and a 5-mm trocar paravertebrally. Under direct visual control, dissection of the retroperitoneal space (dissection of perinephritic adipose tissue, identification of the upper renal pole and dissection of the adrenal gland) was performed using ultrasonic shears. The adrenal gland was mobilized using ultrasonic shears, and middle adrenal veins were

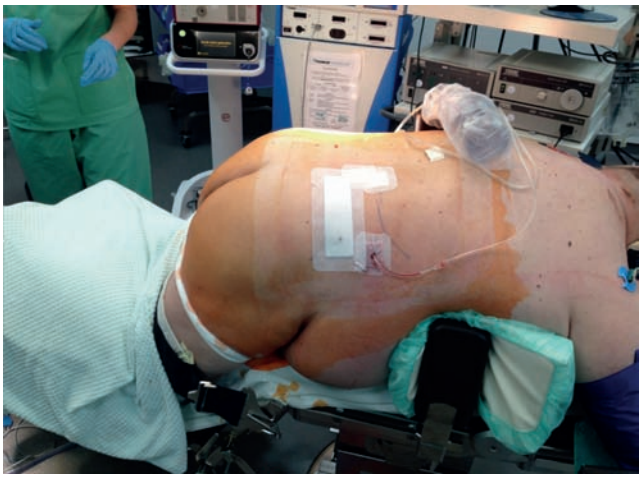

Fig. 1 Patient's operative position during retroperitoneoscopic adrenalectomy

interrupted between clips. The adrenal gland was inserted in a plastic bag and extracted through the widened incision (where the camera trocar had been). Drain was not left on the regular basis; it was an individual decision of the operating surgeon depending on the course of the surgery.

Statistical Analysis

Descriptive statistics were used for data processing. Differences between study subgroups were assessed using the *t* test, Wilcoxon (Mann–Whitney) test and Pearson's chi-squared test. All the statistical tests were evaluated at the significance level of 5 %. A *P* value of <0.05 was considered statistically significant. Statgraphics Plus 5.0 and Statistica version 8 were used for all statistical analyses.

Results

During the study period (August 2007 through March 2013), 137 subsequent patients underwent posterior retroperitoneoscopic adrenalectomy and were included in the study. There were 74 women (54 %) and 63 men (46 %) with a mean age of 52±15 years (median 51, range 16–85 years). Mean BMI was 28±3 kg/m^2 (median 28 kg/m^2, range 21–47 kg/m^2). The majority of patients (80.3 %) were preoperatively classified as ASA class I or II.

Forty-one patients (30 %) with a BMI ≥30 kg/m^2 were included in the obese patient subgroup (mean subgroup BMI of 34.1±3.5 kg/m^2). Ninety-six patients with a BMI <30 kg/m^2 were included in the non-obese patient subgroup (mean BMI 26.6±2.1 kg/m^2). The demographic and clinical characteristics of both subgroups and the results of statistical comparisons are clearly presented in Table 1.

Mean tumour size was 5.2±2.2 cm (median 4.5 cm, range 2.2–14 cm) and did not statistically differ between the study subgroups. Bilateral posterior retroperitoneoscopic adrenalectomy was performed in 12 patients (8.7 %). Indications for resection are presented in Table 1; aldosteronism and incidentaloma were the most frequent indications in the non-obese subgroup, and aldosteronism and Cushing syndrome were the most frequent indications in the obese subgroup.

Perioperative and postoperative outcomes of posterior retroperitoneoscopic adrenalectomy are summarized in Table 2. Mean operative time was 71±27 min (median 60 min, range 32–150 min) for all patients. A significantly longer operative time was recorded in the obese patient subgroup (84±30 min) compared with non-obese patients (65±24 min). The mean blood loss noted during retroperitoneoscopic adrenalectomy was 29±89 mL (median 0 mL, range 0–500 mL); there was no difference between obese and non-obese patients. Surgery with no blood loss was performed in 119 patients (87 %). We did not encounter any serious complications during posterior retroperitoneoscopic adrenalectomy in our study group. One patient required conversion to open surgery because of adhesions.

Table 1 Demographics, clinical data and tumour characteristics of the study groups

Parameter	BMI <30 (n =96)	BMI ≥30 (n =41)	p-value	Total (n =137)
Age (years, mean±SD)	51±15	53±14	*0.467*	52±15
Gender, n (%)				
Female	49 (51)	25 (61)	*0.285*	74 (54)
Male	47 (49)	16 (39)		63 (46)
BMI (kg/m^2, mean±SD)	26.6±2.1	34.1±3.5	*0.000**	28.1±3.0
ASA, n (%)				
I	36 (37.5)	5 (12.2)	*0.001**	41 (29.9)
II	48 (50)	21 (51.2)		69 (50.4)
III	12 (12.5)	15 (36.6)		27 (19.7)
Tumour size (cm, mean±SD)	5.4±2.3	4.7±1.6	*0.056*	5.2±2.2
Histopathology finding				
Aldosteronism	20 (20.8)	6 (14.6)		26 (18.8)
Cushing's disease	9 (9.4)	3 (7.3)		12 (8.8)
Virilizing adenoma	2 (2.1)	0 (0)		2 (1.5)
Pheochromocytoma	30 (31.3)	10 (24.4)		40 (29.2)
Incidentalomas	8 (8.3)	5 (12.2)		13 (9.5)
Angiomyolipoma	1 (1)	1 (2.4)		2 (1.5)
Secondary tumours	26 (27.1)	16 (39.1)		42 (30.7)

Data are expressed as mean±SD. * statistically significant. *P* values of <0.05 were considered statistically significant

Histopathology evaluation of harvested specimens (adrenal glands) revealed that there was no evidence of tumour disruption and no positive resection margins within patients in our study groups. Postoperative complications were observed within the first 30 days after surgery in 22 patients, a 16 % postoperative morbidity rate. The details of noted complications are shown in Table 2. According to the Clavien–Dindo classification [21], all detected postoperative complications were of degree I or II (less serious). Postoperative complications were noted more frequently in obese patients (26.8 vs. 11.5 %); this difference was statistically significant. The postoperative mortality was 0 % in both subgroups. The mean postoperative hospital stay was 2.7±1.1 days (median 2 days, range 1–7 days). The hospital stay was significantly longer in the obese patient subgroup.

After the surgery, follow-up of patients with adrenal gland benign tumours was done by endocrinologists. In total, there were 42 patients (30.7 %) with malignant secondary tumours of the adrenal gland in our study groups (Table 1). Follow-up of these patients was managed by a surgeon on the regular basis—clinical examination and ultrasonography each 3 months; PET/CT after 1 year. Disease recurrence (distant metastases) was detected in 4 patients during

Table 2 Perioperative and postoperative clinical outcomes

Parameter	BMI <30 (n =96)	BMI ≥30 (n =41)	p-value	Total (n =137)
Operative time (minutes, mean±SD)	65±24	84±30	*0.0006**	71±27
Operative blood loss (ml, mean±SD)	29±96	28±70	*0.939*	29±89
Conversion rate, n (%)	0 (0)	0 (0)		0 (0)
Morbidity within 30 days, n (%)	11 (11.5)	11 (26.8)	*0.025**	22 (16.0)
Wound complications (haematoma)	4 (4.2)	4 (9.7)		8 (5.8)
Urinary retention	3 (3.1)	2 (4.8)		5 (3.6)
Atelectasis	2 (2.1)	5 (12.2)		7 (5.1)
Pneumonia	2 (2.1)	0 (0)		2 (1.5)
Mortality within 30 days, n (%)	0 (0)	0 (0)		0 (0)
Hospital stay (days, mean±SD)	2.5±0.9	3.1±1.2	*0.003**	2.7±1.1

Data are expressed as mean±SD. * statistically significant. *P* values of <0.05 were considered statistically significant

the follow-up—2 patients with lung cancer and 2 patients with colorectal cancer. One of these 4 patients had to be reoperated—open transabdominal approach was performed in an effort to remove paraaortal positive lymph nodes and perivesically located tumour.

Discussion

Minimally invasive adrenalectomy is considered to be the gold standard surgical treatment for small, benign adrenal gland lesions [3, 11]. The earlier transperitoneal approach is currently being replaced with the retroperitoneoscopic approach. Despite previous concerns regarding the limited operating space and worsened surgeon's orientation in the retroperitoneum, retroperitoneoscopic adrenalectomy is overtaking the transperitoneal approach in a growing number of surgical departments worldwide. Adaptation to the technique is reported to occur after performance of 20–40 surgeries [22, 23].

The most prominent advantages of the retroperitoneoscopic approach are the direct approach to the gland (especially when the dorsal approach is used), lower number of trocars used, lower risk of injury to abdominal organs, possibility of safely performing the operation in patients after multiple previous abdominal surgeries and more favourable postoperative course [24, 25].

The retroperitoneoscopic technique can be performed though either a lateral or a dorsal approach. The ability to use higher pressures during the dorsal approach (up to 25 mmHg) enables a good view over the operative field, better haemorrhage control [20] and a shorter operative time in comparison with the lateral approach [9, 26]. A recent meta-analysis based on the results of 22 studies was performed by Constantinides et al. [11] and compared laparoscopic and retroperitoneoscopic adrenalectomies. A total of 1257 patients underwent laparoscopic adrenalectomy; the retroperitoneoscopic lateral approach was performed in 471 patients, and the retroperitoneoscopic dorsal approach was performed in 238 patients. Only 2 out of the 22 studies included in the meta-analysis were prospective and randomized. According to this meta-analysis, retroperitoneoscopic adrenalectomy produced equivalent perioperative results to the laparoscopic transperitoneal approach but was associated with a better postoperative course and significantly shortened postoperative hospital stay.

Only a few studies, with small numbers of included patients, have compared transabdominal and purely dorsal retroperitoneoscopic approaches. In a prospective randomized study, Rubinstein et al. [9] reported a significant difference only in recovery time, which was shorter following dorsal retroperitoneoscopic adrenalectomy. In a retrospective study, Berber et al. [27] observed greater blood loss and longer hospital stays in patients who underwent the transperitoneal laparoscopic approach. Lee et al. [28] reported shorter operative times and a more favourable postoperative course in patients who underwent the retroperitoneoscopic dorsal approach. In contrast, Ramacciato et al. [29] reported shorter operative times and less blood loss in association with the transabdominal approach. In a meta-analysis of 21 studies, Nigri et al. [30] did not find any differences in operative time, blood loss, postoperative course, mortality or morbidity between the transperitoneal and dorsal retroperitoneoscopic approaches. These conclusions are similar to those of Constantinides et al. [11] in the meta-analysis mentioned above.

Regarding management of possible perioperative complications, dorsal retroperitoneoscopic approach could be more difficult compared to that of the transabdominal approach. The potentially acute venous bleeding could be managed by the increased high pressure of retrocapnoperitoneum, but there is a connection to a potential gas embolization. Another option is acute tamponade of the operation field through a small incision and the change of patient's prone position to supine position. In our study group, it was not necessary to solve such complications. The reason of the only conversion in our study were adhesions; our solution was manually assisted retroperitoneoscopy.

In general, obese patients represent an expanding and high-risk group of surgical patients, particularly with respect to wound and septic complications [14]. Although BMI is surely a risk factor for conversion during laparoscopic adrenalectomy, the technique can be safely performed in obese patients [18], maintaining the advantages of minimally invasive surgery such as a better postoperative course and quicker recovery [15]. An increasing number of published reports have described dorsal retroperitoneoscopic adrenalectomies performed in obese patients, with good tolerance of the prone position [16, 17, 31]. Fazeli-Matin et al. [15] prefer the retroperitoneoscopic approach in obese patients, while Agha et al. [19] recommend the lateral retroperitoneoscopic approach in patients with a BMI over 35 kg/m^2. Dickson et al. [32] advise a careful retroperitoneoscopic approach in obese patients, but these authors successfully performed the technique in 8 patients with a BMI over 40 kg/m^2. Aksoy et al. [17], in performing robotic adrenalectomy, prefer a dorsal retroperitoneoscopic approach for tumours less than 6 cm in diameter but advise a transperitoneal approach for larger tumours.

In our study, obese patients (BMI over 30 kg/m^2) represented one third of the entire study group, which corresponds with the obesity prevalence in the population of the Czech Republic and Germany. The subgroups were comparable with respect to demographic data (age, sex) and tumour characteristics (size, histology), although we observed a tendency for smaller tumours to occur more frequently in the obese patient subgroup. A greater number of higher ASA classification patients were observed in the obese patient subgroup, which corresponds with the supposedly higher comorbidity of obese patients. The significantly longer operative time observed in obese patients resulted from the more difficult orientation in excessive retroperitoneal adipose tissue and the worsened manipulation with laparoscopic instruments through the thick layer of subcutaneous fat. The operative times recorded for our subgroups were comparable to previously published results, in which the operative times for retroperitoneoscopic adrenalectomy in non-selected patients were reported to have a range of 45–248 min [31].

In our study, conversion to an open approach occurred in 1 patient (0.7 %), which is in line with the reported conversion rate of 0–36 % in the published literature (1–22 % for the transperitoneal approach, 2–14 % for the dorsal retroperitoneoscopic approach and 4–36 % for the lateral retroperitoneoscopic approach) [11]. The postoperative complications observed in our study group were not serious (all were classified as degree I or II according to the Clavien–Dindo classification), and they were managed without any surgical intervention, radiological intervention or intensive care. Postoperative morbidity was higher in the obese patient subgroup; this difference was statistically significant. The higher frequency of postoperative complications in obese patients corresponds with other recently published data [11]. Subcostal nerve injury is a possible complication after posterior retroperitoneoscopic adrenalectomy as a consequence of the pressure of subcostally located trocar on the ribs. The pain is usually temporary. We have noted subcostal pain in 8 patients (5.8 %) 1 month after the surgery. Six months after the surgery, patients were without subcostally located pain, but intermittent vertebral pain was observed. The clear connection between vertebral pain and surgery was unambiguous.

The length of the postoperative hospital stay was significantly longer in the obese patient subgroup, which might have resulted from the higher number of postoperative complications and the lower ability of obese patients to recover from surgery. However, our results contrast with those of Kazaure et al. [13], who did not identify a longer postoperative stay after adrenalectomy in obese patients.

To the best of our knowledge, this study is the first among the available literature to focus on dorsal retroperitoneoscopic adrenalectomy in obese patients. The limitation of our study is its non-randomized, retrospective design.

Conclusion

Dorsal retroperitoneoscopic adrenalectomy can be safely performed in morbidly obese patients, maintaining the advantages of minimally invasive surgery. Avoiding the abdominal approach is beneficial for patients, particularly for the obese population. The prolonged operative time and postoperative hospital stay, in addition to the higher risk of postoperative complications, that occurred in obese patients were acceptable in accordance with the generally higher risks and worsened results associated with surgeries in obese patients.

Ethical Approval All procedures performed in the study were in accordance with the ethical standards of the University hospital and Faculty of Medicine, University of Ostrava, Czech Republic, in accordance with the ethical standards of the Helsinki Declaration of 1975, as revised in 2000. For this type of study, formal consent is not required.

Conflict of Interest Dr. Zonča, Dr. Bužga, Dr. Ihnát and Dr. Martínek do not have a conflict of interest. The authors are all independent from funders. The sponsors had no influence in the writing of the manuscript. No other relationships or activities exist that could appear to have influenced the submitted work.

References

1. Snow LL. Endoscopic general surgery: an update. Laser Highlights. 1991;2:1–3.
2. Gagner M, Lacroix A, Bolte E. Laparoscopic adrenalectomy in Cushing's syndrome and pheochromocytoma. N Engl J Med. 1992;327:1033.
3. Smith CD, Weber CJ, Merson JR. Laparoscopic adrenalectomy: a new gold standard. World J Surg. 1999;23:389.

4. Zacharias M, Haese A, Jurczok A, et al. Transperitoneal laparoscopic adrenalectomy: outline of the preoperative management, surgical approach, and outcome. Eur Urol. 2006;49:448–59. doi:10.1016/j.eururo.2006.01.014.
5. Gaur DD. Laparoscopic operative retroperitoneoscopy: use of a new device. J Urol. 1992;148:1137–9.
6. Mandressi A, Buizza C, Antonelli D, et al. Retroperitoneoscopy. Ann Urol (Paris). 1995;29:91–6.
7. Mercan S, Seven R, Ozarmagan S. Endoscopic retroperitoneal adrenalectomy. Surgery. 1995;118:1071–5.
8. Walz MK, Peitgen K, Krause U, et al. Die dorsale Adrenalektomie – eine operative Technik. Zentralbl Chir. 1995;120:53–8.
9. Rubinstein M, Gill IS, Aron M, et al. Prospective, randomized comparison of transperitoneal versus retroperitoneal laparoscopic adrenalectomy. J Urol. 2005;174:442–5. doi:10.1097/01.ju.0000165336.44836.2d.
10. Mazzaglia PJ, Vezeridis MP. Laparoscopic adrenalectomy: balancing the operative indications with the technical advances. J Surg Oncol. 2010;101:739–44. doi:10.1002/jso.21565.
11. Constantinides VA, Christakis I, Touska P, et al. Systematic review and meta-analysis of retroperitoneoscopic versus laparoscopic adrenalectomy. Br J Surg. 2012;99:1639–48. doi:10.1002/bjs.8921.
12. Pierpont YN, Dinh TP, Salas RE, et al. Obesity and surgical wound healing: a current review, ISRN Obesity Volume 2014, Article ID 638936, 13 pages, doi.10.1155/2014/638936.
13. Kazaure HS, Roman SA, Sosa JA. Obesity is a predictor of morbidity in 1,629 patients who underwent adrenalectomy. World J Surg. 2011;35:1287–95. doi:10.1007/s00268-011-1070-2.
14. Muth A, Taft C, Hammarstedt L, et al. Patient-reported impacts of a conservative management programme for the clinically inapparent adrenal mass. Endocrine. 2013;44:228–36. doi:10.1007/s12020-012-9856-z. mPublished online Dec 20, 2012.
15. Fazeli-Matin S, Gill IS, Hsu TH, et al. Laparoscopic renal and adrenal surgery in obese patients: comparison to open surgery. J Urol. 1999;162:665–9. doi:10.1097/00005392-199909010-00005.
16. Varela E. Retroperitoneoscopic adrenalectomy for pheochromocytoma in morbidly obese. Obes Surg. 2009;19:1180–2. doi:10.1007/s11695-009-9805-y.
17. Aksoy E, Taskin HE, Aliyev S, et al. Robotic versus laparoscopic adrenalectomy in obese patients. Surg Endosc. 2013;27:1233–6. doi:10.1007/s00464-012-2580-1.
18. Shen ZJ, Chen SW, Wang S, et al. Predictive factors for conversion of laparoscopic adrenalectomy: a 13-year review of 456 cases. J Endourol. 2007;21:1333–7. doi:10.1089/end.2006.450.
19. Agha A, Breitenbuch P, Gahli N, et al. Retroperitoneoscopic adrenalectomy: lateral versus dorsal approach. J Surg Oncol. 2008;97:90–3. doi:10.1002/jso.20793.
20. Walz MK, Peitgen K, Walz MV, et al. Posterior retroperitoneoscopic adrenalectomy: lessons learned within five years. World J Surg. 2001;25:728–34. doi:10.1007/s00268-001-0023-6.
21. Dindo D, Demartines N, Clavien PA. Classification of surgical complications: a new proposal with evaluation in a cohort of 6336 patients and results of a survey. Ann Surg. 2004;240:205–13. doi:10.1097/01.sla.0000133083.54934.ae.
22. Guerrieri M, Campagnacci R, De Sanctis A, et al. The learning curve in laparoscopic adrenalectomy. J Endocrinol Investig. 2008;31:531–6.
23. Schreinemakers JM, Kiela GJ, Valk GD, et al. Retroperitoneal endoscopic adrenalectomy is safe and effective. Br J Surg. 2010;97:1667–72. doi:10.1002/bjs.7191.
24. Lin Y, Li L, Zhu J, et al. Experience of retroperitoneoscopic adrenalectomy in 195 patients with primary aldosteronism. Int J Urol. 2007;14:910–3. doi:10.1111/j.1442-2042.2007.01860.x.
25. Zhang X, Fu B, Lang B. Technique of anatomical retroperitoneoscopic adrenalectomy with report of 800 cases. J Urol. 2007;177:1254–7. doi:10.1016/j.juro.2006.11.098.
26. Suzuki K. Laparoscopic adrenalectomy: retroperitoneal approach. Urol Clin N Am. 2001;28:85–95.
27. Berber E, Tellioglu G, Harvey A, et al. Comparison of laparoscopic transabdominal lateral versus posterior retroperitoneal adrenalectomy. Surgery. 2009;146:621–5. doi:10.1016/j.surg.2009.06.057.
28. Lee CR, Walz MK, Park S, et al. A comparative study of the transperitoneal and posterior retroperitoneal approaches for laparoscopic adrenalectomy for adrenal tumors. Ann Surg Oncol. 2012;19:2629–34. doi:10.1245/s10434-012-2352-0.
29. Ramacciato G, Nigri GR, Petrucciani N, et al. Minimally invasive adrenalectomy: a multicenter comparison of transperitoneal and retroperitoneal approaches. Am Surg. 2011;77:409–16.
30. Nigri G, Rosman AS, Petrucciani N, et al. Meta-analysis of trials comparing laparoscopic transperitoneal and retroperitoneal adrenalectomy. Surgery. 2013;153:111–9. doi:10.1016/j.surg.2012.05.042.
31. Zonča P, Cambal M, Labas P, et al. Retroperitoneoscopic adrenalectomy with dorsal approach. Rozhl Chir. 2012;91:235–40.
32. Dickson PV, Jimenez C, Chisholm GB, et al. Posterior retroperitoneoscopic adrenalectomy: a contemporary American experience. J Am Coll Surg. 2011;212:659–65. doi:10.1016/j.jamcollsurg.2010.12.023.

4. The impact of standard protocol implementation on the quality of colorectal cancer pathology reporting

Ihnát P, Delongová P, Horáček J, Ihnát Rudinská L, Vávra P, Zonča P

Originally published in World Journal of Surgery, 2015, vol. 39, no. 1, p. 259-265.

World J Surg (2015) 39:259–265
DOI 10.1007/s00268-014-2796-4

World Journal of Surgery

ORIGINAL SCIENTIFIC REPORT

The Impact of Standard Protocol Implementation on the Quality of Colorectal Cancer Pathology Reporting

Peter Ihnát · Patricie Delongová · Jaroslav Horáček · Lucia Ihnát Rudinská · Petr Vávra · Pavel Zonča

Published online: 19 September 2014

Abstract

Background The aim of the study is to assess the influence of standardized protocol implementation on the quality of colorectal cancer histopathology reporting.

Methods A standardized protocol was created based on the recommendations of The College of American Pathologists. The impact of this protocol was measured by comparing frequencies of assessed parameters in histopathology reports before and after implementation.

Results In total, 177 histopathology reports were included in this study. The numbers of harvested lymph nodes were 12.4 ± 5.2 (colon) and 12.6 ± 5.4 (rectum) before protocol; and 17.1 ± 6.5 (colon), and 16.6 ± 7.0 after protocol implementation; differences were statistically significant. The recommended minimum of 12 lymph nodes was not achieved in 42.8 % (colon) and 45.7 % (rectum) of specimens before, and in 10.4 % (colon) and 17.7 % (rectum) of specimens after protocol implementation; differences were statistically significant. There were no differences in histopathology assessment of proximal and distal resection margins, grading assessment, TNM staging recording, and number of positive findings of microscopic tumor aggressiveness. The findings of tumor budding, tumor satellites, and assessment of microscopic tumor aggressiveness were more frequent after protocol implementation. Histopathology reports of rectal specimens contained assessments of the macroscopic quality of mesorectum, circumferential resection margin, and neoadjuvant therapy effect (if administered) only after protocol introduction.

Conclusions A standardized protocol is a valuable and effective tool for improving the quality of histopathology reporting. Its implementation is associated with more precise specimen evaluation, higher numbers of harvested lymph nodes, and improved completeness of histopathology reports.

Introduction

Histopathological evaluation of colorectal cancer specimens is a critical component of patient management in the postoperative period. It determines the adequacy and quality of surgical resection, indicates the requirement for adjuvant therapy, and determines prognosis [1–3]. Of many parameters included in the histopathology report, the most powerful tools for assessing prognosis are the depth of tumor invasion,

P. Ihnát (✉) · P. Vávra · P. Zonča
Department of Surgical Studies, Faculty of Medicine, University of Ostrava, Syllabova 19, Zábřeh, 703 00 Ostrava, Czech Republic
e-mail: peterihnat@yahoo.com

P. Ihnát · P. Vávra · P. Zonča
Department of Surgery, University Hospital Ostrava, Ostrava, Czech Republic

P. Delongová · J. Horáček · L. Ihnát Rudinská
Department of Pathology, University Hospital Ostrava, Ostrava, Czech Republic

P. Delongová · J. Horáček · L. Ihnát Rudinská
Department of Pathology and Forensic Medicine, Faculty of Medicine, University of Ostrava, Ostrava, Czech Republic

the number of harvested/positive lymph nodes, and positive/negative status of resected margins [1–4].

Detailed specimen examination and retrieval of as many lymph nodes as possible is essential to provide an accurate prognosis. A minimum of 12 harvested lymph nodes for colorectal cancer is recommended by all current guidelines [1, 5, 6]. However, several population-based studies have reported that an inadequate number of lymph nodes are examined in a high portion of patients [7–10].

The College of American Pathologists has developed a proposal of a standardized protocol for the evaluation of specimens from patients with primary carcinoma of the colon and rectum [5]. The protocol was created in an effort to assist pathologists in providing higher quality specimen examination and reporting.

The aim of this study is to assess if the implementation of a standardized protocol for the evaluation of colorectal cancer specimens improves the completeness and quality of histopathology reporting.

Materials and methods

A standardized histopathology protocol for the assessment of colorectal cancer specimens was created on the basis of recommendations from The College of American Pathologists [5], and in accordance with the National Comprehensive Cancer Network (NCCN) guidelines for colorectal cancer. The protocol involves reporting histopathology data pertaining to the precise macroscopic evaluation of the specimen, detailed microscopic examination, and the 7th edition tumor, node, metastasis (TNM) staging system (Table 1). The standardized protocol was introduced into clinical practice in the University Hospital Ostrava on January 1, 2013.

Prior to standard protocol implementation, short multidisciplinary meeting (for colorectal surgeons, radiologists, clinical oncologists, and pathologists) was organized. The adherence to NCCN guidelines for colorectal cancer (and its importance) was emphasized, and standard protocol for histopathology reporting was introduced. Head of pathology department asked all pathologists to examine each colorectal specimen with regard to all parameters within the protocol. Completion of all standard protocol parameters was stated as imperative. In an effort to create ideal conditions, all pathologists were assured and offered enough time for precise examination of each specimen. After introduction, histopathological evaluation of all colorectal cancer specimens was performed using the standardized protocol.

All colorectal resections were performed by a surgical team comprised of five experienced colorectal surgeons. Surgical resection technique has not changed during the study. Great emphasis was put on achieving negative resections margins and on providing colorectal cancer specimens with sufficient lymph nodes for examination. Surgeons were employing technique of Total Mesorectal Excision (TME) during rectal resections and technique of Complete Mesocolic Excision (CME) during colon resections.

Table 1 Features recorded in standardized histopathology protocol for colorectal cancer specimen examination

Macroscopic evaluation
Tumor localisation and type of surgical procedure
Specimen dimensions (cm)
Tumor dimension (cm)
Macroscopic tumor perforation
Macroscopic quality mesorectum
Minimal distance of tumor from
Distal resection margin
Proximal resection margin
Circumferential resection margin
Microscopic evaluation
Histologic type of tumor
Degree of tumor differentiation (grading)
Evaluation of neoadjuvant treatment effect
Lymph-vascular invasion
Perineural invasion
Tumor deposits (satellites)
Tumor „budding“
Lymphocyte infiltration of the tumor
Pathologic disease staging (pTNM)
Primary Tumor (pT)
Regional Lymph Nodes (pN)
Number of harvested lymph nodes
Number of positive lymph nodes
Distant Metastasis (pM)
Results of molecular–genetic examination (KRAS, BRAF etc.)

For the purposes of this study, histopathology reports from all colorectal resection specimens in our institution from 2012 and 2013 were identified and assessed for study eligibility. The inclusion criterion was resected colon or rectal carcinoma in the study period (January 1, 2012 to December 31, 2013, inclusive). The exclusion criterion was rectal carcinoma resection by means of operative rectoscope (transanal endoscopic microsurgery), because lymphadenectomy is not routinely performed during this procedure, and well-differentiated neuroendocrine neoplasms (carcinoid tumors).

The study design does not require randomization. Approval from the local ethical committee was acquired. The primary goal of the study was to evaluate the influence of a standardized histopathology protocol on the quality of

histopathology reporting by means of comparing frequencies of reported parameters (such as number of lymph nodes, assessment of macroscopic quality of mesorectum, and resection margins reporting) before and after protocol implementation.

Histopathology reports of all included patients were analyzed. Acquired data were statistically analyzed using descriptive statistics, *t* test, Wilcoxon (Mann–Whitney) test, Pearson's χ^2 test, and Fisher's exact test. Statistical tests were evaluated at a significance level of 5 %.

Results

During the study period, 177 patients (67 women, 110 men) who underwent colorectal cancer resection in the University Hospital Ostrava were included in this comparative study. In 2013, colorectal cancer specimens were evaluated using the standardized protocol (48 colon and 45 rectal specimens). In 2012, specimens were evaluated without this protocol, and instead evaluated according to former traditions and practices of the pathology department (49 colon and 35 rectal specimens).

Demographics, clinical data, and statistical testing of differences between the study groups are summarized in Table 2. Both groups had similar demographic data (age and gender) and were comparable with regard to body mass index (BMI) and tumor location. There were no statistical differences between any of these aforementioned characteristics (p value >0.05). Histopathology reports included in the study underwent detailed analysis. Frequencies of all followed parameters before and after protocol implementation, as well as statistical testing of noted differences, are clearly presented in Table 3 (colon cancer specimens) and Table 4 (rectal cancer specimens).

The number of harvested lymph nodes in colon cancer specimens was 12.4 ± 5.2 in 2012 (before protocol implementation) and 17.1 ± 6.5 in 2013 (after protocol implementation). The number of lymph nodes in rectal cancer specimens was 12.6 ± 5.4 in 2012, and 16.6 ± 7.0 in 2013. Differences were statistically significant for both colon and rectal specimens (p value <0.05).

A minimum of 12 resected lymph nodes was not achieved in 21 (42.8 %) colon specimens in 2012, and in 5 (10.4 %) colon specimens in 2013. Similarly, this minimum was not achieved in 16 (45.7 %) rectal specimens in 2012, and in 8 (17.7 %) rectal specimens in 2013 after protocol implementation; these differences were statistically significant for both colon and rectal specimens (p value <0.05).

The workup of mesenteric fat has not changed before and after protocol introduction. No special methods like lymph node revealing solutions were used to increase lymph node harvest. The fat of colorectal specimens with small numbers of harvested lymph nodes had never been re-evaluated before protocol implementation. After protocol implementation, the fat had been re-evaluated (due to colorectal surgeon's request) in 24 out of 93 specimens (25.8 %). Assessment of the macroscopic quality of mesorectum was not done in 2012; after protocol implementation it was done for 39 (86.6 %) rectal specimens. There were 22 specimens (56.4 %) evaluated by pathologists as *complete excision*, 6 specimens (15.4 %) evaluated as *nearly complete excision*, and 11 specimens (28.2 %) evaluated as *incomplete excision*. Specimens evaluated as *incomplete excision* were noticed more frequently after APR (abdominoperinal resection) than after LAR (low anterior resection).

Table 2 Demographics and clinical data of the study groups

Parameter	2012 (n = 84)	2013 (n = 93)	p value	Total (n = 177)
Age (years, mean ± SD)	66.8 ± 10.1	66.6 ± 10.4	0.645	66.7 ± 10.2
Gender, n (%)				
Female	29 (34.5)	38 (40.9)	0.385	67 (37.9)
Male	55 (65.5)	55 (59.1)		110 (62.1)
BMI (kg/m^2, mean ± SD)	27.7 ± 4.5	27.6 ± 4.4	0.823	27.6 ± 4.4
Tumor location, n (%)				
Right colon	25 (29.7)	25 (26.9)	0.665	50 (28.2)
Left colon	24 (28.6)	23 (24.7)		47 (26.6)
Rectum	35 (41.7)	45 (48.4)		80 (45.2)

All colorectal specimens from both study groups were assessed with regard to proximal and distal resection margins (every histopathology report contained data pertaining to the positivity/negativity of the proximal and distal resection margins). Circumferential resection margin (CRM) was not assessed in rectal specimens in 2012, but in 2013 CRM was evaluated in 42 (93.3 %) rectal specimens. Of these 42 rectal specimens assessed in 2013, the CRM was positive in 7 cases (15.5 %).

Grading (degree of tumor differentiation) and TNM staging were recorded in all histopathology reports before and after protocol implementation. Assessment of microscopic tumor aggressiveness (intravascular invasion and perineural growth) was recorded in histopathology reports more frequently after protocol introduction. Intravascular invasion assessment was done in 68.7 % (protocol used) versus 44.9 % (protocol not used) of colon cancer cases, and in 84.4 % (protocol used) versus 42.8 % (protocol not used) of rectal cancer cases. Perineural growth assessment was performed in 35.4 % (protocol used) versus 18.3 % (protocol not used) of colon cancer specimens, and in

Table 3 Summary of pathology reports analysis (COLON cancer specimens)

Parameter	Protocol not used (year 2012) ($n = 49$)	Protocol used (year 2013) ($n = 48$)	p value
Number of harvested lymph nodes (mean ± SD)	12.4 ± 5.2	17.1 ± 6.5	<0.001*
Less than 12 lymph nodes in specimen, n (%)	21 (42.8)	5 (10.4)	<0.001*
Proximal and distal resection margins			
Assessment, n (%)	49 (100)	48 (100)	–
Positivity, n (%)	0 (0)	0 (0)	
Grading assessment, n (%)	49 (100)	48 (100)	–
TNM stage noted, n (%)	49 (100)	48 (100)	–
Intravasc. invasion			
Assessment, n (%)	22 (44.9)	33 (68.7)	0.018*
Positivity, n (%)	9 (18.3)	8 (16.6)	0.826
Perineural growth			
Assessment, n (%)	9 (18.3)	17 (35.4)	0.058
Positivity, n (%)	2 (4.1)	2 (4.1)	1.000
Tumor budding or satellites, n (%)	4 (8.1)	7 (14.6)	0.356
Cancer stage, n (%)			
I	11 (22.5)	12 (25.0)	0.270
II	20 (40.8)	11 (22.9)	
III	12 (24.5)	18 (37.5)	
IV	6 (12.2)	7 (14.6)	

* Statistically significant

Table 4 Summary of pathology reports analysis (RECTAL cancer specimens)

Parameter	Protocol not used (year 2012) ($n = 35$)	Protocol used (year 2013) ($n = 45$)	p value
Number of harvested lymph nodes (mean ± SD)	12.5 ± 5.4	16.6 ± 7.0	0.002*
Less than 12 lymph nodes in specimen, n (%)	16 (45.7)	8 (17.7)	0.007*
Assessment of macroscopic quality of mesorectum, n (%)	0 (0)	39 (86.6)	–
Proximal and distal resection margins			
Assessment, n (%)	35 (100)	45 (100)	–
Positivity, n (%)	2 (5.7)	3 (6.6)	1.000
Circumferential resection margin			
Assessment, n (%)	0 (0)	42 (93.3)	–
Positivity, n (%)	0 (0)	7 (15.5)	–
Grading noted, n (%)	35 (100)	45 (100)	–
TNM stage noted, n (%)	35 (100)	45 (100)	–
Intravasc. invasion			
Assessment, n (%)	15 (42.8)	38 (84.4)	< 0.001*
Positivity, n (%)	6 (17.1)	8 (17.7)	0.941
Perineural growth			
Assessment, n (%)	11 (31.4)	32 (71.1)	< 0.001*
Positivity, n (%)	3 (8.5)	6 (13.3)	0.724
Tumor budding or satellites, n (%)	2 (5.7)	11 (24.4)	0.032*
Effect of neoadjuvant therapy assessment, n (%)	0 (0)	17 (100)	
Cancer stage, n (%)			
I	5 (14.3)	7 (15.5)	0.211
II	17 (48.6)	13 (28.9)	
III	9 (25.7)	21 (46.7)	
IV	4 (11.4)	4 (8.9)	

* Statistically significant

71.1 % (protocol used) versus 31.4 % (protocol not used) of rectal cancer specimens. The frequency of findings representative of microscopic tumor aggressiveness (intravascular invasion and perineural growth) were very similar before and after protocol implementation for both colon and rectal cancer specimens. Positive microscopic findings of tumor budding or tumor satellites were noted more frequently in histopathology reports after protocol introduction; the frequency rose from 8.1 to 14.6 % in colon cases, and from 5.7 to 24.4 % in rectal cases. Both changes were statistically significant (p value <0.05).

There were 12 patients in 2012 and 17 patients in 2013 who received neoadjuvant chemoradiotherapy (which strongly influences number of harvested lymph nodes). Out of these patients, 9 patients in 2012 and 5 patients in 2013 had less than 12 lymph nodes harvested. The effect of neoadjuvant therapy was not assessed in any rectal specimens in 2012. After protocol implementation, it was assessed for all rectal specimens that underwent neoadjuvant therapy; one complete response (no residual tumor) had been observed.

Analysis of cancer stages before and after protocol implementation revealed very similar numbers of stage I and stage IV tumors. There were more stage III and less stage II tumors after protocol implementation. This fact was observed for both—colon and rectal cancer specimens. However, the differences were not statistically significant (p value >0.05).

Discussion

The correlation between the number of harvested colorectal lymph nodes from patients with colorectal cancer and prognosis has been demonstrated in many studies [1, 2, 4, 11, 12]. This link is the main reason why there is an intense effort to obtain the maximum possible number of lymph nodes from each colorectal specimen in clinical practice. Many professional healthcare organizations, such as the American College of Surgeons, NCCN, American Society of Clinical Oncology, have acknowledged the number of harvested lymph nodes as an important measure of cancer care quality [4].

The number of lymph nodes that are harvested is influenced by many factors, which can be divided into patient-related factors and factors related to cancer care management. The impact of patient-related factors, such as a patient's age, gender, the size of the tumor, and tumor site (colon or rectum), on the number of harvested lymph nodes has been demonstrated in recent studies [3, 4, 8, 13, 14].

Apart from patient-related factors, the number of retrieved lymph nodes depends on cancer care management factors, including the use of neoadjuvant therapy, the extent of the surgical dissection, and the precision of the pathologist's examination of the specimen. Undoubtedly, the extent of the surgical dissection directly affects patient prognosis; the surgeon has to perform a radical surgical resection with the intention of achieving negative resection margins and to provide the pathologist with sufficient lymph nodes for examination.

The completeness and precision of specimen assessment by the pathologist is another key factor of cancer care management. It is for these reasons why several techniques have been described to increase lymph node harvest, such as fat clearance using xylene and alcohol or lymph node revealing solutions [1, 11]. According to the results of our study, implementing a standardized pathology protocol can be a very effective and valuable method for augmenting these efforts.

Although standard protocol does not give any technical advice, higher numbers of harvested lymph nodes after protocol implementation in our institution were probably a consequence of several factors: more time allowed for each specimen examination; more precise examination (pathologists evaluated several new parameters after protocol implementation such as CRM, effect of neoadjuvant treatment, and tumor deposits); re-evaluation of specimens with low numbers of harvested lymph nodes; and enforcement of the protocol implementation by head of pathology department.

Patients with stage II or III colorectal carcinoma and a low number of harvested lymph nodes have shorter survival and a higher risk of cancer recurrence [2, 11, 12, 15]. The association between patient survival and the number of harvested lymph nodes is the outcome of several factors, the most prominent being the concept of stage migration (also called Will Rogers phenomenon).

In 1985, Fenstein et al. described the principle of stage migration as patient relocation into a more accurate disease category as a consequence of the identification of previously unrecognized metastatic disease using improved methods or techniques [16]. Stage migration resulting from better pathology reporting or improved surgical techniques consequently leads to better patient prognosis.

There were more stage III and less stage II tumors after protocol implementation in our study (for both—colon and rectal cancer specimens). As a consequence, higher numbers of patients received adjuvant therapy (chemo or chemoradiotherapy) after protocol implementation. Although the difference was not statistically significant, slightly better long-term outcome could be expected after standard protocol implementation.

On the basis of the aforementioned stage migration concept, Sarli et al. suggested routine postoperative chemotherapy in all patients with stage II colorectal cancer and a low number of harvested lymph nodes [11]. Miller at el. pointed out the fact that patients treated at low-volume centers usually have a lower number of harvested lymph nodes compared with patients from high-volume centers [17]. These patients are therefore at an obvious risk of having their disease under-staged.

A very wide range of mean harvested lymph nodes from colorectal cancer specimens is reported in published studies. Although several authors proclaim average findings of 16 or 18 lymph nodes in specimens [3, 18], many other authors report low numbers of harvested lymph nodes [2, 8, 9, 14, 19].

The mean number of harvested lymph nodes in our study appeared sufficient even prior to implementation of the standard protocol implementation, as we routinely examined more than 12 for both colon and rectal specimens. However, the increase in mean lymph nodes harvested after protocol implementation (17.1 ± 6.5 lymph nodes from colon and 16.6 ± 7.0 nodes from rectal specimens) was statistically significant. This improvement indicates that using a standardized protocol helps to increase the number of lymph nodes resected and allows for more precise examination of colorectal specimens.

Despite satisfactory mean numbers of lymph nodes resected before protocol implementation, the situation was still not ideal, owing to the fact that some patients had fewer than 12 lymph nodes harvested; before protocol introduction, almost half of our patients had an insufficient number of lymph nodes harvested (42.8 % of patients with colon cancer and 45.7 % of patients with rectal cancer). After protocol implementation, an insufficient number of lymph nodes harvested was found in only 10.4 % of colon

specimens and 17.7 % of rectal specimens. This statistically significant improvement can surely be regarded as the most important benefit of standardized protocol introduction in our institution.

The positive association between standardized protocol implementation and higher numbers of harvested lymph nodes has been previously reported by Buchwald et al. The authors registered an average finding of 14.7 lymph nodes before and 16.8 lymph nodes after protocol implementation [18]. Similarly, Beattie et al. reported average findings of eight lymph nodes before, and 12 lymph nodes after protocol implementation [19].

Evaluation of the macroscopic quality of mesorectum and CRM examination were not done in our institution before standardized protocol implementation. This is in stark contradiction with the recommendations of all available guidelines, because both parameters are considered to be gold standards for histopathology evaluation of rectal cancer specimens. Protocol implementation helped us establish evaluation of mesorectal quality and CRM in all rectal carcinoma specimens.

CRM examination is fundamental in rectal carcinoma management, because it is the single most accurate prognostic factor in local recurrence prediction, and a very important factor for predicting distant metastasis development and patient survival [20–22]. Moreover, CRM evaluation offers precious feedback to the operating surgeon regarding the quality of the total mesorectal excision, and to radiologists concerning the accuracy of preoperative CRM estimation [23].

Recommendations for colorectal cancer management are based on radical tumor removal with negative resection margins and adequate regional lymph node dissection. From a critical perspective, many patients in our institution before protocol introduction were managed without observing these two main principles: assessment of surgical radicality was insufficient (because we did not perform CRM assessment) and almost half of our patients had an insufficient number of lymph nodes examined. Standardized protocol introduction led to major improvements in adhering to both of the aforementioned principles. Therefore, we appraise it as very valuable and effective tool for improving the quality of cancer care.

In conclusion, the implementation of a standardized histopathology protocol results in more precise evaluation of colorectal cancer specimens, higher numbers of harvested lymph nodes, improved completeness of information obtained, and higher quality histopathology reports. These characteristic are obvious prerequisites for more accurate disease staging, correct indications of consequent treatment, and improved survival of patients with colorectal cancer.

Acknowledgments The authors thank medical statistician Ing. Hana Tomášková, Ph.D, for helping with the statistical analysis.

Conflict of interest The authors declare that they have no conflict of interest.

References

1. Rojo A, Sancho P, Alonso O et al (2010) Update on the surgical pathology standards on rectal cancer diagnosis, staging and quality assessment of surgery. Clin Trans Oncol 12:431–436
2. Jestin P, Pahlman L, Glimelius B et al (2005) Cancer staging and survival in colon cancer is dependent on the quality of the pathologists specimen examination. Eur J Cancer 41:2071–2078
3. Shen SS, Haupt BX, Ro JY et al (2009) Number of lymph nodes examined and associated clinicopathologic factors in colorectal carcinoma. Arch Pathol Lab Med 133:781–786
4. Chang GJ, Rodriguez-Bigas MA, Skibber JM et al (2007) Lymph node evaluation and survival after curetive resection of colon cancer: systematic review. J Natl Cancer Inst 99(6):433–441
5. Washington MK, Berlin J, Branton P et al (2009) Protocol for the examination of specimens from patients with primary carcinoma of the colon and rectum. Arch Pathol Lab Med 133:1539–1551
6. Goldstein NS (2002) Lymph node recoveries from 2427 pT3 colorectal resection specimens spanning 45 years. Recommendations for a minimum number of recovered lymph nodes based on predictive probabilities. Am J Surg Pathol 26:179–189
7. Bull AD, Biffin AH, Mella J et al (1997) Colorectal cancer pathology reporting: a regional audit. J Clin Pathol 50:138–142
8. Baxter NN, Virnig DJ, Rothenberger DA et al (2005) Lymph node evaluation in colorectal cancer patients: a population-based study. J Natl Cancer Inst 97:219–225
9. Dušek M, Chlumská A, Mukenšnabl P et al (2013) Examination of lymph nodes in resected colon segments with colorectal carcinoma. Rozhl Chir 92:250–254
10. Lemmens VE, Verheij CD, Janssen-Heijnen ML et al (2006) Mixed adherence to clinical practice guidelines for colorectal cancer in the Southern Netherlands in 2002. Eur J Surg Oncol 32:168–173
11. Sarli L, Bader G, Iusco D et al (2005) Number of lymph nodes examined and prognosis of TNM stage II colorectal cancer. Eur J Cancer 41:272–279
12. Kim YW, Kim NK, Min BS et al (2009) The influence of the number of retrieved lymph nodes on staging and survival in patients with stage II and III rectal cancer undergoing tumor-specific mesorectal excision. Ann Surg 249:965–972
13. Ostadi MA, Harnish JL, Stegienko S et al (2007) Factors affecting the number of lymph nodes retrieved in ciolorectal cancer specimens. Surg Endosc 21:2142–2146
14. Johnson PM, Malatjalian D, Porter GA (2002) Adequacy of nodal harvest in colorectal cancer: a consecutive cohort study. J Gastrointest Surg 6(6):883–888
15. Namm J, Ng M, Roy-Chowdhury S et al (2008) Quantitating the impact of stage migration on staging accuracy in colorectal cancer. J Am Coll Surg 207(6):882–887
16. Feinstein AR, Sosin DM, Wells CK (1985) The Will Rogers phenomenon: stage migration and new diagnostic techniques as a source of misleading statistics for survival in cancer. N Engl J Med 312:1604–1608
17. Miller EA, Woosley J, Martin CF et al (2004) Hospital-to-hospital variation in lymph node detection after colorectal resection. Cancer 101(5):1065–1071
18. Buchwald P, Olofsson F, Lörinc E et al (2011) Standard protocol for assessment of colon cancer improves the quality of pathology. Colorectal Dis 13(3):e33–e36

19. Beattie GC, McAdam TK, Elliott S et al (2003) Improvement in quality of colorectal cancer pathology reporting with a standardized proforma—a comparative study. Colorectal Dis 5:558–562
20. How P, Shihab O, Tekkis P et al (2011) A systematic review of cancer related patient outcomes after anterior resection and abdominoperineal excision for rectal cancer in the total mesorectal excision era. Surg Oncol 20:149–155
21. Nagtegaal ID, Quirke P (2008) What is the role for the circumferential margin in the modern treatment of rectal cancer? J Clin Oncol 26(2):303–312
22. Wibe A, Rendedal PR, Svensson E et al (2002) Prognostic significance of the circumferential resection margin following total mesorectal excision for rectal cancer. Br J Surg 89:327–334
23. Ihnát P, Martínek L, Ihnát Rudinská L et al (2013) Circumferential resection margin in the modern treatment of rectal carcinoma. Rozhl Chir 92:297–303

5. The time factor in the LDI (Laser Doppler Imaging) diagnosis of burns

Štětinský J, Klosová H, Kolářová H, Šalounová D, Bryjová I, Hledík S

Originally published in Lasers in Surgery and Medicine, 2015, vol. 47, no. 2, p. 196-202.

Lasers in Surgery and Medicine 47:196–202 (2015)

The Time Factor in the LDI (Laser Doppler Imaging) Diagnosis of Burns

Jiří Štětinský, MD,[1,2]* Hana Klosová, MD,[1] Hana Kolářová,[2] Dana Šalounová, PhD,[3] Iveta Bryjová, Msc,[4,5] and Stanislav Hledík, PhD[6]

[1]*Burn Center, University Hospital Ostrava, 17. Listopadu 1790 708 52, Ostrava-Poruba, Czech Republic*
[2]*Department of Medical Biophysics, Faculty of Medicine, Palacky University, Hněvotínská 3, Olomouc, Czech Republic*
[3]*Department of Mathematical Method in Economy, Faculty of Economy, Technical University of Ostrava, Sokolská 33, Ostrava, Czech Republic*
[4]*Department of Cybernetics and Biomedical Engineering, Faculty of Electrical Engineering and Computer Science, Technical University of Ostrava, 17. Listopadu 15/2172 708 33, Ostrava-Poruba, Czech Republic*
[5]*Faculty of Medicine, University of Ostrava, Syllabova 19 703 00, Ostrava, Czech Republic*
[6]*Institute of Physics, Silesian University in Opava, Bezručovo nám. 13 746 01, Opava, Czech Republic*

Background and Objective: The not quite rare occurrence of inaccurate clinical diagnoses of burns in early post-burn days leads to an inappropriate conservative treatment strategy, or unnecessary surgery. LDI (Laser Doppler Imaging) objectively evaluates skin blood circulation, which correlates with the depth of the burn and the length of healing. The aim of this work was to suggest cutoff values for detecting burns without healing potential within 3 weeks, which should have undergone surgery.
Method: The burned area's average blood perfusion of 148 burns was measured on 115 patients, using the Laser Doppler Imager PIM III. A total of 268 measurements were performed from the one to the ninth post-burn day (PBD). The perfusion values were compared to the healing time or histology in the case of the surgical treatment. Cutoff values indicating surgery were investigated in various post-burn days; the ROC analysis was used.
Results: This work suggest statistically significant increasing cutoff values for indication to surgery ($P = 0.05$). From the third to the fifth day 148.5 perfusion units (PU), from the sixth to the seventh day 186.0 PU, from the eighth to the ninth PBD 269.5 PU. The cutoff value is not possible to establish until the second day.
Conclusion: LDI is a useful method for wound healing prediction and an indication of the necessity of surgery. We have demonstrated that the diagnosis of the healing capacity of LDI needs to take into account the factor of time. Lasers Surg. Med. 47:196–202, 2015.

Key words: healed; perfusion unit (PU); perfusion scan; postburn day (PBD); unhealed

INTRODUCTION

Inaccurate diagnosis occurs about 35 percent of the time, based on the clinical assessment of burn depth [1]. Inaccurate diagnoses lead to inadequate local treatment and prolonged wound healing, which increases the risk of hypertrophic scar, scar disruption or unnecessarily extended hospitalization [2]. And with unnecessary surgery comes the need for other medical examinations, the stress from surgery and anaesthesia, blood transfusions and also a significant economic impact [3]. To achieve complication-free healing, good functional and aesthetic results, faster physiological skin functions restoration and reduced risk of functional disorders (Fig. 1), the appropriate timing of surgery is essential [4,5,6].

The aim of this work is to suggest a decision making algorithm for choice of the treatment of strategy, according to Laser Doppler Imaging (LDI) assesment and the time of measurement. The work was carried out on the basis of blood perfusion monitoring in the burn wounds, during the first 9 days post injury. The decisive fact was that wounds with healing time exceeding 3 weeks should be operated early. We were particularly looking for a cutoff value for surgical indication. Some works refer to LDI accuracy till the fifth postburn day [7,8,9,10], but the observed facts are different. We investigated cutoff perfusion values indicating surgery up to the ninth postburn day. The first 5 days are important for early surgical indication, necrectomy and skin grafting. The following days then, for the healing course control of the wounds treated conservatively. This is important especially for the wounds with a cutoff perfusion value. The need for an objective diagnosis after the fifth postburn day is advantageous in the case of later admission

Conflict of Interest Disclosures: All authors have completed and submitted the ICMJE Form for Disclosure of Potential Conflicts of Interest and have disclosed the following: The authors declare no significant conflicts of interest with regard to this publication.
Contract grant sponsor: Project No.1 RVO-FNOs/2012.
*Correspondence to: Jiří Štětinský, MD, Burn Centre, University Hospital Ostrava, 17. Listopadu 1790, 708 52 Ostrava-Poruba, Czech Republic. E-mail: jiri.stetinsky@centrum.cz
Accepted 4 August 2014
Published online 6 February 2015 in Wiley Online Library (wileyonlinelibrary.com).
DOI 10.1002/lsm.22291

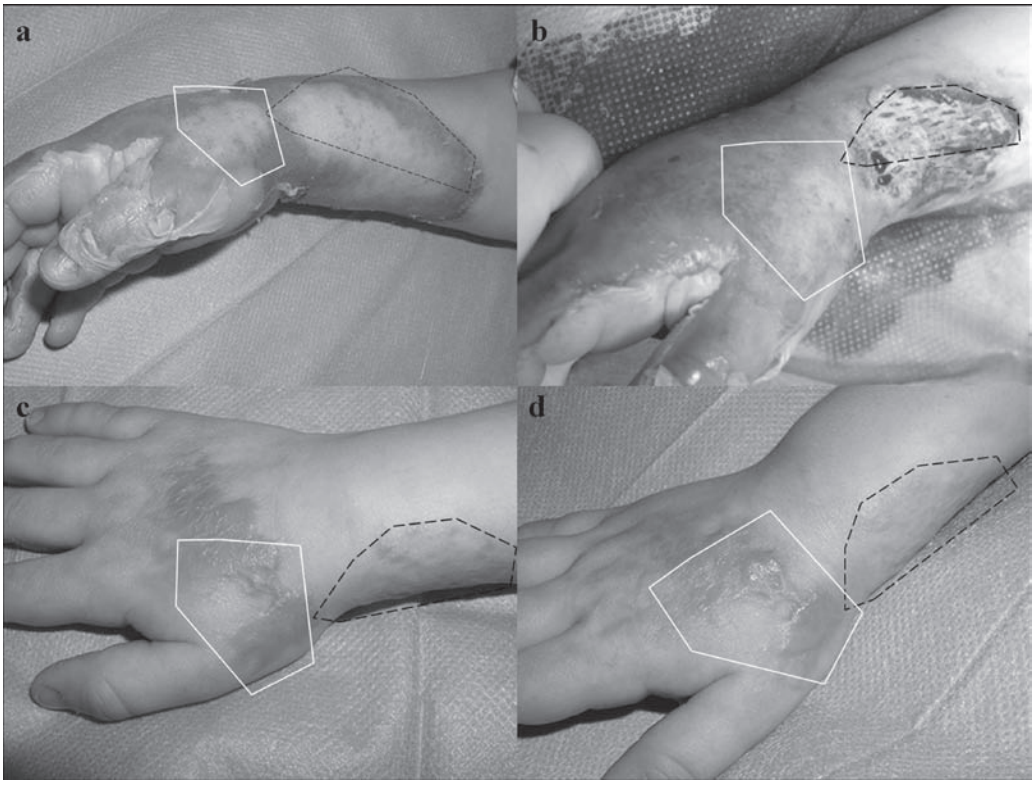

Fig. 1. A 4-year-old child scalded by hot soup underwent surgery on his wrist (area depicted by black dotted line). As the parents did not agree with skin grafting on the back of the hand (depicted in white), this part of the body was treated conservatively and the healing time exceeded 21 days; **a**) The sixth postburn day, deep burns at both regions - 140 perfusion units. **b**) The split skin graft was applied at the wrist only. **c**) The third postburn month, conservatively treated part with hypertrophic scar, requiring complex scar therapy, the grafted part had no tendency to hypertrophy. **d**) The seventh postburn month: hypertrophic scar on the back of the hand (white marked area), the quality of the grafted part is very similar to the healthy skin (area depicted in black).

or technical impossibility to measure it previously. Based on our experience, physicians experienced in LDI scan evaluations are not available sometimes and the uncertainty in diagnostic occurs also after the fifth PBD.

Laser Doppler Imager (LDI) is a noncontact scanner (Fig. 2), allowing the diagnosis of the burn depth based on a noninvasive examination of skin microcirculation and the proven correlation between the blood supply and the depth of burns. The LDI uses the well known Doppler effect by analysing the back-scattered laser beam. The ratio between shifted and non-shifted beams and signal intensity corresponds with the velocity of red blood cells and their number resp.[11]. The perfusion value is an output expressed by the amount of arbitrarily set perfusion units (PU). The perfusion value is coded in a two-dimensional color map (Fig. 3). That LDI color map is represented by six basic colors, with optional color scale distribution. For our purposes we spread the color range to 480 PUs. Dark blue represents the lowest perfusion and is equal to the number of perfusion units ranging from 0 PU to 80 PU. The perfusion increase corresponds with the color changes in the following order: light blue (80–160 PU), green (160–240

Fig. 2. A PIM III no contact scanner, produced by PerimedAB (Stockholm), was used during the investigation of the wound area at the back of the hand. The distance between the device and the examined area is 20 cm.

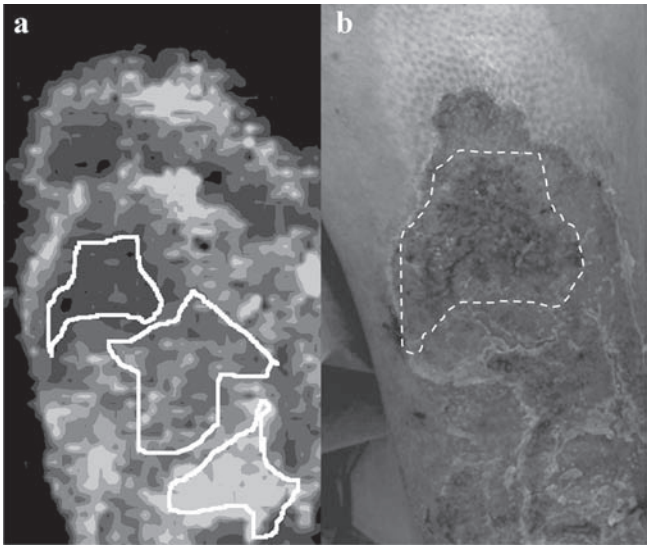

Fig. 3. **a**) Example of two-dimensional color map, converted to gray scale, representing perfusion scan on the burned thigh (the sixth postburn day) a white line shows three areas of interest, where individual perfusions are 120 PU (the deepest burn—outlined in the upper left area of the image—unhealed), 291 PU (the middle area—healed), 556 PU (the most superficial lowest area—healed). **b**) The 22nd postburn day, wound is still not healed.

PU), yellow (240–320 PU), orange (320–400 PU) and finally red (400–480 PU), which represents the highest perfusion. The number of perfusion units is determined by both the concentration and flow velocity of erythrocytes.

METHODS

The study protocol was reviewed and approved by the Institutional Review Board of Ostrava University Hospital. All adult patients or legal representatives of children signed the informed consent form with LDI measurements.

Inclusion and Exclusion Criteria

The inclusion criteria for this study were as follows: signed informed consent form, compliance of patient, inpatient, normothermia before measurement, histological assesment in the case of surgical treatment and the photographic documentation of the healing process.

The exclusion criteria were as follows: non-compliance of patient (both adults and children), fever, any macroscopic signs of infection, polytrauma, skin diseases, and cortico-steroid therapy.

Subjects

The study group contains 115 patients, 85 (74%) males, 30 (26%) females. The mean age of patients was 41.49 years (2–88). The average age of males was 44.59, females 49.74. The distribution of patients by age is shown in Figure 4a. The predominated mechanism of injury was fire at 57% of patients, 37% were scalded, and 6% of patients

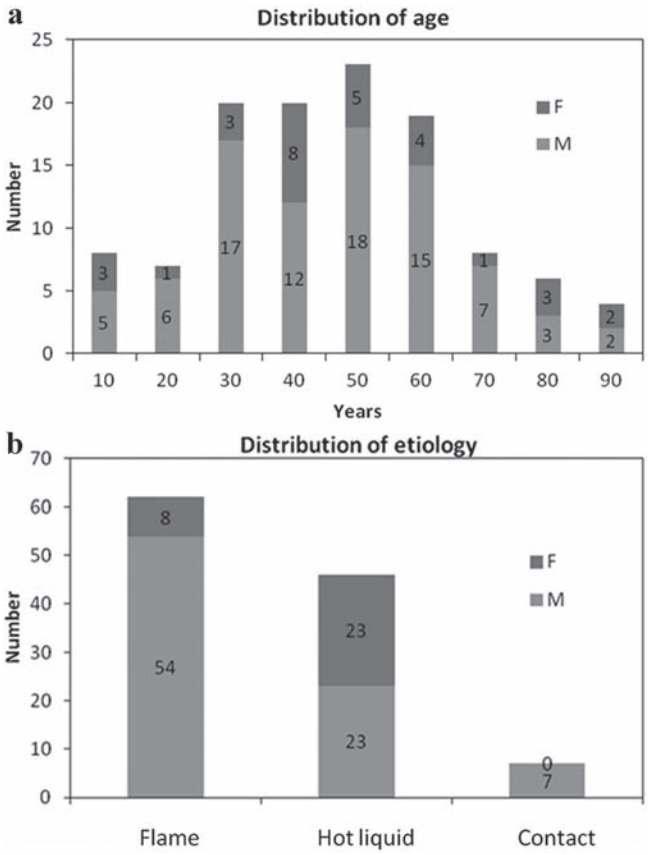

Fig. 4. **a**) The distribution of burned patients by age, patients between 30 and 60 years of age made up 70% of all patients treated. **b**) The distribution of burned patients by etiology.

sustained burns by contact with a hot object (Fig. 4b). The extent of burns was on average 8.8% TBSA, ranged from 0.5 to 45%.

In this prospective observational study 148 burn wounds on 115 patients in total were assessed by LDI from January 2010 till June 2013; 63 wounds were assessed by LDI several times with an interval of 48 hours in different days during 9 days period. The time of measurement was recorded and measurements were divided into groups by days. In total, 268 measurements were performed by the laser Doppler imager within nine postburn days. On the first day, 21 wounds were measured, the second day 32 wounds, the third day 34 wounds, the fourth day 36 wounds, the fifth day 45 wounds, the sixth day 38 wounds, the seventh day 22 wounds, the eighth day 22 and the ninth day 19 wounds. The whole period was divided into four intervals according to existing knowledge and an increasing perfusion trend: 53 wounds were assessed by the second day after injury (the interval called early perfusion). The evaluation of the LDI in this period is the most controversial due to local edema. Ninety-nine wounds were assessed from the third to the fifth day (an interval called blood perfusion 1). This interval is recommended by the manufacturers as the most appropriate for LDI scanning. Sixty wounds were assessed on the sixth and

TABLE 1. The Characteristic of Groups in Four Intervals, Count, Mean, Median of PU

	Healed	Unhealed	*P*-value
Early Perfusion			<0.0005
Count	32	21	
Mean	249	96	
Median	207	85	
Blood perfusion 1			<0.0005
Count	64	35	
Mean	338	98	
Median	281	88	
Blood perfusion 2			<0.0005
Count	36	24	
Mean	434	99	
Median	433	102	
Blood perfusion 3			<0.0005
Count	23	18	
Mean	645	103	
Median	668	84	

Early perfusion (till the second postburn day), Blood perfusion 1 (from the third to the fifth day), Blood perfusion 2 (on the sixth and seventh day), Blood perfusion 3 (on the eighth and ninth day). The differences between groups are statistically significant.

the seventh day (an interval called Blood perfusion 2), 41 wounds were assessed on the eighth and the ninth postburn day (an interval called Blood perfusion 3). Table 1 shows the count of wounds in each time period and its mean and median, see also Fig. 5.

The patients were measured by LDI as soon as possible, but never during the primary treatment of wound, because of the pain and psychological trauma associated with thermal injury. Attention has been focused mainly on mid dermal and deep dermal burns. It is very difficult to differentiate the depth of dermal damage clinically.

Two physicians familiar with LDI performed the LDI examination. Another burn surgeon determined the therapeutic plan. When conservative treatment was chosen, photographic documentation of the healing process in the measured area was taken. In the case of necrectomy, the sample of tissue in the LDI measured part of the wound was taken for histological examination, which is still the golden standard in diagnosis of burn depth [12,13].

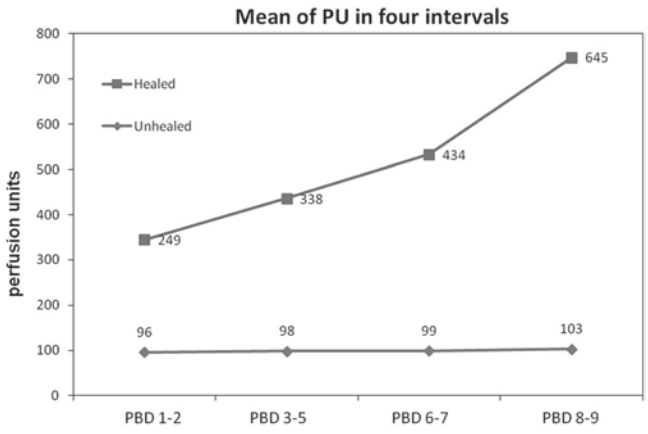

Fig. 5. The mean of PU in four intervals shows the increasing perfusion trend in the group of healed within 3 weeks, no development of perfusion in group of unhealed (underwent surgery or healed after 3 weeks).

Patients were categorized into two groups according to the state of healing on the 21st day or the histological analysis in the case of surgical treatment. Group 1, so-called Healed, contains patient with a demonstrably healed measured site on the 21st day. Group 2, so-called Unhealed, contains wounds without reepitelization in a measured area on the 21st day or wounds after the necrectomy, with the histological finding of full thickness injury. (The hematoxylin eosin technique was used during the histological examination).

Instrumentation

Laser Doppler imager PIM III (Perimed AB company, Stockholm) with an integrated camera was used for burn wound perfusion assessment. The PIM III uses a diode laser with a beam wavelength of 640 nm, low power of 1 mW (laser class IIb) and the beam diameter of 1 mm. A depth of beam penetration is set at approx. 1 mm by the manufacturer. A distance between each measured point was 1–2 mm, the average scan area measured 150 cm^2, with 4,300 points on average. (Maximum scanned area measured 2,500 cm^2 with 65,000 measured points). The position of the scanner head during the assesment was slightly off perpendicular to the wound surface [14], as the lower angle impairs the signal intensity. The distance between the scanner head and the wound surface ranged from 15 to 20 cm. A laser device with this performance requires no special protective equipment. A non-contact scanning method also eliminates the risk of contamination.

The examination was carried out during dressing changes, after removing the bandages and debridement, in a room with a constant temperature of 22°C, relative humidity ranging from 30% to 50%, in daylight. A single measurement took approximately 2 minutes, depending on the size of the scanned area.

The measurements were performed in the morning, when bandages had run. The silver sulfadiazine or polyvinylpyrrolidone iodine were the most frequently used agents for a topical treatment. Wounds treated especially with Dermazin were carefully wiped off because of the demonstrated impact of Dermazin on the absorption of laser radiation [14].

Repeated measurements, even after several days, were conducted on the same site. To achieve identical localization during the examination, we followed the wound edge, which was compared with the previous scan and simultaneous photo. The diameters of scans were repeated as well (Fig. 6).

When evaluating the LDI scans, common inflammation on the edges of deep wounds, distorting the average perfusion was excluded from the assessment of wound perfusion; the region of interest is inside this rim (Fig. 7). Blisters, imitating LDI image of deep burns, were also removed. The LDI scans

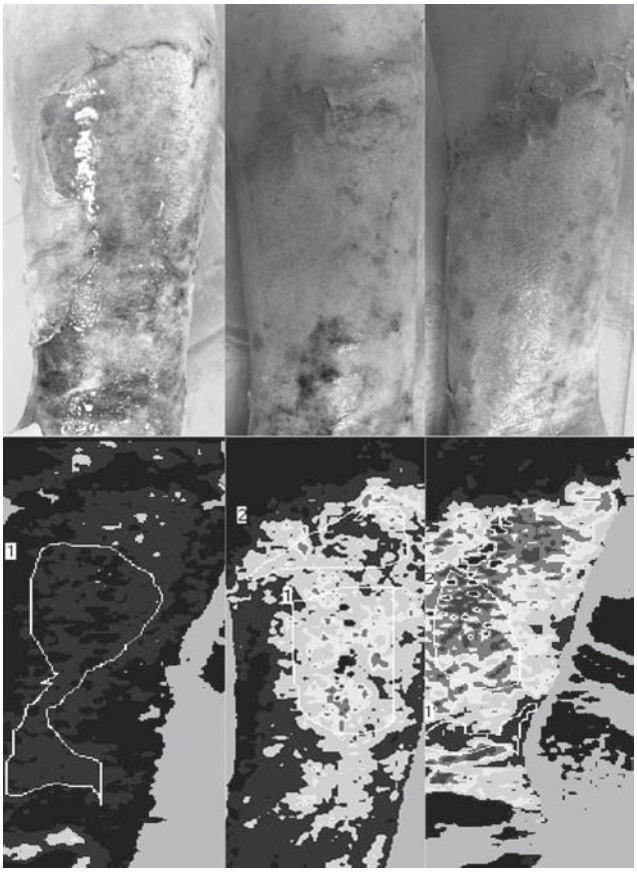

Fig. 6. Repeated perfusion scan of the same wounds the first (170 PU), the third (465 PU), fifth (668 PU) postburn day showing a gradual increase in perfusion. There were no significant clinical changes in burns during this period. The wound was healed on the 16th day.

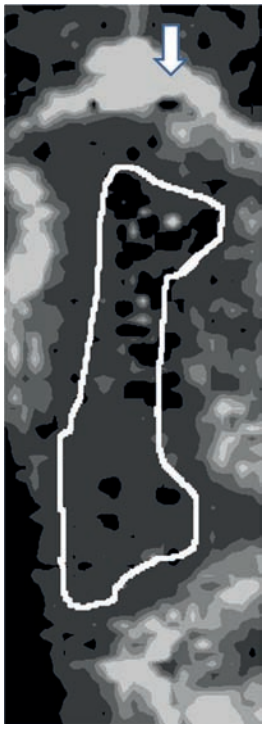

Fig. 7. Perfusion scan of a burned arm with inflammatory rim (white in grey scale) at the edge of burns (arrowed). The rim would significantly effect the resulting perfusion. The measured area (the fourth postburn day-92 PU), marked by a white line, does not contain this inflammatory rim.

were thoroughly compared with the appearance of a wound while marking areas of interest. The average perfusion of the scanned area, its size, number of points, and time of measurement was recorded by the software.

Data Analysis

Data analysis was performed with IBM SPSS software version 18. A two-sided value of $P = 0.05$ was considered statistically significant for all analyses.

We assessed the differences in wound perfusion between groups of healed and nonhealed in all observed intervals. The median test was used.

To obtain the cutoff value, with the optimal sensitivity and specificity, for surgery indication at each time period, we established ROC curves.

RESULTS

Group 1 contains 90 wounds in total healed within 3 weeks: 23 wounds healed within 2 weeks, 67 healed in the third week. Group 2 (unhealed) contains 58 wounds: 43 wounds underwent surgical treatment with skin grafting and histological examination of damaged skin, 15 wounds were treated conservatively and their healing time exceeded 3 weeks, on average 28.2 (23–34).

There is evidence for differences in wound perfusion between the groups in all observed intervals (all $P < 0.0005$).

The cutoff value for surgical indication, with the satisfactory level of sensitivity and specificity, was not able to be established for the first and second PBD, so-called "Early blood perfusion," as the perfusion values of both groups overlapped too much. Cutoff value for the second interval, from the third to the fifth PBD (Blood perfuison 1), for indication to surgical treatment, was determined at 148.5 PU, with sensitivity 94%, specificity 95%. Cutoff value for the third interval, which is on the sixth and the seventh PBD (Blood perfusion 2), was determined at 186.0 PU, with sensitivity 100% and specificity 94%. Cutoff value for the fourth interval, on the eighth and the ninth postburn day (Blood perfusion 3) was determined at 269.5 PU, with sensitivity and specificity of 100%. These results are shown in Table 2.

Patients in group 1 showed a significant increase of perfusion in the third interval (from the sixth to the seventh day) and the fourth (from the eighth to the ninth PBD) interval, compared to the second one, from the third to the fifth PBD ($P = 0.018$ and $P < 0.0005$ using the Friedman

TABLE 2. ROC Curve Analysis of Three Intervals

	Area	*P*-value	Cutoff Val	Positive N	Negative N	Sens %	Spec %
Blood Perfusion 1<	0.944	<0.0005	148.5	35	64	94.3	95.3
Blood Perfusion 2<	0.986	<0.0005	186.0	24	36	100.0	94.4
Blood Perfusion 3<	1.00	<0.0005	269.5	18	23	100.0	100.0

Area, Area under the ROC curve; *P*-value, significance for null hypothesis: Area = 0.5; Cutoff Val, cut off value for surgery indication; Positive N, number of positive indication; Negative N, number of negative indication; Sens %, sensitivity (%); Spec %, specificity (%).

test and pairwise comparisons), which means that the blood perfusion changes faster with the passing days.

DISCUSSION

In this work, the standard values for determining the surgical treatment, using the LDI assesment, were established up to the ninth postburn day. The time factor should be taken into account for a proper evaluation of the LDI scan.

Low perfusion measured up to the second postburn day cannot indicate surgical treatment; low perfusion may be misleading. Perfusion is very low in the group of unhealed (third degree burns, deep dermal burns) as well as in the group of healed (mid dermal burn), especially when they were caused by flame. This fact occurs also immediately after removing the blisters [19]. The cutoff value to indicate surgical treatment was determined for the time period from the third to the ninth PBD. These values were statistically significant.

The increasing wound perfusion in the group of the healed contrasts with the consistently low perfusion in the group of unhealed, which could help by predicting the wound behavior in the case of two measurements. The increasing trend is shown in Fig. 5.

Development of blood flow in the group of healed patients is a reflection of emerging inflammatory response with vasodilatation, which is also the image of microcirculation throughput. On the other hand, microcirculation is largely damaged in the group of nonhealed, so that the vasodilatation, which would provide the metabolic needs of the tissues, is not possible. A detailed analysis of the increase in perfusion will be the issue of further research.

In the first 2 days post-injury, compression of vascular supply prevails in the burned areas due to the local edema. This may falsely imitate the destruction of microcirculation. Till the second PBD we could indicate only conservative treatment, not operation. Regarding the increasing perfusion trend, we can treat wounds conservatively with perfusion higher than 148.5 PU, which is a cutoff for the following time interval (third to fifth PBD).

Rapid increase in blood flow during the first 48 hours was also described by other authors [15–19]. Our findings correlate with these works.

CONCLUSION

With our set values, we can proceed with the perfusion scan at different times during the first 9-day period post injury. While it is appropriate to perform the examination as soon as possible, as well as schedule the treatment strategy, it is often necessary to also later objectify healing potential. This method should help the clinician in both situations.

ACKNOWLEDGEMENT

The authors would like to acknowledge the financial support from the Institutional Support Project No.1 RVO-FNOs/2012.

REFERENCES

1. Watts AMI, Tyler MPH, Perry ME, Roberts AHN, McGrouther DA. Burn depth and its histological measurement. Burns 2001;27:154–160.
2. Lawrence KHC, Ward D, Lam L, Holland AJA. The impact of laser Doppler imaging on time to grafting decisions in pediatric burns. J Burn Care Res 2010;31:328–332.
3. Klein MB, Hollinworth W, Rivala FP, Kramer CB, Askay W, Heimbach DM, Gibran NS. Hospital costs associated with pediatric burn injury. J Burn Care Res 2008;29:632–637.
4. Scott JR. Watson SB. 7 Surgical management of burns. Baillire's Clin Anaesthesiol 1997;11:473–495.
5. Cubison TCS, Pape SA, Parkhouse N. Evidence for the link between healing time and the development of hypertrophic scars (HTS) in paediatric burns due to scald injury. Burns 2006;32:992–999.
6. Sjoberg F, Danielsson P, Anderson L, Steinwall I, Zdolsek J, Ostrup L. Utility of an intervention scoring system in documenting effects of changes in burn treatment. Burns 2000;26:553–559.
7. Hemington-Gorse SJ. A comparison of laser Doppler imaging with other measurement techniques to assess burn depth. J wound care 2005;14:151–153.
8. Jeng JC, Bridgeman A, Shivnan L, Thornton PM, Alam H, Clarke TJ. Laser Doppler imaging determines need for excision and grafting in advance of clinical judgment: a prospective blinded trial. Burns 2003;29:665–670.
9. La Hei ER, Holland AJ, Martin HCO. Laser Doppler imaging of paediatric burns: burn wound outcome can be predicted independent of clinical examination. Burns 2006;32:550–553.
10. Cho JK, Moon DJ, Kim SG, Lee HG, Chung SP, Chung SP. Relationship between healing time and mean perfusion units of laser Doppler imaging (LDI) in pediatric burns. Burns 2009;35:818–823.
11. Watkins D, Holloway GA. An instrument to measure cutaneous blood flow using the Doppler shift of laser light. IEEE Trans Biomed Eng 1978;25:28–33.
12. Riordan CL, McDonough M, Davidson JM, Corley R, Perlov C, Barton R. Noncontact laser Doppler imaging in burn depth analysis of the extremities. J Burn Care Rehabil 2003;24:177–186.
13. Brown RFR, Rice P, Bennet NJ. The use of laser Doppler imaging as an aid in clinical management decision making in the treatment of vesicant burns. Burns 1998;24:692–698.

14. Droog EJ, Steenbergen W, Sjoberg F. Measurement of depth of burns by laser Doppler perfusion imaging. Burns 2002; 28:561–568.
15. Kloppenberg WH, Beerthuizen GIJM, Duis HJ. Perfusion of burn wounds assessed by Laser Doppler Imaging is related to burn depth and healing time. Burns 2001;27:359–363.
16. Atiles L, Mileski W, Spann K, Pardue G, Hunt J, Barter C. Early assesment of pediatric burn wounds by laser Doppler flowmetry. J Burn Care Rehabil 1995;16:596–601.
17. Holland AJ, Martin HC, Cass DT. Laser Doppler imaging prediction of burn wound outcome in children. Burns 2002; 28:11–17.
18. Niazi ZBM, Essen TJH, Rapini R, Scoty D, McLean NR, Blafl MJM. New laser Doppler scanner, a valuable adjunct in burn depth assessment. Burns 1993;19:485–489.
19. Hoeksema H, Van de Skipe K, Tondu T, Hamdi M, Landuyt K, Blondeel P. Accuracy of early burn depth assessment by laser Doppler imaging on different days post burn. Burns 2009; 35:36–45.

6. Transcranial sonography of brainstem structures in panic disorder

Šilhán P, Jelínková M, Walter U, Praško JP, Herzig R, Langová K, Školoudík D

Originally published in Psychiatry Research: Neuroimaging, 2015, vol. 234, no. 1, p. 137-143.

Psychiatry Research: Neuroimaging 234 (2015) 137–143

Contents lists available at ScienceDirect

Psychiatry Research: Neuroimaging

journal homepage: www.elsevier.com/locate/psychresns

Transcranial sonography of brainstem structures in panic disorder

Petr Šilhán [a,1], Monika Jelínková [b,c,1], Uwe Walter [d], Ján Pavlov Praško [e], Roman Herzig [f], Kateřina Langová [g], David Školoudík [b,h,*]

[a] Department of Psychiatry, University Hospital, Ostrava, Czech Republic
[b] Department of Neurology, University Hospital, 17 listopadu 1780, CZ-708 56 Ostrava, Czech Republic
[c] Department of Neurology, Hospital Karviná-Ráj, Czech Republic
[d] Department of Neurology, University of Rostock, Rostock, Germany
[e] Department of Psychiatry, Faculty of Medicine and Dentistry, Palacký University, University Hospital, Olomouc, Czech Republic
[f] Department of Neurology, Charles University Faculty of Medicine, University Hospital, Hradec Králové, Czech Republic
[g] Department of Biophysics, Faculty of Medicine and Dentistry, Institute of Molecular and Translational Medicine, Palacký University, Olomouc, Czech Republic
[h] Department of Nursing, Faculty of Health Science, Palacký University, Olomouc, Czech Republic

ARTICLE INFO

Article history:
Received 22 August 2014
Received in revised form
23 May 2015
Accepted 2 September 2015
Available online 8 September 2015

Keywords:
Panic disorder
Transcranial sonography
Brainstem raphe

ABSTRACT

Panic disorder has been associated with altered serotonin metabolism in the brainstem raphe. The aim of study was to evaluate the BR echogenicity on transcranial sonography (TCS) in panic disorder. A total of 96 healthy volunteers were enrolled in the "derivation" cohort, and 26 healthy volunteers and 26 panic disorder patients were enrolled in the "validation" cohort. TCS echogenicity of brainstem raphe and substantia nigra was assessed on anonymized images visually and by means of digitized image analysis. Significantly reduced brainstem raphe echogenicity was detected more frequently in panic disorder patients than in controls using both visual (68% vs. 31%) and digitized image analysis (52% vs. 12%). The optimal cut-off value of digitized brainstem raphe echogenicity indicated the diagnosis of panic disorder with a sensitivity of 64% and a specificity of 73%, and corresponded to the 30th percentile in the derivation cohort. Reduced brainstem raphe echogenicity was associated with shorter treatment duration, and, by trend, lower severity of anxiety. No relationship was found between echogenicity of brainstem raphe or substantia nigra and age, gender, severity of panic disorder, or severity of depression. Patients with panic disorder exhibit changes of brainstem raphe on TCS suggesting an alteration of the central serotonergic system.

1. Introduction

Panic disorder is an anxiety disorder characterized by recurrent unexpected panic attacks accompanied by somatic and psychological symptoms. It may also include behavioral changes and ongoing worry about the implications or concern about having other attacks, and about one in three people with panic disorder develops agoraphobia (American Psychiatric Association, 2000). Substantial comorbidity between panic disorder and other anxiety disorders or major depression has been described (Kessler et al., 2003).

The monoamine neurotransmitter serotonin (5-hydroxytryptamine; 5-HT) plays an important role in the pathophysiology of anxiety and panic attacks (Bell and Nutt, 1998; Baldwin et al., 2005). Panic disorder is associated with reduced availability of the postsynaptic inhibitory serotonergic receptor, the serotonin-1A (5-HT1A) subtype, which is also known to play a key role in depression. The areas with the most significant reductions are brainstem raphe (BR), amygdala, orbitofrontal cortex, and anterior lateral temporal cortex (Nash et al., 2008). Positron emission tomography (PET) studies have shown lower 5-HT1A binding in anterior cingulate, posterior cingulate, and BR in patients with panic disorder (Neumeister et al., 2004).

Transcranial sonography (TCS) is a non-invasive diagnostic method that displays tissue echogenicity of the brain through the intact skull. It allows one to differentiate brain structures, for example, brainstem, substantia nigra (SN), red nucleus, BR, thalamus and ventricular system (Walter et al., 2007a). TCS demonstrates reduced echogenicity of BR in patients with major depressive disorder, obsessive–compulsive disorder, but also in Parkinson's, Huntington's or Wilson's diseases with depression (Becker et al., 1995; Berg et al., 1999; Walter et al., 2005, 2007b; Mijajlovic, 2010; Krogias et al., 2011b; Mavrogiorgou et al., 2013). It has been

* Corresponding author at: Department of Neurology, University Hospital Ostrava, 17 listopadu 1780, CZ-708 56 Ostrava, Czech Republic.
E-mail address: skoloudik@hotmail.com (D. Školoudík).
[1] Equal contribution.

http://dx.doi.org/10.1016/j.pscychresns.2015.09.010
0925-4927/

suggested that reduced BR echogenicity might reflect an alteration of the central serotonergic system (Becker et al., 2001; Walter et al., 2007c).

In view of the previously reported similarities of BR 5-HT receptor alteration in major depressive and panic disorders, we hypothesized that BR alteration might also be detected by TCS in patients with panic disorder. In major depressive disorder, an increased frequency of abnormal SN hyperechogenicity has also been found; a TCS finding thought to reflect an alteration of the nigrostriatal dopaminergic system (Walter et al., 2007b). We therefore compared the echogenicity of BR and SN in patients with panic disorder and healthy controls using visual evaluation and a novel digitized image analysis tool.

2. Methods

2.1. Patients and control subjects

One-hundred healthy volunteers were examined as members of the derivation cohort in the neurosonological laboratory during 1 month for the evaluation of normal values for BR and SN for visual measurements and digitized image analysis. Healthy controls were recruited from the University Hospital Volunteer Database. Only volunteers with the BDI-score 0–13 and the BAI-score of 0–16 points were included. Two months later, 26 out of 33 screened patients with panic disorder and 26 age- and sex-matched healthy volunteers were examined as members of the validation cohort.

We enrolled patients with panic disorder who met the Diagnostic and Statistical Manual of Mental Disorders, 4th Edition, Text Revision (DSM-IV-TR) criteria for panic disorder, with or without agoraphobia, using the Mini-International Neuropsychiatric Interview (MINI) version 5.0.0 (American Psychiatric Association, 2000; Sheehan et al., 1998). Exclusion criteria for both the derivation and the validation cohort included the presence of any other current Axis I psychiatric disorder using the MINI, the history of any other psychiatric disorder, and current or past serious medical or neurological disorders.

Participants who exhibited low quality of the TCS B-mode image due to insufficient temporal bone windows, as tested by digitized image analysis, were excluded from the study (4 healthy volunteers and 1 panic disorder patient). The image quality was evaluated using the developed B-mode Assist System as an integral part of digitized image analysis (Blahuta et al., 2013; Skoloudík et al., 2014). Images with a mean value of brightness intensity $I \geq 25$ in all 5×5 mm pixels were considered to be of low quality.

The entire study was conducted in accordance with the Helsinki Declaration of 1975 (revised in 2004 and 2008). The study was approved by the Ethics Committee of University Hospital Ostrava, Czech Republic. All patients provided written informed consent.

2.2. Clinical examination and psychological tests

Patients with panic disorder and healthy volunteers were subjected to MINI version 5.0.0 to assess DSM-IV-TR Axis I disorders, physical and neurological examination, and completed the Beck Anxiety Inventory (BAI) and Beck Depression Inventory (BDI). In patients with panic disorder, clinical severity of their symptoms was assessed using the Panic Disorder Severity Scale (PDSS). Clinical Global Impression (CGI), Hamilton Anxiety Scale (HAMA), 17-item Hamilton Depression Scale (HAMD-17), Sheehan Disability Scale (SDS), Dissociative Experiences Scale (DES), and Somatoform Dissociation Questionnaire (SDQ-20) were performed in all patients. Age, sex, education level, tobacco use, alcohol consumption, duration of panic disease, type, dose and duration of treatment, number of antidepressants used, presence and duration of agoraphobia, and hand preference (right- or left-handedness) were collected for statistical analysis.

2.3. TCS

The BR and SN were imaged in all participants from both the right and the left temporal bone windows in the axial mesencephalic plane using the ultrasound system MyLab Twice (Esaote S.p.A., Genova, Italy) with a 2.5-MHz phased-array transducer (PA240). The examination was performed through a temporal bone window with the following standard parameters (Skoloudík et al., 2014): penetration depth of 16 cm, penetration high, dynamic range 7 (50 dB), frequency 1–4 MHz, enhancement 3, density 2, view 9, persistence 7, dynamic compression 0, gain 26%, gray map 0, S view off, 2 focuses in 5 and 10 cm, mechanical index 0.9, tissue indices TIs 1.0, TIB 1.0 and TIC 2.1.

The butterfly-shaped structure of the mesencephalic brainstem and the region of BR and SN were depicted as clearly as possible from the transversal plane (Fig. 1) using slow craniocaudal probe motion. One image of BR and SN, and one video (lasting for at least 5 s) were obtained and saved from both the right and the left temporal bone windows. Personal data and examination times were deleted and all acquired anonymized images and videos were encoded with a unique key. All examinations were performed by a single sonographer (MJ) who was blinded to the diagnoses.

2.4. Visual manual measurement and digital image analysis

Semiquantitative visual evaluation of BR was performed and BR was evaluated as normal or disrupted. Echogenicity of BR was rated as reduced when its structure was interrupted or not detectable, i.e. isoechogenic with the adjacent brain tissue (Walter et al., 2007a; Berg et al., 2006, 2008). Isoechogenic BR with the adjacent brain tissue was evaluated separately. Manual SN echogenic size measurements were performed on axial mesencephalic scans automatically after zooming and freezing of the image. Manual encircling of the outer circumference of the ipsilateral echogenic SN area was performed to evaluate the echogenic area of SN (Berg et al., 2008). For all subsequent processing steps of the digital analysis and measurement, images without SN or BR area

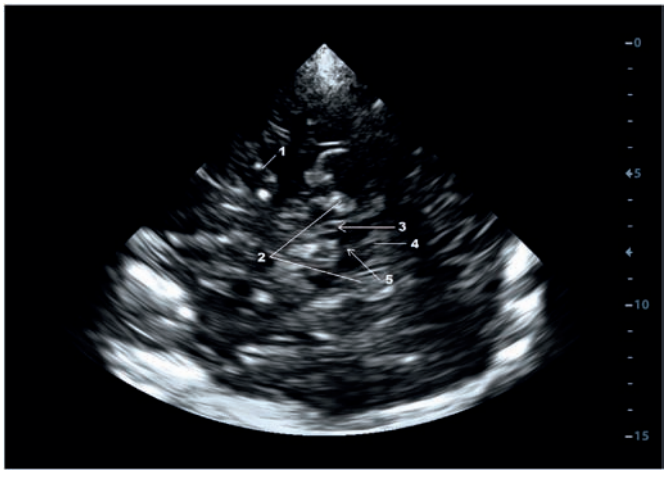

Fig. 1. Transcranial sonography: brainstem with substantia nigra and brainstem raphe imaged from transtemporal approach, axial mecencephalic plane. 1 – Middle cerebral artery, 2 – perimesencephalic cisterns, 3 – substantia nigra, 4 – fourth ventricle, and 5 – brainstem raphe.

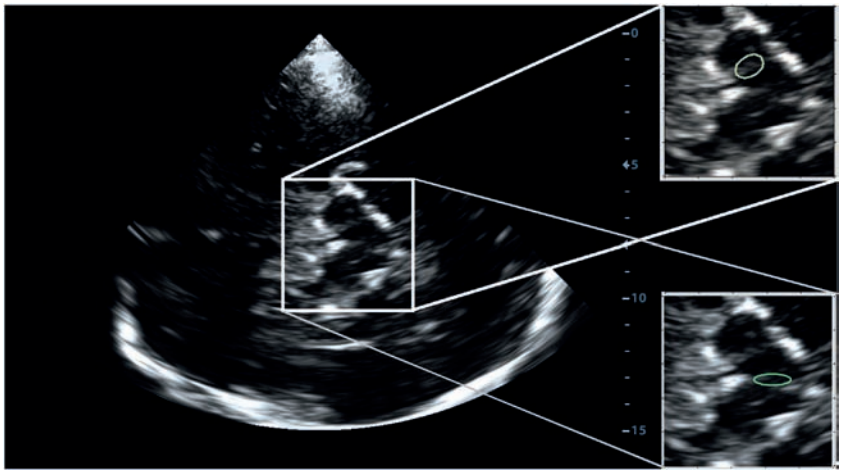

Fig. 2. Placement of the region of interest for digital analysis in the transcranial sonography brainstem images.

encircling were converted to the 8-bit gray scale (intensity value I=0–255). The designed algorithm allowed region of interest (ROI)-based processing on grayscale images with intensities of 0–255, binary thresholding, and computation of areas inside the two specific elliptical ROIs for ipsilateral SN and BR. The size and shape of both specific ROIs were based on histological images of SN and BR (Fig. 2) and the same ROIs were used for digital analysis of all images (Blahuta et al., 2013; Skoloudík et al., 2014). Input images were uploaded into the application and cropped to the window of 50×50 mm from the native axis by the image. A predefined elliptical ROI was manually placed in the region of the BR by a blinded sonographer (DŠ) with a 15-year experience in TCS. In the second step, the predefined elliptical ROI was manually placed in the region of the SN. The algorithm computed the hyperechogenic area for each I (0–255) inside the total area of the specific elliptical ROI circumscribed in the BR and ipsilateral SN. The echogenicity indices as a total sum of hyperechogenic areas for each I (area under the curve; AUC) were counted for BR and SN from both the right and the left temporal bone windows. The detailed methodology was described previously (Blahuta et al., 2013). The higher value obtained from both measurements was used for analysis. The healthy volunteers BR and SN images obtained from the right temporal bone window were evaluated visually and using the digital image analysis twice by one rater (DS) in a 2-week period and once by second rater (ML) for the evaluation inter-rater and intra-rater agreements.

The 10th percentile of BR echogenicity index and the 90th percentile value of SN echogenicity index both obtained on digitized image analysis in the healthy volunteers group were set as border values for BR and SN, respectively. The difference between the border value and the counted value of each image in the validation cohort was used for differentiation between normal and hypoechogenic (for BR) or normal and hyperechogenic (for SN) images.

2.5. Statistical analysis

The sample size of the study was based on an expected 30% difference in BR echogenicity index between healthy volunteers and panic disorder patients. Pre-study calculations showed that a minimum of 26 patients in each group was needed to reach a significant difference with an α value of 0.05 (two-tailed) and a β value of 0.8, assuming that 10% of participants will present with an insufficient bone window.

The higher values of manually measured echogenic SN areas and BR and SN echogenicity indices obtained using digital image analysis from the right and the left temporal bone window were used for statistical analysis. The Shapiro–Wilk test was used for testing the correspondence of the calculated parameters to a normal distribution. Data with a normal distribution were reported as mean $\pm$ standard deviation. All parameters not fitting a normal distribution were presented as median and interquartile range (IQR). Student's t test (for BR and SN digital image analysis and manual measurement of echogenic SN area) and Fisher's exact test (for visual evaluation of BR) were used for comparisons between panic disorder patients and healthy volunteers. Statistical significance was defined as $p < 0.0125$ after Bonferroni correction. Pearson correlation coefficient was used for the evaluation of the inter-rater and the intra-rater agreement.

Spearman's correlation coefficient was used for correlation between TCS measured BR echogenicity index and age, BAI, BDI, PDSS, CGI, HAMA, HAMD-17, SDS, DES and SDQ-20 tests results. Mann–Whitney U test (for evaluation of age, BAI, BDI, PDSS, CGI, HAMA, HAMD-17, SDS, DES, SDQ-20, duration of panic disorder, presence and duration of agoraphobia, duration of treatment, and number of currently administered antidepressant drugs) and Fisher's exact test (for the evaluation of sex, hand preference, education level, smoking, and alcohol consumption) were used for comparison between patients with normal and abnormal BR. Pearson correlation coefficient was used for the evaluation of the correlation between the dose of serotonin reuptake inhibitors (SSRIs) or venlafaxine (paroxetin equivalent dose) and both visual BR evaluation and BR echogenicity index. Statistical significance was defined as $p < 0.0025$ after Bonferroni correction.

Receiver operating characteristic (ROC) curve analysis for panic disorder diagnosis using both measurements of AUC and optimal cut-off point determination were created. All data was analyzed using SPSS version 17.0 software (SPSS, Chicago, IL, USA).

3. Results

After excluding individuals (4 healthy volunteers and 1 patients with panic disorder) with low image quality on TCS and 7 panic disorder patients with concomitant depression, 96 healthy volunteers in the derivation cohort (46 male, mean age 39.3 $\pm$ 9.1 years), and 25 panic disorder patients (10 male, mean age 38.0 $\pm$ 8.0 years) and 26 age- and sex-matched controls (10 male, mean age 38.0 $\pm$ 7.8 years) in the validation cohort were evaluated. Demographic and baseline characteristics of panic disorder patients and controls are presented in Table 1. The groups did not differ in age and sex distribution.

Table 1
Demographic data.

	Panic disorder patients	Healthy subjects	*p* Value
Number	25	26	NA
Mean age ± SD; years	38.0 ± 8.0	38.0 ± 7.8	0.83
Male gender; *n* (%)	10 (40.0)	10 (38.5)	1.00
BAI; median (range)	30 (7–49)	2.5 (0–16)	< 0.001
BDI; median (range)	19 (0–26)	2.5 (0–13)	< 0.001

BAI – Beck Anxiety Inventory; BDI – Beck Depression Inventory; NA – not applicable; SD – standard deviation.

Abnormal BR on TCS was detected more frequently in the panic disorder patients than in the controls using visual and digital image analyses (Table 2). There was no subject with BR evaluated as isoechogenic with the adjacent brain tissue (non-detectable). Pearson correlation coefficients for intra-rater and inter-rater agreement of visual BR evaluation and BR echogenicity index were 0.91 and 0.75, and 0.97 and 0.95, respectively ($p < 0.01$ in all cases).

The BR echogenicity index obtained on digitized analysis was significantly lower in the panic disorder patients than in the controls (10.56 ± 3.81 vs. 13.72 ± 3.82; $p=0.006$). BR echogenicity index was, by trend, correlated negatively with age ($r=-0.469$, $p=0.037$) and positively with score on the BAI ($r=0.451$, $p=0.046$). Panic disorder patients with visually abnormal BR had shorter disease duration than those with normal BR (3.6 vs. 8.0 years; $p=0.004$), and consecutively, shorter panic disorder treatment duration (1.1 vs. 4.1 years; $p=0.025$). They did not differ with respect to sex, handedness, education level, tobacco use, alcohol consumption, total number of antidepressive drugs, presence and duration of agoraphobia, and scores on the following psychometric tests: BAI, BDI, PDSS, CGI, HAMA, HAMD-17, SDS, DES and SDQ-20 (Table 3). Panic disorder patients and healthy controls did not differ with respect to SN echogenicity index (13.71 ± 3.87 vs. 15.89 ± 4.19; $p=0.27$) or SN area (0.18 ± 0.07 cm^2 vs. 0.17 ± 0.05 cm^2; $p=0.39$). No significant correlations were found between the dose of SSRIs (23 patients) or venlafaxine (2 patients) and both the visual BR evaluation ($r=0.34$, $p=0.10$) and BR echogenicity index ($r=0.13$, $p=0.55$), respectively.

ROC curve analysis for panic disorder diagnosis using the BR echogenicity index obtained on digitized image analysis is shown in Fig. 3. AUC was 0.745 (95% confidence interval [CI]: 0.607–0.882; $p=0.003$). The optimal cut-off value for BR echogenicity index was > 11.5 with accuracy of 68.6% (95% CI: 54.1–80.9%), sensitivity of 64.0% (95% CI: 42.5–82.0%), specificity of 73.1% (95% CI: 52.2–88.4%), negative predictive value of 67.9% (95% CI: 47.7–84.1%) and positive predictive value of 69.6% (95% CI: 47.1–86.8%) for diagnosis of panic disorder. The specified cut-off value corresponded to the 30th percentile but not the pre-defined 10th percentile of BR echogenicity index in the healthy derivation cohort.

4. Discussion

To the best of our knowledge, this is the first study to assess BR on TCS in patients with panic disorder. Our results demonstrated alteration of BR in panic disorder patients on both visual assessment and digital image analysis.

Hypoechogenicity of BR is a characteristic finding in patients with unipolar depression, depression associated with Parkinson's, Huntington's or Wilson's disease, but not in healthy adults and patients with schizophrenia, multiple sclerosis with depression, or Parkinson's disease without concomitant depression (Becker et al., 1995; Berg et al., 1999; Walter et al., 2005, 2007b; Mijajlovic, 2010; Krogias et al., 2011b; Mavrogiorgou et al., 2013). In contrast to unipolar depression, TCS findings in bipolar depression patients indicate most frequently preserved structural integrity of BR (Krogias et al., 2011a). If bipolar disorder was associated with hypoechogenic BR, depressive symptoms were reported to be more severe. In patients with unipolar depressive disorder, hypoechogenic BR was associated with responsivity to SSRIs, including low-dose venlafaxine, while patients with normal echogenic BR responded better to non-SSRI antidepressant drugs (Walter et al., 2007c). In the present study, BR hypoechogenicity was frequently found in panic disorder patients, which supports the idea of a similar relationship between BR echogenicity and responsivity to SSRI. Nevertheless, BR echogenicity did not correlate significantly with SSRI or venlafaxine doses. Also studies with loudness dependence of the auditory evoked potentials (LAEDP) did not demonstrate differences in LAEDP between panic disorder or anxiety patients and healthy volunteers (Park et al., 2010; Eser et al., 2009).

The fact, that patients with pathological BR showed the shorter disease duration represents another interesting point in the present study. This could be caused by a vulnerability of patients with abnormal BR to develop depression and, the exclusion of patients with concomitant depression occurring in the early stages of the disease might be associated with the shorter disease duration in the analyzed set of panic disorder patients.

Changes in BR echogenicity are thought to reflect changes in tissue impedance and point toward an alteration of the brainstem microarchitecture, which could be due to a shift in tissue cell density, a change in interstitial matrix composition, or an alteration of fiber tract integrity (Berg et al., 1999; Becker et al., 2001). The present study shows that digitized image analysis allows quantification of BR echogenicity, which appears to be a more reliable tool for assessment of BR echogenicity than visual assessment. This is not surprising, given the difficulties of rating BR echogenicity (Walter et al., 2007c). Nevertheless, this finding should be confirmed in further studies. One may hypothesize that visual inspection and digitized image analysis might "pick up" different aspects of BR TCS image morphology.

In contrast, a correlation between echogenicity measures and clinical scores may be more reliably detected. Here, digitized analysis revealed, albeit only by trend after Bonferroni correction,

Table 2
Primary study results.

	Panic disorder patients	Healthy subjects	*p* Value
BR echogenicity index measured using digitized analysis; mean ± SD	10.56 ± 3.81	13.72 ± 3.82	0.006
Hypoechogenic BR – digitized analysis; *n* (%)	13 (52.0)	3 (11.5)	0.007
Disrupted BR – visual evaluation; *n* (%)	17 (68.0)	8 (30.8)	0.012
SN echogenicity index measured using digitized analysis; mean ± SD	13.71 ± 3.87	15.89 ± 4.19	0.270
Visual manual measurement of echogenic SN area; mean ± SD; cm^2	0.18 ± 0.07	0.17 ± 0.05	0.390
Hyperechogenic SN – digitized analysis; *n* (%)	2 (4.0)	2 (3.8)	1.000
Hyperechogenic SN – manual measurement; *n* (%)	5 (20.0)	1 (3.9)	0.070

BR – brainstem raphe; SD – standard deviation; SN – substantia nigra

Table 3
Differences and correlation in followed factors between panic disorder patients with normal and pathological TCS findings of brainstem raphe.

	Normal BR (visual)	Disrupted BR (visual)	*p* Value	Normal BR (digitized analysis)	Hypoechogenic BR (digitized analysis)	*p* Value	Spearman correlation coefficient (digitized analysis)	*p* Value
Mean age ± SD; years	40.5 ± 7.1	36.8 ± 8.3	0.242	36.3 ± 7.3	39.6 ± 7.9	0.304	−0.469	0.037
Male gender; *n* (%)	3 (37.5)	7 (41.2)	1.0	3 (25.0)	7 (53.8)	0.151	NA	NA
BAI; median, (IQR)	32.5 (15.75–41.25)	25 (14.5–36)	0.366	31 (27.25–42)	25 (12–33)	0.064	0.451	0.046
BDI; median,(IQR)	19 (4.75–20)	19 (7.5–21.5)	0.726	18.5 (12.75–20.5)	19 (4–21)	0.234	0.120	0.613
PDSS; median (IQR)	15.5 (9.75–18.75)	14 (12–16.5)	0.704	16.5 (11.75–18)	14 (13–16)	0.331	0.060	0.803
CGI; median (IQR)	5.5 (4–6)	5 (4.5–6)	0.830	6 (4–6)	5 (5–6)	0.560	0.053	0.824
HAMA; median (IQR)	18.5 (12.75–27.75)	17 (15.5–21)	0.977	19.5 (15.75–25)	16 (15–18)	0.074	0.191	0.420
HAMD-17; median (IQR)	12.5 (8.25–18.5)	13 (10–17.5)	0.620	12.5 (11.75–18.5)	14 (10–17)	0.821	0.049	0.837
SDS; median (IQR)	23 (10–30.75)	23 (15.5–27.5)	0.930	25.5 (20–29.25)	20 (14–24)	0.172	0.237	0.315
DES; median (IQR)	120 (34.25–203.25)	183 (87.5–359)	0.145	107.5 (59.75–232)	183 (135–299)	0.854	−0.241	0.307
SDQ-20; median (IQR)	24 (22.25–26.75)	23 (21.5–25.5)	0.500	23.5 (22–26)	24 (20–25)	0.794	0.094	0.694
Right-handedness; *n* (%)	1 (12.5)	7 (41.2)	0.205	2 (16.7)	6 (46.2%)	0.254	NA	NA
Education level (basic/secondary/higher or university education); *n* (%)	1 (12.5)/6 (75.0)/1 (12.5)	3 (17.6)/12 (70.6)/2 (11.8)	1.0	3 (25)/8 (66.7)/1 (8.3)	1 (7.7)/10 (76.9)/2 (15.4)	0.452	NA	NA
Smoking (no / 1–5 per day / > 5 per day); *n* (%)	6 (75.0)/0 (0)/2 (25.0)	5 (29.4)/2 (11.8)/10 (58.8)	0.078	6 (50)/1 (8.3)/5 (41.7)	5 (38.5)/1 (7.7)/7 (53.8)	0.754	NA	NA
Alcohol consumption (no / ≤ 2 units per week / > 2 units per week); *n* (%)	4 (50.0)/3 (37.5)/1 (12.5)	10 (58.8)/5 (29.4)/2 (11.8)	0.771	5 (41.7)/6 (50.0)/1 (8.3)	9 (69.2)/2 (15.4)/2 (15.4)	0.486	NA	NA
Number of used antidepressive drugs; mean ± SD	1.9 ± 0.6	1.5 ± 1.4	0.155	1.5 ± 0.6	1.8 ± 1.5	0.587	−0.067	0.780
Mean duration of panic disorders ± SD; years	8.0 ± 3.6	3.6 ± 5.4	0.004	7.4 ± 5.9	2.8 ± 2.9	0.034	0.295	0.207
Mean duration of agoraphobia ± SD; years	7.9 ± 7.3	2.7 ± 4.3	0.072	6.7 ± 6.2	2.2 ± 4.2	0.072	0.212	0.371
Mean treatment duration ± SD; years	4.1 ± 4.3	1.1 ± 1.8	0.025	2.5 ± 3.3	1.7 ± 2.8	0.521	0.026	0.915

BAI – Beck Anxiety Inventory, BDI – Beck Depression Inventory, BR – brainstem raphe, CGI – Clinical Global Impression, DES – Dissociative Experiences Scale, HAMA – Hamilton Anxiety Scale, HAMD-17–17-item Hamilton Depression Scale, PDSS – Panic Disorder Severity Scale, SD – standard deviation, SDQ-20 – Somatoform Dissociation Questionnaire, SDS – Sheehan Disability Scale, TCD – transcranial sonography.

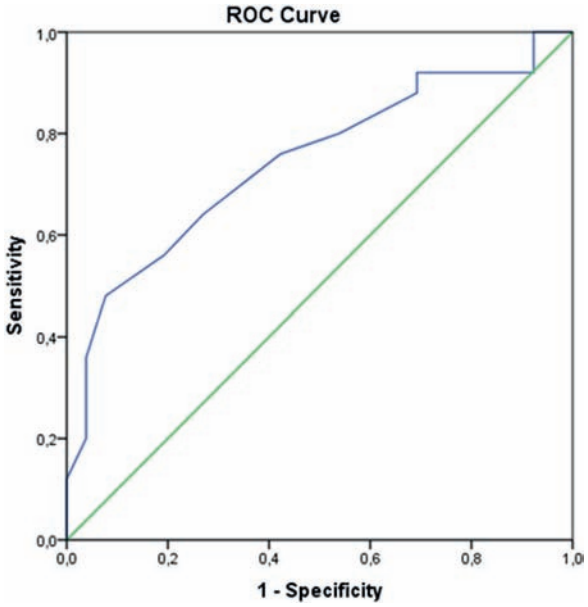

Fig. 3. Receiver operating characteristic (ROC) curve for panic disorder diagnosis.

a positive correlation between BR echogenicity and severity of anxiety on the BAI score. A similar relationship has been reported in patients with depressive disorders in whom a (visually assessed) reduced BR echogenicity was related to a lower mean score on the HAMD scale (Walter et al., 2007c). Applying the same digitized image analysis software tool, the echogenicity values of other brain structures, for example, the basal ganglia, were clearly correlated with independently obtained disease severity scores and postmortem histochemical data (Walter et al., 2014a, 2014b). It needs to be elucidated in further studies whether BR abnormalities detected on TCS are related to disease severity in depressive and panic disorder patients. Recent TCS study on patients with major depressive disorder showed an association of BR hypoechogenicity with higher frequency of suicidal ideation (Budisic et al., 2010), but no data are available for patients with panic disorder without depression.

Several limitations of the present study should be mentioned. First, a limited number of participants were enrolled. Second, the TCS examination was performed by a single well-trained investigator. Less-trained investigators could have difficulties in adequately imaging BR and SN within the brainstem. Magnetic resonance–TCS fusion imaging with virtual navigation technology could be helpful in this case. Third, the quality of the TCS images was influenced by the quality of the ultrasound machine and its preset parameters. For digital analysis, the optimal quality of the TCS image was evaluated by the developed software. Finally, strictly standardized ultrasound system settings had to be used. In particular, gross changes in settings influencing the image brightness (e.g. gain or dynamic range) could potentially lead to bias.

5. Conclusion

Alteration of BR echogenicity on TCS, thought to reflect an alteration of the central serotonergic system, is frequently detected in patients with panic disorder. Further studies are warranted to confirm this finding, and to establish whether these changes are related to disease severity, presence of different disease subtypes and, responsivity to SSRIs and other therapeutic approaches.

Contributorship statement

Petr Šilhán, MD: study conception and design, psychiatric examinations, data collection, paper preparation.

Monika Jelínková, MD: study conception and design, TCS examinations, data collection, visual evaluation of TCS images, paper preparation.

Prof. Uwe Walter, MD, Ph.D.: revising manuscript critically for important intellectual content.

Prof. Ján Pavlov Praško, MD, Ph.D.: data interpretation, paper preparation.

Prof. Roman Herzig, MD, Ph.D., FESO: revising manuscript critically for important intellectual content.

Kateřina Langová, MA, Ph.D.: statistic analysis and interpretation of data.

Assoc. Prof. David Školoudík, MD, Ph.D.: digital image analyses, drafting of the manuscript and final approval of the manuscript submitted.

Competing interest statement

Nothing to declare.

References

American Psychiatric Association, 2000. Diagnostic and Statistical Manual of Mental Disorders, Fourth Edition, Text Revision. American Psychiatric Press, Washington, DC.

Baldwin, D.S., Anderson, I.M., Nutt., D.J., Bandelow, B., Bond, A., Davidson, J.R., den Boer, J.A., Fineberg, N.A., Knapp, M., Scott, J., Wittchen, H.U., 2005. Evidence-based guidelines for the pharmacological treatment of anxiety disorders: recommendations from the British Association for Psychopharmacology. J. Psychopharmacol. 19, 567–596.

Becker, G., Becker, T., Struck, M., Lindner, A., Burzer, K., Retz, W., Bogdahn, U., Beckmann, H., 1995. Reduced echogenicity of brainstem raphe specific to unipolar depression: a transcranial color-coded real-time sonography study. Biol. Psychiatry 38, 180–184.

Becker, G., Berg, D., Lesch, K.P., Becker, T., 2001. Basal limbic system alteration in major depression: a hypothesis supported by transcranial sonography and MRI findings. Int. J. Neuropsychopharmacol. 4, 21–31.

Bell, C.J., Nutt, D.J., 1998. Serotonin and panic. Br. J. Psychiatry 172, 465–471.

Berg, D., Behnke, S., Walter, U., 2006. Application of transcranial sonography in extrapyramidal disorders: Updated recommendations. Ultraschall der Medizin 27, 12–19.

Berg, D., Godau, J., Walter, U., 2008. Transcranial sonography in movement disorders. Lancet Neurol. 7, 1044–1055.

Berg, D., Supprian, T., Hofmann, E., Zeiler, B., Jager, A., Lange, K.W., Reiners, K., Becker, T., Becker, G., 1999. Depression in Parkinson's disease: brainstem midline alteration on transcranial sonography and magnetic resonance imaging. J. Neurol. 246, 1186–1193.

Blahuta, J., Soukup, T., Jelinkova, M., Bartova, P., Cermak, P., Herzig, R., Skoloudik, D., 2013. A new program for highly reproducible automatic evaluation of the substantia nigra from transcranial sonographic images. Biomed. Pap. Med. Fac. Univ. Palacky Olomouc Czech Repub. 2013 (April), 22 (Epub ahead of print).

Budisic, M., Karlovic, D., Trkanjec, Z., Lovrencic-Huzjan, A., Vukovic, V., Bosnjak, J., Demarin, V., 2010. Brainstem raphe lesion in patients with major depressive disorder and in patients with suicidal ideation recorded on transcranial sonography. Eur. Arch. Psychiatry Clin. Neurosci. 260, 203–208.

Eser, D., Leicht, G., Baghai, T., Pogarell, O., Schüle, C., Karch, S., Nothdurfter, C., Rupprecht, R., Mulert, C., 2009. Impact of loudness dependency of auditory evoked potentials on the panic response to CCK-4. J. Psychiatr. Res. 43, 393–400.

Kessler, R.C., Berglund, P., Demler, O., Jin, R., Koretz, D., Merikangas, K.R., Rush, A.J., Walters, E.E., Wang, P.S., 2003. National comorbidity survey replicationThe epidemiology of major depressive disorder: results from the national comorbidity survey replication (NCS-R). J. Am. Med. Assoc. 289, 3095–3105.

Krogias, C., Hoffmann, K., Eyding, J., Scheele, D., Norra, C., Gold, R., Juckel, G., Assion, H.J., 2011a. Evaluation of basal ganglia, brainstem raphe and ventricles in bipolar disorder by transcranial sonography. Psychiatry Res. 194, 190–197.

Krogias, C., Strassburger, K., Eyding, J., Gold, R., Norra, C., Juckel, G., Saft, C., Ninphius, D., 2011b. Depression in patients with Huntington disease correlates with alterations of the brain stem raphe depicted by transcranial sonography. J. Psychiatry Neurosci. 36, 187–194.

Mavrogiorgou, P., Nalato, F., Meves, S., Luksnat, S., Norra, C., Gold, R., Juckel, G., Krogias, C., 2013. Transcranial sonography in obsessive–compulsive disorder.

J. Psychiatr. Res. 47, 1642–1648.
Mijajlovic, M.D., 2010. Transcranial sonography in depression. Int. Rev. Neurobiol. 90, 259–272.
Nash, J.R., Sargent, P.A., Rabiner, E.A., Hood, S.D., Argyropoulos, S.V., Potokar, J.P., Grasby, P.M., Nutt, D.J., 2008. Serotonin 5-HT1A receptor binding in people with panic disorder: positron emission tomography study. Br. J. Psychiatry 193, 229–234.
Neumeister, A., Bain, E., Nugent, A.C., Carson, R.E., Bonne, O., Luckenbaugh, D.A., Eckelman, W., Herscovitch, P., Charney, D.S., Drevets, W.C., 2004. Reduced serotonin type 1A binding in panic disorder. J. Neurosci. 24, 589–591.
Park, Y.M., Lee, S.H., Kim, S., Bae, S.M., 2010. The loudness dependence of the auditory evoked potential (LDAEP) in schizophrenia, bipolar disorder, major depressive disorder, anxiety disorder, and healthy controls. Prog. Neuropsychopharmacol. Biol. Psychiatry 34, 313–316.
Sheehan, D.V., Lecrubier, Y., Sheehan, K.H., Amorim, P., Janavs, J., Weiller, E., Hergueta, T., Baker, R., Dunbar, G.C., 1998. The mini-international neuropsychiatric interview (M.I.N.I.): the development and validation of a structured diagnostic psychiatric interview for DSM-IV and ICD-10. J. Clin. Psychiatry 59 (Suppl. 20), 22–33.
Skoloudik, D., Jelinkova, M., Blahuta, J., Cermak, P., Soukup, T., Bartova, P., Langova, K., Herzig, R., 2014. Transcranial sonography of the substantia nigra: digital image analysis. AJNR Am. J. Neuroradiol. 35, 2273–2278.
Walter, U., Behnke, S., Eyding, J., Niehaus, L., Postert, T., Seidel, G., Berg, D., 2007a. Transcranial brain parenchyma sonography in movement disorders: state of the art. Ultrasound Med. Biol. 33, 15–25.
Walter, U., Hoeppner, J., Prudente-Morrissey, L., Horowski, S., Herpertz, S.C., Benecke, R., 2007b. Parkinson's disease-like midbrain sonography abnormalities are frequent in depressive disorders. Brain 130, 1799–1807.
Walter, U., Krolikowski, K., Tarnacka, B., Benecke, R., Czlonkowska, A., Dressler, D., 2005. Sonographic detection of basal ganglia lesions in asymptomatic and symptomatic Wilson disease. Neurology 64, 1726–1732.
Walter, U., Prudente-Morrissey, L., Herpertz, S.C., Benecke, R., Hoeppner, J., 2007c. Relationship of brainstem raphe echogenicity and clinical findings in depressive states. Psychiatry Res. 155, 67–73.
Walter, U., Blitzer, A., Benecke, R., Grossmann, A., Dressler, D., 2014a. Sonographic detection of basal ganglia abnormalities in spasmodic dysphonia. Eur. J. Neurol. 21, 349–352.
Walter, U., Skowrońska, M., Litwin, T., Szpak, G.M., Jabłonka-Salach, K., Skoloudík, D., Bulska, E., Członkowska, A., 2014b. Lenticular nucleus hyperechogenicity in Wilson's disease reflects local copper, but not iron accumulation. J. Neural Trans. 121, 1273–1279.

7. Comparison between uroflowmetry and sonouroflowmetry in recording of urinary flow in healthy men

Krhut J, Gärtner M, Sýkora R, Hurtík P, Burda M, Luňáček L, Zvarová K, Zvara P

Originally published in International Journal of Urology, 2015, vol. 22, no. 8, p. 761-765.

INTERNATIONAL JOURNAL OF UROLOGY
International Journal of Urology (2015) **22**, 761–765 doi: 10.1111/iju.12796

Original Article: Clinical Investigation

Comparison between uroflowmetry and sonouroflowmetry in recording of urinary flow in healthy men

Jan Krhut,[1,2] Marcel Gärtner,[3] Radek Sýkora,[1] Petr Hurtík,[4] Michal Burda,[4] Libor Luňáček,[1] Katarína Zvarová[5] and Peter Zvara[2,6]

[1]Department of Urology, University Hospital, [2]Department of Surgical Studies, Ostrava University, [3]Department of Obstetrics and Gynecology, University Hospital, and [4]Institute for Research and Applications of Fuzzy Modeling, Centre of Excellence IT4Innovations, Ostrava University, Ostrava, Czech Republic; [5]Department of Physiology, Slovak Medical University, Bratislava, Slovakia; and [6]Department of Surgery, University of Vermont, Burlington, Vermont, USA

Abbreviations & Acronyms
PCC = Pearson's correlation coefficient
Q_{ave} = average flow rate
Q_{max} = maximum flow rate
SUF = sonouroflowmetry
UF = uroflowmetry

Correspondence: Jan Krhut M.D., Ph.D., Department of Urology, University Hospital, Tr. 17. listopadu 1790, 708 52 Ostrava, Czech Republic. Email: jan.krhut@fno.cz

Received 20 January 2015; accepted 22 March 2015
Online publication 18 May 2015

Objectives: To evaluate the accuracy of sonouroflowmetry in recording urinary flow parameters and voided volume.
Methods: A total of 25 healthy male volunteers (age 18–63 years) were included in the study. All participants were asked to carry out uroflowmetry synchronous with recording of the sound generated by the urine stream hitting the water level in the urine collection receptacle, using a dedicated cell phone. From 188 recordings, 34 were excluded, because of voided volume <150 mL or technical problems during recording. Sonouroflowmetry recording was visualized in a form of a trace, representing sound intensity over time. Subsequently, the matching datasets of uroflowmetry and sonouroflowmetry were compared with respect to flow time, voided volume, maximum flow rate and average flow rate. Pearson's correlation coefficient was used to compare parameters recorded by uroflowmetry with those calculated based on sonouroflowmetry recordings.
Results: The flow pattern recorded by sonouroflowmetry showed a good correlation with the uroflowmetry trace. A strong correlation (Pearson's correlation coefficient 0.87) was documented between uroflowmetry-recorded flow time and duration of the sound signal recorded with sonouroflowmetry. A moderate correlation was observed in voided volume (Pearson's correlation coefficient 0.68) and average flow rate (Pearson's correlation coefficient 0.57). A weak correlation (Pearson's correlation coefficient 0.38) between maximum flow rate recorded using uroflowmetry and sonouroflowmetry-recorded peak sound intensity was documented.
Conclusions: The present study shows that the basic concept utilizing sound analysis for estimation of urinary flow parameters and voided volume is valid. However, further development of this technology and standardization of recording algorithm are required.

Key words: sound recording, urinary flow, voided volume, wireless data transfer.

Introduction

Voiding dysfunction is highly prevalent and has a major impact on the quality of life of a large proportion of men. UF is a widely used non-invasive test for evaluation of bladder emptying.[1] It is carried out on an outpatient basis, at specified procedure areas and involves having the person urinate into the uroflowmeter often at a predetermined time. This process is unnatural and requires "on-demand" voiding often with either low or very high bladder filling. It leads to significant test-to-test variability. It has been therefore recommended that uroflowmetry should be repeated, which requires time-consuming and costly repeated clinic visits.[2,3] This is the reason why the demand for smaller, more practical devices has grown and led to the emergence of portable uroflowmeters. These have not been fully adopted into routine practice, because they are costly and difficult to operate, which is especially troublesome for elderly patients.[4]

SUF represents a new approach to recording urinary flow patterns and measuring of urinary flow parameters. It captures the sound generated when urine stream is hitting the water level in the toilet bowl. It then uses a web-based algorithm to store the sound file in a digital form on a secure website, where it is subsequently analyzed. It uses a physical principle adopted from technologies that have been developed for estimation of the intensity of rain fall on a large body of water or the flow through turbines in hydroelectric plants.[5] The literature data describing attempts

to analyze sound associated with urine flow in urology exist; however, they are sparse, with the last article dating back to 1991.[6] The goal of the present pilot study was to compare the urinary flow parameters acquired using SUF with those recorded by standard uroflowmetry in healthy male volunteers in controlled settings.

Methods

Preclinical testing

In the initial preclinical experiments, we tested a number of cellular phones in order to select the type, with hardware parameters optimal for recording of the sound produced by the urinary stream falling on the water surface. We designed a set-up in which a stream with a constant flow rate was falling onto the water level in the collecting chamber filled with 3000 mL of water, and positioned on top of the gravimetric uroflowmetry device Flowmaster (MMS, Enschede, the Netherlands). Three different flow rates (6, 20, 60 mL/s) were tested. We carried out multiple synchronous UF/SUF recordings. We then compared the UF-recorded flow parameters and the pattern of the trace with a related sound, recorded with SUF. The experimental setting allowed for identification of parameters that can significantly modify the sound signal intensity. We tested the distance between the sound source and the microphone, the height of the stream, depth of the water in the receptacle, direction of the urine stream as well as the size of the room in which the recording was carried out. In addition, significant variability in the quality of the sound recording was noted between individual cell phone and smart phone types. Based on these experiments, we selected a Samsung GT-B2710 (Samsung, Seoul, Korea) for the use in the subsequent clinical trial. Trace patterns and parameters recorded using this cell phone produced the highest consistency and best correlation with UF recordings among the tested phone units.

Clinical trial

A total of 25 healthy male volunteers (age 18–63 years) were included in the study. All study procedures were approved by the institutional review board of the University Hospital, Ostrava, Czech Republic, and the study conformed to the provisions of the Declaration of Helsinki (as revised in Edinburgh 2000). After giving informed consent, participants were asked to carry out the uroflowmetry synchronous with sound recording using standardized conditions that included use of a cell phone that was selected in the preclinical portion of the study. A constant distance between the phone and the water level in the collecting device was used, with the phone positioned on the table next to the participant, 150 cm from the water level. All men carried out the urination in standing position when experiencing a normal desire to void. The experimental setting is shown in Figure 1.

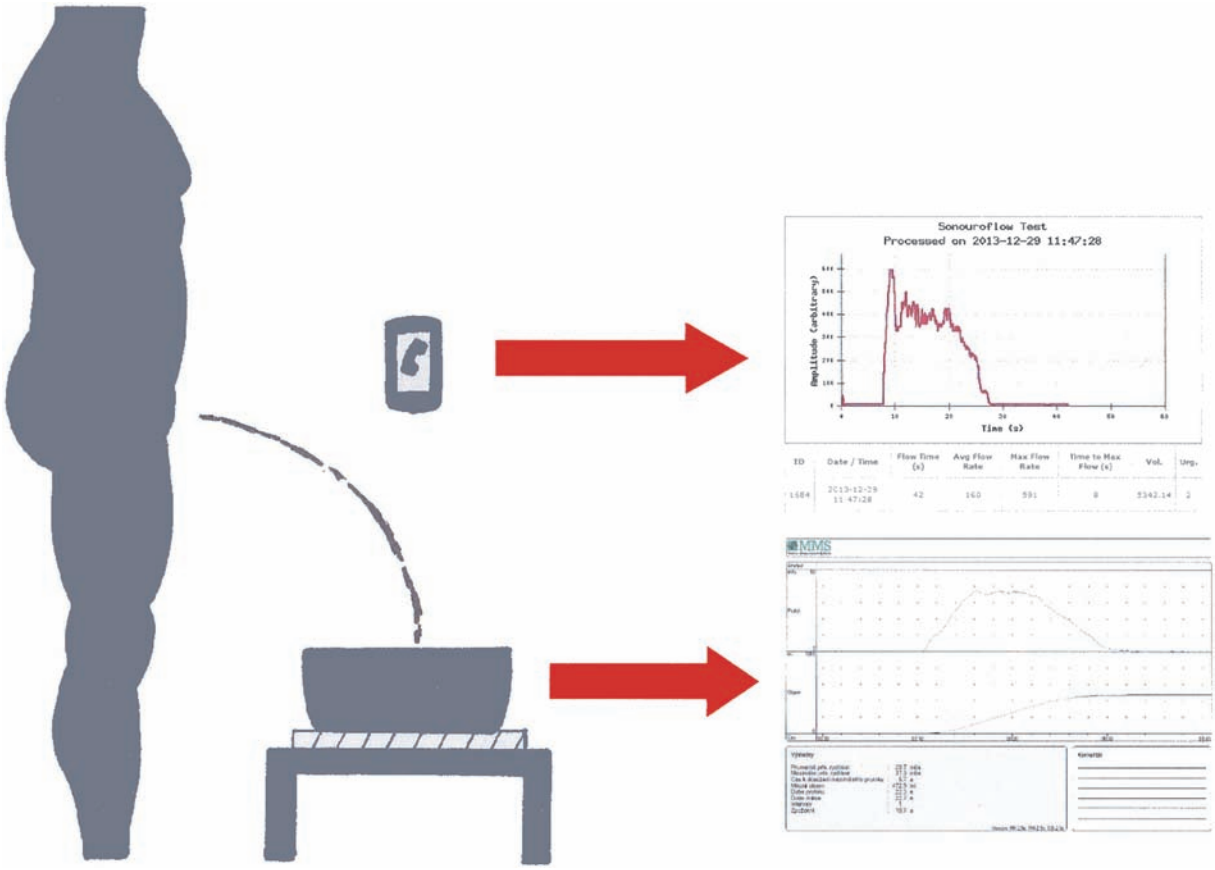

Fig. 1 Experimental setting.

Data analysis

From a total of 188 recordings, 34 were excluded from the final analysis, because of voided volume <150 mL, or technical problems encountered during recording. Amplitude of the sound was then recorded from the remaining SUF records and visualized in a form of a trace representing the intensity of the sound signal over time. A median convolution technique was applied to smooth the data plot and suppress sound artifacts generated during the sound signal recording. This allowed us to eliminate an artificial spike at the beginning of each SUF recording. Subsequently the matching datasets of UF and SUF were compared as follows: flow time recorded using UF was compared with the duration of the sound signal recorded by SUF; UF-recorded voided volume was compared with the calculated area under the SUF curve; and UF-recorded Q_{ave} and Q_{max} were compared with the average and peak intensity of the sound signal.

Statistical analysis

A linear model was fitted to calculate the urinary flow parameters and voided volume from data obtained by SUF. PCC was used to compare the parameters recorded by UF with those calculated based on SUF recordings. A PCC value of >0.7 was considered to be indicative of a strong correlation, 0.5– 0.7 signified a moderate correlation and PCC 0.3–0.5 was indicative of a weak correlation. In addition, the error between SUF and UF was analyzed and calculated as the difference between UF-measured and SUF-estimated parameters. The standard deviation of the error was an indicator of accuracy. Approximately 68% of all UF-parameter values fell within the interval of the estimated SUF-parameter ±standard deviation of the error. A 95% confidence interval of the error specifies the interval that includes 95% of all cases.

Results

Urinary flow pattern

The flow pattern recorded by SUF showed a good visual correlation with the UF trace. The artifact (spike) at the beginning of each recording was highly reproducible and was subsequently filtered out by the median convolution filter (Fig. 2).

Correlation between the flow time, flow parameters and voided volume

A strong correlation (PCC 0.87) was documented between UF recorded flow time and duration of the sound signal recorded with SUF. A moderate correlation (PCC 0.68) was observed in voided volume measured by UF and voided volume determined by calculating the area under the SUF curve. The values calculated using SUF showed a moderate correlation to UF-recorded parameters for Q_{ave} (PCC 0.57) and a weak correlation (PCC 0.38) for Q_{max}. These two values were calculated based on recorded average and peak sound intensity, respectively. The relationship between parameters obtained by either UF or SUF for each individual test are shown using scattergrams (Figs 3–6). Means and standard deviations of all recorded UF parameters as well as the PCC, standard deviation of the error and confidence intervals of the error are summarized in Table 1. Error is defined as the difference between flow parameters and voided volume measured by UF and those estimated by SUF.

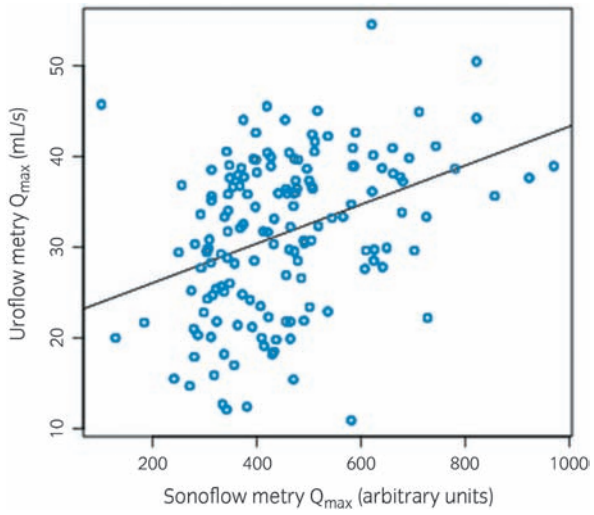

Fig. 3 Scattergram representing the correlation between Q_{max} recorded by UF (*y*-axis) and corresponding Q_{max} estimated by SUF (*x*-axis).

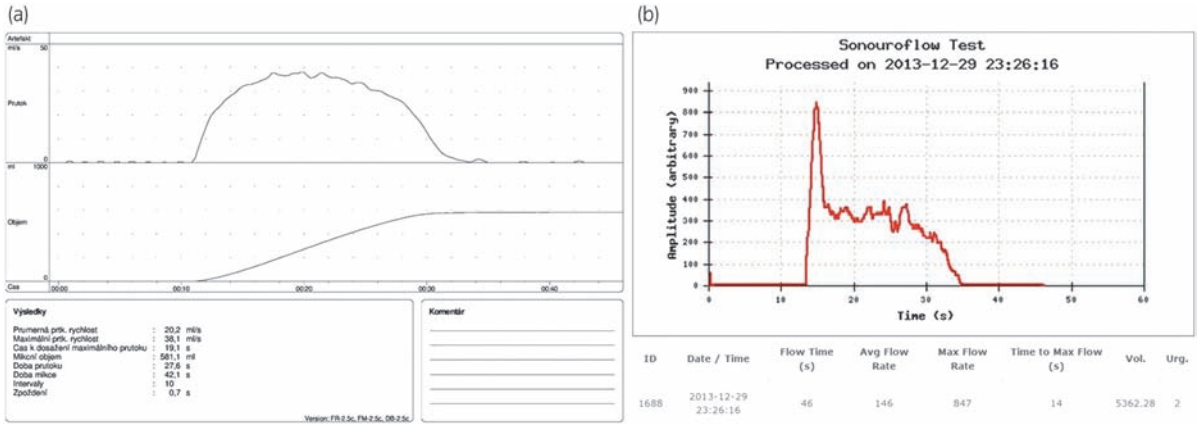

Fig. 2 Side-by-side comparison between the recordings of a single micturition. (a) Uroflowmetry trace. (b) Sound generated during micturition, recorded by a telephone, electronically analyzed and transformed into a trace – sonourogram.

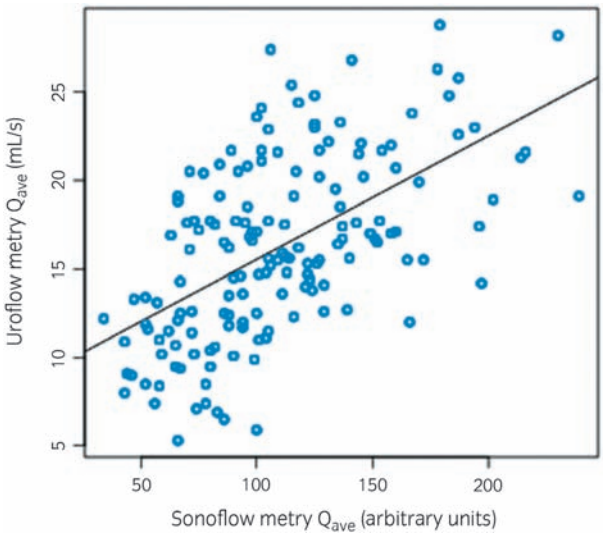

Fig. 4 Scattergram representing the correlation between Q_{ave} recorded by UF (*y*-axis) and corresponding Q_{ave} estimated by SUF (*x*-axis).

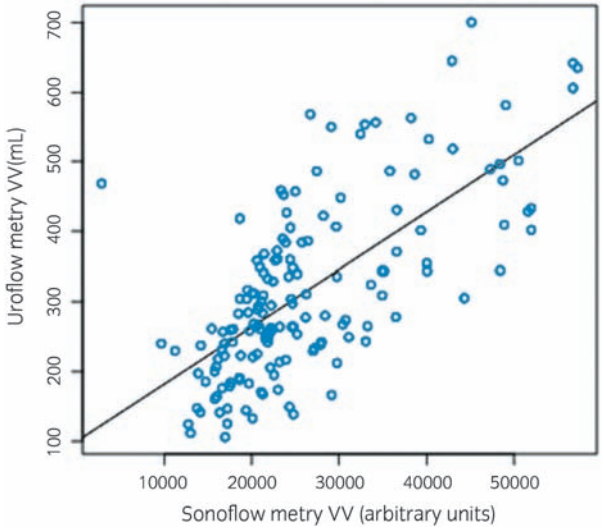

Fig. 5 Scattergram representing the correlation between voided volume (VV) recorded by UF (*y*-axis) and corresponding voided volume estimated based on SUF area under the curve (*x*-axis).

Discussion

The present pilot study documents that that intensity of the sound associated with urine stream falling on the water level in a toilet bowl could be used to estimate urinary flow parameters and voided volume. SUF therefore has a potential to become a user friendly, reliable and portable method for electronic recording of voiding pattern, voided volume and urinary flow parameters.

The idea of using sound analysis in the diagnosis of voiding dysfunction is not new. It was anecdotally mentioned a long time ago that urologists attempted to detect lower urinary tract dysfunction simply by listening to the patient voiding. Attempts to quantify the relationship between the sound of the urine flow and the urinary flow pattern have been described previously.

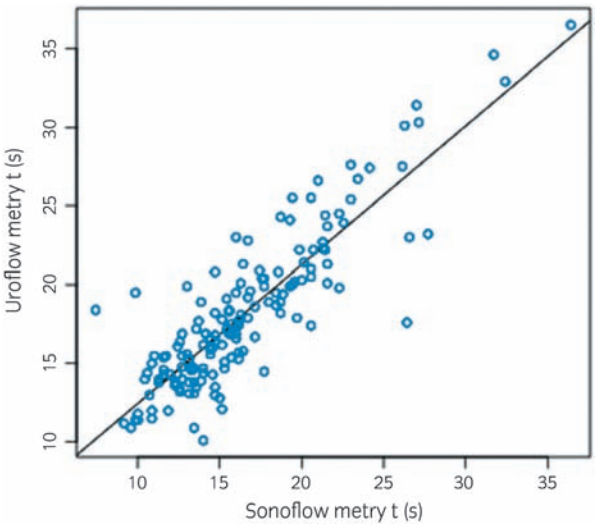

Fig. 6 Scattergram representing the correlation between flow time (t) recorded by UF (*y*-axis) and corresponding duration of the sound signal obtained by SUF (*x*-axis).

Table 1 Correlation between the flow time, flow parameters and voided volume

Variable	Mean	SD	PCC	Error St Dev	Error Conf Int95
Q_{max}	34.53	8.61	0.38	7.97	±15.754
Q_{ave}	16.23	5.10	0.57	4.18	±8.258
Voided volume	315.16	126.84	0.68	92.41	±182.573
Flow time	18.15	4.87	0.87	2.39	±4.726

Koiso *et al*. used a sensor positioned on the surface of the perineum of 25 men to record the sound of urine flowing through the urethra.[6] Using spectral analysis, they detected the flow turbulence in patients who were believed to have a bladder outflow obstruction and no such turbulence in healthy individuals. Although authors studied this technique in a comprehensive manner and published several communications, this technique had never become a part of routine practice. A major limitation of the present study was an absence of objective verification of bladder outflow obstruction.

The present results show a strong correlation between UF and SUF in flow time, and a moderate correlation with respect to estimation of the voided volume and Q_{ave}. The correlation in Q_{max} was weak. The standard deviation in the error (differences between the UF-measured and SUF-estimated voided volume and Q_{max}) was approximately 25–30%.

We acknowledge that at this stage of the development of this method, the level of accuracy is clearly inferior to that obtained by UF. We, however, suggest that the portability and ease of use of this technique leads to substantial advantages. It allows for multiple recordings at home, under natural conditions, reducing intra-individual test-to-test variability and limiting the need for hospital visits.[7] At this time, we believe that SUF could benefit patients in several clinical situations. Those include a possibility of remote evaluation of men undergoing the trial without catheter after acute urinary retention, and in the treatment follow up of patients receiving medical treatment for lower urinary tract symptoms. Even in the absence of the

exact quantification of the urinary flow parameters, the SUF-determined flow pattern combined with the estimated voided volume could identify patients in need of additional detailed evaluation and treatment.

The present trial identified several technical problems that could lead to improvements of SUF accuracy if solved. The most fundamental are related to the cell phone microphone technology and variation in quality of mobile network reception. The majority of recently released cell phones are equipped with a noise cancellation system. This feature is designed to filter out the background noise that does not resemble a human voice. This feature proved to have a detrimental effect on the accuracy of the parameters recorded with SUF. The laboratory part of this trial showed that more advanced cell phone technology (especially that used in latest generations of smart phones) is associated with an unacceptably high degree of signal processing, making these devices unsuitable for SUF. Use of cell phone technology makes this method dependent on the availability of the mobile signal (reception). Reduced signal quality led to generation of random artifacts in the course of SUF recording. We believe that both these limitations necessitate changing the platform used for recording to a specialized recording device using a designated microphone without artificial sound signal modulation.

The sound that SUF records and analyzes is the result of complex physical events that take place during the contact of urine with the water surface. The majority of the sound is attributed to oscillations of air bubbles, which form just below the water surface. This splashing phenomenon is generated by a large number of various size bubbles, resulting in wide acoustic spectra. The algorithm used accounts for this complexity. This is the reason why the SUF data could not have been expressed in decibels, but rather arbitrary units had to be used. Findings from the acoustic literature as well as the present data show that flow rate is a dominant parameter determining the sound intensity; however, we recognize that SUF accuracy and repeatability is dependent on a number of factors. The most important proved to be the microphone distance from the sound source and the height of the stream.[5] A modality allowing standardization of these parameters would need to be developed as well, before SUF could be used as a standard diagnostic tool.

The present study supports the feasibility of the basic concept of using sound analysis for estimation of urinary flow parameters and voided volume. However, it also identifies areas in which this technology needs improvement.

Acknowledgments

The authors thank Dr Jerry Blaivas for valuable input, Travis Mann-Gow for critical review and editorial assistance, and Jiri Krhut for supplying the schematic drawing. The work of Petr Hurtik and Michal Burda was supported by the European Regional Development Fund, Project of IT4Innovations Centre of Excellence (CZ.1.05/1.1.00/02.0070, VP6).

Conflict of interest

P Zvara and K Zvarova are partners in the commercial enterprise that developed and patented this technology. The remaining authors declare no conflict of interest.

References

1 Gravas S, Descazeaud A, Drake M *et al*. Guidelines on the Management of Non-Neurogenic Male Lower Urinary Tract Symptoms (LUTS), incl. Benign Prostatic Obstruction (BPO), EAU, 2014.

2 Kranse R, van Mastrigt R. Causes for variability in repeated pressure-flow measurements. *Urology* 2003; **61**: 930–4.

3 Reynard JM, Yang Q, Donovan JL *et al*. The ICS-'BPH' Study: uroflowmetry, lower urinary tract symptoms and bladder outlet obstruction. *Br. J. Urol.* 1998; **82**: 619–23.

4 Porru D, Scarpa RM, Prezioso D, Bertaccini A, Rizzi CA. Home and office uroflowmetry for evaluation of LUTS from benign prostatic enlargement. *Prostate Cancer Prostatic Dis.* 2005; **8**: 45–9.

5 Ogcaronuz HM, Prosperetti A. Numerical calculation of the underwater noise of rain. *J. Fluid Mech.* 1991; **228**: 417–42.

6 Koiso K, Nemoto R, Ohtani M. Urophonographic studies of benign prostatic hypertrophy. *J. Urol.* 1991; **145**: 1071–7.

7 Zvarova K, Ursiny M, Giebink T, Liang K, Blaivas JG, Zvara P. Recording urinary flow and lower urinary tract symptoms using sonouroflowmetry. *Can. J. Urol.* 2011; **18**: 5689–94.

8.

Treatment strategies for colorectal carcinoma with synchronous liver metastases: Which way to go?

Ihnát P, Vávra P, Zonča P

Originally published in World Journal of Gastroenterology, 2015, vol. 21, no. 22, p. 7014-7021.

World Journal of Gastroenterology

Submit a Manuscript: http://www.wjgnet.com/esps/
Help Desk: http://www.wjgnet.com/esps/helpdesk.aspx
DOI: 10.3748/wjg.v21.i22.7014

World J Gastroenterol 2015 June 14; 21(22): 7014-7021
ISSN 1007-9327 (print) ISSN 2219-2840 (online)

SYSTEMATIC REVIEWS

Treatment strategies for colorectal carcinoma with synchronous liver metastases: Which way to go?

Peter Ihnát, Petr Vávra, Pavel Zonča

Peter Ihnát, Petr Vávra, Pavel Zonča, Department of Surgical Studies, Faculty of Medicine, University of Ostrava, Ostrava 70300, Czech Republic
Peter Ihnát, Petr Vávra, Pavel Zonča, Department of Surgery, University Hospital Ostrava, Ostrava 70852, Czech Republic

Author contributions: Ihnát P and Zonča P performed the literature search; Ihnát P and Vávra P wrote the paper; Zonča P revised the paper.

Conflict-of-interest: All authors declare that they have no personal, political or financial conflicts of interest.
Data sharing: No additional data are available.

Correspondence to: Peter Ihnát, MD, PhD, MBA, Department of Surgical Studies, Faculty of Medicine, University of Ostrava, Syllabova 19, Ostrava 70300,
Czech Republic. peterihnat@yahoo.com
Telephone: + 42-597-375701
Fax: + 42-597-375054

Received: December 28, 2014
Peer-review started: December 29, 2014
First decision: January 22, 2015
Revised: February 6, 2015
Accepted: April 3, 2015
Article in press: April 3, 2015
Published online: June 14, 2015

Abstract

AIM: To offer an up-to-date review of all available treatment strategies for patients with synchronous colorectal liver metastases (CLM).

METHODS: A comprehensive literature search was performed to identify articles related to the management of patients with synchronous CLM. A search of the electronic databases PubMed, MEDLINE, and Google Scholar was conducted in September 2014. The following search terms were used: synchronous colorectal liver metastases, surgery, stage Ⅳ colorectal cancer, liver-first approach, and up-front hepatectomy. These terms were employed in various combinations to maximize the search. Only articles written in English were included. Particular attention was devoted to studies and review articles that were published within the last six years (2009-2014). Additional searches of the cited references from primary articles were performed to further improve the review. The full texts of all relevant articles were accessed by two independent reviewers.

RESULTS: Poor long-term outcomes of patients with synchronous CLM managed by a traditional treatment strategy have led to questions about the timing and sequence of possible therapeutic interventions. Thus, alternative paradigms called reverse strategies have been proposed. Presently, there are four treatment strategies available: (1) primary first approach (or traditional approach) comprises resection of the primary colorectal tumor followed by chemotherapy; subsequent liver resection is performed 3-6 mo after colorectal resection (provided that CLM are still resectable); (2) simultaneous resection of the primary colorectal tumor and CLM during a single operation presents intriguing options for a highly select group of patients, which can be associated with significant postoperative morbidity; (3) liver-first (or chemotherapy-first) approach comprises preoperative chemotherapy (3-6 cycles) followed by liver resection, adjuvant chemotherapy, and resection of the primary colorectal tumor (it is best suited for patients with

asymptomatic primary tumors and initially unresectable or marginally resectable CLM); and (4) up-front hepatectomy (or "true" liver-first approach) includes liver resection followed by adjuvant chemotherapy, colorectal resection, and adjuvant chemotherapy (strategy can be offered to patients with asymptomatic primary tumors and initially resectable CLM).

CONCLUSION: None of the aforementioned strategies appears inferior. It is necessary to establish individual treatment plans in multidisciplinary team meetings through careful appraisal of all strategies.

Key words: Colorectal cancer; Liver-first approach; Reverse strategy; Simultaneous resection; Up-front hepatectomy

Core tip: There are four treatment strategies available for synchronous liver metastases of colorectal carcinoma (CLM): (1) primary first approach comprises resection of the primary colorectal tumor followed by chemotherapy and liver resection; (2) simultaneous resection of liver and colorectal primary tumor; (3) liver-first (or chemotherapy-first) approach comprises preoperative chemotherapy, liver resection, adjuvant chemotherapy, and resection of the primary colorectal tumor (best for asymptomatic primary tumors and initially unresectable or marginally resectable CLM); and (4) up-front hepatectomy (or "true" liver-first approach) includes liver resection followed by adjuvant chemotherapy and colorectal resection (for asymptomatic primary tumors and initially resectable CLM).

Ihnát P, Vávra P, Zonča P. Treatment strategies for colorectal carcinoma with synchronous liver metastases: Which way to go? *World J Gastroenterol* 2015; 21(22): 7014-7021 Available from: URL: http://www.wjgnet.com/1007-9327/full/v21/i22/7014.htm DOI: http://dx.doi.org/10.3748/wjg.v21.i22.7014

INTRODUCTION

The liver is the most common site of colorectal cancer metastases. At the time of diagnosis, approximately 25% of patients have synchronous colorectal liver metastases (CLM)[1]. These patients are thought to have less favorable cancer biology, and are less likely to become long-term survivors compared to patients with metachronous CLM[2]. The endeavor to improve outcomes of patients with synchronous CLM led to questions about the timing and sequence of possible therapeutic interventions[3,4]. Several alternative treatment strategies have been proposed, such as simultaneous resection, the liver-first approach, and an up-front hepatectomy approach.

A search of the scientific literature shows that there is currently no complex review available that summarizes the pros and cons of all four possible treatment strategies with respect to the management of patients with synchronous CLM. Moreover, authors usually do not clearly distinguish the up-front hepatectomy from the liver-first approach, though several principal distinctions between both strategies are evident.

The aim of the present paper is to offer an up-to-date review of all four available strategies for the treatment of patients with colorectal cancer and synchronous CLM. This article summarizes the current data concerning the rationale, benefits, and potential drawbacks of the particular strategies (primary-first, simultaneous approach, liver-first approach, and up-front hepatectomy).

MATERIALS AND METHODS

A comprehensive literature search was performed to identify articles related to therapeutic strategies for patients with colorectal cancer and simultaneous CLM. The search combined the following terms: synchronous colorectal liver metastases, surgery, stage Ⅳ colorectal cancer, liver-first approach, and up-front hepatectomy. Sources included MEDLINE, PubMed, and Google Scholar databases. Particular attention was devoted to studies and review articles that were published within the last six years (2009-2014).

RESULTS

Current treatment strategies

Although there have been significant improvements in the management of stage Ⅳ colorectal cancer in the last few decades, only radical surgical resection of both the primary tumor and CLM can offer long-term survival for patients presenting with CLM[1,5,6]. Surgery is performed with the intent to achieve minimal intraoperative blood loss and low postoperative morbidity and mortality, because these factors have been shown to compromise not only short-term results, but also long-term outcomes[7-9].

The management of patients with colorectal cancer and synchronous CLM is multimodal and comprises surgery, chemotherapy, and radiotherapy. Multimodality and the need for surgery at the two different sites (colorectal primary tumor and CLM) enable various sequences and timing for therapeutic modalities. Poor long-term outcomes of the traditional treatment strategy (primary-first approach) led to the proposal of alternative paradigms for patient management, called reverse strategies. Presently, four therapeutic strategies are available: the primary-first approach, simultaneous resection, a liver-first approach, and up-front hepatectomy.

Primary-first approach

The primary first approach, often referred to as

the "classical" or "traditional" approach, includes resection of the primary colorectal tumor followed by chemotherapy (plus radiotherapy for rectal primaries). Liver resection is performed 3-6 mo after colorectal resection (provided CLM are still resectable).

The rationale for the primary-first approach is twofold: colorectal primary tumors are thought to be a likely source of subsequent metastases and also the source of symptoms. The main advantage of the strategy is that it avoids potential complications from the primary tumor and decreases the risk of potential progression of the primary tumor during liver surgery or initial chemotherapy[3,4]. Conversely, the main drawback of the primary-first approach is the progression of CLM beyond resectability during the primary tumor resection (especially in patients with postoperative complications after colorectal resection)[3].

Because of frequent CLM progression beyond resectability, only few patients benefit from the traditional strategy. In 2012, analysis based on the LiverMetSurvey revealed that < 30% of patients underwent the complete treatment plan of primary-first strategy (from primary tumor resection to liver resection)[10]. Conversely, reverse strategy enables completion of the treatment plan in almost 80% of patients[3,11].

Simultaneous resection

Simultaneous resection of colorectal primary and synchronous CLM presents an intriguing option for many surgeons. The simultaneous resection can be employed with or without preoperative chemotherapy; adjuvant chemotherapy is applied after the surgery (plus radiotherapy for rectal primaries).

The strategy of simultaneous resection had been proposed in the effort to avoid delaying surgical resection of metastatic liver disease[12]. The main advantage of this strategy is the removal of all macroscopic cancer during a single operation followed by systemic chemotherapy with minimal delay. Conversely, the main disadvantage of this strategy is that it is associated with significantly increased postoperative morbidity and possibly mortality[12-14]. Increased risk of infectious liver complications (due to bacterial contamination from intestinal resection), increased risk of anastomotic complications (due to impaired liver function), and limited extent of feasible liver resection have been reported[13,14]. There is also some evidence that simultaneous resection may have a negative effect on progression-free survival[15].

Several studies have demonstrated that reasonable postoperative morbidity and mortality can be achieved if colorectal resection is combined with minor hepatectomy. In recent series of simultaneous resections, postoperative morbidity in the range of 5% to 48% was reported when minor hepatectomies were performed, and from 33% to 55% when major hepatectomies were performed simultaneously with colorectal resection[13-16]. Perioperative mortality of ⩽ 5% was noted, but a higher number can be expected when major hepatectomies are performed.

Simultaneous resection is best suited for highly select patients; many authors recommend considering simultaneous resection only if one of the intended surgical resections is minor. It is reasonable to perform rectal resection simultaneously only with minor hepatectomy (< 3 segments), or to perform major liver resection (⩾ 3 segments) simultaneously with (right-sided) colon resection[14,16,17]. However, major hepatectomies should be pursued only in very carefully selected patients by an experienced hepatobiliary team. A patient's general health status and comorbidities also have to be considered.

Liver-first (chemotherapy-first) approach

The reverse treatment strategy was first introduced by Mentha *et al*[3] in 2008. The liver first approach comprises initial preoperative chemotherapy (3-6 cycles) followed by liver resection and subsequent resection of the primary colorectal tumor. Chemotherapy (possibly with radiotherapy for rectal primaries) is administered between colorectal and liver resection.

The introduction of modern potent cytotoxic drugs (oxaliplatin-based and irinotecan-based) in combination with targeted agents (directed against epidermal growth factor receptor or vascular endothelial growth factor) resulted in improved tumor response rates (up to 60% of tumors) and prolonged survival of patients with colorectal cancer[16,18]. Effectiveness of modern chemotherapy regimens (in adjuvant settings) led to the application of chemotherapy, also in neoadjuvant settings, for patients with colorectal carcinoma and synchronous CLM. It is believed that the prognosis of patients with stage Ⅳ colorectal cancer is determined mainly by the curability of CLM and not by the primary tumor or its potential complications[3,4,14].

As a matter of fact, preoperative chemotherapy is the initial treatment modality during the liver-first approach, which is why the term "chemotherapy-first" is suggested to be more accurate for this strategy[17]. The expression "chemotherapy-first" emphasizes the main rationale of the reverse strategy, which is to provide early systemic treatment to patients with stage Ⅳ colorectal cancer.

Benefits of the chemotherapy-first approach are: (1) early application of systemic treatment; (2) lowering the risk of CLM progression; and (3) the possibility of CLM downsizing or converting unresectable CLM to resectable.

As stage Ⅳ colorectal cancer presents as systemic disease, it seems reasonable to offer systemic chemotherapy as soon as possible after the diagnosis is established. Moreover, patients with synchronous CLM are supposed to have more aggressive tumors with less favorable cancer biology. By using preoperative

chemotherapy administration, effective systemic treatment is not delayed by colorectal surgery and its possible postoperative complications[3,4,12].

The risk of CLM progression is significantly lower when the chemotherapy-first approach is employed, compared to the traditional strategy[3,12,17]. Furthermore, preoperative chemotherapy offers the opportunity for initial disease control and CLM downsizing. Liver metastasis shrinkage after preoperative chemotherapy enables surgeons to perform more conservative liver surgery more often and to achieve R0 resection in more patients. Preoperative chemotherapy application also allows for the assessment of tumor response to chemotherapy. In theory, another possible advantage of preoperative chemotherapy is the elimination of micrometastatic disease and the eradication of dormant cancer cells[17,19].

Fears of complications arising from unresected primary tumors (such as bleeding, obstruction, or perforation) in the course of initial chemotherapy and liver resection represent principal arguments against the reverse strategy. Nevertheless, primary tumor complications in patients with stage Ⅳ colorectal cancer are very rare according to several studies. The vast majority (> 90%) of patients with initially asymptomatic colorectal primary tumors and synchronous CLM who receive modern chemotherapy regimens never require surgical intervention because of primary tumor-related complications[20]. Besides, Scheer *et al*[21] demonstrated that primary tumor resection provided only minimal palliative benefit to these patients. This is why systemic chemotherapy regimens are advocated as initial treatment modalities for asymptomatic primary tumors with synchronous CLM. If the tumor does not respond to preoperative chemotherapy in patients with initially unresectable CLM, useless colorectal surgery can be avoided[14,19].

Recently, an international multidisciplinary panel generated a consensus concerning the reverse strategy[22]. The most important recommendations were as follows. First, the reverse strategy should be considered for all patients with predominant hepatic disease and asymptomatic primary tumor. Second, preoperative chemotherapy should be offered to patients with asymptomatic colorectal cancer and synchronous CLM (resectable, marginally resectable, and unresectable). Third, at least four courses of first-line chemotherapy should be given. Fourth, the use of doublet or triplex chemotherapy regimens combined with targeted therapy is recommended. Fifth, chemotherapy duration should be as short as possible and liver resection should be performed as soon as technically possible. Lastly, tumor response and patient reassessment should be performed 2 mo after starting chemotherapy.

In the last decade, many (> 400) papers focusing on liver-first strategy evaluation have been published. However, according to several recent systematic reviews[4,17,23], scientific evidence for the justification of the liver-first approach is very limited. For instance, there are no randomized controlled trials, and many papers have very limited scientific validity (such as reviews, case reports, letters, editorials, and abstracts). There are only four cohort retrospective studies reporting outcomes of a total of 121 patients with colorectal cancer and synchronous CLM managed by the liver-first approach[4,17,23]. In these studies, postoperative morbidity was in the range of 11% to 37%; postoperative mortality was < 4%. Disease recurrence rates were 25%-70%; three-year survival rates varied in the range of 41% to 79%, and five-year survival rates were 31%-39%[3,12,24,25]. The majority (66%-81%) of patients completed the entire liver-first strategy treatment plan (preoperative chemotherapy to colorectal resection). This is in contrast to < 30% of patients completing the primary-first strategy[3,10,12,24,25].

The reverse strategy is best suited for patients with an asymptomatic primary tumors and advanced hepatic metastases[4,16,17,22]. There is general agreement that patients with unresectable or borderline resectable CLM should be offered aggressive doublet or triplex chemotherapy regimen combined with targeted therapy as the initial treatment modality, followed by liver resection, if technically amenable. The optimal initial treatment strategy for patients with initially resectable synchronous CLM is debatable.

Up-front hepatectomy

Surgical resection represents the only treatment modality that can offer long-term survival to patients with synchronous resectable CLM. The limited evidence for preoperative (neoadjuvant) chemotherapy employment led to the proposal of an up-front hepatectomy strategy, which is in fact the "true" liver-first approach. The common sequence of up-front hepatectomy strategy comprises liver resection, adjuvant chemotherapy, colorectal resection, and adjuvant chemotherapy. The strategy was originally proposed by Grundmann *et al*[26] in 2008 for patients with asymptomatic colorectal carcinoma and synchronous resectable CLM.

There are several benefits to preoperative chemotherapy administration for the treatment of resectable synchronous CLM: testing tumor chemoresponsiveness, elimination of micrometastatic disease (in theory), and the possibility of tumor shrinkage enabling more conservative liver surgery in some cases; the benefits were discussed in detail in the previous section[11,14,19].

The main drawbacks of preoperative chemotherapy include liver toxicity, missing lesions, and risk of tumor progression. Chemotherapy induces pathologic changes in the liver parenchyma, which are dependent on the number of chemotherapy cycles (such as steatosis, chemotherapy-associated steatohepatitis, and sinusoidal obstruction syndrome). In addition, chemotherapy increases the risk of systemic toxicity, postoperative bleeding, and infection (by inducing neutropenia)[19,27,28]. A recent meta-analysis demonstrated a high variability in the frequency of

chemotherapy-induced hepatotoxicity[18]. Hepatic steatosis was detected after regimens with 5-flurouracil in 6%-76% of patients, steatohepatitis was observed after irinotecan-based regimens in 3%-8% of patients, and sinusoidal obstruction syndrome was noted after oxaliplatin-based regimens in 5%-51% of patients[18]. Chemotherapy-induced liver injury results in worse postoperative outcomes of subsequent liver resections. Increased postoperative morbidity has been demonstrated by several studies, though no impact on postoperative mortality was observed[29-33]. Especially after extended surgical resection performance, preoperative chemotherapy may contribute to the development of liver failure.

CLM that respond well to preoperative chemotherapy may no longer be visible on CT or during surgery. Tumor disappearance was noted in 2%-36% of patients after preoperative chemotherapy[28]. Problematic identification of invisible lesions during surgery is associated with a higher risk of incomplete (non-radical) resection and disease early recurrence[34]. Furthermore, lesion disappearance (on CT scans) does not mean complete pathologic response. Benoist *et al*[19] demonstrated that > 80% of invisible metastases (invisible lesions on CT scans after chemotherapy) contained viable tumor cells at the time of resection. When the "watch and see" policy is applied (after disappearance on imaging techniques), local recurrence was reported in 38%-74% of patients[34,35].

The risk of tumor progression in the course of preoperative chemotherapy is another drawback of its routine use in the management of patients with initially resectable CLM. According to recent systematic reviews and meta-analyses, CLM progression (changing from resectable to unresectable disease) was observed in 7%-37% of patients undergoing preoperative chemotherapy. However, some authors suggest that disease progression during preoperative chemotherapy is a consequence of highly aggressive tumor biology and may in fact prevent unnecessary postoperative surgical morbidity and mortality[36,37].

The European Colorectal Metastases Treatment Group in its Multidisciplinary International Consensus recommends preoperative chemotherapy for patients with initially resectable synchronous CLM[22]. These recommendations are based mainly on the results of the EORTC 40983 trial, which are a slightly misleading. The EORTC trial evaluated outcomes of 364 patients with resectable CLM divided into two groups: (1) patients managed with three cycles of preoperative FOLFOX, liver resection, and three cycles of postoperative FOLFOX; and (2) patients undergoing liver resection alone without chemotherapy. In other words, the EORTC trial unfortunately did not compare the effect of preoperative chemotherapy (patients in the FOLFOX group) with patients undergoing liver resection plus adjuvant chemotherapy (the FOLOFX group was only compared with patients undergoing surgery alone). In the FOLFOX group, there was significantly longer progression-free survival at three years (35.4% *vs* 28.1%), but overall survival was not increased. Moreover, higher numbers of postoperative complications were recorded in the FOLFOX group compared to patients undergoing surgery alone (25% *vs* 16%)[29].

In an effort to overcome the aforementioned handicap of the EORTC trial, several studies have been executed. For instance, Adam *et al*[38] compared 169 patients treated with preoperative chemotherapy with a retrospective group of 1302 patients who underwent surgery and adjuvant chemotherapy; postoperative complications were more frequent in the neoadjuvant group (37% *vs* 24%). No impact on survival or disease-free interval was found in the neoadjuvant group, but improved survival was found in patients treated with surgery and adjuvant chemotherapy. Reddy *et al*[39] published very similar results in favor of adjuvant chemotherapy. Additional studies (with several hundreds of patients) also showed no significant differences between the outcomes of patients receiving preoperative chemotherapy compared to those without preoperative chemotherapy[40-42].

The aforementioned pros and cons of preoperative chemotherapy administration make it difficult to determine which strategy is the best option for patients with synchronous resectable CLM. The need for prospective randomized trials of neoadjuvant *vs* adjuvant chemotherapy is emphasized by all authors. However, recent systematic reviews and meta-analyses focusing on the preoperative chemotherapy evaluation concluded that "routine use of neoadjuvant chemotherapy for patients with clearly resectable lesions is not recommended due to a lack of benefit on survival"[18]. Many authors share the same conviction and recommend performing up-front hepatectomy in patients with synchronous initially resectable CLM[11,14,19,27,40,42-44].

DISCUSSION

Proposal of a decision strategy

With regard to current published data and according to all aforementioned benefits and drawbacks of particular strategies, we propose the following decision treatment scheme for patients with synchronous CLM.

Patients with colorectal cancer and synchronous CLM should undergo careful clinical examination focused on determining a patient's performance status, comorbidities, and tumor stage. It is necessary to establish an individual treatment plan for each patient in a multidisciplinary team meeting that includes experienced colorectal and hepatobiliary surgeons.

The traditional strategy (primary-first approach) is best suited for patients with symptomatic primary tumors and synchronous CLM. Assessment of the simultaneous approach execution should be conducted in patients with limited CLM extent, especially when

one of the intended surgical resections is minor (minor hepatectomy or right-sided colon resection). Patients with unresectable or marginally resectable CLM should be offered the chemotherapy-first approach. The administration of a duplex or triplex chemotherapy regimen combined with targeted therapy is recommended. Evaluation of tumor response and patient reassessment is advised after two months, followed by liver resection if technically amendable. Patients with initially resectable CLM should be offered up-front hepatectomy as a first-line treatment strategy.

The management of patients with colorectal cancer and synchronous CLM is complex and multiple factors must be considered (such as location and extent of primary tumor and CLM, presence of symptoms, patient's general health status, and comorbidities). None of the aforementioned treatment strategies (primary-first, simultaneous resection, chemotherapy-first, or up-front hepatectomy) appears inferior to the others[23]. However, the optimal treatment strategy is still unclear because of limited available evidence[4,17,23]. It is necessary to establish an individual treatment plan for each patient with synchronous CLM in multidisciplinary team meetings through careful appraisal of all strategies with the aim of avoiding unnecessary surgical complications and to achieve long-term cures.

COMMENTS

Background

Although there have been significant improvements in the management of stage Ⅳ colorectal cancer in the last few decades, only radical surgical resection of both the primary tumor and liver metastases can offer long-term survival. The management of patients with colorectal cancer and synchronous colorectal liver metastases (CLM) is multimodal, comprising surgery, chemotherapy, and radiotherapy. Multimodality and the need for surgery at the two different sites (primary colorectal tumor and CLM) enable various sequences and timing for therapeutic modalities.

Research frontiers

A search of the scientific literature shows there is currently no complex review available that summarizes the pros and cons of all four possible treatment strategies with respect to the management of patients with synchronous CLM. Moreover, authors usually do not clearly distinguish the up-front hepatectomy from the liver-first approach, although several principal distinctions between both strategies are evident.

Innovations and breakthroughs

In this paper, the authors offer a comprehensive review of all four different therapeutic strategies that are currently available for patients with synchronous CLM: primary-first approach, simultaneous resection, liver-first approach, and up-front hepatectomy. Authors summarize up-to-date data on the rationale, benefits, and potential drawbacks of the particular strategies. Based on the available published data, authors propose a decision scheme (between particular strategies) for patients with synchronous CLM.

Applications

The present review offers comprehensive insight into current treatment options available for patients with synchronous CLM. The proposed decision scheme may work as a helpful tool for multidisciplinary teams when establishing a treatment plan for particular patients.

Terminology

Primary-first approach comprises resection of colorectal primary followed by chemotherapy and subsequent liver resection. Simultaneous resection is resection of the primary colorectal tumor and CLM during a single operation. Liver-first (or chemotherapy-first) approach comprises preoperative chemotherapy (3-6 cycles) followed by liver resection, adjuvant chemotherapy, and resection of the primary colorectal tumor. Up-front hepatectomy (or "true" liver-first approach) includes liver resection followed by adjuvant chemotherapy, colorectal resection, and adjuvant chemotherapy.

Peer-review

The topic of this review is important, and the publication is well written and readable. The discussion is well organized as findings correspond with the literature.

REFERENCES

1 **McMillan DC**, McArdle CS. Epidemiology of colorectal liver metastases. *Surg Oncol* 2007; **16**: 3-5 [PMID: 17493802]

2 **Tsai MS**, Su YH, Ho MC, Liang JT, Chen TP, Lai HS, Lee PH. Clinicopathological features and prognosis in resectable synchronous and metachronous colorectal liver metastasis. *Ann Surg Oncol* 2007; **14**: 786-794 [PMID: 17103254]

3 **Mentha G**, Roth AD, Terraz S, Giostra E, Gervaz P, Andres A, Morel P, Rubbia-Brandt L, Majno PE. 'Liver first' approach in the treatment of colorectal cancer with synchronous liver metastases. *Dig Surg* 2008; **25**: 430-435 [PMID: 19212115 DOI: 10.1159/000184734]

4 **De Rosa A**, Gomez D, Brooks A, Cameron IC. "Liver-first" approach for synchronous colorectal liver metastases: is this a justifiable approach? *J Hepatobiliary Pancreat Sci* 2013; **20**: 263-270 [PMID: 23325126 DOI: 10.1007/s00534-012-0583-x]

5 **Manfredi S**, Lepage C, Hatem C, Coatmeur O, Faivre J, Bouvier AM. Epidemiology and management of liver metastases from colorectal cancer. *Ann Surg* 2006; **244**: 254-259 [PMID: 16858188]

6 **Van den Eynde M**, Hendlisz A. Treatment of colorectal liver metastases: a review. *Rev Recent Clin Trials* 2009; **4**: 56-62 [PMID: 19149763]

7 **Giuliante F**, Ardito F, Vellone M, Ranucci G, Federico B, Giovannini I, Nuzzo G. Role of the surgeon as a variable in long-term survival after liver resection for colorectal metastases. *J Surg Oncol* 2009; **100**: 538-545 [PMID: 19722234 DOI: 10.1002/jso.21393]

8 **Ito H**, Are C, Gonen M, D'Angelica M, Dematteo RP, Kemeny NE, Fong Y, Blumgart LH, Jarnagin WR. Effect of postoperative morbidity on long-term survival after hepatic resection for metastatic colorectal cancer. *Ann Surg* 2008; **247**: 994-1002 [PMID: 18520227 DOI: 10.1097/SLA.0b013e31816c405f]

9 **Farid SG**, Aldouri A, Morris-Stiff G, Khan AZ, Toogood GJ, Lodge JP, Prasad KR. Correlation between postoperative infective complications and long-term outcomes after hepatic resection for colorectal liver metastasis. *Ann Surg* 2010; **251**: 91-100 [PMID: 19858702 DOI: 10.1097/SLA.0b013e3181bfda3c]

10 **Andres A**, Toso C, Adam R, Barroso E, Hubert C, Capussotti L, Gerstel E, Roth A, Majno PE, Mentha G. A survival analysis of the liver-first reversed management of advanced simultaneous colorectal liver metastases: a LiverMetSurvey-based study. *Ann Surg* 2012; **256**: 772-778; discussion 778-779 [PMID: 23095621 DOI: 10.1097/SLA.0b013e3182734423]

11 **Straka M**, Skrovina M, Soumarova R, Kotasek R, Burda L, Vojtek C. Up front hepatectomy for metastatic rectal carcinoma - reversed, liver first approach. Early experience with 15 patients. *Neoplasma* 2014; **61**: 447-452 [PMID: 25027742]

12 **Brouquet A**, Mortenson MM, Vauthey JN, Rodriguez-Bigas MA, Overman MJ, Chang GJ, Kopetz S, Garrett C, Curley SA, Abdalla EK. Surgical strategies for synchronous colorectal liver metastases in 156 consecutive patients: classic, combined or reverse strategy? *J Am Coll Surg* 2010; **210**: 934-941 [PMID: 20510802 DOI: 10.1016/j.jamcollsurg.2010.02.039]

13 **Fahy BN**, Fischer CP. Synchronous resection of colorectal primary and hepatic metastasis. *J Gastrointest Oncol* 2012; **3**: 48-58 [PMID: 22811869 DOI: 10.3978/j.issn.2078-6891.2012.004]

14 **Grundmann RT**. Current state of surgical treatment of liver metastases from colorectal cancer. *World J Gastrointest Surg* 2011; **3**: 183-196 [PMID: 22224173 DOI: 10.4240/wjgs.v3.i12.183]

15 **de Haas RJ**, Adam R, Wicherts DA, Azoulay D, Bismuth H, Vibert E, Salloum C, Perdigao F, Benkabbou A, Castaing D. Comparison of simultaneous or delayed liver surgery for limited synchronous colorectal metastases. *Br J Surg* 2010; **97**: 1279-1289 [PMID: 20578183 DOI: 10.1002/bjs.7106]

16 **Tsoulfas G**, Pramateftakis MG. Management of rectal cancer and liver metastatic disease: which comes first? *Int J Surg Oncol* 2012; **2012**: 196908 [PMID: 22778934 DOI: 10.1155/2012/196908]

17 **Jegatheeswaran S**, Mason JM, Hancock HC, Siriwardena AK. The liver-first approach to the management of colorectal cancer with synchronous hepatic metastases: a systematic review. *JAMA Surg* 2013; **148**: 385-391 [PMID: 23715907 DOI: 10.1001/jamasurg.2013.1216]

18 **Lehmann K**, Rickenbacher A, Weber A, Pestalozzi BC, Clavien PA. Chemotherapy before liver resection of colorectal metastases: friend or foe? *Ann Surg* 2012; **255**: 237-247 [PMID: 22041509 DOI: 10.1097/SLA.0b013e3182356236]

19 **Benoist S**, Brouquet A, Penna C, Julié C, El Hajjam M, Chagnon S, Mitry E, Rougier P, Nordlinger B. Complete response of colorectal liver metastases after chemotherapy: does it mean cure? *J Clin Oncol* 2006; **24**: 3939-3945 [PMID: 16921046]

20 **Poultsides GA**, Servais EL, Saltz LB, Patil S, Kemeny NE, Guillem JG, Weiser M, Temple LK, Wong WD, Paty PB. Outcome of primary tumor in patients with synchronous stage IV colorectal cancer receiving combination chemotherapy without surgery as initial treatment. *J Clin Oncol* 2009; **27**: 3379-3384 [PMID: 19487380 DOI: 10.1200/JCO.2008.20.9817]

21 **Scheer MG**, Sloots CE, van der Wilt GJ, Ruers TJ. Management of patients with asymptomatic colorectal cancer and synchronous irresectable metastases. *Ann Oncol* 2008; **19**: 1829-1835 [PMID: 18662955 DOI: 10.1093/annonc/mdn398]

22 **Adam R**, De Gramont A, Figueras J, Guthrie A, Kokudo N, Kunstlinger F, Loyer E, Poston G, Rougier P, Rubbia-Brandt L, Sobrero A, Tabernero J, Teh C, Van Cutsem E. The oncosurgery approach to managing liver metastases from colorectal cancer: a multidisciplinary international consensus. *Oncologist* 2012; **17**: 1225-1239 [PMID: 22962059 DOI: 10.1634/theoncologist.2012-0121]

23 **Lykoudis PM**, O'Reilly D, Nastos K, Fusai G. Systematic review of surgical management of synchronous colorectal liver metastases. *Br J Surg* 2014; **101**: 605-612 [PMID: 24652674 DOI: 10.1002/bjs.9449]

24 **Verhoef C**, van der Pool AE, Nuyttens JJ, Planting AS, Eggermont AM, de Wilt JH. The "liver-first approach" for patients with locally advanced rectal cancer and synchronous liver metastases. *Dis Colon Rectum* 2009; **52**: 23-30 [PMID: 19273952 DOI: 10.1007/DCR.0b013e318197939a]

25 **de Jong MC**, van Dam RM, Maas M, Bemelmans MH, Olde Damink SW, Beets GL, Dejong CH. The liver-first approach for synchronous colorectal liver metastasis: a 5-year single-centre experience. *HPB* (Oxford) 2011; **13**: 745-752 [PMID: 21929676 DOI: 10.1111/j.1477-2574.2011.00372.x]

26 **Grundmann RT**, Hermanek P, Merkel S, Germer CT, Grundmann RT, Hauss J, Henne-Bruns D, Herfarth K, Hermanek P, Hopt UT, Junginger T, Klar E, Klempnauer J, Knapp WH, Kraus M, Lang H, Link KH, Löhe F, Merkel S, Oldhafer KJ, Raab HR, Rau HG, Reinacher-Schick A, Ricke J, Roder J, Schäfer AO, Schlitt HJ, Schön MR, Stippel D, Tannapfel A, Tatsch K, Vogl TJ. [Diagnosis and treatment of colorectal liver metastases - workflow]. *Zentralbl Chir* 2008; **133**: 267-284 [PMID: 18563694 DOI: 10.1055/s-2008-1076796]

27 **Neumann UP**, Seehofer D, Neuhaus P. The surgical treatment of hepatic metastases in colorectal carcinoma. *Dtsch Arztebl Int* 2010; **107**: 335-342 [PMID: 20532128 DOI: 10.3238/arztebl.2010.0335]

28 **Khan K**, Wale A, Brown G, Chau I. Colorectal cancer with liver metastases: neoadjuvant chemotherapy, surgical resection first or palliation alone? *World J Gastroenterol* 2014; **20**: 12391-12406 [PMID: 25253940 DOI: 10.3748/wjg.v20.i35.12391]

29 **Nordlinger B**, Sorbye H, Glimelius B, Poston GJ, Schlag PM, Rougier P, Bechstein WO, Primrose JN, Walpole ET, Finch-Jones M, Jaeck D, Mirza D, Parks RW, Collette L, Praet M, Bethe U, Van Cutsem E, Scheithauer W, Gruenberger T. Perioperative chemotherapy with FOLFOX4 and surgery versus surgery alone for resectable liver metastases from colorectal cancer (EORTC Intergroup trial 40983): a randomised controlled trial. *Lancet* 2008; **371**: 1007-1016 [PMID: 18358928 DOI: 10.1016/S0140-6736(08)60455-9]

30 **Morris-Stiff G**, Tan YM, Vauthey JN. Hepatic complications following preoperative chemotherapy with oxaliplatin or irinotecan for hepatic colorectal metastases. *Eur J Surg Oncol* 2008; **34**: 609-614 [PMID: 17764887]

31 **Zorzi D**, Laurent A, Pawlik TM, Lauwers GY, Vauthey JN, Abdalla EK. Chemotherapy-associated hepatotoxicity and surgery for colorectal liver metastases. *Br J Surg* 2007; **94**: 274-286 [PMID: 17315288]

32 **Khan AZ**, Morris-Stiff G, Makuuchi M. Patterns of chemotherapy-induced hepatic injury and their implications for patients undergoing liver resection for colorectal liver metastases. *J Hepatobiliary Pancreat Surg* 2009; **16**: 137-144 [PMID: 19093069 DOI: 10.1007/s00534-008-0016-z]

33 **Karoui M**, Penna C, Amin-Hashem M, Mitry E, Benoist S, Franc B, Rougier P, Nordlinger B. Influence of preoperative chemotherapy on the risk of major hepatectomy for colorectal liver metastases. *Ann Surg* 2006; **243**: 1-7 [PMID: 16371728]

34 **Mentha G**, Terraz S, Morel P, Andres A, Giostra E, Roth A, Rubbia-Brandt L, Majno P. Dangerous halo after neoadjuvant chemotherapy and two-step hepatectomy for colorectal liver metastases. *Br J Surg* 2009; **96**: 95-103 [PMID: 19109800 DOI: 10.1002/bjs.6436]

35 **Tanaka K**, Takakura H, Takeda K, Matsuo K, Nagano Y, Endo I. Importance of complete pathologic response to prehepatectomy chemotherapy in treating colorectal cancer metastases. *Ann Surg* 2009; **250**: 935-942 [PMID: 19953712]

36 **Adam R**, Wicherts DA, de Haas RJ, Ciacio O, Lévi F, Paule B, Ducreux M, Azoulay D, Bismuth H, Castaing D. Patients with initially unresectable colorectal liver metastases: is there a possibility of cure? *J Clin Oncol* 2009; **27**: 1829-1835 [PMID: 19273699 DOI: 10.1200/JCO.2008.19.9273]

37 **Stein A**, Schmoll HJ. Systemic treatment of liver metastases from colorectal cancer. *Ther Adv Med Oncol* 2013; **5**: 193-203 [PMID: 23634197 DOI: 10.1177/1758834012473347]

38 **Adam R**, Bhangui P, Poston G, Mirza D, Nuzzo G, Barroso E, Ijzermans J, Hubert C, Ruers T, Capussotti L, Ouellet JF, Laurent C, Cugat E, Colombo PE, Milicevic M. Is perioperative chemotherapy useful for solitary, metachronous, colorectal liver metastases? *Ann Surg* 2010; **252**: 774-787 [PMID: 21037433 DOI: 10.1097/SLA.0b013e3181fcf3e3]

39 **Reddy SK**, Zorzi D, Lum YW, Barbas AS, Pawlik TM, Ribero D, Abdalla EK, Choti MA, Kemp C, Vauthey JN, Morse MA, White RR, Clary BM. Timing of multimodality therapy for resectable synchronous colorectal liver metastases: a retrospective multi-institutional analysis. *Ann Surg Oncol* 2009; **16**: 1809-1819 [PMID: 18979139 DOI: 10.1245/s10434-008-0181-y]

40 **Lubezky N**, Geva R, Shmueli E, Nakache R, Klausner JM, Figer A, Ben-Haim M. Is there a survival benefit to neoadjuvant versus adjuvant chemotherapy, combined with surgery for resectable colorectal liver metastases? *World J Surg* 2009; **33**: 1028-1034 [PMID: 19234865 DOI: 10.1007/s00268-009-9945-1]

41 **Zhu D**, Zhong Y, Wei Y, Ye L, Lin Q, Ren L, Ye Q, Liu T, Xu J, Qin X. Effect of neoadjuvant chemotherapy in patients with resectable colorectal liver metastases. *PLoS One* 2014; **9**: e86543 [PMID: 24466143 DOI: 10.1371/journal.pone.0086543]

42 **Nanji S**, Cleary S, Ryan P, Guindi M, Selvarajah S, Al-Ali H, Grieg P, McGilvary I, Taylor B, Wei A, Moulton CA, Gallinger S. Up-front hepatic resection for metastatic colorectal cancer results in favorable long-term survival. *Ann Surg Oncol* 2013; **20**: 295-304 [PMID: 23054102 DOI: 10.1245/s10434-012-2424-1]

43 **Wieser M**, Sauerland S, Arnold D, Schmiegel W, Reinacher-Schick A. Peri-operative chemotherapy for the treatment of

resectable liver metastases from colorectal cancer: A systematic review and meta-analysis of randomized trials. *BMC Cancer* 2010; **10**: 309 [PMID: 20565923 DOI: 10.1186/1471-2407-10-309]

44 **Chua TC**, Saxena A, Liauw W, Kokandi A, Morris DL. Systematic review of randomized and nonrandomized trials of the clinical response and outcomes of neoadjuvant systemic chemotherapy for resectable colorectal liver metastases. *Ann Surg Oncol* 2010; **17**: 492-501 [PMID: 19856028 DOI: 10.1245/s10434-009-0781-1]

P- Reviewer: Kiss I **S- Editor**: Yu J
L- Editor: AmEditor **E- Editor**: Liu XM

9. Immunoglobulin G4, autoimmune pancreatitis and pancreatic cancer

Bojková M, Dítě P, Dvořáčková J, Novotný I, Floreánová K, Kianička B, Uvírová M, Martínek A

Originally published in Digestive Diseases: Clinical Reviews, 2015, vol. 33, no. 1, p. 86-90.

Review Article

Digestive Diseases

Dig Dis 2015;33:86–90
DOI: 10.1159/000368337

Immunoglobulin G4, Autoimmune Pancreatitis and Pancreatic Cancer

Martina Bojková[a, d] Petr Dítě[a, d] Jana Dvořáčková[b, d] Ivo Novotný[e] Katarina Floreánová[f] Bohuslav Kianička[g, h] Magdalena Uvírová[c, d] Arnošt Martínek[a, d]

[a]Academic Centre of Gastroenterology, Department of Internal Medicine and [b]Department of Pathology, University Hospital Ostrava, [c]Cytogenetic and Cytobioptic Laboratory AGEL Ostrava, and [d]Faculty of Medicine, University of Ostrava, Ostrava, [e]Department of Gastroenterology, Masaryk Oncological Institute, [f]Department of Internal Gastroenterological Medicine, University Hospital Brno, [g]2nd Department of Internal Medicine, St. Ann's University Hospital, and [h]Faculty of Medicine, Masaryk University Brno, Brno, Czech Republic

Key Words
Immunoglobulin G4 · Autoimmune pancreatitis · Pancreatic cancer

Abstract
Background: Immunoglobulin G4 (IgG4)-related diseases are a group of diseases characterized by enlargement of the affected organs, elevation of serum IgG4, massive infiltration of affected organs with lymphocytes and plasma cells with IgG4 positivity and tissue fibrosis. Type I autoimmune pancreatitis is one form of IgG4-related disease. For IgG4-related diseases, various localizations are described for up to 10% of malignancies. The aim of our study was to examine IgG4 serum levels and pancreatic tissue with respect to the simultaneous presence of autoimmune pancreatitis in patients with pancreatic cancer. ***Methods:*** IgG4 serum levels were examined In 106 patients with histologically confirmed pancreatic cancer. The level of 135 mg/dl was considered as the normal value. Pancreatic tissue was histologically examined with respect to the presence of markers of autoimmune pancreatitis. ***Results:*** A higher IgG4 level than the cut-off value of 135 mg/dl was proven in 11 patients with pancreatic cancer. Of these 11 patients, 7 had levels twice the normal limit (65.6%). Autoimmune pancreatitis was diagnosed in these individuals. In the case of 1 patient, it was basically an unexpected finding; another patient was initially diagnosed with autoimmune pancreatitis. Repeated biopsy of the pancreas at the time of diagnosis did not confirm the presence of tumour structures, therefore steroid therapy was started. At a check-up 6 months after starting steroid therapy, the condition of the patient improved subjectively and IgG4 levels decreased. However, endosonographically, malignancy was suspected, which was subsequently confirmed histologically. This patient also demonstrated an IgG4 level twice the normal limit. ***Conclusion:*** IgG4-related diseases can be accompanied by the simultaneous occurrence of malignancies, which also applies to autoimmune pancreatitis. Chronic pancreatitis is considered a risk factor for pancreatic cancer. It cannot be reliably confirmed whether this also applies to autoimmune pancreatitis. In accordance with other works, however, it is evident that, despite the described high sensitivity and specificity for IgG4 elevation in the case of autoimmune pancreatitis, even levels twice the normal limit are demonstrable in some individuals with pancreatic cancer, without the presence of autoimmune pancreatitis. We believe that patients with IgG4-related disease, including autoimmune pancreatitis, must be systematically monitored with respect to the potential presence of malignancy.

Introduction

Immunoglobulin G4 (IgG4)-related diseases are characterized by enlargement of the affected organs, elevated IgG4 serum levels, abundant infiltration of affected tissues with plasma cells containing IgG4, and significant tissue fibrosis [1]. Typical representations of IgG4-related diseases include Mikulicz syndrome and an autoimmune form of pancreatitis [2]. A level of IgG4 higher than 135 mg/dl, or its 2-fold elevation rank, is among the criteria in diagnosing autoimmune pancreatitis [3]. In recent years, however, a number of conditions have appeared with elevated IgG4 levels which were not IgG4-related diseases. Such diseases also include pancreatic cancer, therefore differential diagnostics is gaining importance in order to rule out or confirm cancer [4].

In 2012, Yamamoto et al. [5] published a report evaluating a representative group of persons with IgG4-related diseases in terms of the simultaneous presence of malignancy. In the studied group of 106 persons, the presence of a malignant tumour was detected in 11 cases (10.6%). Localization of tumours was in the lungs and intestine, and lymphoma was also present – both non-Hodgkin and MALToma. Although no pancreatic cancer was detected in this study, the potential relationship between autoimmune pancreatitis and pancreatic cancer has been described in other studies [6, 7]. However, IgG4 levels, corresponding to the values reported as one of the criteria for diagnosing autoimmune pancreatitis, were detected not only in patients with autoimmune pancreatitis but also in a portion of the persons with primary pancreatic carcinoma [8].

The aim of our study was to examine a group of persons with histologically confirmed pancreatic cancer and to test the IgG4 serum levels – and specifically to investigate whether histomorphometric signs of autoimmune pancreatitis are present in the pancreatic tissue.

Materials and Methods

In our study, during the years 2011–2013, we examined the IgG4 serum level and pancreatic tissue samples for the presence of criteria for autoimmune pancreatitis in a group of 106 people with histologically confirmed pancreatic cancer.

The evaluated group consisted of 88 men (75.8%) with an average age of 61.4 years and 28 women (24.2%) with an average age of 58.7 years. We detected a number of comorbidities for which the patients with pancreatic cancer were treated. Some comorbidities, however, are a risk factor for pancreatic carcinogenesis (table 1).

In the studied group of 106 persons, 11 patients (10.1%) demonstrated IgG4 serum levels higher than 135 mg/dl, this level being considered a diagnostic criterion for autoimmune pancreatitis. A 2-fold increase was found in 7 of the 11 persons (65.6%; table 2).

Table 1. Comorbidities in 106 persons with proven pancreatic cancer

	Men	Women
Diagnosis, n	86	20
Average age, years	61.4	59.8
Diabetes mellitus, n	12 (12.8%)	4 (20.0%)
Chronic pancreatitis, n	3 (3.5%)	1 (5.0%)
Ulcerative disease, n	2 (2.3%)	0
Hepatopathy, n	10 (11.6%)	2 (10.0%)
Ischaemic heart disease, n	6 (6.9%)	1 (5.0%)
Arterial hypertension, n	8 (9.3%)	4 (20.0%)
Obesity (BMI >30), n	5 (5.8%)	3 (15.0%)

Table 2. Elevated IgG4 serum levels in patients with pancreatic cancer

Patient	Age, years	Sex	IgG4, mg/dl	Autoimmune pancreatitis
1	51	M	151.0	No
2	71	M	280.4	No
3	64	F	308.6	No
4	52	M	514.2	Yes
5	60	M	148.4	No
6	59	F	203.6	No
7	65	M	487.0	Yes
8	70	M	149.4	No
9	62	M	274.0	No
10	55	F	288.6	No
11	53	M	390.3	No

Average age: men, 60.5 years (range 51–71); women, 59.3 years (range 55–64). Average IgG4 in 11 persons with serum IgG4 level ≥135 mg/dl was 263 mg/dl.

The group of patients with elevated IgG4 levels consisted of 8 men with an average age of 61.5 years (range 51–71) and 3 women with an average age of 59.3 years (range 55–64). None of these persons had sought treatment for diseases with immune changes, rheumatological disease or allergy. The average value of IgG4 in all patients with pancreatic cancer and elevated IgG4 levels was 263 mg/dl.

In 2 persons with elevated IgG4 serum levels, pancreatic changes besides those typical for pancreatic cancer were proven at histological examination , characterizing autoimmune pancreatitis.

Patient 1

Patient 1 was a 52-year-old man. He was a regular smoker of 10–15 cigarettes daily since the age of 25 and only occasionally drank alcohol. He had never been seriously ill, but since 30 years of age he had been treated for gastroduodenal peptic ulcer disease.

In his family profile, his father was treated for arterial hypertension, his mother was healthy and his grandfather died of colorectal cancer.

He was examined due to dyspepsia, dull epigastric pain and subicterus, resulting in a suspected diagnosis of a focal form of autoimmune pancreatitis. However, with the consent of the patient, fine needle biopsy of the pancreatic head was performed under endosonographic guidance with negative results in terms of malignancy. The IgG4 serum level was increased – 514.2 mg/dl. Steroid therapy was started for the patient at a dose of 40 mg of prednisone per os daily, and the dose was reduced by 5 mg weekly to 10 mg/day; this dose was administered for 3 months. When the patient came for a check-up, subjectively he was feeling better, but he had lost 2 kg in weight – jaundice was not present; the IgG4 level had decreased to 281.5 mg/dl, but it was not normalized. At a check-up endosonographic examination, suspected malignancy of the pancreatic head was stated. The patient underwent surgery and adenocarcinoma was found with metastasis to the lymph nodes, and at the same time there were histological signs of autoimmune pancreatitis.

Patient 2

Patient 2 was a 65-year-old man. He was obese, an occasional smoker and an abstainer from alcohol consumption. He had been treated for arterial hypertension, autoimmune thyroiditis and type 2 diabetes mellitus, which had been proven 4 years before the diagnosis of pancreatic cancer. The reason for the examination was painless obstructive jaundice. In his family profile, there was no cancer or autoimmune disease.

During IgG4 examination, a high value of 487 mg/dl was detected in the blood serum at the endosonographic examination; the finding was evaluated as carcinoma of the pancreatic head. Surgery was performed, and adenocarcinoma of the pancreatic head was histologically proven, together with histomorphometric features of autoimmune pancreatitis.

While the first patient was initially diagnosed with autoimmune pancreatitis, in the case of the second patient it was basically an unexpected appearance of autoimmune pancreatitis with pancreatic cancer.

Discussion

IgG4-related diseases affect many organs such as the pancreas, biliary tract, liver, central nervous system, thyroid gland, prostate, kidney, retroperitoneum, and lymph nodes [9]. The clinical symptomatology is logically dependent upon the particular affected organ. Clinical symptomatology is typically insignificant; it affects mainly middle-aged and elderly men, and the effect of steroid therapy is frequent. Infiltration of affected organs with IgG4-positive plasma cells and high IgG4 serum levels are typical signs of the disease. The intensity of fibrotic changes varies according to the nature of the affected organ. The diagnostic problem is that a number of other conditions that do not rank among the IgG4-related diseases show elevated IgG4 serum levels. The presence of IgG4-positive plasma cells is a frequent finding in patients with rheumatoid synovitis or inflammatory diseases of the skin or oral cavity. Elevated IgG4 serum levels have also been reported in some cancers, including pancreatic cancer [10].

Autoimmune pancreatitis is one of the conditions where an elevated IgG4 serum level exceeding the value of 135 mg/dl is included in the diagnostic characteristics [11]. In the study by Hamano et al. [3], the sensitivity and specificity of serum level exceeding 135 mg/dl was higher than 95%. The diagnostic criteria for autoimmune pancreatitis are determined on the basis of a consensus published in 2011 by a group of experts [12]. Currently, there are two clinically significant forms of autoimmune pancreatitis which, in addition to some common features, have characteristics typical of their differential diagnosis. Type 1 autoimmune pancreatitis, known as lymphoplasmacellular pancreatitis, mainly affects individuals aged about 60 years, and its course is often initially presented with obstructive jaundice and only mild belly pain or discomfort. Most patients have elevated IgG4 serum levels and tissue infiltration with plasma cells and lymphocytes in the presence of IgG4. More than half of all type 1 autoimmune pancreatitis cases are accompanied by a finding of extrapancreatic organ lesions.

Type 2 autoimmune pancreatitis affects people a decade younger than type 1. IgG4 positivity is very low, about 40% of cases are simultaneously diagnosed with idiopathic intestinal inflammation (which does not apply to type 1 autoimmune pancreatitis) and in about one third of the persons, clinical symptoms may mimic acute pancreatitis [13] (table 3).

The autoimmune form occurs either in the form of diffuse involvement of the gland or as a focal or multifocal form [14]. The focal form of autoimmune pancreatitis, especially if painless obstructive jaundice is present simultaneously, is often difficult to distinguish from pancreatic cancer. Ghazale et al. [15] examined IgG4 serum levels in 135 patients with pancreatic cancer and a value higher than 135 mg/dl was detected in 13 persons (10%). None of the examined patients with pancreatic cancer, however, showed a level of IgG4 higher than twice the normal limit. Raina et al. [8] detected higher IgG4 serum levels in 5 patients (7%) out of 71 persons with pancreatic carcinoma; none of those 5 patients was diagnosed with autoimmune pancreatitis. In this group of people with pancreatic carcinoma, the average IgG4 value was 160.8 mg/dl. Kamisawa et al. [4] detected a high level of IgG4, which exceeded the normal limit of 135 mg/dl twice

Table 3. Differential diagnosis between autoimmune pancreatitis and pancreatic cancer: important points

	Autoimmune pancreatitis	Pancreatic cancer
Clinical features		
Exocrine insufficiency	Frequently	Rarely
Cachexia, anorexia	Rarely	Frequently
Pain	Rarely	Frequently
Extrapancreatic disease	Non-metastatic lesions	Metastatic lesions
Serology		
Autoantibodies	IgG4 >135 mg/dl	IgG4 <100 mg/dl
Carbohydrate antigen 19-9	<200 U/ml	>200 U/ml
Amylase, lipase	Mid-elevation (2- or 3-fold)	Usually normal
Imaging		
CT	Diffuse (sausage-shaped pancreas with hypointense rim) or focal	Focal
	Diffuse or focal stenosis of the pancreatic duct	Focal stenosis of the duct Infiltration of adjacent tissues and distant metastases
MR elastography	Homogeneous stiffness pattern	Heterogeneous stiffness pattern
ERCP	Diffuse or focal narrowing of the duct >3.5 cm No post-stenotic duct dilatation	Focal narrowing or obstruction of the duct <3.4 cm Post-stenotic duct dilatation >5.2 mm
	Strictures in the proximal half of the common bile duct	No strictures in the proximal half of the common bile duct
Secretion-enhanced MRCP	Duct-penetrating sign	No specific sign
EUS	Hypoechoic diffuse or focal enlargement with hyperechoic spots	Absence of hyperechoic spots
EUS elastography	Homogeneous stiffness pattern	Heterogeneous stiffness pattern
Contrast-enhanced EUS	Homogeneously hypervascular	Mainly hypovascular
Histology	Pattern of lymphoplasmacytosis, sclerosing pancreatitis or idiopathic duct-destructive pancreatitis	Ductal adenocarcinoma
Treatment	Response to corticosteroids	No response to corticosteroids

(433 mg/dl), in a patient with pancreatic cancer. Immunohistochemical examination showed a high occurrence of IgG4-positive plasma cells in the tumour tissue and low positivity of these cells in the surrounding pancreatic tissue. Abundant IgG4 positivity was also proven in the nearby lymph nodes.

Incidences of adenocarcinoma of the pancreas with simultaneous autoimmune pancreatitis are usually published as case reports [6, 7, 10]. In the case report by Loos et al. [11], a 67-year-old woman was diagnosed with autoimmune pancreatitis. However, it was not possible to clearly distinguish it from carcinoma of the head of the pancreas; therefore, pylorus-preserving pancreaticoduodenectomy was performed. The histological examination of the biopsy showed no signs of malignant process. Changes in the sense of autoimmune pancreatitis were proven, and 18 months after the diagnosis of autoimmune pancreatitis the woman was re-examined for ascites. The examination confirmed metastatic adenocarcinoma of the pancreas in the area of autoimmune pancreatitis. In 2012, Siokawa et al. [16] showed that not only IgG4-related diseases in general, but also autoimmune pancreatitis in particular (as one of the IgG4-related diseases), represent a risk factor in inducing carcinogenesis. In a group of 108 persons with a diagnosis of autoimmune pancreatitis – according to Asian criteria –

a total of 18 cancers were detected in 15 persons (13.9%). The highest risk of cancers was found in the first year after diagnosis of autoimmune pancreatitis. In 6 out of 8 people treated with steroids with a diagnosis of autoimmune pancreatitis, a cancerous lesion was detected before starting steroid therapy. Most frequently, malignancy was detected in the stomach, lungs and prostate. It is evident that patients with autoimmune pancreatitis are at risk of malignant tumours of various localizations. In our study we have found an increase in IgG4 in 10% of patients; in more than 65% of these patients, the value was more than twice the normal limit. In 1 patient who was initially observed for autoimmune pancreatitis and treated with steroids, we also confirmed pancreatic cancer histologically 5 months after the diagnosis of autoimmune pancreatitis. In another patient with a finding of pancreatic cancer, IgG4 autoimmune pancreatitis was surprisingly identified as well at histological revision of pancreatic tissue; IgG4 positivity was not detected in the tumour tissue. Although chronic pancreatitis is a potential risk factor for pancreatic cancer, it cannot be clearly confirmed that autoimmune pancreatitis or IgG4-related diseases in general were the cause of pancreatic cancer. However, patients with a diagnosis of autoimmune pancreatitis should be regularly monitored and the armamentarium of tests should be supplemented with examinations that may reveal potential cancerous changes.

References

1 Takahashi H, Yamamoto M, Suzuki C, et al: The birthday of a new syndrome: IgG4-related disease constitutes a clinical entity. Autoimmune Rev 2010;9:591–594.

2 Vlachou PA, Khalili K, Jang H-J, et al: IgG4-related sclerosing disease: autoimmune pancreatitis and extrapancreatic manifestations. Radiographics 2011;31:1379–1402.

3 Hamano H, Kawa S, Hirouchi A, et al: High serum IgG4 concentration in patients with sclerosing pancreatitis. N. Engl. J. Med 2001; 344:732–738.

4 Kamisawa T, Chen PY, Tu Y, et al: Pancreatic cancer with a serum IgG4 concentration. World J Gastroenterol 2006;12:6225–6228.

5 Yamamoto M, Takahashi H, Tabeya T, et al: Risk of malignancies in IgG4-related disease. Mod Rheumatol 2012;22:414–418.

6 Inoue H, Miyatani H, Sawada Y: A case of pancreatic cancer with autoimmune pancreatitis. Pancreas 2006;33:208–209.

7 Wilkiewicz AK, Kennedy EP, Keneyon I, et al: Synchronous autoimmune pancreatitis and infiltrating pancreatic ductal adenocarcinoma: case report and review of the literature. Human Pathol 2008;39:1548–1551.

8 Raina A, Krasinskas AM, Greer JB, et al: Serum immunoglobulin G fraction 4 levels in pancreatic cancer: elevations not associated with autoimmune pancreatitis. Arch Pathol Lab Med 2007;112:48–53.

9 Umehara M, Okazaki K, Masaki Y, et al: Comprehensive diagnostic criteria for IgG4-related disease. Mod Rheumatol 2012;22:21–30.

10 Pezzilli R, Vecchiarelli S, DiMarco MC, et al: Pancreatic ductal adenocarcinoma related with autoimmune pancreatitis. Case Rep Gastroenterol 2011;5:378–385.

11 Loos M, Esposito I, Hedderich DM, et al: Autoimmune pancreatitis complicated by carcinoma of the pancreatobiliary system. Pancreas 2011;40:151–154.

12 Shimozegawa T, Chari ST, Frulloni L, et al: International consensus diagnostic criteria for autoimmune pancreatitis: guidelines of the International Association of Pancreatology. Pancreas 2011;40:352–358.

13 Kamisawa T, Chari ST, Lerch MM, et al: Recent advances in autoimmune pancreatitis type 1 and type 2. Gut 2013;62:1373–1380.

14 Psarras K, Baltatris MF, Pavlidis ET: Autoimmune pancreatitis versus pancreatic cancer a comprehensive review with emphasis on differential diagnosis. Hepatobiliary Pancreat Dis Int 2011;10:465–473.

15 Ghazale A, Chari ST, Smyrk TC, et al: Value of serum IgG4 in the diagnosis of autoimmune pancreatitis and in distinguishing it from pancreatic cancer. Am J Gastroenterol 2007;102:1646–1653.

16 Siokawa M, Kodama Y, Ypshimura K, et al: Risk of cancer in patients with autoimmune pancreatitis. Am J Gastroenterol 2013;108: 610–618.

10. Patients with chronic rhinosinusitis and simultaneous bronchial asthma suffer from significant extraesophageal reflux

Zeleník K, Matoušek P, Formánek M, Urban O, Komínek P

Originally published in International Forum of Allergy & Rhinology, 2015, vol. 5, no. 10, p. 944-949.

Patients with chronic rhinosinusitis and simultaneous bronchial asthma suffer from significant extraesophageal reflux

Karol Zeleník, MD, PhD[1,2], Petr Matoušek, MD, PhD[1,2], Martin Formánek, MD[2,3], Ondřej Urban, MD, PhD[2,3] and Pavel Komínek, MD, PhD, MBA[1,2]

Background: **The aim of this study was to determine the severity of extraesophageal reflux (EER) in patients with various degrees of chronic rhinosinusitis (CRS), and particularly in patients with simultaneous bronchial asthma.**

Methods: **Patients with different severity of CRS were invited to participate in the study. Group I consisted of patients with CRS without nasal polyps or bronchial asthma; group II consisted of patients with CRS with nasal polyps but without bronchial asthma; group III consisted of patients with CRS with nasal polyps and bronchial asthma. The age, gender, Reflux Symptom Index, severity of EER evaluated using the Restech system, and number of previous functional endoscopic sinus surgeries (FESSs) were compared between groups.**

Results: **A total of 90 patients (30 in each group) were recruited for the study. Pathological EER was significantly often present in group III when compared with group I and group II in all parameters analyzed (RYAN score, number of EER episodes, total percentage of time below pH 5.5). Furthermore, patients from group III had undergone more surgeries in the past.**

Conclusion: **Patients with CRS with nasal polyps and simultaneous bronchial asthma suffer from significant EER. Antireflux therapy can be recommended for these patients. However, the effect has to be confirmed in further studies.**

Key Words:
chronic rhinosinusitis; extraesophageal reflux; oropharyngeal pH monitoring; bronchial asthma; antireflux therapy

***How to Cite this Article*:**
Zeleník K, Matoušek P, Formánek M, Urban O, Komínek P. Patients with chronic rhinosinusitis and simultaneous bronchial asthma suffer from significant extraesophageal reflux. *Int Forum Allergy Rhinol.* 2015;5:944–949.

Chronic rhinosinusitis (CRS) is 1 of the most common chronic diseases affecting adults in the United States.[1,2] Despite intensive conservative as well as surgical treatment, some patients do not respond to standardized protocols appropriately, and suffer from so called refractory CRS.[3,4] Many factors have been cited as possible reasons for this; eg, immunodeficiency, fungal sinusitis, bacterial biofilms, vasculitis, structural abnormalities, cystic fibrosis, sarcoidosis, and others.[4–6]

During the last decade, extraesophageal reflux (EER) has been hypothesized to be 1 of the possible factors contributing to the worsening of CRS.[7] To date, only a few studies have tried to elucidate the relationship between CRS and reflux.[8–18] In most of them, history and/or esophageal pH monitoring has been used to determine the presence and severity of gastroesophageal and extraesophageal reflux. The results of these studies suggest that patients with refractory CRS and CRS which persists after functional endoscopic sinus surgery (FESS) have more hypopharyngeal or nasopharyngeal reflux episodes when compared with patients who have no recurrence after FESS.[8–13] Moreover, treatment of reflux led to improvement of refractory CRS in some studies.[16–18] Despite these promising results, the relationship between EER and CRS remains indeterminate due to its complexity; it is not clear whether antireflux treatment is indicated for those patients and who would benefit from it. According to the European Position Paper on Rhinosinusitis and Nasal Polyps (EPOS), evidence of a relationship

[1]*Department of Otorhinolaryngology–Head and Neck Surgery, University Hospital Ostrava, Ostrava, Czech Republic;* [2]*Faculty of Medicine, University of Ostrava, Ostrava, Czech Republic;* [3]*Department of Gastroenterology, Vítkovice Hospital, Ostrava, Czech Republic*

Correspondence to: Karol Zeleník, MD, PhD, Department of Otorhinolaryngology–Head and Neck Surgery, University Hospital Ostrava 17. listopadu 1790, 708 52 Ostrava-Poruba, Czech Republic; e-mail: karol.zelenik@fno.cz

Funding sources for the study: Ministry of Health of the Czech Republic (grant IGA MZCR NT13500–4/2012).

Potential conflict of interest: None provided.
Public clinical trial registration: http://clinicaltrials.gov/show/NCT01819454. The Diagnostics of Extraesophageal Reflux With the Restech System in Patients With Chronic Rhinosinusitis.

Received: 8 April 2015; Revised: 26 April 2015; Accepted: 2 May 2015
DOI: 10.1002/alr.21560
View this article online at wileyonlinelibrary.com.

between CRS and EER is at level III, and further study of the relationship is recommended.[19]

An analogous medical dilemma involves the relationship between bronchial asthma and EER. Many patients with bronchial asthma suffer from reflux (30–90%), but questions remain about their treatment with proton pump inhibitors (PPIs). It is still not clear how to select asthmatic patients with EER who would best respond to antireflux therapy.[20–23] Therefore, identifying the characteristics of a reflux-related asthma phenotype is very important, and more research is needed in this area.[21]

The aim of the present study was to determine the severity of EER in patients with various degrees of CRS, and particularly in patients with simultaneous bronchial asthma. Such a study has not been performed to date. We assumed that patients with simultaneous CRS and bronchial asthma would suffer from the most severe reflux and would therefore be good candidates for antireflux therapy.

Patients and methods

This prospective case-series study was approved by the Ethics Committee of the University Hospital Ostrava and was performed in accordance with the Declaration of Helsinki, good clinical practice, and applicable regulatory requirements. The study was registered on ClincialTrials.gov under the identifier NCT01819454. Written informed consent was obtained from all subjects before initiating any procedure.

Study design

Patients with different degrees of severity of CRS were invited to participate in the study. Participants were divided into 3 groups. Group I consisted of patients with CRS without nasal polyps or bronchial asthma; group II consisted of patients with CRS with nasal polyps but without bronchial asthma; group III consisted of patients with CRS with nasal polyps and bronchial asthma. We decided to include 30 patients in each group to have homogeneous groups for further statistical analysis.

Inclusion criteria

Patients 18 to 64 years old who were followed at the Ear/Nose/Throat (ENT) clinic of a tertiary hospital, who had been diagnosed with CRS with/without nasal polyps (according to the EPOS definition),[19] and had been scheduled for FESS for persistent symptoms of CRS were invited to participate in the study. Only patients who had been treated with nasal topical corticosteroids for at least the 2 years prior to the study and who had been put on systemic steroids (20 mg of prednisolone daily for 10 days) at least twice during the second of the 2 years were invited to participate. Only nonsmokers were asked to participate in the study. Patients with simultaneous bronchial asthma were enrolled in group III. Only patients with a diagnosis of bronchial asthma made by a respiratory physician and who had been treated with inhaled corticosteroids for at least the 2 years prior to the study were included. If patients had undergone FESS in the past, only those who were operated on in our department were enrolled in the study. All patients underwent preoperative computed tomography (CT) scan, which showed polypoid thickening of the sinus mucosa, and the diagnosis of CRS was confirmed during consecutive FESS.

Exclusion criteria

Patients with prediagnosed cystic fibrosis based on a positive sweat test or DNA alleles, immunodeficiency (congenital or acquired), congenital mucociliary problems (eg, primary ciliary dyskinesia), noninvasive fungal balls and invasive fungal disease, systemic vasculitis and granulomatous diseases, and neoplasia of the nose or sinuses were excluded from the study.

Demographic data and history

The age, gender, history of nasal and systemic corticosteroid therapy, history of bronchial asthma and its treatment with inhaled corticosteroids, and number of FESSs (no surgery, 1 to 2 surgeries, 3 or more surgeries) within the previous 5 years was ascertained. In addition, patients were asked to complete the Reflux Symptom Index (RSI) questionnaire introduced by Belafsky et al.[24] The RSI questionnaire is standardized and widely used in the assessment of EER symptoms.

Twenty-four-hour monitoring of oropharyngeal pH

Twenty-four-hour monitoring of oropharyngeal pH was carried out 24 to 36 hours prior to the FESS using the Restech® system (Respiratory Technology Corporation, San Diego, CA). The Restech pH catheter was calibrated in solutions of pH 7 and pH 4 prior to use. The sensor was inserted through the nasal cavity until the flashing light-emitting diode (LED) was seen in the back of the subject's throat and then positioned so that the flashing light was 5 to 10 mm below the uvula. The catheter was secured to the patient's face and then passed over the ear and secured to the neck. The transmitter at the end of the catheter was either taped to the skin or attached to the subject's clothing using a clip-on case. A data recorder was attached to the subject's belt. Patients were asked not to shower during the recording period and instructed to record, directly to the device and manually to a diary, the time they spent eating and drinking and their position (upright, supine) during the 24-hour period. If there was any discrepancy, periods logged in the device were modified according to the diary. Time spent eating and drinking was excluded from the analyses of pharyngeal pH recordings. A standardized RYAN composite score was calculated automatically using the software supplied. A RYAN score is a composite pH score for pharyngeal acid exposure calculated from volunteers without reflux problems. A composite pH score was calculated for the pH threshold identified by

TABLE 1. Demographic data and RSI of overall study group and individual groups I, II, and III

	Overall group	Group I	Group II	Group III
Age (years), mean ± SD	46.0 ± 13.6	39.3 ± 12.5	44.3 ± 11.7	54.4 ± 12.2
Gender, n				
Male	47	11	19	17
Female	43	19	11	13
RSI, mean ± SD	10.5 ± 4.1	8.7 ± 4.9	9.7 ± 4.0	13.2 ± 3.3

RSI = Reflux Symptom Index; SD = standard deviation.

applying the same method used to calculate the composite pH score for esophageal pH monitoring (DeMeester score). The sum of the 3 component scores (percent time below threshold, number of reflux episodes, and duration of the longest episode) equals the pharyngeal composite pH score.[25] Patients with pathological RYAN composite scores in the vertical (higher than 9.4) and/or horizontal (higher than 6.8) position were classified as having pathological EER. The number of EER episodes and total percentage of time below pH 5.5 were also assessed.

Statistical analysis

The age, gender, RSI, the severity of EER evaluated using the Restech system and number of previous FESS were compared between group I, group II, and group III. The statistical analysis was performed using Stata 13 software (Stata Corp, College Station, TX). The following statistical tests were used: arithmetic mean, standard deviation, Pearson's chi-squared test, Fisher's exact test, analysis of variance (ANOVA), odds ratio (OR) calculation with 95% confidence intervals, and logistic regression. The statistical tests were assessed on a significance level of 5%.

Results

A total of 107 consecutive patients who had met the inclusion and exclusion criteria were invited to participate in the study from September 2012 to December 2014. A total of 90 patients (30 in each group) agreed to participate. Enrollment of patients was terminated when all groups consisted of 30 patients. All enrolled patients tolerated the Restech catheter well and completed the 24-hour oropharyngeal pH study. There were no errors associated with oropharyngeal pH monitoring and no missing data. Therefore, all 90 patients were included in further statistical analysis.

Demographic data

Demographic data of the overall study group and individual groups I, II, and III are summarized in Table 1. The overall study group consisted of 47 males (aged 46.7 ± 13.5 years) and 43 females (aged 45.2 ± 13.7 years). There was no difference in age between males and females ($p = 0.594$). Patients in group III were significantly older in comparison with patients in group I and group II ($p < 0.001$). There was no difference in gender between groups ($p = 0.099$) (Table 1).

RSI

RSI was significantly higher in group III when compared with group I and group II ($p < 0.05$); there was no difference between group I and group II (Table 1).

Results of oropharyngeal pH monitoring

Data from oropharyngeal pH monitoring for groups I, II, and III are summarized in Table 2. Pathological EER in the upright position was significantly often present in group III when compared with group I ($p < 0.001$) and group II ($p < 0.004$). Moreover, EER was present in group II significantly often when compared with group I ($p < 0.005$). The average RYAN score in the upright position differed significantly between groups ($p = 0.0001$). The highest average RYAN score was noted in group III and the lowest in group I (Table 2, Fig. 1).

Pathological EER in the supine position was significantly often diagnosed in group III when compared with

TABLE 2. Data from oropharyngeal pH monitoring for groups I, II, and III

	Group I	Group II	Group III
Reflux upright, n (% of patients with proved EER)	6/30 (20%)	17/30 (57%)	28/30 (97%)
RYAN score upright (mean ± SD)	5.3 ± 10.7	61.3 ± 103.7	408 ± 453.8
Reflux supine, n (% of patients with proved EER)	5/30 (17%)	9/30 (30%)	15/30 (50%)
RYAN score supine (mean ± SD)	3.1 ± 2.3	5.9 ± 7.1	18.8 ± 25.7
Number of episodes (mean ± SD)	3.0 ± 3.7	18 ± 18.7	43.7 ± 61.5
Percent of time below pH 5.5 (mean ± SD)	0.2 ± 0.3	0.9 ± 1.6	5.2 ± 11.3

EER = extraesophageal reflux; SD = standard deviation.

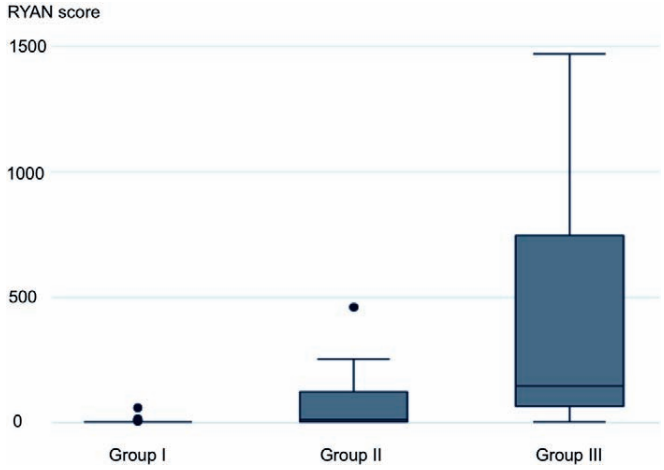

FIGURE 1. Graph showing average upright RYAN score for groups I, II, and III.

group I ($p < 0.008$). No other statistical difference was noted. The average RYAN score in the supine position differed significantly between groups ($p = 0.0042$) as well (Table 2).

Number of EER episodes differed significantly between group I and group II ($p < 0.05$) and between group I and group III ($p < 0.05$). Moreover, the total percentage of time below pH 5.5 differed significantly between group I, group II, and group III ($p = 0.0001$). The longest time under pH 5.5 was recorded in group III, whereas the shortest time under pH 5.5 was recorded in group I (Table 2).

Number of previous FESSs

Altogether, 50% (15/30) of patients from group III had undergone more than 2 prior FESSs within the previous 5 years, whereas only 2 of 30 (6%) and none of 30 (0%) patients, in group II and group I, respectively, had undergone more than 2 prior FESSs. The difference was significant ($p < 0.001$). In the group of patients with >2 prior FESSs within the previous 5 years, the number of patients with pathological EER and average RYAN score was significantly higher when compared with no previous FESS group and the group with 1 to 2 previous FESSs ($p < 0.001$ and $p = 0.0001$, respectively) (Table 3, Fig. 2).

Discussion

EER has recently been cited as a possible risk factor for many respiratory symptoms, signs, and diseases; eg, hoarseness, laryngitis, globus, cough, laryngospasm, bronchial asthma, recurrent and chronic otitis media, and CRS.[26–29] Of these conditions, the relationship between CRS and EER is the least studied; only a few studies having been conducted within the last decade.[8–18] These studies have found more hypopharyngeal or nasopharyngeal reflux episodes in patients with refractory CRS and/or early recurrence of nasal polyps after FESS when compared with patients who had no recurrence. The authors conclude that antireflux therapy should be considered in patients with refractory CRS.[8–13] No others factors that could help us identify patients with CRS and also with EER who are suitable for antireflux therapy have been discussed so far.

TABLE 3. Number of previous FESSs within the last 5 years in groups I, II, and III[a]

	No previous FESS	1–2 previous FESSs	>2 previous FESSs
Group I	27	3	0
Group II	13	15	2
Group III	2	13	15
Reflux upright	12/42 (28.6%)	22/31(71%)	17/17 (100%)
RYAN score upright	15.9 ± 36.8	186 ± 299.8	458 ± 499.6

[a]Reflux upright and RYAN score upright are listed for groups with different numbers of previous FESSs.
FESS = functional endoscopic sinus surgery.

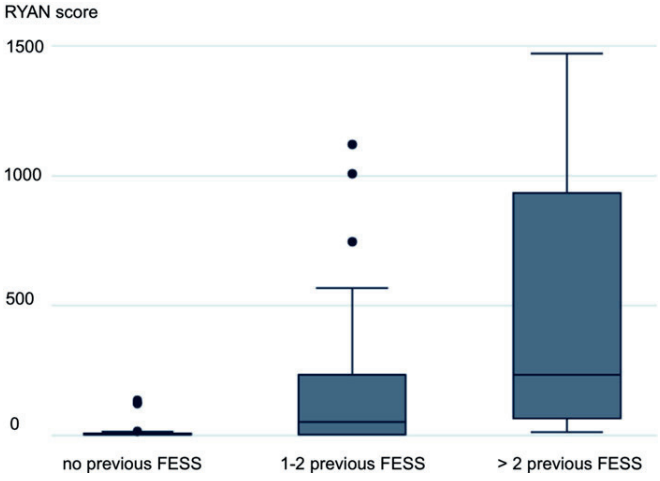

FIGURE 2. Graph showing average upright RYAN score for groups with no previous FESS, 1 to 2 previous FESSs, and >2 previous FESSs.

Regarding the relationship of bronchial asthma and reflux, asthmatic patients have more gastroesophageal reflux disease and more EER symptoms than the general population. There is not a clear understanding of why this is the case. Consensus exists on the antireflux treatment of patients with bronchial asthma and simultaneous "classical" symptoms of gastroesophageal reflux disease (pyrosis, regurgitation).[30] However, empirical PPIs therapy in adults with asthma results only in a small statistically significant improvement in morning peak expiratory flow rate. The magnitude of this improvement is unlikely to be of meaningful clinical significance. Because of many controversies, inconsistent results, and insufficient evidence, the empirical use of PPIs for routine treatment of asthmatic patients with only extraesophageal symptoms is not recommended.[23,30] As in the case of patients with CRS, there is a need to identify the phenotype of asthmatic patients who would respond to antireflux therapy.[23,30,31]

EER is considered to be a frequent cofactor of many respiratory symptoms, signs and diseases, including CRS and bronchial asthma. As a result, antireflux therapy, most often using PPIs, has been widely introduced as the recommended treatment for these extraesophageal manifestations. However, treatment of patients with suspected EER using PPIs is often disappointing. This applies not only to patients with CRS, but more generally to patients with most extraesophageal manifestations (dysphonia, reflux, cough, etc.). Most studies attempting to prove the superiority of PPIs over placebos in the treatment of EER have failed.[26]

Two main reasons are considered as possible reasons for this failure. The first is that EER is not diagnosed properly (often only on the basis of symptoms), and therefore many patients diagnosed as having EER do not really suffer from EER; hence, naturally antireflux therapy will not work. Which is to say that difficulties in treating EER patients arise from the inability to diagnose EER accurately and to select those patients who are suitable candidates for antireflux therapy. In the search for "antireflux therapy responders," 2 general assumptions can be made. First, there exist some signs (eg, age, gender, body mass index [BMI], specific symptoms, certain characteristics, another diagnosis, etc.) whose presence in a particular patient can predict a better response to antireflux therapy. The second is an assumption regarding pH studies. Generally speaking, if stricter criteria are used for diagnosing pathological EER, a higher positive response rate to the treatment will be achieved.[29,32]

The second explanation for failure to respond to PPIs may have to do with the fact that pepsin plays the main role in some patients with EER.[33] In these patients, the treatment should be focused not only on the acidity cut-back but also on the reduction of the reflux episodes and minimization of the negative pepsin effect.[34,35]

The ideal method for diagnosis of EER in patients with CRS and bronchial asthma would be one that could accurately predict their response to antireflux treatment. Unfortunately, such a method does not exist at present. It can only be assumed that patients with more serious symptoms, signs, and/or more severe EER detected by pH monitoring are at higher risk for developing EER-related respiratory disease, and would be potential candidates for antireflux treatment.

In the present study, the hypothesis that patients with simultaneous CRS and bronchial asthma would suffer from the most severe reflux and would therefore be suitable candidates for antireflux therapy was formulated. Patients with different types of CRS were examined for the presence and severity of EER; patients with simultaneous bronchial asthma were enrolled in group III. The results of pH analysis showed that pathological EER was significantly often present in group III when compared with group I and group II in all parameters analyzed (RYAN score in the upright and supine positions, number of EER episodes, total percentage of time below pH 5.5). In almost all (28/30) patients from group III, pathological EER was confirmed, whereas in group I and group II, EER was confirmed only in 6 of 30 and 17 of 30 patients, respectively. Also of interest is the finding that the average RYAN score in the upright position (408) was many times higher, when compared with the physiological threshold (9.4). On the other hand, patients from group I with CRS without nasal polyps and without bronchial asthma essentially did not suffer from EER. Only in 6 patients from group I was a very little reflux detected, and the average RYAN score for group I was even below the physiological threshold (5.3). The results confirmed the study hypothesis that patients with CRS and simultaneous bronchial asthma suffer from significant EER. Besides, it was also revealed that patients with CRS without nasal polyps rarely suffer from EER.

Analysis of demographic data showed that patients from group III were significantly older (54 years), when compared with group I and group II (39 and 44 years, respectively). This is consistent with the fact that increasing age has been confirmed as a risk factor for new onset of gastroesophageal reflux disease.[36]

Symptoms of EER are heterogeneous, nonspecific, and of very limited diagnostic value. Therefore, the RSI was developed by Belafsky et al.[24] Use of the RSI for the diagnosis of EER in patients with CRS has not been reported so far. In the present study, significantly higher RSI (13.2) was noted in patients with CRS and simultaneous bronchial asthma when compared with other groups. However, the RSI was only slightly higher than 13, which is the threshold given by Belafsky et al.[24] Moreover, when considering standard deviations, the RSI goes below the threshold established and accordingly does not identify patients with EER. Therefore, we can only conclude that RSI might be helpful in the diagnosis of EER in patients with CRS.

Altogether, 50% (15/30) of patients from group III had undergone more than 2 previous FESS within the previous 5 years, while only 2 of 30 (6%) and none of 30 (0%) patients, in group II and group I, respectively, had undergone more than 2 prior FESSs. This means that CRS in group III was not controlled well. This is in accordance with the results of previous studies, which compared the severity of EER in patients with refractory CRS and/or early recurrence of nasal polyposis after FESS with patients with well controlled CRS. These studies found more hypopharyngeal or nasopharyngeal reflux episodes in patients with early recurrence of nasal polyposis after FESS.[8–13]

Although important, diagnosis of EER in patients with CRS is not easy. Currently, 24-hour dual-probe esophageal pH monitoring or impedance is considered the best diagnostic method for EER. However, the position of the sensor, which is placed in the esophagus or hypopharynx, does not reflect the amount of reflux content that reaches the nasopharynx. Therefore, a diagnostic method that is able to detect pH in the oropharynx or nasopharynx would seem to be indicated for the diagnosis of EER in patients with CRS.

Twenty-four-hour measuring of oropharyngeal pH with the Restech system has became widespread within the

last decade. This method is less invasive and much better tolerated.[25,37] However, there are some disadvantages of this method as well. In particular, the absence of a distal sensor, which means that it is necessary to rely on data about meal periods and the position of the patient as recorded by the patient. Nevertheless, the majority of studies comparing esophageal and oropharyngeal pH measurement (simultaneous monitoring in 1 patient) have established good reciprocal correlation between these 2 methods.[25,38] In the present study, the oropharyngeal Restech catheter was tolerated well by all patients and there were no errors or missing data. Therefore, 24-hour oropharyngeal pH monitoring seems to be a good diagnostic tool for making the diagnosis of EER in patients with CRS.

One limitation of this study should be mentioned. Group III had significantly older patients than group I or group II. This can be seen in 2 ways. The first explanation is that older patients suffer often from reflux and their reflux is more severe and consequently it worsens CRS and bronchial asthma. And therefore they need more surgeries. The second explanation might be that patients in group III are older and need more surgeries because they suffer from CRS longer. We tried to eliminate this potential bias when the number of previous FESSs was ascertained within the last 5 years before the study. The ongoing studies should take into account this potential weakness in their methodology.

Conclusion

According to the results of the present study it can be concluded that patients with CRS with nasal polyps and simultaneous bronchial asthma suffer from significant EER. Patients suffering from CRS with nasal polyps and simultaneous bronchial asthma who have had more than 2 prior surgeries for CRS seem to be the most suitable candidates for antireflux treatment. However, the effect of antireflux therapy in these particular patients has to be confirmed in further studies.

References

1. Anand VK. Epidemiology and economic impact of rhinosinusitis. *Ann Otol Rhinol Laryngol Suppl*. 2004;193:3–5.
2. Benninger MS, Ferguson BJ, Hadley JA, et al. Adult chronic rhinosinusitis: definitions, diagnosis, epidemiology, and pathophysiology. *Otolaryngol Head Neck Surg*. 2003;129(Suppl):S1-S32.
3. Desrosiers M. Refractory chronic rhinosinusitis: pathophysiology and management of chronic rhinosinusitis persisting after endoscopic sinus surgery. *Curr Allergy Asthma Rep*. 2004;4:200–207.
4. Slavin RG. Resistant rhinosinusitis: what to do when usual measures fail. *Allergy Asthma Proc*. 2003;24:303–306.
5. Drilling A1, Coombs GW, Tan HL, et al. Cousins, siblings, or copies: the genomics of recurrent *Staphylococcus aureus* infections in chronic rhinosinusitis. *Int Forum Allergy Rhinol*. 2014;4:953–960.
6. Danielsen KA, Eskeland O, Fridrich-Aas K, et al. Bacterial biofilms in patients with chronic rhinosinusitis: a confocal scanning laser microscopy study. *Rhinology*. 2014;52:150–155.
7. Lupa M, DelGaudio JM. Evidence-based practice: reflux in sinusitis. *Otolaryngol Clin North Am*. 2012;45:983–992.
8. DelGaudio JM. Direct nasopharyngeal reflux of gastric acid is a contributing factor in refractory chronic rhinosinusitis. *Laryngoscope*. 2005;115:946–957.
9. Loehrl TA, Smith TL, Darling RJ, et al. Autonomic dysfunction, vasomotor rhinitis, and extraesophageal manifestations of gastroesophageal reflux. *Otolaryngol Head Neck Surg*. 2002;126:382–387.
10. Ulualp SO, Toohill RJ, Hoffmann R, et al. Possible relationship of gastroesophagopharyngeal acid reflux with pathogenesis of chronic sinusitis. *Am J Rhinol*. 1999;13:197–202.
11. Jecker P, Orloff LA, Wohlfeil M, et al. Gastroesophageal reflux disease (GERD), extraesophageal reflux (EER) and recurrent chronic rhinosinusitis. *Eur Arch Otorhinolaryngol*. 2006;263:664–667.
12. Ozmen S, Yucel OT, Sinici I, et al. Nasal pepsin assay and pH monitoring in chronic rhinosinusitis. *Laryngoscope*. 2008;118:890–894.
13. Phipps CD, Wood WE, Gibson WS, et al. Gastroesophageal reflux contributing to chronic sinus disease in children: a prospective analysis. *Arch Otolaryngol Head Neck Surg*. 2000;126:831–836.
14. Wong IW, Omari TI, Myers JC, et al. Nasopharyngeal pH monitoring in chronic sinusitis patients using a novel 4 channel probe. *Laryngoscope*. 2004;114:1582–1585.
15. Wise SK, Wise JC, DelGaudio JM. Association of nasopharyngeal and laryngopharyngeal reflux with postnasal drip symptomatology in patients with and without rhinosinusitis. *Am J Rhinol*. 2006;20:283–289.
16. Vaezi MF, Hagaman DD, Slaughter JC, et al. Proton pump inhibitor therapy improves symptoms in postnasal drainage. *Gastroenterology*. 2010;139:1887–1893.
17. DiBaise JK, Olusola BF, Huerter JV, et al. Role of GERD in chronic resistant sinusitis: a prospective, open label, pilot trial. *Am J Gastroenterol*. 2002;97:843–850.
18. Pincus RL, Kim HH, Silvers S, et al. A study of the link between gastric reflux and chronic sinusitis in adults. *Ear Nose Throat J*. 2006;85:174–178.
19. Fokkens WJ, Lund VJ, Mullol J, et al. European Position Paper on Rhinosinusitis and Nasal Polyps 2012. *Rhinol Suppl*. 2012;(23):3 p preceding table of contents, 1–298.
20. Kiljander TO, Laitinen JO. The prevalence of gastroesophageal reflux disease in adult asthmatics. *Chest*. 2004;126:1490–1494.
21. Harding SM, Guzzo MR, Richter JE. The prevalence of gastroesophageal reflux in asthma patients without reflux symptoms. *Am J Respir Crit Care Med*. 2000;162:34–39.
22. Amarasiri LD, Pathmeswaran A, deSilva HJ, Ranasinha CD. Prevalence of gastrooesophageal reflux disease symptoms and reflux-associated respiratory symptoms in asthma. *BMC Pulm Med*. 2010;10:49.
23. Parsons JP, Mastronarde JG. Gastroesophageal reflux disease and asthma. *Curr Opin Pulm Med*. 2010;16:60–63.
24. Belafsky PC, Postma GN, Koufman JA. Validity and reliability of the reflux symptom index (RSI). *J Voice*. 2002;16:274–277.
25. Ayazi S, Lipham JC, Hagen JA, et al. A new technique for measurement of pharyngeal pH: normal values and discriminating pH threshold. *J Gastrointest Surg*. 2009;13:1422–1429.
26. Karkos PD, Wilson JA. Empiric treatment of laryngopharyngeal reflux with proton pump inhibitors: a systematic review. *Laryngoscope*. 2006;116:144–148.
27. Madanick RD. Extraesophageal presentations of GERD: where is the science? *Gastroenterol Clin North Am*. 2014;43:105–120.
28. Moore JM, Vaezi MF. Extraesophageal manifestations of gastroesophageal reflux disease: real or imagined? *Curr Opin Gastroenterol*. 2010;26:389–394.
29. Zeleník K, Matoušek P, Urban O, Schwarz P, Stárek I, Komínek P. Globus pharyngeus and extraesophageal reflux: simultaneous pH <4.0 and pH <5.0 analysis. *Laryngoscope*. 2010;120:2160–2164.
30. Chan WW, Chiou E, Obstein KL, Tignor AS, Whitlock TL. The efficacy of proton pump inhibitors for the treatment of asthma in adults: a meta-analysis. *Arch Intern Med*. 2011;171:620–629.
31. McCallister JW, Parsons JP, Mastronarde JG. The relationship between gastroesophageal reflux and asthma: an update. *Ther Adv Respir Dis*. 2011;5:143–150.
32. Zelenik K, Matousek P, Tedla M, Syrovatka J, Kominek P. Extraesophageal reflux: what is the best parameter for pH-monitoring data analysis from the perspective of patient response to proton pump inhibitors? *Gastroenterol Res Pract*. 2013;2013:736486.
33. Samuels TL, Johnston N. Pepsin as a causal agent of inflammation during nonacidic reflux. *Otolaryngol Head Neck Surg*. 2009;141:559–563.
34. Johnston N, Wells CW, Samuels TL, Blumin JH. Rationale for targeting pepsin in the treatment of reflux disease. *Ann Otol Rhinol Laryngol*. 2010;119:547–558.
35. Johnston N, Dettmar PW, Strugala V, Allen JE, Chan WW. Laryngopharyngeal reflux and GERD. *Ann N Y Acad Sci*. 2013;1300:71–79.
36. Hallan A, Bomme M, Hveem K, Møller-Hansen J, Ness-Jensen E. Risk factors on the development of new-onset gastroesophageal reflux symptoms. A population-based prospective cohort study: the HUNT study. *Am J Gastroenterol*. 2015;110:393–400.
37. Wiener GJ, Tsukashima R, Kelly C, et al. Oropharyngeal pH monitoring for the detection of liquid and aerosolised supraesophageal gastric reflux. *J Voice*. 2009;23:498–504.
38. Chheda NN, Seybt MW, Schade PR, Postma GN. Normal values for pharyngeal pH monitoring. *Ann Otol Rhinol Laryngol*. 2009;118:166–171.

11. Plasma cell leukemia: from biology to treatment

Jelínek T, Kryukov F, Říhová L, Hájek R

Originally published in European Journal of Haematology, 2015, vol. 95, no. 1, p. 16-26.

European Journal of Haematology

European Journal of Haematology 95 (16–26)

REVIEW ARTICLE

Plasma cell leukemia: from biology to treatment

Tomas Jelinek[1], Fedor Kryukov[2], Lucie Rihova[3], Roman Hajek[1,2,3]

[1]University Hospital Ostrava, Department of Haematooncology, Ostrava; [2]University of Ostrava, Faculty of Medicine, Ostrava; [3]University Hospital Brno, Department of Clinical Haematology, Brno, Czech Republic

Abstract

Plasma cell leukemia (PCL) is a very aggressive and rare form of malignant monoclonal gammopathy characterized by the presence of plasmocytes in peripheral blood. It is classified as primary PCL occuring '*de novo*', or as secondary PCL in patients with relapsed/refractory multiple myeloma. Primary PCL is a distinct clinicopathological entity from myeloma with different cytogenetic abnormalities and molecular findings, which are usually found only in advanced multiple myeloma. The clinical course is aggressive with short remissions and reduced overall survival. The diagnostic criteria are based on the percentage (>20%) and absolute number (2×10^9/L) of plasma cells in peripheral blood. After establishing diagnosis, induction therapy should begin promptly which is aimed to rapid disease control and to minimize the risk of early death. Intensive chemotherapy regimens and bortezomib-based regimens, followed by high-dose therapy with autologous stem cell transplantation, are recommended. Allogeneic transplantation can be considered in younger patients. This article reviews recent knowledge of this hematological malignancy that is associated with a very poor prognosis.

Key words plasma cell leukemia; multiple myeloma; bone marrow transplantation; bortezomib

Correspondence Tomas Jelinek, University Hospital Ostrava, Department of Haematooncology, Ostrava, Czech Republic. Tel: +420597374587; Fax: +420597372092; e-mail: tomas.jelinek@fno.cz

Accepted for publication 24 October 2014 doi:10.1111/ejh.12533

Plasma cell leukemia (PCL) is an uncommon form of plasma cell dyscrasia but the most aggressive of human monoclonal gammopathies. The incidence of PCL in Europe is estimated to be 0.04 cases per 100,000 persons per year (1), ranging between 2 and 4% of patients with multiple myeloma [MM] (2, 3). Similar to MM, PCL is more common in African Americans than in Caucasians (4). The definition of PCL was created in the seventies by R. Kyle, a famous nestor of American hematology. It is claimed that it was just an empirical, intuitive determination of the percentage of plasma cells in peripheral blood (PB). These diagnostic criteria are still valid; however, efforts are being made to change them due to recent scientific findings (5). Plasma cell leukemia is defined by the presence of more than 20% of plasma cells in PB and an absolute plasma cell count greater than 2×10^9/L (6, 7). PCL is classified as primary (pPCL) when it presents 'de novo' and as secondary (sPCL) when it is observed as a leukemic transformation of relapsed or refractory multiple myeloma. Primary and secondary PCLs are two different clinical entities, although they have something in common—peripheral plasmacytosis and poor prognosis. Primary PCL is highly sensitive to aggressive chemotherapy (almost 100%), but because of its aggressiveness, it relapses early and its clinical outcome is poor (8). On the other hand, secondary PCL, a leukemic transformation of refractory MM, represents an end stage of disease with less than 50% response to treatment, thus leading to death. The aim of this article is to provide an overview of the definition of PCL, diagnostics, criteria of response, and treatment recommendations of primary and secondary PCLs.

Biology of PCL

Plasma cell dyscrasias are characterized by proliferation of plasma cells that are mainly localized in the bone marrow (BM). Typically, in initial stages of MM, tumor cells are strongly dependent on the BM microenvironment, which is essential for their growth, survival, and protection against apoptosis-inducing drugs. Furthermore, PCL cells have high potential to egress to peripheral blood stream and to form extramedullary disease. This dissemination from the BM is not only caused just by different expression of adhesion

Table 1 Comparison of immunophenotypic markers in pPCL vs. in MM

	$CD19^+$ PCs	$CD56^+$ PCs	$CD20^+$ PCs	$CD27^+$ PCs	$CD28^+$ PCs	$CD117^+$ PCs	$CD44^+$ PCs	$nestin^+$ PCs
(A) Relative expression of markers on $CD38^+$ $CD138^+$ PCs								
MM BM (n = 110) median of relative expression [%] (min–max)	0.38 (0.0–66.0)	96.3 (0.5–100.0)	0.2 (0.0–90.8)	16.8 (0.6–99.7)	3.1 (0.1–98.9)	4.5 (0.0–99.4)	84.8 (1.0–99.6)	5.3 (0.0–99.4)
pPCL PB (n = 11) median of relative expression [%] (min–max)	0.1 (0.0–94.7)	19.4 (0.4–99.9)	2.5 (0.0–94.4)	0.4 (0.0–50.6)	0.1 (0.0–99.6)	0.1 (0.0–30.2)	98.1 (2.3–100.0)	21.8 (0.1–99.1)
pPCL BM (n = 10) median of relative expression [%] (min–max)	0.1 (0.0–92.6)	48.9 (0.2–99.3)	2.4 (0.0–92.8)	0.6 (0.0–18.5)	1.8 (0.0–99.9)	0.0 (0.0–37.5)	77.0 (49.8–99.7)	53.6 (0.2–99.1)
(B) Positivity of expressed markers on $CD38^+$ $CD138^+$ PCs								
MM BM (n = 110) positivity [%]	6.4 (7/110)	75.5 (83/110)	8.2 (9/110)	31.8 (35/110)	20.9 (23/110)	31.8 (35/110)	84.3 (43/51)	30.5 (18/59)
pPCL PB (n = 11) positivity [%]	18.2 (2/11)	45.5 (5/11)	18.2 (2/11)	18.2 (2/11)	18.2 (2/11)	9.1 (1/11)	83.3 (5/6)	50.0 (3/6)
pPCL BM (n = 10) positivity [%]	20.0 (2/10)	60.0 (6/10)	30.0 (3/10)	0.0 (0/10)	33.3 (3/9)	11.1 (1/9)	100.0 (4/4)	75.0 (3/4)

molecules and chemokine receptors, but also by the presence of several molecular aberrations (9).

The typical markers of plasmocytes (CD38 and CD138) are equally expressed in MM and in pPCL, but some antigens have different expression. For example, in pPCL cases, decreased expression of CD56 is a common finding in comparison to MM (10). CD56 antigen is a neuronal cell adhesion molecule responsible for anchoring plasmocytes to the BM stroma, preventing the circulation of plasma cells to peripheral blood as well as their extramedullary migration (10, 11). Moreover, our results showed even lower expression of CD56 in peripheral blood than in the BM of pPCL (own unpublished data). Normal plasma cells (PCs) usually express CD19, which is absent in neoplastic PCs, and in contrast to it, CD20 is usually negative in normal PCs and has been shown to be positive in 30% of MM cases (12). García-Sanz *et al.* (10) and Tembhare *et al.* (13) have reported data about CD20 expression coming from small case series, but their results were controversial. Recently, it has been discovered that overexpression of CD27 in pPCL is connected to the activation of NFκB leading to higher anti-apoptotic activity (14). Surprisingly, the described high expression of CD27 on plasma cells from pPCL was not confirmed by Morgan *et al.* and by our group as well (15, 16). Antigen CD44, involved in cell–cell interactions, cell adhesion, and migration, is highly expressed in pPCL as well as in extramedullary relapses of MM, which was analyzed by our group and others (Table 1) (17). In summary, the principal immunophenotypic difference between pPCL and MM is that pPCL tumor cells are less often positive for CD27, CD56, CD71, CD117, and HLA-DR, but more often express CD20, CD44, CD45, CD19, and CD23 (9). Hitherto, it is not possible to accurately define typical immunophenotype for primary PCL.

In pPCL, the genetic abnormalities are already present at the time of diagnosis, whereas during the process of progression from monoclonal gammopathy of undetermined significance (MGUS) to MM, and finally to sPCL, there is a gradual accumulation of genetic events leading to the acquisition of more aggressive phenotype of malignant plasma cells (9). Hyperdiploidy and primary IgH translocations are considered to be the initial immortalizing oncogenic events standing at the inception of immortal plasma cell clone. Two of the largest studies showed that most cases were non-hyperdiploid consisting mostly of complex hypodiploid or pseudodiploid karyotypes (18, 19). Regarding IgH translocations, chromosome 14q32 translocations are found in a great number of pPCL and sPCL patients (82–87%), as expected in non-hyperdiploid multiple myeloma cases. In pPCL IgH translocations, 11q13 (cyclin D1) is involved almost exclusively, supporting a central relation to pathogenesis of pPCL, while in sPCL, multiple partner oncogenes are involved, including 11q13, 4p16 (FGFR3/MMSET – Fibroblast growth factor 3/Multiple myeloma SET domain), and

16q23 (MAF), recapitulating MM (3). Genomic aberrations such as *t*(4,14), del(13q14), del(17p), 1q21 gains, and del (1p21) are adverse risk factors in MM, but their significance in PCL is not clear (as they usually signify more aggressive behavior, which is ubiquitous in PCL) (20–27).

The prevalence of poor risk chromosomal abnormalities such as del(17p), ampl(1q21), MYC abnormalities, and RAS mutations is significantly higher in both pPCL and sPCL in comparison with newly diagnosed multiple myeloma (28). In cases of deletions of 17p13 and TP 53 inactivations, there were studies that reported a prevalence of deletion in MM 17p13.1 as a late event found only in 10% of patients and TP53 coding mutations in only 3% (29). Furthermore, deletion of TP53 was complemented by functionally relevant TP53 coding mutations in 24% of PCL patients, contributing to a substantial prevalence of allelic TP53 inactivation of 56% in pPCL and 83% in sPCL. Inactivation of p53 function can also occur via overexpression of negative regulatory elements, such as mouse double minute 2 homolog (MDM2), or by decreased activity of CDKN2A (p14ARF), a negative regulator of MDM2 (30, 31). Mutations of K-RAS or N-RAS at codons 12, 13, or 61, characterized as functionally activating, are found in 27% of pPCL and 15% of sPCL (3). Nevertheless, the prevalence of K-RAS or N-RAS mutations in sPCL is comparable to that reported in MM (21%), suggesting just a little selective pressure for RAS activation in secondary leukemic transformation from MM (32) (Fig. 1).

Genomic and clinical differences between PCL and MM have been recognized. The presence of p53 deletion in a high-level karyotypic complexity, hypodiploidy, 13q deletions, and 1q gains could define an advanced stage of plasma cell disease characterized by poor prognosis and resistance to therapy (32).

Clinical and laboratory features

Due to relatively low incidence and prevalence of this disease, most clinical data come from isolated case reports and small retrospective studies (3, 10, 33), only one prospective study has been published up to date (34). The median age of patients with primary PCL (65 years) is about 10 years younger than the median age of common myeloma population (6) and patients with secondary PCL (3). The period from the origin of the disease to the development of the first clinical features is very short, which is the same as in acute leukemias (weeks). Patients with PCL present with more serious symptoms than patients with MM, the most frequent are dyspnea and pallor, due to severe anemia or hemorrhagic diathesis due to thrombocytopenia. The cause of these symptoms is usually extensive infiltration of the bone marrow by plasma cells with anaplastic and plasmablastic morphology (Fig. 2).

According to aggressive clinical course, there is a higher proportion of patients with pPCL who have significant leukocytosis as well as elevated serum level of lactate dehydrogenase and ß2-microglobulin than patients with MM (35). The presence of lytic bone lesions is lower than in patients with MM (pPCL 35%, sPCL 53%, MM 80%); this is probably related to higher aggressiveness of pPCL or different biology of the disease (3, 36). During physical examination, patients may present with hepatosplenomegaly, lymphadenopathy, pulmonary findings connected with pleural effusion, neurologic deficit due to central nervous system involvement, and extramedullary soft-tissue plasmacytomas. Unlike in patients with MM, considerably higher proportion of patients with PCL secrete only free-light chains (15% vs. 26–44% resp.) (6).

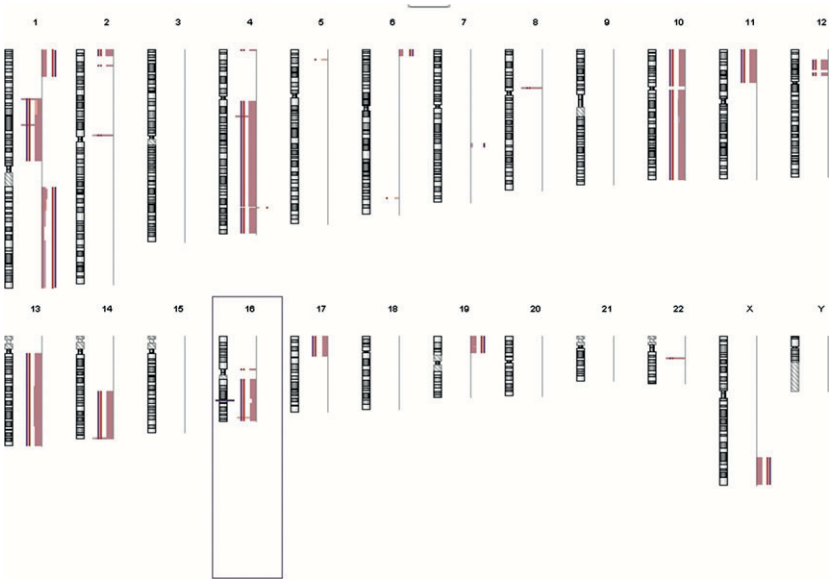

Figure 1 The array CGH analysis of patient's genome revealed copy number alterations ranging from small regions to whole chromosomes. Monosomies of chromosome 10 and chromosome 13 were observed. Large deletions were located at chromosomes 4 and 1 involving cytogenetic bands 4q12-q32.3, and 1p33-p13.2, respectively. However, smaller interstitial or terminal deletions located at 11p, 12p, 14p, 16p, and 17p were also observed. By contrast, both arms of chromosome 1 were also affected by gain of chromosomal material, predominantly affecting bands 1p36.33 - p36.13 and 1q21.1-q44. Smaller gains were also present at 6p, 19p, and chromosome X. Case report was kindly presented by Integrated Laboratory of Molecular Cytogenetics (Department of Experimental Biology, Faculty of Science, Masaryk University, Brno, Czech Republic).

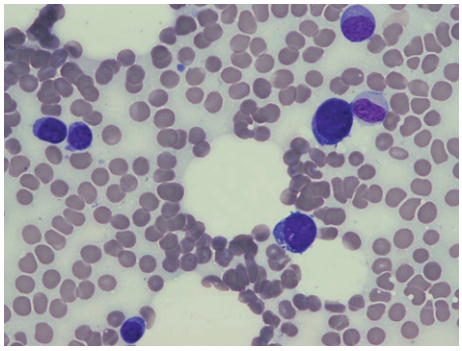

Figure 2 Plasma cell leukemia, bone marrow, microscope OLYMPUS BX41, May - Grünwald - Giemsa panoptical staining, original magnification 1000x, Jana Zuchnicka, MD, Faculty Hospital Ostrava.

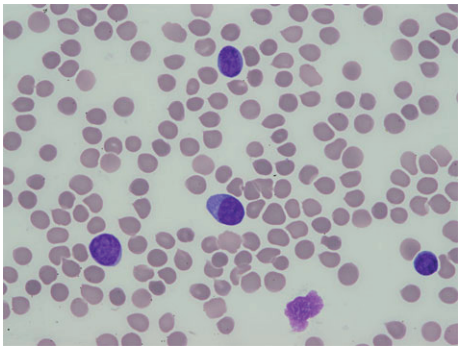

Figure 3 Plasma cell leukemia, peripheral blood, microscope OLYMPUS BX41, May – Grünwald - Giemsa panoptical staining, original magnification 1000x, Jana Zuchnicka, MD, Faculty Hospital Ostrava.

Diagnostic criteria

There are two main originally determined diagnostic criteria of PCL – absolute count of plasma cells in PB greater than 2×10^9/L and more than 20% of circulating plasma cells (6). These criteria have never been evaluated prospectively, and it is not clear whether they exactly distinguish PCL from MM. These criteria are valid especially when the morphological evaluation is used. When the flow cytometry is used to evaluate circulating plasma cells, it is possible that even lower number of plasma cells can signify the development of plasma cell leukemia. The control mechanisms responsible for keeping plasma cells from egression to PB are poorly understood. In fact, small amount of plasma cells can be found in a broad spectrum of plasma cell dyscrasias, including newly diagnosed MM, smoldering MM, and sometimes even MGUS (37, 38). During differential diagnosis, it is always important to distinguish malignant causes of peripheral plasmacytosis from non-malignant conditions, such as severe sepsis, infectious mononucleosis, and particularly serum sickness with presence of polyclonal plasma cells (39).

It is not absolutely clear whether both criteria are needed for establishing the diagnosis of PCL. In many studies, it was considered sufficient to meet only one of these two criteria (>20% circulating plasma cells or absolute count greater than 2×10^9/L in PB). For example, in patients who underwent intensive treatment resulting in poor BM reserve and leukopenia, they may meet the percentage criterion, but may not meet the absolute criterion. Perhaps meeting only one of these criteria should be enough for diagnosing this entity. The correct and timely diagnosis of PCL is dependent on the ability of the haematologists to recognize plasma cells in peripheral blood smear (Fig. 3). Careful examination of peripheral blood with conventional microscope should be performed in all patients with MM and clinical suspicion of PCL, such as leukocytosis or elevation of lactate dehydrogenase.

Many myeloma experts admit that diagnostic criteria should be changed, but there is no consensus in which way. Present criteria, even when only one is met, probably underestimate the real incidence of this diagnosis. The presence of blastic type of plasma cells in the BM is considered as a negative prognostic factor (40), while the presence of even very small amount of circulating plasma cells is a sign of aggressive proliferative process. In many cases, it is probably an early-diagnosed PCL that can rapidly develop the picture of severe disease in the absence of adequate treatment. In our own experience with 16 PCL patients (both pPCL and sPCL), the median of peripheral plasmacytosis was 13% by conventional morphology and 29.9% by flow cytometry at the time of diagnosis. Moreover, the median percentage of plasma cells in the bone marrow was 69.6% by conventional morphology and 51.1% by flow cytometry. In all cases, there was higher percentage of plasma cells in the BM than in PB by conventional morphology, but in 12.5% of patients (2/16), there was higher percentage of plasma cells in PB than in BM by flow cytometry (own unpublished data). The importance of modern methods, dominantly flow cytometry, used for detecting early PCL must be prospectively evaluated in multicentric studies in newly diagnosed patients. Therefore, there is no consensus in re-evaluating the diagnostic criteria at this time.

Criteria of response and survival

Specific response criteria for PCL have not been formulated yet. Usually, the general MM response criteria are used for patients with PCL. According to leukemic nature of the disease, precise evaluation of plasmocytes is very important. They should be evaluated in peripheral blood as well as in the bone marrow by morphology and flow cytometry. Also, the level of serum free-light chains (FLC) should be measured because of the relative higher percentage of light-chain only or oligosecretory forms of PCL. According to the work done by Fernandez and experts from International Myeloma Working Group (IMWG), there were proposed response criteria for pPCL that combine the requirements for acute leukemias and multiple myeloma (5, 41) (Table 2). In fact,

Table 2 Response criteria for plasma cell leukemia (adopted from Fernandez, Kyle *et al.* 2013 and van de Donk, Lokhorst *et al.* 2012)

Category	Bone marrow criteria[1]	Peripheral blood criteria[1]	Serologic criteria[2]	Other criteria
MRD-negative CR (sCR as defined below plus)	MRD-negative BM[3] by multicolor flow cytometry or allele-specific oligonucleotide PCR[4]	MRD-negative peripheral blood by multicolor flow cytometry or allele-specific oligonucleotide PCR[4]		
Stringent Complete Remission (sCR) (CR as defined below plus)	Bone marrow plasma cells <5% and no malignant plasma cell by flow cytometry	No plasma cells in peripheral blood	Normal FLC ratio and negative serum and urine immunofixation	Absence of extramedullary disease
Complete remission (CR)	Bone marrow plasma cells <5%	No plasma cells in peripheral blood	Normal FLC ratio and negative serum and urine immunofixation	Absence of extramedullary disease
Very Good Partial response (VGPR)	Bone marrow plasma cells <5%	No plasma cells in peripheral blood	≥90% reduction of serum M-protein 24 h urinary M-protein <100 mg per 24 h[5]	Absence of extramedullary disease
Partial response (PR)	Bone marrow plasma cells from 5% to 25%	Peripheral plasma cell from 1% to 5%	≥50% reduction of serum M-protein and reduction in 24 h urinary M-protein by ≥90% and <200 mg per 24 h[6]	≥50% reduction in the size of soft tissue plasmacytomas
Stable disease (SD)	Not meeting the criteria of either partial response or progressive disease			
Progressive disease (PD)	>25% increase in plasma cells in the bone marrow aspirate or absolute increase ≥10%	Plasma cells >5% increase in peripheral blood	The difference between involved and uninvolved FLC levels; the absolute increase must be > 100 mg/L >25% increase in the level of the serum M-protein with an absolute increase ≥5 g/L >25% increase in the 24 h urinary light chain excretion with and absolute increase ≥200 mg/24 h	Hypercalcemia Definite increase in lytic bone lesions Definite increase in the size or number of soft tissue plasmacytomas
Relapse from CR	More than 5% increase in the bone marrow plasma cells[7]	Reappearance of peripheral blood plasma cells at any level	Reappearance of original M-protein in serum and/or urine immunofixation	Any extramedullary disease Any new lytic bone lesion Hypercalcemia

[1]It is recommended that at least 200 leukocytes on blood smears and 500 nucleated cells on marrow smears be counted.
[2]It should be maintained for a minimum of 6 weeks. In case of discrepancy or undetectable serological parameter, the patient must be classified according to bone marrow criteria.
[3]Confirmation with repeat BM biopsy is not needed.
[4]Sensitivity attainable with 8-color multiparameter flow cytometry and allele-specific oligonucleotide PCR is 10^{-6}.
[5]If the serum and urine M-protein are unmeasurable, *a* ≥ 90% decrease in the difference between involved and uninvolved FLC levels is required instead of the M-protein.
[6]If the serum and urine M-protein are unmeasurable, *a* ≥ 50% decrease in the difference between involved and uninvolved FLC levels is required instead of the M-protein.
[7]Relapse from CR has the 5% cut-off vs. 10% for other categories of relapse.

there are four main categories that are necessary to evaluate (i) plasma cell count in BM; (ii) plasma cell count in peripheral blood; (iii) serologic criteria (serum M-protein, urinary M-protein, FLC); and (iv) evaluation of extramedullary disease. For achieving partial remission (PR), there must be ≤5% of plasma cells in peripheral blood and ≤25% of

plasma cells in BM. It is required to attain complete clearance of plasma cells from peripheral blood and ≤5% in BM by conventional morphology to qualify for complete remission (CR); for stringent CR, there must be no detection of malignant plasma cells in BM by flow cytometry. In accordance with IMWG, other authors added MRD (minimal residual disease)-negative CR, which is defined as MRD-negative BM and peripheral blood by multicolor flow cytometry or allele-specific oligonucleotide PCR (9). In addition, high frequency of extramedullary disease justifies the evaluation by imaging techniques such as magnetic resonance imaging (MRI) and FDG positron emission tomography/computer tomography (PET/CT).

Prognosis and survival

The prognosis of patients with PCL is very poor in the most of cases. The median survival by published small trials was short and ranged from 7 to 13 months, and the median survival of more than 5 years was in less than 10% of patients (42, 43). In the largest recently published epidemiological study, the median survival in 231 patients was just 4 months (44). The best survival data were achieved in patients undergoing autologous stem cell transplantation (ASCT), where the survival was longer than 3 years in 64% of patients (45). It is important to highlight that the significant survival improvement observed in MM in the past decade has not been seen in PCL (44). These discouraging survival results in primary PCL are due to two facts: (1) its aggressive presentation with complications leading to early death within the first months after diagnosis and (2) the lack of effective therapy to achieve sustained responses. Early mortality reflects the aggressiveness of the disease. In the French study, 28% (11/40) of patients died within the first month after diagnosis (18). The sPCL is usually a terminal event with median overall survival (OS) of only one month (7). Among the unfavorable prognostic factors, the same parameters are shared as in newly diagnosed MM, but their prevalence is significantly higher. These risk factors include elevated ß2-microglobulin (10), low serum albumin, hypercalcemia (33), elevated serum lactate dehydrogenase, worse performance status, and advanced age (46).

Also, the response to treatment has its prognostic value. Patients who are resistant to initial therapy have a very bad prognosis with estimated median overall survival (OS) of just several months (33, 46). Because most studies in pPCL are small and retrospective with heterogeneous treatments, the value of the cytogenetic abnormalities with prognostic impact in MM remains unclear in pPCL (9). In the Italian retrospective study, the presence of complex karyotype, hypodiploidy del(13q), del(17p), del(1p), or ampl(1q) was associated with reduced OS (33). On the other hand, Avet-Loiseau *et al.* showed that pPCL patients with *t*(11,14) had a longer OS (18).

Treatment modalities

The treatment of PCL should start immediately after the diagnosis is confirmed to eliminate the risk of early death because of irreversible disease complications. It is important to note that these recommendations are based on incomplete data and on the expert opinions, and there are no randomized clinical trials in patients with PCL because of rarity of this entity. In addition to other acute leukemias, the induction therapy should be as intensive as possible according to patients' tolerability to combined intensive chemotherapeutical regimens containing bortezomib. The use of bortezomib improves the treatment outcome, and this substance has become a backbone in the treatment of PCL (47). Based on expert opinions, strategies to improve long-term survival including high-dose therapy with ASCT are always considered, if there are no contraindications. The role of consolidation and maintenance therapy has not been evaluated yet. Also, the impact of tandem autologous transplantation as well as allogeneic transplantation should be defined. Patients younger than 50 years of age with suitable donor (related or unrelated) should be considered for allogeneic transplantation with myeloablative regimen (Fig. 4). Bortezomib-based regimens should be used in patients not eligible for ASCT to achieve rapid treatment response (47). The treatment of secondary PCL or relapsed pPCL depends on the treatment response to the previous therapies and the time to progression. Many patients could temporarily benefit from bortezomib-based regimens or the intensive regimens (e.g. hyper-CVAD [hyper-fractionated cyclophosphamide, vincristine, doxorubicin, dexamethasone] or dexamethasone-PACE [cisplatin, doxorubicin, cyclophosphamide, etoposide]). These patients can also be enrolled into clinical trials if they are fit enough.

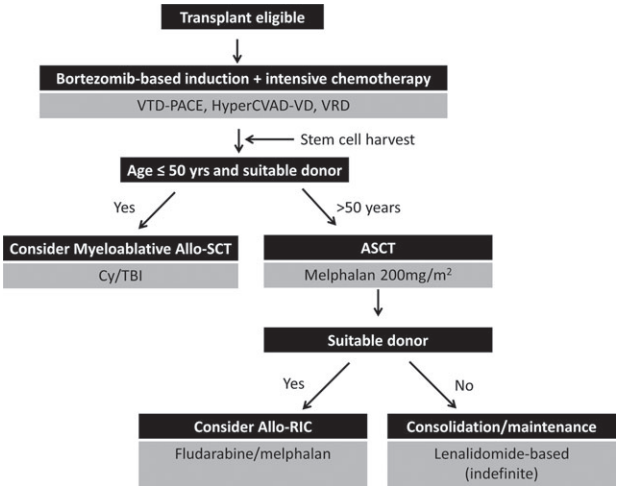

Figure 4 Treatment algorithm of pPCL for transplant eligible patients.

Conventional chemotherapeutic regimens

The treatment results of pPCL after conventional chemotherapy without novel agents [immunomodulatory drugs (IMIDs) or proteasome inhibitors (PIs)] are unsatisfactory with median OS about 7 months. The only limited benefit appears in terms of OS, in using combined conventional regimens, such as VAD (vincristine, doxorubicin, dexamethasone) in comparison with regimens containing only alkylating agents plus corticosteroids (2, 10, 48). There have been efforts performed to improve poor outcomes of PCL by intensification of conventional regimens in concert with therapeutic strategies in other types of acute leukemia. Intensive regimes such as hyperCVAD (49) or PACE and dominantly their combinations with bortezomib (VTD-PACE /bortezomib, thalidomide, dexamethasone – cisplatin, doxorubicin, cyclophosphamide, etoposide, hyperCVAD-VD /hyperfractionated cyclophosphamide, vincristine, doxorubicin, dexamethasone – bortezomib, dexamethasone) are currently recommended (5).

Proteasome inhibitors

There is increasing evidence that the use of proteasome inhibitors (PIs) improves outcomes of patients with PCL. Until now, there has been limited experience particularly with bortezomib. This proteasome inhibitor showed clinical activity in patients with pPCL as well as sPCL (50). This group of agents (PIs) are tested because of their efficacy in acute leukemias. Although the clinical trials were only performed with bortezomib, novel PIs like carfilzomib or others should also be tested because of their effect on inhibition of immunoproteasome (51). The Italian group reported results of retrospective analysis of 12 patients with relapsed pPCL and sPCL treated with bortezomib and its combinations (48). Response rate was 92% (11/12) with two patients with complete remission. The median progression-free survival (PFS) and overall survival were 8 and 12 months, respectively. These authors also reported a similar high response in patients with newly diagnosed pPCL treated with bortezomib in several combinations (VD – bortezomib, dexamethasone, $n = 3$; VTD – bortezomib, thalidomide, dexamethasone, $n = 2$; BDD – bortezomib, doxorubicin, dexamethasone, $n = 6$; MPV – melphalan, prednisone, bortezomib, $n = 1$). There was a high overall response rate 79% (23/29), including 28% (8/29) of patients with CR. In total, there were 83% (24/29) of patients who underwent ASCT. According to the aggressiveness of this disease and high-risk patients, only a few died during induction therapy – 17% (5/29) (47). There are other studies dominantly with small number of patients, which prove the benefit of bortezomib in the treatment of PCL (52), as well as combinations of bortezomib with dexamethasone, melphalan, or doxorubicin (53, 54). Recently, the results of the first retrospective study using the combination of novel agents in the treatment of sPCL were published. Nine patients with sPCL received the combination of lenalidomide, bortezomib, and dexamethason (VRD) with overall response rate (ORR) of 44% and median OS of only 5.13 months. The authors recommend trying VRD for one cycle; if no response is seen, an alternative approach should be utilized (55).

Immunomodulatory agents

Conventional treatment with usual dosage used in patients with MM is not effective. The role of thalidomide is even negligible (56) and was associated with severe pulmonary and cardiac toxicity (57, 58). Lenalidomide, a more potent immunomodulatory drug, resulted only in transient responses (59, 60). A multicentric prospective phase II clinical trial studied 23 patients with pPCL treated with lenalidomide and dexamethasone as a first-line therapy (34). Patients received 25 mg of lenalidomide in days 1–21 and 40 mg of dexamethasone once a week in a 28-day cycle. Patients that were eligible for ASCT proceeded to ASCT or they continued in long-term primary therapy. The initial ORR was 73.9% (17/23) of patients. In the 34th month of follow-up, the median progression-free survival (PFS) and median OS were 14 and 28 months, respectively.

High-dose myeloablative chemotherapy with hematopoietic stem cell support (autologous transplantation)

Because of a very poor prognosis of this plasma cell dyscrasia, the intensive high-dose chemotherapy followed by autologous stem cell transplantation should be offered to all patients, if their age and clinical conditions allow for such approach. In the Mayo Clinic series, patients who received ASCT had longer median OS in comparison to those who received only chemotherapy (34 vs. 11 months; $P = 0.09$). Indubitably, these results are a little bit distorted due to selection bias in favor of the transplant group (3). Large retrospective analysis of 97 patients with pPCL who underwent ASCT was generated by the CIBMTR (Center for International Blood and Marrow Transplant Research). PFS and OS were at 3 years 34% and 62%, respectively. These results demonstrated for the first time an OS longer than 3 years (45). The largest clinical study, which was conducted by EBMT (European Group for Blood and Marrow Transplantation), retrospectively analyzed clinical data of 272 patients with pPCL compared with 20 844 multiple myeloma patients undergoing ASCT between 1980 and 2006 (61). Results showed that the behavior of pPCL is very similar to the behavior of high-risk myeloma patients, which tends to have higher response rates to induction therapy and ASCT; however, they have a short duration of response (DOR) and rapid relapse. Although CR rates before and after autologous

transplantation were higher in pPCL patients (at 100 days after ASCT 41.2% in pPCL patients vs. 28.2% in MM patients; $P \leq 0.001$), median PFS (14.3 vs. 27.4 months; $P \leq 0.001$) and OS (25.7 vs. 62.3 months; $P \leq 0.001$) were significantly longer in MM patients. Despite the fact that certain proportion of patients achieved a relatively good response to initial treatment and underwent ASCT, they did not attain longer survival. On the other hand, ASCT is currently recommended for increasing the chance of prolonged survival in pPCL patients. The role of tandem ASCT has not been completely evaluated yet and represents an interesting opportunity to improve depth and duration of remission. Other strategies of consolidation after the first ASCT include combined regimens such as VTD, RD, or VRD, and they need to be prospectively evaluated. In addition, it is very important to explore other therapeutic approaches, such as the use of novel drugs in induction, consolidation, or maintenance therapy. Based on biological features of pPCL related with early reoccurrence of disease, the best strategy should probably be the starting consolidation and/or maintenance therapy as soon as the stable engraftment is documented (5).

Allogeneic stem cell transplantation

Allogeneic stem cell transplantation (allo-SCT) in patients with pPCL is the only potentially curative method, although this potential is limited, accompanied by high transplantation-related mortality (45, 49). The advantage of allo-SCT lies in establishing graft-versus-tumor (GVT) effect and graft-versus-pPCL (GVpPCL), respectively, as previously described in multiple myeloma (62, 63). One of the largest retrospective analyses presented outcomes of 147 patients with pPCL after upfront autologous (n = 97) or allogeneic (n = 50) hematopoietic stem cell transplantation (HSCT) reported to the CIBMTR between 1995 and 2006. This study showed that 39% (19/50) of patients who underwent allo-SCT had survived more than 3 years after transplantation (45). Despite a significant number of patients in these series, only a few of them were treated with novel agents (bortezomib, thalidomide, lenalidomide) as a part of their induction regimen. Due to the progression of disease, 85% of patients died in the ASCT group, whereas in allogeneic transplant group, 22% died, almost four times less. Nevertheless, transplantation-related mortality (TRM) at 3 years was significantly higher in allogeneic transplant group (auto-SCT vs. allo-SCT, 5% vs. 41%), so it resulted in a 3-year OS of 64% and 39% for the ASCT and allo-SCT group, respectively (45). In 2008, the EBMT described their experience with 85 patients who underwent allogeneic transplantation in comparison to 411 patients who underwent autologous SCT for PCL. As seen in previous experiences with allo-SCT described by the CIBMTR, there was a high early mortality; however, there was also a clear plateau in survival at 20% (64). Allogeneic approach gives hope for very limited number of patients with pPCL according to age, availability of suitable donor, and early peritransplant mortality. Patients with pPCL can be treated with ASCT, followed by allo-SCT 3–6 months later (9). In patients with sPCL, allo-SCT is not indicated at all. Because of the rarity of this disease, all patients should be treated within the clinical trials. The European Myeloma Network is preparing a new EMN plasma cell leukemia study in EMN trial consortium (EMN12/HO129 PCL). Patients will be treated with carfilzomib, lenalidomide, and dexamethasone in induction, consolidation, and maintenance. In addition, younger patients will receive the tandem of ASCT and allo-SCT or, in case of no suitable donor, tandem ASCT (personal communication with Henk Lokhorst, MD, PhD). For patients with refractory/relapsed PCL, it is possible to take part in several commercial studies such as phase I clinical trial NCT01248923, in which patients will receive the study drug ARRY-520 (a kinesin spindle inhibitor) and bortezomib with or without dexamethasone (65).

Conclusion

Plasma cell leukemia is a very rare aggressive monoclonal gammopathy. The diagnostic process depends primarily on morphological evaluation of peripheral blood with plasmocytes findings. The diagnostic criteria are widely discussed and can be modified. There are also discussions about treatment criteria suggesting the use of combined evaluation of treatment response. Plasma cell leukemia treatment is based on intensive chemotherapeutic regimens in combination with novel agents, especially with bortezomib. Induction treatment should begin immediately after diagnosis is confirmed, and the best strategies to improve long-term survival are high-dose chemotherapy followed by autologous transplantation of stem cells or allogeneic transplantation in younger patients. Nevertheless, the current treatment outcomes remain unsatisfactory and majority of patients have poor prognosis. Because of the rarity of this disease, all the patients should be treated within the clinical trials with the protocol including novel agents as a part of intensive induction and consolidation as well as maintenance therapy. The treatment of secondary PCL or relapse of primary PCL is very difficult, the treatment armamentarium may include also modern drugs with different mechanism of action such as monoclonal antibodies elotuzumab and daratumumab, spindle kindle inhibitor ARRY-520, or inhibitors of histone deacetylase.

Acknowledgments

TJ wrote the manuscript and reviewed the clinical part of manuscript. FK and LR proofread the paper and reviewed the biological part of manuscript. The overall proofreading and work coordination was provided by RH. The authors would like to thank Jana Zuchnicka MD. (Department of Haematooncology, University Hospital Ostrava) for morphological

images of plasma cell leukemia, RNDr. Henrieta Greslikova and assProf. RNDr. Petr Kuglik, CSc. (Babak Myeloma Group, Department of Pathological Physiology, Faculty of Medicine, Masaryk University) for CGH array PCL and Mgr. Eva Jarosova (University Hospital Ostrava, University of Ostrava) for administrative support. This work was supported by the Czech Ministry of Health under project RVO-FNOs/2012. The project was also supported by the grants of University of Ostrava, 2012. The financial support is assigned by the Ministry of Education, Youth and Sports.

References

1. Sant M, Allemani C, Tereanu C, De Angelis R, Capocaccia R, Visser O, *et al.* Incidence of hematologic malignancies in Europe by morphologic subtype: results of the HAEMACARE project. *Blood* 2010;**116**:3724–34.
2. Dimopoulos MA, Palumbo A, Delasalle KB, Alexanian R. Primary plasma cell leukaemia. *Br J Haematol* 1994;**88**:754–9.
3. Tiedemann RE, Gonzalez-Paz N, Kyle RA, Santana-Davila R, Price-Troska T, Van Wier SA, *et al.* Genetic aberrations and survival in plasma cell leukemia. *Leukemia* 2008;**22**:1044–52.
4. Yamamoto JF, Goodman MT. Patterns of leukemia incidence in the United States by subtype and demographic characteristics, 1997–2002. *Cancer Causes Control CCC* 2008;**19**:379–90.
5. Fernández de Larrea C, Kyle RA, Durie BGM, Ludwig H, Usmani S, Vesole DH, *et al.* Plasma cell leukemia: consensus statement on diagnostic requirements, response criteria and treatment recommendations by the International Myeloma Working Group. *Leukemia* 2013;**27**:780–91.
6. Kyle RA, Maldonado JE, Bayrd ED. Plasma cell leukemia. Report on 17 cases. *Arch Intern Med* 1974;**133**:813–18.
7. Noel P, Kyle RA. Plasma cell leukemia: an evaluation of response to therapy. *Am J Med* 1987;**83**:1062–8.
8. Bladé J, Kyle RA. Nonsecretory myeloma, immunoglobulin D myeloma, and plasma cell leukemia. *Hematol Oncol Clin North Am* 1999;**13**:1259–72.
9. Van de Donk NWCJ, Lokhorst HM, Anderson KC, Richardson PG. How I treat plasma cell leukemia. *Blood* 2012;**120**:2376–89.
10. García-Sanz R, Orfão A, González M, Tabernero MD, Bladé J, Moro MJ, *et al.* Primary plasma cell leukemia: clinical, immunophenotypic, DNA ploidy, and cytogenetic characteristics. *Blood* 1999;**93**:1032–7.
11. Pellat-Deceunynck C, Barillé S, Jego G, Puthier D, Robillard N, Pineau D, *et al.* The absence of CD56 (NCAM) on malignant plasma cells is a hallmark of plasma cell leukemia and of a special subset of multiple myeloma. *Leukemia* 1998;**12**:1977–82.
12. Rawstron AC, Orfao A, Beksac M, Bezdickova L, Brooimans RA, Bumbea H, *et al.* Report of the European Myeloma Network on multiparametric flow cytometry in multiple myeloma and related disorders. *Haematologica* 2008;**93**:431–8.
13. Tembhare PR, Subramanian PG, Sehgal K, Yajamanam B, Kumar A, Gadge V, *et al.* Immunophenotypic profile of plasma cell leukemia: a retrospective study in a reference cancer center in India and review of literature. *Indian J Pathol Microbiol* 2011;**54**:294–8.
14. Guikema JEJ, Hovenga S, Vellenga E, Conradie JJ, Abdulahad WH, Bekkema R, *et al.* CD27 is heterogeneously expressed in multiple myeloma: low CD27 expression in patients with high-risk disease. *Br J Haematol* 2003;**121**:36–43.
15. Guikema JEJ, Vellenga E, Abdulahad WH, Hovenga S, Bos NA. CD27-triggering on primary plasma cell leukaemia cells has anti-apoptotic effects involving mitogen activated protein kinases. *Br J Haematol* 2004;**124**:299–308.
16. Morgan TK, Zhao S, Chang KL, Haddix TL, Domanay E, Cornbleet PJ, *et al.* Low CD27 expression in plasma cell dyscrasias correlates with high-risk disease: an immunohistochemical analysis. *Am J Clin Pathol* 2006;**126**:545–51.
17. Kraj M, Kopeć-Szlęzak J, Pogłód R, Kruk B. Flow cytometric immunophenotypic characteristics of plasma cell leukemia. *Folia Histochem Cytobiol Pol Acad Sci Pol Histochem Cytochem Soc* 2011;**49**:168–82.
18. Avet-Loiseau H, Daviet A, Brigaudeau C, Callet-Bauchu E, Terré C, Lafage-Pochitaloff M, *et al.* Cytogenetic, interphase, and multicolor fluorescence in situ hybridization analyses in primary plasma cell leukemia: a study of 40 patients at diagnosis, on behalf of the Intergroupe Francophone du Myélome and the Groupe Français de Cytogénétique Hématologique. *Blood* 2001;**97**:822–5.
19. Chesi M, Robbiani DF, Sebag M, Chng WJ, Affer M, Tiedemann R, *et al.* AID-dependent activation of a MYC transgene induces multiple myeloma in a conditional mouse model of post-germinal center malignancies. *Cancer Cell* 2008;**13**:167–80.
20. Avet-Loiseau H, Attal M, Moreau P, Charbonnel C, Garban F, Hulin C, *et al.* Genetic abnormalities and survival in multiple myeloma: the experience of the Intergroupe Francophone du Myélome. *Blood* 2007;**109**:3489–95.
21. Fonseca R, Barlogie B, Bataille R, Bastard C, Bergsagel PL, Chesi M, *et al.* Genetics and cytogenetics of multiple myeloma: a workshop report. *Cancer Res* 2004;**64**:1546–58.
22. Fonseca R, Van Wier SA, Chng WJ, Ketterling R, Lacy MQ, Dispenzieri A, *et al.* Prognostic value of chromosome 1q21 gain by fluorescent in situ hybridization and increase CKS1B expression in myeloma. *Leukemia* 2006;**20**:2034–40.
23. Hanamura I, Stewart JP, Huang Y, Zhan F, Santra M, Sawyer JR, *et al.* Frequent gain of chromosome band 1q21 in plasma-cell dyscrasias detected by fluorescence in situ hybridization: incidence increases from MGUS to relapsed myeloma and is related to prognosis and disease progression following tandem stem-cell transplantation. *Blood* 2006;**108**:1724–32.
24. Chang H, Ning Y, Qi X, Yeung J, Xu W. Chromosome 1p21 deletion is a novel prognostic marker in patients with multiple myeloma. *Br J Haematol* 2007;**139**:51–4.

25. Chang H, Qi X, Trieu Y, Xu W, Reader JC, Ning Y, *et al.* Multiple myeloma patients with CKS1B gene amplification have a shorter progression-free survival post-autologous stem cell transplantation. *Br J Haematol* 2006;**135**:486–91.
26. Chang H, Qi XY, Samiee S, Yi Q-L, Chen C, Trudel S, *et al.* Genetic risk identifies multiple myeloma patients who do not benefit from autologous stem cell transplantation. *Bone Marrow Transplant* 2005;**36**:793–6.
27. Shaughnessy JD, Zhan F, Burington BE, Huang Y, Colla S, Hanamura I, *et al.* A validated gene expression model of high-risk multiple myeloma is defined by deregulated expression of genes mapping to chromosome 1. *Blood* 2007;**109**:2276–84.
28. Chiecchio L, Dagrada GP, Ibrahim AH, Dachs Cabanas E, Protheroe RKM, Stockley DM, *et al.* Timing of acquisition of deletion 13 in plasma cell dyscrasias is dependent on genetic context. *Haematologica* 2009;**94**:1708–13.
29. Chng WJ, Price-Troska T, Gonzalez-Paz N, Van Wier S, Jacobus S, Blood E, *et al.* Clinical significance of TP53 mutation in myeloma. *Leukemia* 2007;**21**:582–4.
30. Eymin B, Gazzeri S, Brambilla C, Brambilla E. Mdm2 overexpression and p14(ARF) inactivation are two mutually exclusive events in primary human lung tumors. *Oncogene* 2002;**21**:2750–61.
31. Stott FJ, Bates S, James MC, McConnell BB, Starborg M, Brookes S, *et al.* The alternative product from the human CDKN2A locus, p14(ARF), participates in a regulatory feedback loop with p53 and MDM2. *EMBO J* 1998;**17**:5001–14.
32. Albarracin F, Fonseca R. Plasma cell leukemia. *Blood Rev* 2011;**25**:107–12.
33. Pagano L, Valentini CG, De Stefano V, Venditti A, Visani G, Petrucci MT, *et al.* Primary plasma cell leukemia: a retrospective multicenter study of 73 patients. *Ann Oncol Off J Eur Soc Med Oncol ESMO* 2011;**22**:1628–35.
34. Musto P, Simeon V, Martorelli MC, Petrucci MT, Cascavilla N, Di Raimondo F, *et al.* Lenalidomide and low-dose dexamethasone for newly diagnosed primary plasma cell leukemia. *Leukemia* 2014;**28**:222–5.
35. Dimopoulos MA, Barlogie B, Smith TL, Alexanian R. High serum lactate dehydrogenase level as a marker for drug resistance and short survival in multiple myeloma. *Ann Intern Med* 1991;**115**:931–5.
36. Hameed A, Brady JJ, Dowling P, Clynes M, O'Gorman P. Bone disease in multiple myeloma: pathophysiology and management. *Cancer Growth Metastasis* 2014;**7**:33–42.
37. Kumar S, Rajkumar SV, Kyle RA, Lacy MQ, Dispenzieri A, Fonseca R, *et al.* Prognostic value of circulating plasma cells in monoclonal gammopathy of undetermined significance. *J Clin Oncol Off J Am Soc Clin Oncol* 2005;**23**:5668–74.
38. Nowakowski GS, Witzig TE, Dingli D, Tracz MJ, Gertz MA, Lacy MQ, *et al.* Circulating plasma cells detected by flow cytometry as a predictor of survival in 302 patients with newly diagnosed multiple myeloma. *Blood* 2005;**106**:2276–9.
39. Shtalrid M, Shvidel L, Vorst E. Polyclonal reactive peripheral blood plasmacytosis mimicking plasma cell leukemia in a patient with Staphylococcal sepsis. *Leuk Lymphoma* 2003;**44**:379–80.
40. Al-Sahmani M, Trnavska I, Sevcikova S, Antosova M, Antosova L, Kissova J, *et al.* Prognostic significance of morphological assessment of plasma cells in multiple myeloma. *Neoplasma* 2011;**58**:554–60.
41. Döhner H, Estey EH, Amadori S, Appelbaum FR, Büchner T, Burnett AK, *et al.* Diagnosis and management of acute myeloid leukemia in adults: recommendations from an international expert panel, on behalf of the European LeukemiaNet. *Blood* 2010;**115**:453–74.
42. Colović M, Janković G, Suvajdzić N, Milić N, Dordević V, Janković S. Thirty patients with primary plasma cell leukemia: a single center experience. *Med Oncol Northwood Lond Engl* 2008;**25**:154–60.
43. Peijing Q, Yan X, Yafei W, Dehui Z, Zengjun L, Junyuan Q, *et al.* A retrospective analysis of thirty-one cases of plasma cell leukemia from a single center in China. *Acta Haematol* 2009;**121**:47–51.
44. Ramsingh G, Mehan P, Luo J, Vij R, Morgensztern D. Primary plasma cell leukemia: a surveillance, epidemiology, and end results database analysis between 1973 and 2004. *Cancer* 2009;**115**:5734–9.
45. Mahindra A, Kalaycio ME, Vela-Ojeda J, Vesole DH, Zhang M-J, Li P, *et al.* Hematopoietic cell transplantation for primary plasma cell leukemia: results from the Center for International Blood and Marrow Transplant Research. *Leukemia* 2012;**26**:1091–7.
46. Vela-Ojeda J, García-Ruiz Esparza MA, Rosas-Cabral A, Padilla-González Y, García-Chávez J, Tripp-Villanueva F, *et al.* Intermediate doses of melphalan and dexamethasone are better than vincristine, adriamycin, and dexamethasone (VAD) and polychemotherapy for the treatment of primary plasma cell leukemia. *Ann Hematol* 2002;**81**:362–7.
47. D'Arena G, Valentini CG, Pietrantuono G, Guariglia R, Martorelli MC, Mansueto G, *et al.* Frontline chemotherapy with bortezomib-containing combinations improves response rate and survival in primary plasma cell leukemia: a retrospective study from GIMEMA Multiple Myeloma Working Party. *Ann Oncol Off J Eur Soc Med Oncol ESMO* 2012;**23**:1499–502.
48. Musto P, Rossini F, Gay F, Pitini V, Guglielmelli T, D'Arena G, *et al.* Efficacy and safety of bortezomib in patients with plasma cell leukemia. *Cancer* 2007;**109**:2285–90.
49. Saccaro S, Fonseca R, Veillon DM, Cotelingam J, Nordberg ML, Bredeson C, *et al.* Primary plasma cell leukemia: report of 17 new cases treated with autologous or allogeneic stem-cell transplantation and review of the literature. *Am J Hematol* 2005;**78**:288–94.
50. Esparís-Ogando A, Alegre A, Aguado B, Mateo G, Gutiérrez N, Bladé J, *et al.* Bortezomib is an efficient agent in plasma cell leukemias. *Int J Cancer J Int Cancer* 2005;**114**:665–7.
51. Niewerth D, Dingjan I, Cloos J, Jansen G, Kaspers G. Proteasome inhibitors in acute leukemia. *Expert Rev Anticancer Ther* 2013;**13**:327–37.
52. Lebovic D, Zhang L, Alsina M, Nishihori T, Shain KH, Sullivan D, *et al.* Clinical outcomes of patients with plasma cell

leukemia in the era of novel therapies and hematopoietic stem cell transplantation strategies: a single-institution experience. *Clin Lymphoma Myeloma Leuk* 2011;**11**:507–11.
53. Al-Nawakil C, Tamburini J, Bardet V, Chapuis N, Bourry E, Roux C, *et al.* Bortezomib, doxorubicin and dexamethasone association is an effective option for plasma cell leukemia induction therapy. *Leuk Lymphoma* 2008;**49**:2012–14.
54. Libby E, Candelaria-Quintana D, Moualla H, Abdul-Jaleel M, Rabinowitz I. Durable complete remission of primary plasma cell leukemia with the bortezomib plus melphalan and prednisone (VMP) regimen. *Am J Hematol* 2010;**85**:733–4.
55. Jimenez-Zepeda VH, Reece DE, Trudel S, Chen C, Tiedemann R, Kukreti V. Lenalidomide (Revlimid), bortezomib (Velcade) and dexamethasone for the treatment of secondary plasma cell leukemia. *Leuk Lymphoma* 2015;**56**:232–5.
56. Petrucci MT, Martini V, Levi A, Gallucci C, Palumbo G, Del Bianco P, *et al.* Thalidomide does not modify the prognosis of plasma cell leukemia patients: experience of a single center. *Leuk Lymphoma* 2007;**48**:180–2.
57. Ballanti S, Mastrodicasa E, Bolli N, Lotti F, Capolsini I, Berchicci L, *et al.* Sustained ventricular tachycardia in a thalidomide-treated patient with primary plasma-cell leukemia. *Nat Clin Pract Oncol* 2007;**4**:722–5.
58. Pretz J, Medeiros BC. Thalidomide-induced pneumonitis in a patient with plasma cell leukemia: no recurrence with subsequent lenalidomide therapy. *Am J Hematol* 2009;**84**:698–9.
59. Musto P, Pietrantuono G, Guariglia R, Villani O, Martorelli MC, D'Auria F, *et al.* Salvage therapy with lenalidomide and dexamethasone in relapsed primary plasma cell leukemia. *Leuk Res* 2008;**32**:1637–8.
60. Olivieri A, Attolico I, Cimminiello M, Discepoli G, Cifarelli RA. Lenalidomide can induce graft versus leukemia effect in primary plasma cell leukemia: a case report. *Leuk Res* 2009;**33**:e191–3.
61. Drake MB, Iacobelli S, van Biezen A, Morris C, Apperley JF, Niederwieser D, *et al.* Primary plasma cell leukemia and autologous stem cell transplantation. *Haematologica* 2010;**95**:804–9.
62. Luft T, Moos M, Goldschmidt H, Ho AD, Görner M. Dissociation of putative graft-versus-haematopoiesis and graft-versus-myeloma effects in patients with rapidly progressive multiple myeloma. *Br J Haematol* 2003;**123**:646–53.
63. Tricot G, Vesole DH, Jagannath S, Hilton J, Munshi N, Barlogie B. Graft-versus-myeloma effect: proof of principle. *Blood* 1996;**87**:1196–8.
64. Morris C, Iacobelli S, Gahrton G, Garderet Laurent, Drake Mary, van Biezen Anja, *et al.* Has allogeneic transplantation a role in the management of plasma cell leukaemia? A study on behalf of the myeloma subcomittee of the chronic leukaemia working party of the EBMT. *Blood (ASH Annual Meeting Abstracts)* 2011;**118**: Abstract 2008.
65. Ocio EM, Richardson PG, Rajkumar SV, Palumbo A, Mateos MV, Orlowski R, *et al.* New drugs and novel mechanisms of action in multiple myeloma in 2013: a report from the International Myeloma Working Group (IMWG). *Leukemia* 2014;**28**:525–42.

12.

Addenbrooke´s cognitive examination and individual domain cut-off scores for discriminating between different cognitive subtypes of Parkinson´s disease

Beránková D, Janoušková E, Mračková M, Eliášová I, Košťálová M, Skutilová S, Rektorová I

Originally published in Parkinson´s Disease, [online], 2015, vol. 2015, no. Article ID 579417, p. 1-7.

Hindawi Publishing Corporation
Parkinson's Disease
Volume 2015, Article ID 579417, 7 pages
http://dx.doi.org/10.1155/2015/579417

Research Article

Addenbrooke's Cognitive Examination and Individual Domain Cut-Off Scores for Discriminating between Different Cognitive Subtypes of Parkinson's Disease

Dagmar Berankova,[1,2,3] Eva Janousova,[4] Martina Mrackova,[1,5] Ilona Eliasova,[1,5] Milena Kostalova,[1,6] Svetlana Skutilova,[1,6] and Irena Rektorova[1,5]

[1]*Applied Neuroscience Research Group, CEITEC MU, Masaryk University, 625 00 Brno, Czech Republic*
[2]*Department of Neurology, University Hospital in Ostrava, 708 52 Ostrava, Czech Republic*
[3]*Department of Rehabilitation, Faculty of Medicine, University of Ostrava, 708 52 Ostrava, Czech Republic*
[4]*Institute of Biostatistics and Analyses, Faculty of Medicine, Masaryk University, 625 00 Brno, Czech Republic*
[5]*Department of Neurology, School of Medicine, Masaryk University and St. Anne's Hospital, 656 91 Brno, Czech Republic*
[6]*Second Department of Neurology, School of Medicine, Masaryk University and Brno Teaching Hospital, 625 00 Brno, Czech Republic*

Correspondence should be addressed to Irena Rektorova; irena.rektorova@fnusa.cz

Received 14 June 2015; Accepted 3 August 2015

Academic Editor: Hélio Teive

Objective. The main aim of this study was to verify the sensitivity and specificity of Addenbrooke's Cognitive Examination-Revised (ACE-R) in discriminating between Parkinson's disease (PD) with normal cognition (PD-NC) and PD with mild cognitive impairment (PD-MCI) and between PD-MCI and PD with dementia (PD-D). We also evaluated how ACE-R correlates with neuropsychological cognitive tests in PD. *Methods*. We examined three age-matched groups of PD patients diagnosed according to the Movement Disorder Society Task Force criteria: PD-NC, PD-MCI, and PD-D. ROC analysis was used to establish specific cut-off scores of ACE-R and its domains. Correlation analyses were performed between ACE-R and its subtests with relevant neuropsychological tests. *Results*. Statistically significant differences between groups were demonstrated in global ACE-R scores and subscores, except in the language domain. ACE-R cut-off score of 88.5 points discriminated best between PD-MCI and PD-NC (sensitivity 0.68, specificity 0.91); ACE-R of 82.5 points distinguished best between PD-MCI and PD-D (sensitivity 0.70, specificity 0.73). The verbal fluency domain of ACE-R demonstrated the best discrimination between PD-NC and PD-MCI (cut-off score 11.5; sensitivity 0.70, specificity 0.73) while the orientation/attention subscore was best between PD-MCI and PD-D (cut-off score 15.5; sensitivity 0.90, specificity 0.97). ACE-R scores except for ACE-R language correlated with specific cognitive tests of interest.

1. Introduction

Parkinson's disease (PD) is considered to be a motor disorder, but nonmotor symptoms have recently attracted more attention as they have a major impact on patient quality of life [1, 2]. The major risk factors for developing dementia associated with PD are higher age, more severe Parkinsonism, postural instability with gait difficulty, and mild cognitive impairment at the time of evaluation. The prevalence of dementia in PD is approximately 30%; the cumulative prevalence reaches up to 80% after 8–10 years of the disease progression [3–5]. PD is often associated with some type of cognitive decline even in the absence of fully blown dementia, and mild cognitive impairment (MCI) is present in about 25% of PD patients [6–8].

MCI is characterized by subjective and objective deterioration of cognitive functions with retention of normal social life and daily functioning [9]. Impaired attention and

Table 1: Patient characteristics (n = 69). Characteristics are described as median (min-max).

	Total (n = 69)	PD-NC (n = 22)	PD-MCI (n = 37)	PD-D (n = 10)	p value	Post hoc p values		
						PD-NC × PD-MCI	PD-MCI × PD-D	PD-NC × PD-D
Sex, males (%)	41 (59.4%)	13 (59.1%)	25 (67.6%)	3 (30.0%)	0.100			
Age (years)	68 (49–86)	70 (51–86)	67 (49–81)	65 (54–82)	0.754			
Education (years)	13 (9–18)	13 (12–18)	13 (9–18)	12 (9–18)	**0.006**	0.466	0.062	**0.004**
PD duration (years)	7 (1–22)	7 (3–21)	8 (1–18)	6 (2–22)	0.510			
L-dopa dose (mg/day)	907 (0–2275)	1037 (0–2275)	931 (56–2108)	591 (160–1836)	**0.042**	0.870	0.158	**0.044**
UPDRS III	25 (3–55)	29 (5–49)	25 (5–55)	19 (3–52)	0.333			
MMSE	29 (16–30)	29 (27–30)	29 (27–30)	25 (16–26)	**<0.001**	**0.046**	**<0.001**	**<0.001**
ACE-R	87 (60–99)	93 (80–98)	87 (72–99)	79 (60–87)	**<0.001**	**0.001**	**0.020**	**<0.001**
ACE-R AO	18 (13–18)	18 (17-18)	17 (15–18)	15 (13–18)	**<0.001**	0.130	**<0.001**	**<0.001**
ACE-R M	21 (3–26)	23 (17–26)	19 (12–26)	18 (3–21)	**0.001**	0.057	0.126	**0.001**
ACE-R F	11 (3–14)	13 (6–14)	10 (3–14)	9 (5–12)	**0.001**	**0.005**	0.782	**0.004**
ACE-R L	25 (20–26)	26 (24–26)	25 (20–26)	25 (21–26)	0.176			
ACE-R VA	15 (10–16)	16 (13–16)	15 (12–16)	14 (10–16)	**0.003**	0.250	**0.031**	**0.005**

UPDRS III: Unified Parkinson's Disease Rating Scale.
MMSE: Mini Mental State Examination.
ACE-R: Addenbrooke's Cognitive Examination, global score.
ACE-R AO: Addenbrooke's Cognitive Examination, domain attention and orientation.
ACE-R M: Addenbrooke's Cognitive Examination, domain memory.
ACE-R F: Addenbrooke's Cognitive Examination, domain verbal fluency.
ACE-R L: Addenbrooke's Cognitive Examination, domain language.
ACE-R VA: Addenbrooke's Cognitive Examination, domain visual spatial abilities.

executive functioning are the most common forms of early cognitive deficit in PD [6, 10]. Deficits in memory, visual spatial skills, and language may also occur, in combination with attentional and executive deficits or alone. Impaired executive functions and posterior cortical deficits may predict the development of dementia later in the course of the disease [10–12]. Criteria for MCI in PD (PD-MCI) were formulated by the Movement Disorder Society (MDS) Task Force in their guidelines for the diagnosis of MCI [6]. PD-MCI was defined as a cognitive decline reported by the patient, carer, or clinician with a performance of one to two standard deviations (SD) below the mean for an age-matched control population on two or more tests from a neuropsychological battery as well as the lack of a confounding cause for poor test performance (e.g., depression). Neuropsychological investigations are quite time-consuming and distressing to patients. It is necessary to have screening instruments to identify PD-MCI and dementia in PD (PD-D). While the Mini Mental State Examination (MMSE) cannot distinguish PD with normal cognition (PD-NC) [13], several screening instruments have been developed or validated for screening PD-MCI [14, 15]. We focused on Addenbrooke's Cognitive Examination-Revised (ACE-R) version and its utility in discriminating between PD-NC and PD-MCI and between PD-MCI and PD-D. In addition to global cut-off scores we aimed at providing cut-off values for all cognitive domains evaluated by this screening instrument.

The ACE-R is a brief cognitive screening battery assessing five neuropsychological domains: orientation and attention (ACE-R OA), memory (ACE-R M), verbal fluency (ACE-R F), language (ACE-R L), and visuospatial abilities (ACE-R VA). It incorporates the widely used MMSE but provides a more thorough assessment of cognitive function. As a screening tool for dementia, it has high reliability and validity, and its utility in a number of neurological conditions has been demonstrated [14–19].

ACE-R was translated into Czech [20] and slightly adapted for ease of use [21]. Normative data exist for healthy elderly Czech people [22]. While several previous studies have employed ACE-R in identifying PD-MCI and PD-D (for review, see [23]), none of the studies has identified cut-off scores for individual ACE-R domains. We examined three age-matched groups of PD patients: PD-NC, PD-MCI, and PD-D. We used receiver-operating curve (ROC) analysis in order to establish the specific cut-off scores for ACE-R and its cognitive domains for discriminating among these three groups. We also evaluated how ACE-R correlates with relevant neuropsychological cognitive tests in PD.

2. Materials and Methods

Altogether, 69 patients with PD were enrolled in the study: 22 PD-NC, 37 PD-MCI, and 10 PD-D according to published criteria [5, 6] (Table 1). PD-MCI was defined as a cognitive decline reported by the patient, carer, or clinician, with a performance 1.5 SD below the mean for age-matched control population on two or more tests from the neuropsychological battery (our battery is described in more detail in the text below) as well as the lack of a confounding cause for

poor test performance. This is in accordance with level 1 (comprehensive) MDS criteria for diagnosis of PD-MCI [6].

All of the patients were assessed by a clinician and the presence of a current depressive episode excluded subjects from the study. Beck Depression Inventory was used to evaluate depressive symptoms. Unified Parkinson's Disease Rating Scale, part III: Motor Examination (UPDRS III) was employed to evaluate motor symptoms of PD [24].

All of the assessments were conducted when the patients were in their "on" state on dopaminergic medication. Patients were on levodopa ± dopamine agonist ± COMT (catechol-o-methyltransferase) inhibitor. None of the patients were on antipsychotic treatment at the time of examination. All patients with PD-D received cholinesterase inhibitors. None of the included subjects received deep brain stimulation surgery for PD. The study was approved by the local ethics committee, and all of the patients signed an informed consent form.

Cognitive Assessment Using a Neuropsychological Battery. To detect cognitive decline in the attention domain, we used selected subtests from the Wechsler Adult Intelligence Scale-Revised (WAIS-R): Digit Span (WAIS-R DS), Coding (WAIS-R C), Arithmetic (WAIS-R A) [23, 25–27], and the Stroop Colour and Word Test, part A, word naming (SCWT A), and part B, colour naming (SCWT B) [28].

To detect memory impairment, we used selected subtests from the Wechsler Memory Scale-III (WMS-III): stories for testing logical memory—immediate recall (LMI), stories—delayed recall (LMD), list of words—immediate recall (LWI), delayed recall (LWD), and recognition of the list of words (LWR) [29].

To evaluate executive functions, we used WAIS-R Similarities (WAIS-R S) [25] and SCWT, part C (SCWT C, i.e., colour-word interference) [28], subtests.

To detect impairment of visuospatial functions, we used the Clock Test (CT) [30] and WAIS-R Picture Completion (WAIS-R PC) [25].

To evaluate language domain, we used the Mississippi Aphasia Screening Test (MAST) [31] and letter verbal fluency (VF) [32].

To achieve our goal, all of the patients were also examined by ACE-R [22]. The maximum ACE-R score (i.e., the best performance) is 100 points. In the ACE-R AO domain, it is possible to achieve a maximum of 18 points; in the ACE-R M domain, the maximum is 26 points; in the ACE-R F domain, it is 14 points; in the ACE-R L domain, it is 26 points; and in the ACE-R VA domain, it is 16 points.

To compare the clinical characteristics of the PD-NC, PD-MCI, and PD-D subjects and their results in ACE-R and its subtests, we used Kruskal-Wallis and Chi-square tests. ROC analysis with AUC (95% CI) was performed and used to evaluate subject performance in ACE-R and its subtests in order to distinguish between PD-MCI and PD-NC and between PD-D and PD-MCI. Sensitivity, specificity, positive predictive value (PPV), and negative predictive value (NPV) were calculated for all possible cut-off values. The cut-off points with the highest Youden index (i.e., the maximum sum of sensitivity and specificity) were selected as the best cut-off point values for discriminating between PD-NC and PD-MCI and between PD-MCI and PD-D.

We also performed correlation analysis between each ACE-R domain and specific neurocognitive tests of interest using nonparametric Spearman's rho coefficient, which was corrected for age (i.e., partial correlation coefficients were calculated). We correlated the ACE-R AO domain (attention, orientation) with WAIS-R C, WAIS-R A, WAIS-R DS, and SCWT—A, B. The ACE-R M domain (memory) was correlated with LMI, LMD, LWI, LWD, and LWR. The ACE-R L domain (language) was correlated with MAST and letter VF. The ACE-R F (executive functions) was correlated with WAIS-R S, WAIS-R PC, and SCWT C. Finally, the ACE-R VA domain (visuospatial abilities) was correlated with WAIS-R PC and CT.

The level of significance was set at $\alpha = 0.05$. Statistical analyses were performed by IBM SPSS Statistics software (version 21) and MATLAB R2010b software.

3. Results and Discussion

3.1. Results. A comparison of the clinical characteristics of PD-NC, PD-MCI, and PD-D patients reveals that there were no differences between the groups in sex, age, PD duration, or UPDRS III (Table 1). However, there were differences in education and in daily L-dopa dose. The length of education was significantly shorter in PD-D than in PD-NC (the difference in medians is only one year). The L-dopa dose was significantly lower in PD-D than in PD-NC. There were statistically significant differences among the three patient groups in cognitive tests in MMSE, ACE-R, and all the ACE-R subtests with the exception of ACE-R L. Specifically, scores in MMSE and in ACE-R and its subtests were highest in PD-NC and lowest in PD-D.

Results of ROC analysis including AUC estimates (with 95% confidence intervals) are summarized in Table 2 and visualized via ROC curves in Figure 1. Cut-off scores for global scores of ACE-R and its domains are displayed in Table 2. The ACE-R global cut-off score to differentiate between PD-NC and PD-MCI is 88.5 points (with 0.68 sensitivity and 0.91 specificity) and 82.5 points (with 0.70 sensitivity and 0.73 specificity) to differentiate between PD-MCI and PD-D.

ACE-R and ACE-R M enable discrimination between PD-NC and PD-MCI (with AUC of 0.78 and 0.68, resp.) and between PD-MCI and PD-D (AUC of 0.78 and 0.71, resp.). ACE-R AO and ACE-R VA differentiate between PD-MCI and PD-D (AUC of 0.92 and 0.75, resp.). ACE-R F differentiates between PD-NC and PD-MCI (AUC 0.75). ACE-R L does not enable differentiation among the patient groups (this is shown in Table 1). Table 2 also shows cut-off point estimates based on the Youden index (i.e., the maximum sum of sensitivity and specificity) for ACE-R and its subtests. The cut-off points are also shown in Figure 1.

Partial correlation coefficients between each ACE-R domain and specific neurocognitive tests of interest corrected for patient age are depicted in Table 3. There was no statistically significant correlation between ACE-R AO and WAIS-R

Table 2: AUC estimates calculated in ROC analyses and ROC characteristics at optimal cut-offs.

	AUC (95% CI)	*p* value	Cut-off	Sensitivity (95% CI)	Specificity (95% CI)	PPV	NPV
ACE-R							
PD-NC versus PD-MCI	0.78 (0.66–0.90)	<**0.001**	88.5	0.68 (0.50–0.81)	0.91 (0.69–0.98)	0.93	0.63
PD-MCI versus PD-D	0.78 (0.63–0.93)	**0.007**	82.5	0.70 (0.35–0.92)	0.73 (0.56–0.86)	0.41	0.90
ACE-R AO							
PD-NC versus PD-MCI	0.64 (0.50–0.78)	0.077	17.5	0.51 (0.35–0.68)	0.73 (0.50–0.88)	0.76	0.47
PD-MCI versus PD-D	0.92 (0.77–1.00)	<**0.001**	15.5	0.90 (0.54–0.99)	0.97 (0.84–1.00)	0.90	0.97
ACE-R M							
PD-NC versus PD-MCI	0.68 (0.55–0.82)	**0.020**	22.5	0.76 (0.58–0.88)	0.50 (0.29–0.71)	0.72	0.55
PD-MCI versus PD-D	0.71 (0.54–0.88)	**0.043**	20.5	0.90 (0.54–0.99)	0.46 (0.30–0.63)	0.31	0.94
ACE-R F							
PD-NC versus PD-MCI	0.75 (0.61–0.88)	**0.002**	11.5	0.70 (0.53–0.84)	0.73 (0.50–0.88)	0.81	0.59
PD-MCI versus PD-D	0.62 (0.42–0.82)	0.264	8.5	0.50 (0.20–0.80)	0.76 (0.58–0.88)	0.36	0.85
ACE-R L							
PD-NC versus PD-MCI	0.62 (0.47–0.76)	0.141	24.5	0.35 (0.21–0.53)	0.91 (0.69–0.98)	0.87	0.45
PD-MCI versus PD-D	0.56 (0.34–0.77)	0.585	23.5	0.40 (0.14–0.73)	0.84 (0.67–0.93)	0.40	0.84
ACE-R VA							
PD-NC versus PD-MCI	0.63 (0.48–0.77)	0.110	15.5	0.62 (0.45–0.77)	0.64 (0.41–0.82)	0.74	0.50
PD-MCI versus PD-D	0.75 (0.58–0.93)	**0.015**	14.5	0.60 (0.27–0.86)	0.78 (0.61–0.90)	0.43	0.88

ACE-R: Addenbrooke's Cognitive Examination, global score.
PD-NC: subjects with Parkinson's disease with normal control.
PD-MCI: subjects with Parkinson's disease with mild cognitive impairment.
PD-D: subjects with Parkinson's disease with dementia.
ACE-R AO: Addenbrooke's Cognitive Examination, domain attention and orientation.
ACE-R M: Addenbrooke's Cognitive Examination, domain memory.
ACE-R F: Addenbrooke's Cognitive Examination, domain verbal fluency.
ACE-R L: Addenbrooke's Cognitive Examination, domain language.
ACE-R VA: Addenbrooke's Cognitive Examination, domain visual spatial abilities.

C or between ACE-R L and MAST and letter VF. All other correlations were statistically significant.

3.2. Discussion. Based on the ROC analysis of ACE-R, the best cut-off score for detecting PD-MCI was 88.5 points with 0.68 sensitivity and 0.91 specificity, with AUC of 0.78 (95% confidence interval (CI) 0.66–0.90). Our result accords well with previous study results in PD-MCI [33] where the authors used the same criteria for PD-MCI diagnosis and demonstrated 0.69 sensitivity and 0.84 specificity with the same ACE-R cut-off score. Komadina et al. (2011) found lower sensitivity (0.61) and specificity (0.64) for higher cut-off scores (93 points) but the authors used different criteria for PD-MCI diagnosis [34]. Our best cut-off score for detecting PD-D was 82.5 points with 0.70 sensitivity and 0.73 specificity, with AUC of 0.78 (95% CI 0.63–0.93). Similar results were found by Biundo and co-workers with a lower cut-off score of 80 points [35], while Reyes et al. (2009) reached higher sensitivity (0.92) and specificity (0.93) with the same cut-off score [15]. These discrepancies could have been caused by the fact that different techniques were used to assess the instrumental and basic activities of daily living. We used a semistructured interview performed with both the patients and their caregivers. A limitation of our study might be the small sample size of the PD-D group.

In addition to cut-offs for the total ACE-R score, our study presents cut-off scores of individual cognitive ACE-R domains for predicting PD-MCI and PD-D which is novel. We also demonstrate for the first time that individual ACE-R domains subscores in PD subjects correlate well with relevant tests scores derived from our comprehensive neuropsychological battery. The verbal fluency domain had the highest sensitivity and specificity for discrimination between PD-NC and PD-MCI with a cut-off score of 11.5 points (sensitivity 0.70, specificity 0.73) and AUC of 0.75 (95% CI 0.61–0.88). The memory domain had a cut-off score of 22.5 points (sensitivity 0.76, specificity 0.50) and AUC of 0.68 (95% CI 0.55–0.82). In a study by Komadina et al. [34] the ACE-R verbal fluency domain was found to be the only domain which was significantly different between PD-NC and PD-MCI [34]. This is in line with our study results. However, Komadina et al. [34] did not use the ROC analysis and the authors used different PD-MCI criteria [34]. Therefore, the two studies cannot be directly compared.

Using MDS criteria for PD-MCI diagnosis, Biundo et al. [35] demonstrated that specific neuropsychological tests evaluating executive functions, memory, and visuospatial functions reached significant screening and diagnostic validity in predicting PD-MCI. Interestingly, Cholerton et al. [36] used detailed neuropsychological examination in PD-MCI and factor analysis to show that the verbal fluency category loaded on two factors: with visuospatial skills and with executive functions. In view of these results, it is not surprising that the verbal fluency domain of ACE-R reached

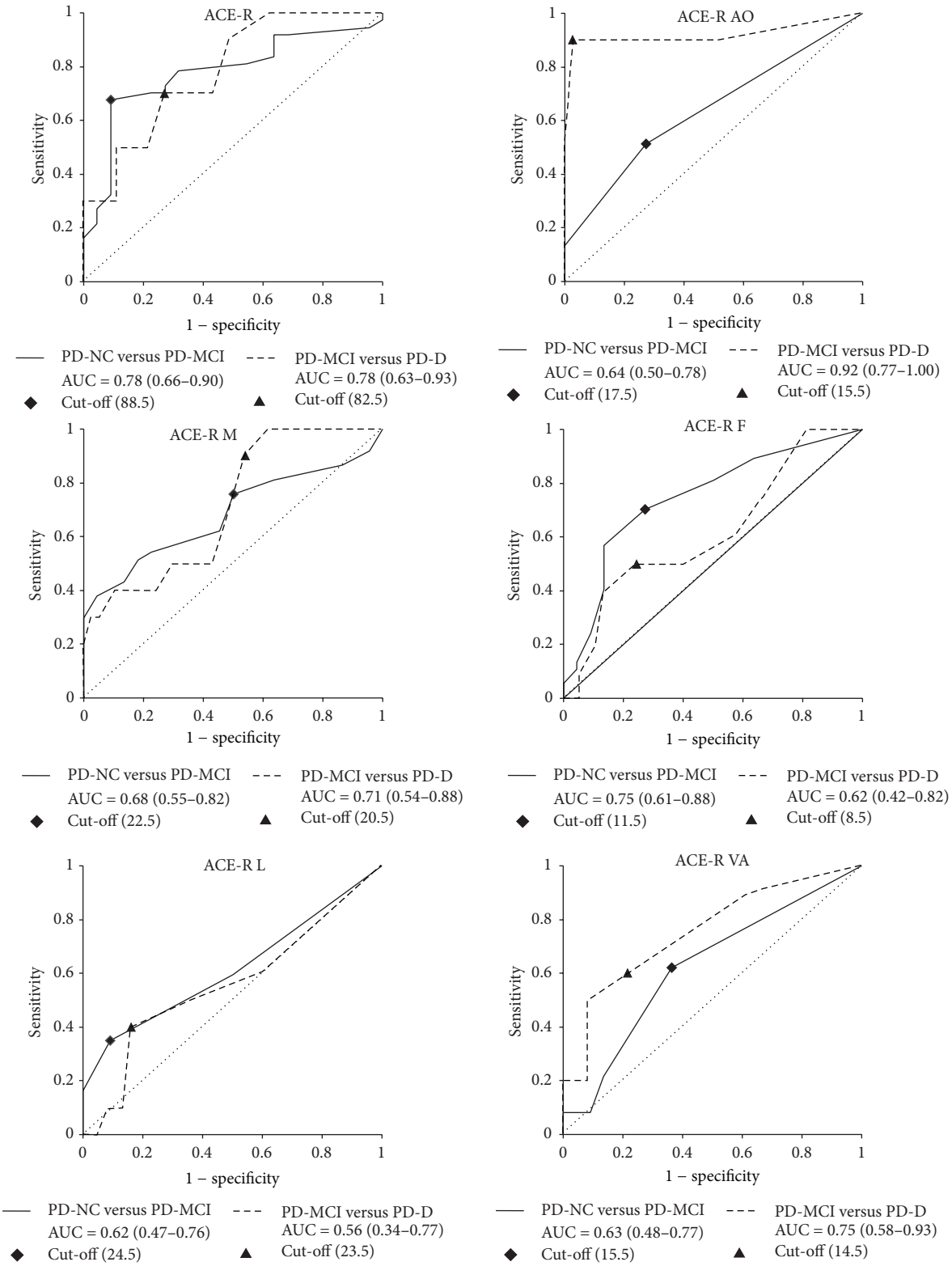

Figure 1: ROC curves distinguishing between patient groups using ACE-R and its subtests. ACE-R OA: orientation and attention domain of ACE-R, ACE-R M: memory domain of ACE-R, ACE-R F: verbal fluency domain of ACE-R, ACE-R L: language domain of ACE-R, ACE-R VA: visuospatial abilities domain of ACE-R, AUC: area under the curve, PD-NC: Parkinson's disease with normal cognition, PD-MCI: Parkinson's disease with mild cognitive impairment, and PD-D: Parkinson's disease with dementia.

Table 3: Correlation coefficients between ACE-R subscores and relevant neuropsychological tests.

	ACE-R AO	ACE-R M	ACE-R L	ACE-R F	ACE-R VA
WAIS-R C	0.242				
WAIS-R A	**0.423***				
WAIS-R DS	**0.311***				
SCWT A	**0.331***				
SCWT B	**0.289**				
LMI		**0.491***			
LMD		**0.408***			
LWI		**0.476***			
LWD		**0.513***			
LWR		**0.483***			
MAST			0.109		
VF			0.194		
WAIS-R S				**0.423***	
SCWT C				**0.545***	
WAIS-R PC					**0.544***
CT					**0.758***

Statistically significant correlation coefficients at $\alpha = 0.01$ level are marked with bold and "$*$" symbol; $\alpha = 0.05$ level is marked with bold only.
WAIS-R C: Coding subtest (WAIS-R); WAIS-R A: Arithmetic subtest (WAIS-R).
WAIS-R DS: Digit Span subtest (WAIS-R), SCWT A: Stroop Colour and Word Test—words part, SCWT B: Stroop Colour and Word Test—colours part, LMI: logical memory subtest—immediate (WMS-III), LMD: logical memory subtest—delayed recall (WMS-III), LWI: list of words—immediate (WMS-III), LWD: list of words—delayed (WMS-III), LWR: list of words—recognition (WMS-III), MAST: Mississippi Aphasia Screening Test, VF: verbal fluency—letter (n, k, and p), WAIS-R S: Similarities subtest (WAIS-R), SCWT C: colours in Stroop Colour and Word test—colour and word part, WAIS-R PC: Picture Completion subtest (WAIS-R), and CT: Clock Test.

the best diagnostic validity in predicting PD-MCI in our study.

The most sensitive and specific ACE-R domain for discrimination between PD-MCI and PD-D was attention and orientation, with a cut-off score of 15.5 points (sensitivity 0.90, specificity 0.97) and AUC of 0.92 (95% CI 0.77–1.00). This domain significantly correlated with neuropsychological tests of interest evaluating attention and psychomotor speed. In the visuospatial abilities domain, a cut-off score of 14.5 points distinguished between PD-MCI and PD-D with sensitivity of 0.60 and specificity of 0.78. The language domain did not reveal good screening validity in predicting either PD-MCI or PD-D. This could have been caused by the fact that our subjects were normal or only very slightly affected in this domain as well as on the MAST. This result is in line with the published literature showing fewer deficits in the language domain in PD [24, 35].

The ACE-R takes 20–30 minutes and yields quite a lot of information about the global level of cognitive functions and about specific cognitive deficits in PD patients. Our cut-off scores for ACE-R and individual ACE-R domains may help in screening for PD-MCI subjects and in assessing their cognitive profile.

We would particularly like to stress our result regarding the orientation and attention domain alone which had very good screening validity for PD-D prediction. The AUC estimates indicate that this subscore was superior to the total ACE-R score in discriminating PD-MCI from PD-D in our dataset (AUC 0.92 versus 0.78). Therefore, this subtest could be recommended for a quick PD dementia screening. However, the whole ACE-R is needed to assess global cognition and specific cognitive profiles in PD-D subjects.

4. Conclusion

While the whole ACE-R is a suitable screening instrument for discriminating among PD-NC, PD-MCI, and PD-D, we also provide for the first time specific ACE-R domains cut-off scores that best distinguish between PD-NC and PD-MCI (verbal fluency and memory domains) and between PD-MCI and PD-D (orientation and attention domain). These parts of ACE-R are easy and quick to administer and may be of help in screening specific PD cognitive subtypes.

Conflict of Interests

The authors declare that there is no conflict of interests regarding the publication of this paper.

Acknowledgments

This work was supported by Grant NT/13499 of the Czech Ministry of Health and by Project "CEITEC—Central European Institute of Technology" (CZ.1.05/1.1.00/02.0068) from the European Regional Development Fund.

References

[1] K. R. Chaudhuri, A. Sauerbier, J. M. Rojo et al., "The burden of non-motor symptoms in Parkinson's disease using a self-completed non-motor questionnaire: a simple grading system," *Parkinsonism and Related Disorders*, vol. 21, no. 3, pp. 287–291, 2015.

[2] P. Martinez-Martin, C. Rodriguez-Blazquez, M. M. Kurtis, K. R. Chaudhuri, and NMSS Validation Group, "The impact of non-motor symptoms on health-related quality of life of patients with Parkinson's disease," *Movement Disorders*, vol. 26, no. 3, pp. 399–406, 2011.

[3] D. Aarsland, K. Andersen, J. P. Larsen, A. Lolk, and P. Kragh-Sørensen, "Prevalence and characteristics of dementia in Parkinson disease: an 8-year prospective study," *Archives of Neurology*, vol. 60, no. 3, pp. 387–392, 2003.

[4] J. Meireles and J. Massano, "Cognitive impairment and dementia in Parkinson's disease: clinical features, diagnosis, and management," *Frontiers in Neurology*, vol. 3, article 88, 15 pages, 2012.

[5] M. Emre, D. Aarsland, R. Brown et al., "Clinical diagnostic criteria for dementia associated with Parkinson's disease," *Movement Disorders*, vol. 22, no. 12, pp. 1689–1707, 2007.

[6] I. Litvan, J. G. Goldman, A. I. Tröster et al., "Diagnostic criteria for mild cognitive impairment in Parkinson's disease:

13. Reference intervals of plasma matrix metalloproteinases 2, 3, and 9 and serum asymmetric dimethylarginine levels

Kušnierová P, Všianský F, Pleva L, Plevová P, Šafarčík K, Švagera Z

Originally published in Scandinavian Journal of Clinical & Laboratory Investigation, 2015, vol. 75, no. 6, p. 508-513.

Scandinavian Journal of Clinical & Laboratory Investigation, 2015; 75: 508–513

Taylor & Francis
Taylor & Francis Group

ORIGINAL ARTICLE

Reference intervals of plasma matrix metalloproteinases 2, 3, and 9 and serum asymmetric dimethylarginine levels

PAVLINA KUSNIEROVA[1,2], FRANTISEK VSIANSKY[2], LEOS PLEVA[3, 4], PAVLINA PLEVOVA[1,5], KRISTIAN SAFARCIK[1,2] & ZDENEK SVAGERA[1,2]

[1]*Department of Biomedical Sciences, Faculty of Medicine, University of Ostrava,* [2]*Institute of Laboratory Medicine, Department of Clinical Biochemistry, University Hospital Ostrava,* [3]*Department of Clinical Studies, Faculty of Medicine, University of Ostrava,* [4]*Cardiovascular Department, University Hospital Ostrava, and* [5]*Department of Medical Genetics, University Hospital Ostrava, Ostrava, Czech Republic*

Abstract

Objective. The present study aimed to verify the reference intervals of plasma matrix metalloproteinases (MMPs) 2, 3, and 9 and serum asymmetric dimethylarginine (ADMA) in a healthy population with an average age corresponding to that of patients with cardiovascular diseases. ***Methods.*** The study included 180 healthy volunteers. Plasma MMP-2, MMP-3, MMP-9, and serum ADMA levels were determined using an enzyme-linked immunosorbent assay. These levels were analyzed for association with age and gender. The Cbstat5, R software, and NCSS 2007 programs were used for statistical analysis. ***Results.*** The average volunteer age was 47.4 years in the group in which MMP-3 and ADMA were analyzed, 40.3 years in the MMP-9 group, and 47.8 years for the MMP-2 group. Serum ADMA levels were determined to be independent of age and gender. Plasma MMP-2 levels were significantly correlated with age ($p = 0.001$), with lower levels detected in persons ≤ 49 years of age. Plasma MMP-3 was significantly associated with both age ($p < 0.0001$) and gender, with lower levels detected in persons of ≤ 47 years of age and among women. Plasma MMP-9 levels were not age dependent, but were associated with gender ($p = 0.014$), showing lower levels in women. ***Conclusions.*** Reference intervals of heparin-plasma MMP-2, MMP-3, and MMP-9 and serum ADMA levels were determined. MMP-2 and MMP-3 levels were found to be age dependent, and MMP-3 and MMP-9 levels were gender dependent.

Key Words: *Adult, age dependence, atherosclerosis, cardiovascular diseases, enzyme-linked immunosorbent assay, gender dependence*

Introduction

Soluble matrix metalloproteinases (MMPs) are enzymes that proteolytically degrade the extracellular matrix, and are thus responsible for connective tissue remodelling. They have been identified as potential biomarkers for delineating cardiovascular risk of plaque rupture and coronary risk. They also may modify cardiovascular tissue remodelling in cases of atherosclerosis and heart failure [1]. Under physiological conditions, MMPs are involved in ontogenetic development [2].

Asymmetric dimethylarginine (ADMA) is the endogenous inhibitor of nitric oxide synthase (SON) – an enzyme that catalyzes the formation of nitric oxide (NO) from arginine. As a signal molecule released from endothelial cells, NO reduces vascular wall tone, thus preventing cell adhesion to the vessel wall, inhibiting platelet activation, and preventing atherosclerosis development. Reduced NO bioavailability is a pathogenetic factor for cardiovascular disease development, with increased ADMA concentrations reportedly associated with increased risk of atherosclerosis [3–5].

The present study aimed to determine reference intervals for the concentration of plasma matrix metalloproteinase 2, 3, and 9 and for the concentration of serum asymmetric dimethylarginine in adults with respect to gender and age.

Material and methods

Patients

The present study included a total of 180 healthy adult volunteers attending the Blood Centre of the

Correspondence: Pavlina Kusnierova, Institute of Laboratory Medicine, Department of Clinical Biochemistry, University Hospital Ostrava, tr. 17.listopadu 1790, 708 52, Ostrava, Czech Republic. Tel: +42 (0)597374144. E-mail: pavlina.kusnierova@fno.cz

(Received 24 September 2014; accepted 30 May 2015)

ISSN 0036-5513 print/ISSN 1502-7686 online
DOI: 10.3109/00365513.2015.1057760

Table I. The average volunteer age, SD and outliers.

Analyte	*N*	Average age (years)	SD (years)	Outliers
ADMA	120	47.4	6.49	–
MMP-3	120	47.4	6.49	–
MMP-9	120	40.3	8.35	4
MMP-2	180	47.8	5.82	7

University Hospital Ostrava. All included volunteers were healthy and were not taking any medication. Each volunteer provided written informed consent for the use of fluid biological material for research purposes. All patient data were handled anonymously. The study was approved by the Ethics Committee of University Hospital Ostrava, Czech Republic, in accordance with the ethical standards of the Helsinki Declaration.

Samples

Heparin plasma was used for measurement of MMP-2, MMP-3, and MMP-9 concentrations and serum in gel-containing tubes for ADMA, all from Sarstedt, Nümbrecht, Germany. Plasma and serum samples were centrifuged at 2500 *g* at 4°C for 6 minutes and aliquoted into two vials (2 mL each) and stored at − 80°C for 2–3 months.

Analytical methods

The enzyme concentrations were measured by immunosorbent assay (ELISA) (BioVendor - Laboratorni Medicina a.s., Brno, Czech Republic).

Statistical methods

Reference intervals were calculated using MedCalc Version 14.12 (origin) [6,7]. Parametric and non-parametric statistical methods were applied, as appropriate, using NCSS 2007 (origin) for calculations and R software for graphical displays. Potential outliers were evaluated by Cook's distance and partitioning of the data according to Harris-Boyd [8]. Z-values above 3 prompted splitting the group.

Associations between measurands were evaluated with Spearman's rank correlation (r_s) or Pearson's product-moment correlation coefficients (r_p), as appropriate. Besides correlation testing, the age dependence of MMP-2 and MMP-3 was evaluated using Piecewise Polynomial Models (Multiphase Models) [9]. Simultaneously, the data sets were tested for normality and skewness. To obtain symmetric data, nonlinear parametric power transformation of data was performed. Due to the nonnormality of the data for all studied analytes, statistical software was used to complete nonlinear transformation of the data.

Results

The average volunteer age, SD and outliers are shown in Table I. The concentrations of MMP-2 and MMP-9 showed statistically significant skewness (Figure 1).

The data for serum ADMA showed no statistically significant dependence on age and gender; thus, we determined total reference values (Table II).

Plasma MMP-2 levels showed statistically significant age dependence ($r_p = 0.171$; $p = 0.02$; $r_s = 0.161$; $p = 0.034$), Figure 2, Table III. Therefore,

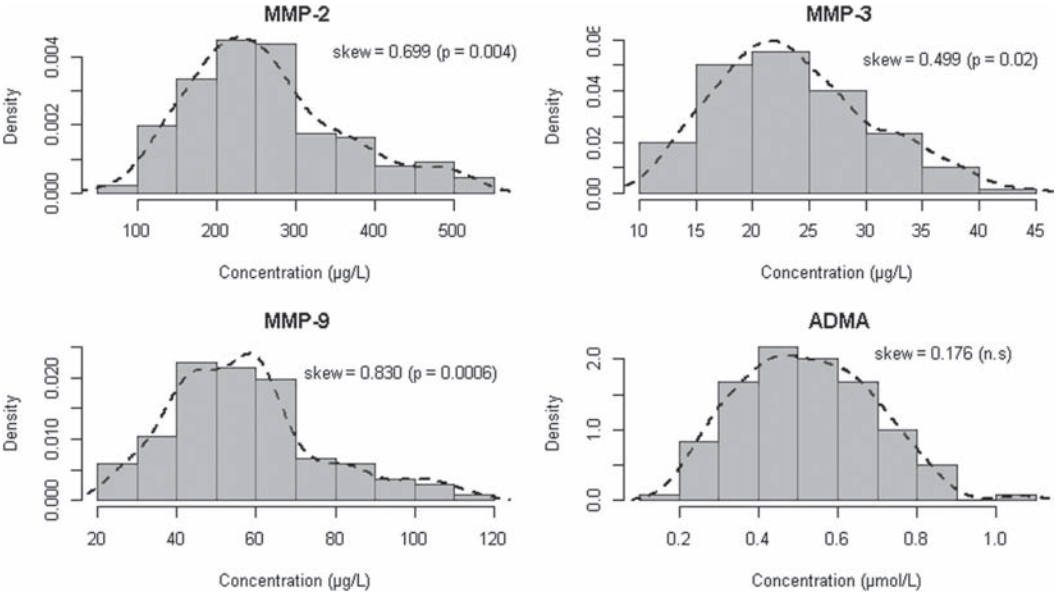

Figure 1. Distribution of the analytes using histograms and the empirical distribution function. $p < 0.05$ was considered to indicate statistical significance; n.s., non-significant.

Table II. Reference intervals for ADMA (µmol/L), 2.5th and 97.5th percentile values, and their 90th confidence intervals.

N	Age (years)	Gender	2.5th	90th confidence interval	97.5th	90th confidence interval	Type of calculation
120	34–61	Both	0.227	0.189–0.267	0.877	0.812–0.945	Parametric (Power transf.)
			0.238	0.205–0.272	0.849	0.735–0.963	Nonparametric (Bootstrap)
			0.228	0.200–0.259	0.889	0.838–0.942	Robust (Power transf.)

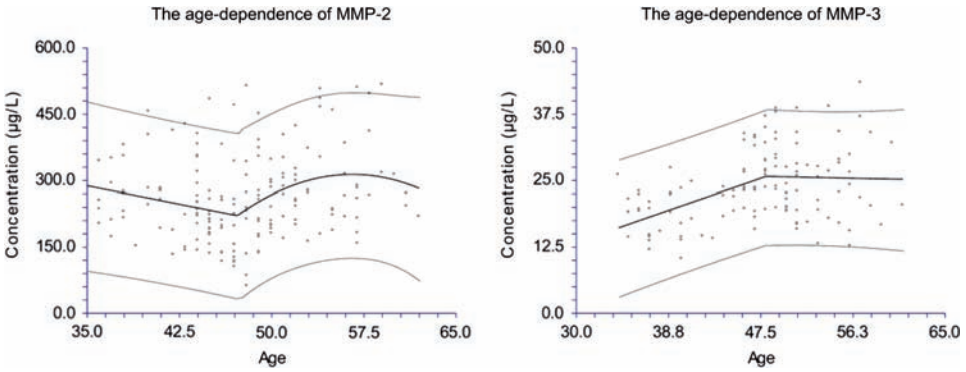

Figure 2. Piecewise Polynomial Models (Multiphase Models) for the age dependence of MMP-2 and MMP-3.

we divided the tested file into two groups: ≤ 49 years and > 50 years. The medians of these age groups were significantly different from each other ($p = 0.001$; $z = 3.15$). Table IV shows the agedependent reference intervals of MMP-2, the 2.5th and 97.5th percentile values, and their confidence intervals.

MMP-3 plasma concentrations were found to be significantly correlated with age ($r_p = 0.355$; $p = 0.00007$; $r_s = 0{,}308$; $p = 0.0006$) as well as with gender ($p \leq 0.001$; $z > 3.0$), Figures 2 & 3, Table III. For this reason, the probands were divided into two age groups: ≤ 47 years and > 47 years. Both of these groups showed statistically significant dependence of the measured values on gender (Table V). As there was only a small number of men in the ≤ 47 years group, the reference interval was not calculated for this group.

Plasma MMP-9 levels showed no statistically significant differences related to age, but show an association with gender ($p = 0.014$; $z = 2.39$). Since the z value was less than 3 and the data showed a non-Gaussian distribution, we calculated the distribution in separate age-dependence subgroups. Table VI shows the reference intervals.

For summary of results see Table VII.

Discussion

To set the reference intervals for MMP-2 MMP-3, MMP-9 and ADMA, we measured the blood concentrations of these analytes in a group of healthy volunteers with an average age of 40–50 years of age. Based on several published studies describing the

Table III. Piecewise Polynomial Models (Multiphase Models) for the age dependence of MMP-2 and MMP-3.

Analyte	Model	Regression equation	Age (years)	R
MMP-2	Linear-Quadratic (Age)	$y = 480.92 - 5.51(\text{Age})$	≤ 49	0.316
		$y = -3074 + 119.8(\text{Age}) - 1.06(\text{Age})^2$	> 50	
MMP-3	Linear/Linear (Age)	$y = -7.24 + 0.69(\text{Age})$	≤ 47	0.412
		$y = 27.76 - 0.042(\text{Age})$	> 47	

Table IV. Age-dependent reference intervals for MMP-2 (µg/L), 2.5th and 97.5th percentile values, and their 90th confidence intervals.

n	Age (years)	Gender	2.5th	90th confidence interval	97.5th	90th confidence interval	Type of calculation
180	35–62	Both	110.0	97.1–124.1	590.9	520.8–670.0	Parametric (Power transf.)
			113.9	93.8–133.9	636.1	536.8–735.4	Nonparametric (Bootstrap)
			108.3	98.1–119.5	488.3	453.3–523.5	Robust (Power transf.)
111	35–49	Both	98.3	83.0–115.2	466.9	417.9–519.1	Parametric (Power transf.)
			96.6	85.5–109.8	469.9	426.9–513.9	Robust (Power transf.)
62	50–62	Both	160.8	144.8–179.0	550.2	456.9–666.7	Parametric (Power transf.)
			157.8	146.3–172.3	555.6	481.1–636.6	Robust (Power transf.)

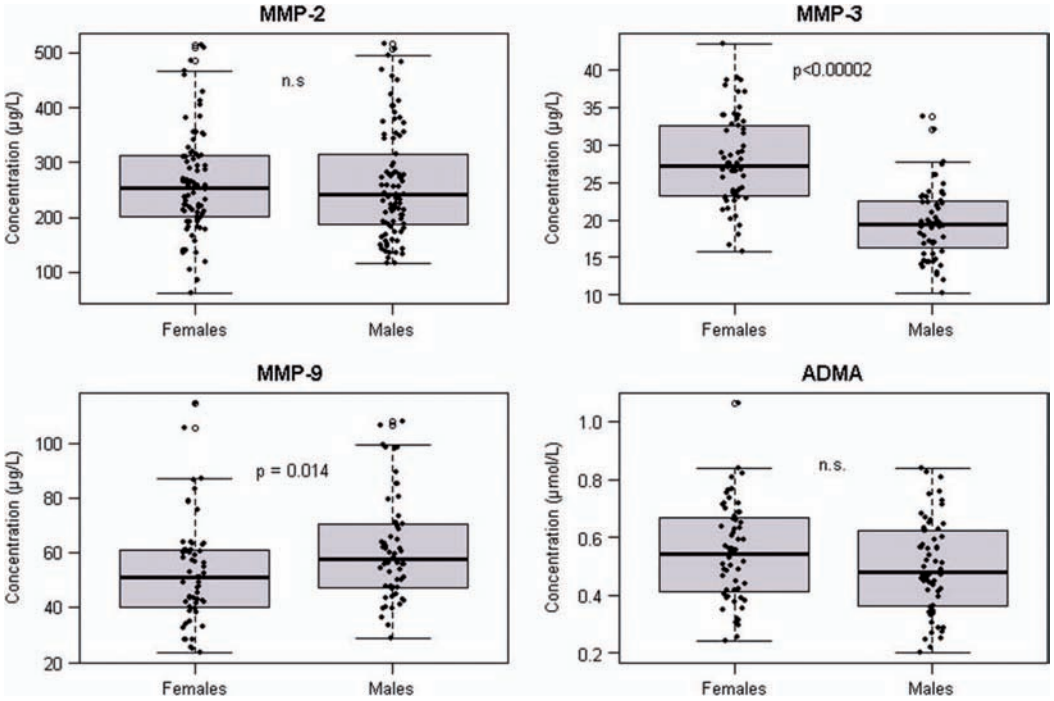

Figure 3. The gender dependence of tested analytes; n.s., non-significant.

discrepancies in MMP concentrations between serum and plasma [10–23], we measured MMP concentrations in heparin plasma and ADMA concentrations in serum.

Our findings indicated that plasma MMP-2 levels were associated with age, showing lower levels in volunteers < 50 years of age and increasing with greater age. No similar data exists in the literature for comparison with these results.

We further found that MMP-3 levels were dependent on both age and gender. Plasma MMP-3 levels were lower in volunteers < 47 years of age. In both age groups, lower MMP-3 values were found in women compared to men. Ribbens et al. [24] previously reported normal MMP-3 levels in 96 healthy controls (46 females and 50 males). That group analyzed MMP-3 level using a one-step sandwich ELISA method with reagents provided by Dr Jaspar, Biosource Europe S.A., Belgium [25]. Compared to their data, our present results showed higher plasma MMP-3 concentrations in both women and men, possibly due to the use of different reagents.

Plasma MMP-9 concentrations differed with respect to gender, showing lower values in women than in men. Iizasa et al. [26] previously studied plasma MMP-9 concentrations in a group of 138 healthy volunteers, using a one-step sandwich enzyme immunoassay kit (Fuji Chemical Industries, Toyama, Japan). They found a normal range of plasma MMP-9 concentrations that was lower than that found in our present study, and that was independent of gender or age. Unfortunately, the authors did not include the age range of their healthy volunteers or the exact specifications of their primary

Table V. Gender- and age-dependent reference intervals of MMP-3 (µg/L), 2.5th and 97.5th percentile values, and their 90th confidence intervals.

n	Age (years)	Gender	2.5th	90th confidence interval	97.5th	90th confidence interval	Type of calculation
120	34–61	Both	12.49	11.20–13.86	39.37	36.19–42.72	Parametric (Power transf.)
			12.68	10.95–14.41	38.79	36.02–41.56	Nonparametric (Bootstrap)
			12.38	11.42–13.47	39.61	36.98–42.19	Robust (Power transf.)
38	34–47	F*	11.11	9.24–13.15	29.91	26.49–33.53	Parametric (Power transf.)
			10.86	9.32–12.85	30.51	27.82–33.69	Robust (Power transf.)
14†		M‡	–	–	–	–	–
22	48–61	F	12.76	11.11–14.69	31.14	25.41–38.40	Parametric (Power transf.)
			12.40	11.09–14.10	32.43	27.08–38.33	Robust (Power transf.)
46		M	18.03	15.84–20.38	42.04	38.00–46.33	Parametric (Power transf.)
			17.73	16.18–19.56	42.70	39.06–45.88	Robust (Power transf.)

*Female; †Reference interval cannot be calculated due to the small number of data; ‡Male

Table VI. Gender-dependent reference intervals of MMP-9 (μg/L), 2.5th and 97.5th percentile values, and their 90th confidence intervals.

n	Age (years)	Gender	2.5th	90th confidence interval	97.5th	90th confidence interval	Type of calculation
116	16–61	Both	27.63	24.55–30.99	103.06	92.85–114.06	Parametric (Power transf.)
			26.45	22.64–30.25	105.89	97.96–113.80	Nonparametric (Bootstrap)
			27.38	24.99–30.14	104.31	95.49–113.1	Robust (Power transf.)
58	20–61	F	24.83	20.93–29.25	98.82	84.28–115.27	Parametric (Power transf.)
			24.38	21.20–28.32	100.98	88.61–114.28	Robust (Power transf.)
58	19–55	M	33.37	29.47–37.77	108.67	93.01–126.8	Parametric (Power transf.)
			32.84	29.94–36.26	110.47	96.28–124.93	Robust (Power transf.)

material, only stating that they used plasma samples. Other published studies have reported that the measured concentrations of MMP-9 as well as other MMPs in blood are strongly influenced by the sampling procedure and by the type of anticoagulant agent used [10–23]. Such differences in methodology could underlie the observed discrepancy between these studies.

We also found that the serum ADMA concentrations in healthy volunteers were independent of age and gender. Ekim et al. [27] used high performance liquid chromatography (HPLC) to determine normal serum ADMA levels in a control group comprising 34 healthy volunteers (20 female and 14 male) with an average age of 46.18 years (SD, 10.39 years). They reported serum ADMA concentrations lower than those found in a comparable age group in our present study. This difference is most likely due to the different methodologies used. Celik et al. [28] used the ADMA direct ELISA Kit (Immunodiagnostic AG, Bensheim, Germany) to determine normal serum ADMA levels in a healthy control group consisting of 31 probands with an average age of 55.06 years (SD, 7.46 years). Their results are comparable to those obtained with HPLC by Ekim et al. [27] and lower than those obtained in our present study using the same methodology but a different diagnostic kit. These differences may be related to the different diagnostic kits used.

In conclusion, in the present study, we determined reference intervals for heparin-plasma MMP-2, MMP-3, and MMP-9 and serum ADMA levels measured by enzyme-linked immunosorbent assay in healthy volunteers. We observed that heparin-plasma MMP-2 and MMP-3 levels were associated with age and heparin-plasma MMP-3 and MMP-9 levels were associated with gender.

Table VII. Summary of results as regards age- and gender-dependence of MMP-2, MMP-3, MMP-9 and ADMA.

Marker	Age dependence	Gender dependence
MMP-2	Yes	No
MMP-3	Yes	Yes
MMP-9	No	Yes
ADMA	No	No

Declaration of interest: The authors report no conflicts of interest. The authors alone are responsible for the content and writing of the paper.

This work was supported by the European Social Fund and the State Budget of Czech Republic [No. CZ. 1.07/2.3.00/20.0040] and by institutional support to the Ministry of Health of Czech Republic [No. 1RVO FNOs/2013].

References

[1] Liu P, Sun M, Sader S. Matrix metalloproteinases in cardiovascular disease. Can J Cardiol 2006;22:25B–30B.

[2] Nagase H, Visse R, Murphy G. Structure and function of matrix metalloproteinases and TIMPs. Cardiovasc Res 2006;69:562–73.

[3] Böger RH. Asymmetric dimethylarginine, an endogenous inhibitor of nitric oxide synthase, explains the "L-arginine paradox" and acts as a novel cardiovascular risk factor. J Nutr 2004;134:2842–7.

[4] Vallance P, Leone A, Calver A, Collier J, Moncada S. Accumulation of an endogenous inhibitor of NO synthesis in chronic renal failure. Lancet 1992;339:572–5.

[5] Böger RH, Bode-Böger SM, Szuba A, Tangphao O, Tsao PS, Chan JR, Blaschke TF, Cooke JP. ADMA: a novel risk factor for endothelial dysfunction. Its role in hypercholesterolemia. Circulation 1998;98:1842–7.

[6] Solberg HE. International Federation of Clinical Chemistry (IFCC). Scientific Committee, Clinical Section. Expert Panel on Theory of Reference Values (EPTRV) and International Committee for Standardization in Haematology (ICSH), Standing Committee on Reference Values. Approved recommendation (1987) on the theory of reference values. Part 5. Statistical treatment of collected reference values. Determination of reference limits. J Clin Chem Clin Biochem 1987;25:645–56. Clin Chim Acta 1987;170:S13–S32.

[7] Clinical and Laboratory Standards Institute (CLSI). Defining, establishing, and verifying reference intervals in the clinical laboratory; approved guideline. CLSI document C28–A3. 3rd ed. Wayne: PA: Clinical and Laboratory Standards Institute; 2008.

[8] Harris EK, Boyd JC. On dividing reference data into subgroups to produce separate reference ranges. Clin Chem 1990;36:265–70.

[9] Seber GAF, Wild CJ. Nonlinear regression. John Wiley & Sons. New York; 1989. ISBN 0471617601.

[10] Mannello F. Effects of blood collection methods on gelatin zymography of matrix metalloproteinases. Clin Chem 2003;49:339–40.

[11] Kodama S, Iwata K, Iwata H, Yamashita K, Hayakawa T. Rapid one-step sandwich enzyme immunoassay for tissue inhibitor of metalloproteinases: an application for rheumatoid arthritis in serum and plasma. J Immunol Meth 1990; 127:103–8.

[12] Jung K, Nowak L, Lein M, Henke W, Schnorr D, Loening SA. Role of specimen collection in preanalytical variation of metalloproteinases and their inhibitors in blood. Clin Chem 1996;46:2043–5.
[13] Lein M, Nowak L, Jung K, Koenig F, Liuchtinghagen R, Schnorr D, Loening SA. Analytical aspects regarding the measurement of metalloproteinases and their inhibitors in blood. Clin Biochem 1997;30:491–6.
[14] Jung K, Laube C, Lein M, Lichtinghagen R, Tschesche H, Schnorr D, Loening SA. Kind of sample as preanalytical determinant of matrix metalloproteinases 2 and 9 and tissue inhibitor of metalloproteinase 2 in blood. Clin Chem 1998;44:1060–2.
[15] Jung K, Lein M, Laube C, Lichtinghagen R. Blood specimen collection methods influence the concentration and the diagnostic validity of matrix metalloproteinase 9 in blood. Clin Chim Acta 2001;314:241–4.
[16] Jung K, Lein M, Roemer A, Lichtinghagen R. Circulating gelatinase B (MMP-9): the impact of preanalytical step of blood collection. Matrix Biol 2002;21:381–2.
[17] Alby C, Abdesselam OB, Foglietti MJ, Beaudeux JL. Preanalytical aspects regarding the measurement of metalloproteinase-9 and tissue inhibitor or metalloproteinase-1 in blood. Clin Chim Acta 2002;325:183–6.
[18] Mannello F, Luchetti F, Canonico B, Papa S. Effect of anticoagulants and cell separation media as preanalytical determinants on zymographic analysis of plasma matrix metalloproteinases. Clin Chem 2003;49:1956–7.
[19] John M, Jung K. Pre-analytical conditions for the assessment of circulating MMP-9 and TIMP-1: consideration of pitfalls. Eur Respir J 2005;26:364–6.
[20] Jung K, Meisser A, Bischof P. Blood sampling as critical preanalytical determinant to use circulating MMP and TIMP as surrogate markers for pathological processes. Int J Cancer 2005;116:1000–1.
[21] Jung K, Gerlach RF, Tanus-Santos JE. Preanalytical pitfalls of blood sampling to measure true circulating matrix metalloproteinase 9 and tissue inhibitors of matrix metalloproteinases. Clin Chim Acta 2006;373:180–1.
[22] Jung K. Sample processing and its preanalytical impact on the measurement of circulating matrix metalloproteinases. Clin Chem Lab Med 2006;44:500–2.
[23] Jung K. Impact of blood sampling on circulating tissue inhibitors of metalloproteinases. Clin Cancer Res 2006; 12:2648.
[24] Ribbens C, Martin y Porras M, Franchimont N, Kaiser MJ, Jaspar JM, Damas P, Houssiau FA, Malaise MG. Increased matrix metalloproteinase-3 serum levels in rheumatic diseases: relationship with synovitis and steroid treatment. Ann Rheum Dis 2002;61:161–6.
[25] Brennan FM, Browne KA, Green PA, Jaspar JM, Maini RN, Feldmann M. Reduction of serum matrix metalloproteinase 3 in rheumatoid arthritis patients following anti-tumor necrosis factor-a (cA2) therapy. Br J Rheumatol 1997;36:643–50.
[26] Iizasa T, Fujisawa T, Suzuki M, Motohashi S, Yasufuku K, Yasukawa T, Baba M, Shiba M. Elevated levels of circulating plasma matrix metalloproteinase 9 in non-small cell lung cancer patients. Clin Cancer Res 1999;5:149–53.
[27] Ekim M, Sekeroglu MR, Balahoroglu R, Ozkol H, Ekim H. Roles of the oxidative stress and ADMA in the development of deep venous thrombosis. Biochem Res Int 2014;2014: 703128.
[28] Celik M, Cerrah S, Arabul M, Akalin A. Relation of asymmetric dimethylarginine levels to macrovascular disease and inflammation markers in type 2 diabetic patients. J Diabetes Res 2014;2014:139215.

14. The rs1803274 polymorphism of the BCHE gene is associated with an increased risk of coronary in-stent restenosis

Pleva L, Kovářová P, Faldynová L, Plevová P, Hilscherová Š, Zapletalová J, Kušnierová P, Kukla P

Originally published in BMC Cardiovascular Disorders, [online], 2015, vol. 15, no. 135, p. 1-9.

Pleva et al. BMC Cardiovascular Disorders (2015) 15:135
DOI 10.1186/s12872-015-0128-8

BMC Cardiovascular Disorders

RESEARCH ARTICLE Open Access

The rs1803274 polymorphism of the *BCHE* gene is associated with an increased risk of coronary in-stent restenosis

L. Pleva[1,2*], P. Kovarova[3,4], L. Faldynova[3,5], P. Plevova[3,5], S. Hilscherova[3,5], J. Zapletalova[6], P. Kusnierova[3,7] and P. Kukla[2]

Abstract

Background: We sought to identify gene polymorphisms that confer susceptibility to in-stent restenosis after coronary artery bare-metal stenting in a Central European population.

Methods: 160 controls without post–percutaneous coronary intervention in-stent restenosis were matched for age, sex, vessel diameter, and diabetes to 160 consecutive cases involving in-stent restenosis of the target lesion within 12 months. Using real time polymerase chain reaction and melting-curve analysis, we detected 13 single-nucleotide polymorphisms in 11 candidate genes - rs1803274 (*BCHE* gene), rs529038 (*ROS1*), rs1050450 (*GPX1*), rs1800849 (*UCP3*), rs17216473 (*ALOX5AP*), rs7412, rs429358 (*ApoE*), rs2228570 (*VDR*), rs7041, rs4588 (*GC*), rs1799986 (*LRP1*) and rs2228671 (*LDLR*). Multivariable logistic regression was used to test for associations.

Results: The rs1803274 polymorphism of *BCHE* was significantly associated with in-stent restenosis (OR 1.934; 95 % CI: 1.181–3.166; $p = 0.009$). No association was found with the other studied SNPs.

Conclusions: The A allele of rs1803274 represents a risk factor for in-stent restenosis in Central European patients after percutaneous coronary intervention with bare-metal stent implantation.

Background

Coronary stent implantation has significantly improved percutaneous coronary intervention (PCI). It has enabled management of early complications of plane balloon angioplasty and prevention of elastic recoil and constrictive remodeling, decreasing the frequency of restenosis after PCI. However, with these improvements has come a new complication: in-stent restenosis (ISR) arising from neointimal hyperplasia. The clinical incidence of ISR after bare-metal stent (BMS) implantation is about 20–35 % and currently represents one of the main limitations of coronary angioplasty [1]. The use of drug-eluting stents has led to a further decrease of ISR occurrence to 5–10 % [1]. The known risk factors for ISR include diabetes mellitus, renal insufficiency, lesion length (20 mm), small vessel diameter (3 mm), treatment of complex lesions (B2/C) [2], chronic total occlusions, venous bypasses, ostial or bifurcation lesions, stent undersizing or underexpansion and necessary implantation of more stents [1]. The increasing number of patients undergoing coronary interventions has led to attempts to find further biochemical and genetic risk factors that would enable more targeted treatment.

Based on a literature review, for the current study, single nucleotide polymorphisms (SNPs) of some candidate genes were selected for having been associated with ISR in different populations (Japanese and North American) or in patients with repeated restenosis, including *BCHE* - butyrylcholinesterase gene, *ROS1* - the closest homolog of the v-Ros oncogene of the avian sarcoma, *GPX1* - glutathione-peroxidase-1 gene, *UCP3* - uncoupling protein 3 gene, and *ALOX5AP* - arachidonate 5-lipoxygenase-activating protein gene. Our aim was to assess associations in our Central European population [3–5]. Furthermore, we focused on a group of genes affecting metabolic processes,

* Correspondence: leos.pleva@volny.cz
[1]Department of Clinical Studies, Medical Faculty, University of Ostrava, Syllabova 19, Ostrava, Zabreh 703 00, Czech Republic
[2]Department of Cardiovascular Diseases, University Hospital Ostrava, Ostrava, Czech Republic
Full list of author information is available at the end of the article

including genes of apolipoprotein E (*APOE*), vitamin D receptor (*VDR*), vitamin D binding protein (*GC*), and two genes of the low density lipoprotein receptor family, low density lipoprotein receptor related protein 1 (*LRP1*) and low density lipoprotein receptor (*LDLR*) which may be involved not only in atherosclerosis but also in inflammation and may influence proliferation and migration of vascular smooth muscle cells (VSMCs), key players in the development of ISR [6–11].

Patient groups and methods

We included 160 consecutive patients treated at the cathlab of the University Hospital Ostrava, Czech Republic, between the years 2010 and 2013, with ISR arising within 12 month after implantation of a bare-metal stent. The control group was searched in the Czech National PCI Registry and consisted of 160 matched patients treated at our cathlab with identical main demographic and clinical risk factors (sex, age, diabetes mellitus, implanted stent diameter ±0.5 mm) in whom ISR was excluded using multi-slice (MS-CT) coronarography scheduled at 12 months after the implantation.

In order to determine frequency of the studied SNPs in the general Czech population, genotyping was also performed in 200 persons (100 Czech man-woman pairs aged 26–66 years).

Selective coronarography

Selective coronarography was performed in a Siemens Axiom device (Forchheim, Germany) using the standard method from the right or left radial approach with 5 F diagnostic catheters and the contrast medium Iomeron 400. Quantitative coronary angiography was performed, and percent diameter stenosis (% DS) was calculated. ISR was defined as a diameter stenosis ≥50 % in the stented segment.

Multi-slice (MS) CT coronarography

All patients were examined without the need for previous premedication with beta-blockers in the Siemens Somatom Definition AS+ device (Forchheim, Germany), a single-source CT scanner in a 128-slice configuration. The maximum intensity projection (MIP) reconstructions and automatic software Vessel analysis were used for evaluation of the lumen. Homogeneous enhancement (visually similar to the CT attenuation in the reference vessels) inside the stent lumen was considered to be normal or unrelated to ISR.

Genotyping of polymorphisms

The evaluated SNPs are listed in Table 1. The polymorphisms are described according to the HGVS nomenclature [12], and their description corresponds to the latest version available in the NCBI and Ensembl gene databases.

Table 1 Selected single nucleotide polymorphisms

Polymorphism			
Gene	Coding DNA level	Protein level	NCBI database
BCHE	c.1699G>A	p.Ala567Thr	rs1803274
ROS1	c.6637G>A	p.Asp2213Asn	rs529038
UCP3	c.-238C>T		rs1800849
GPX1	c.599C>T	p.Pro200Leu	rs1050450
ALOX5AP	c.117–5723G>A		rs17216473
*APOE*2*	c.526C>T	p.Arg176Cys	rs7412
*APOE*4*	c.388 T>C	p.Cys130Arg	rs429358
GC	c.1296 T>G	p.Asp432Glu	rs7041
GC	c.1307C>A	p.Thr436Lys	rs4588
VDR	c.2 T>C	p.Met1Thr	rs2228570
LRP1	c.300C>T	p.Asp100=	rs1799986
LDLR	c.81C>T	p.Cys27=	rs2228671

Genomic DNA was extracted using the MagNA Pure Compact Instrument (Roche, Switzerland). The real-time PCR assays for genotyping of rs1803274 (*BCHE*), rs529038 (*ROS1*), rs1050450 (*GPX1*), and rs1800849 (*UCP3*) were performed on the Rotor-Gene 3000A instrument (Corbett Research/Qiagen, Netherlands) with dual-labeled hydrolysis TaqMan® probes (Eastport, Czech Republic; TIB MolBiol, Germany) and followed by allelic discrimination and/or scatter analysis.

Primers and hybridization probes (TIB MOLBIOL, Germany) were designed to detect rs17216473 (*ALOX5AP*), rs2228570 (*VDR*), rs7041, rs4588 (*GC*), rs2228671 (*LDLR*), and rs1799986 (*LRP1*) genotypes using melting curve analysis on the LightCycler 480 II system (Roche, Switzerland). Primer and probe sequences are available on request.

Using these two methods, sample genotype was determined comparing the curves to positive samples whose genotype was verified by Sanger sequencing using the ABI Big Dye Terminator Cycle Sequencing Detection Kit v.3.1 (Applied Biosystems, USA) and genetic analyzer ABI3130 (Applied Biosystems, USA). Sanger sequencing was also used to determine the genotype of samples with inconclusive result of real-time PCR assay or melting curve analysis.

The *ApoE*2*, **3*, and **4* (rs7412 and rs429358) genotypes were determined using LightMix Kit ApoE C112R C158R (TIB MOLBIOL, Germany).

Ethical statements

The study protocol complied with the Declaration of Helsinki and was approved by the Ethics Committee of the University Hospital Ostrava, Czech Republic. Written informed consent was obtained from each participant.

Statistical analysis

Statistical analysis was performed using SPSS version 15 (SPSS Inc., Chicago, IL, USA). Continuous clinical variables of the groups with non-normal distribution are presented as the median and range (minimum–maximum) or lower and higher quartiles/Med (LQ–HQ)/ and were compared using the non-parametric Mann–Whitney *U* test. Categorical clinical variables are presented as counts and percentages and were compared by the chi-square test. The genotype distribution of each SNP difference between the study and control groups was analyzed by the chi-square test (or the Fisher's exact test in the case of lower frequencies). A p value of less than 0.05 was considered significant. Consistency of the observed genotype frequencies with the Hardy–Weinberg distribution was determined by the chi-square test.

Multiple logistic regression was used to evaluate possible effects of other variables on the association observed between the individual SNPs and ISR.

Results

Basic demographic, clinical, and biochemical characteristics of the cohort are listed in Table 2. The group of patients with ISR and the control group did not differ significantly in the main demographic parameters (age, gender, body mass index) or clinical risk factors (diabetes mellitus). The groups had a similar extent of coronary disease (multi-vessel disease [2VD/3VD], acute coronary syndromes [NSTEMI/STEMI]) and similar lesion characteristics (complex lesion B2/C, length and diameter [±0.5] mm of implanted stents). Furthermore, the group had similar main biochemical parameters (creatinine, TAG, hsCRP). However, total and LDL cholesterol was significantly higher in the control group.

Table 2 Clinical characteristics of all patients (including matched controls) and angiographic parameters of coronary artery lesions

	In-stent restenosis	Controls	p
Age (years)	67.0 (59.0–74.0)	67.0 (62.0–71.0)	0.984
Male/Female	101/59	101/59	1.000[b]
Diabetes mellitus (%)	28.75	28.75	1.000[b]
BMI (kg/m2)	28.4 (25.7–31.2)	29.1 (25.9–32.0)	0.368
Creat (umol/L)	97 (86–115)	99 (87–116)	0.517
Chol (mmol/L)	4.27 (3.73–4.94)	4.50 (3.95–5.55)	0.046
TG (mmol/L)	1.62 (1.12–2.18)	1.58 (1.17–2.21)	0.644
LDL (mmol/L)	2.66 (2.27–3.19)	2.96 (2.45–3.67)	0.003
HDL (mmol/L)	1.25 (1.02–1.51)	1.21 (1.00–1.42)	0.354
hs-CRP (mg/L)	1.71 (0.82–3.76)	1.70 (0.85–3.88)	0.978
ACSy (stemi/nstemi) (%)	62.78	72.50	0.056[b]
Multi vessel dissease (%)	57.5	49.38	0.145[b]
B2/C lesions (%)	68.11	68.48	0.940[b]
Stent diameter (mm)	3.0 (2.0–4.5)[a]	3.0 (2.0–4.0)[a]	0.214
Stent lenght (mm)	19 (8–68)[a]	19 (8–86)[a]	0.680

Data are given as median (lower and higher quartiles) or [a]median (minimim–maximum). Quantitative parameters are given in percents
p, significance of Mann–Whitney *U* test or [b]chi-square test

In the ISR group, the genotype was determined for all the studied SNPs in 149 patients. Due to lack of DNA, in five patients the genotype was obtained only for rs1803274, rs529038, rs1050450, rs7412, rs429358 and rs7041, in three patients only for rs1803274, rs529038, and rs1050450 and in two patients for rs1803274 and rs529038. In the non ISR group, the genotype was established in all patients for all SNPs with the exception of rs1803274 in 2 patients. Three per cent of the analysis had to be repeated and one per cent to be sequenced.

All SNPs were in Hardy–Weinberg equilibrium. The genotype distributions of the studied polymorphisms and minor allele frequencies (MAF) among subjects with ISR and those without restenosis and MAF data for general Czech population are shown in Table 3. With respect to a small number of minor allele homozygotes of various SNPs, a statistical comparison of homozygotes for the wild-type allele and carriers of the minor allele (heterozygotes and homozygotes) was performed.

Evaluation of genotype distributions by the chi-square test (or the Fisher's exact test in the case of lower frequencies) revealed that only the rs1803274 polymorphism of *BCHE* (c.1699G>A, p.Ala567Thr) was associated with an increased risk of ISR (Table 3). The ISR group had a significantly higher occurrence of heterozygous/homozygous carriers of the A allele (GA + AA) ($p = 0.009$) compared to the control group.

Minor allele frequencies (MAF) were calculated in the ISR and the non ISR groups and also in general Czech population. We confirmed a significant difference in rs1803274 MAF between the ISR and non ISR groups ($p = 0{,}007$). There were no significant differences of MAFs for the other SNPs. No difference was also found between nor ISR neither non ISR group versus general Czech population in any SNP (Table 3).

Multivariate logistic regression analysis with adjustment for the prevalence of diabetes mellitus (the main BMS-ISR clinical risk factor) confirmed that the rs1803274 polymorphism of *BCHE* was significantly associated with the prevalence of ISR (Table 3). The A allele carriers (both heterozygous GA and homozygous AA) were at a 1.934 fold (95 % confidence interval [CI]: 1.181–3.166; $p = 0.009$) increased risk of ISR. Thus, the 1699A allele of the *BCHE* polymorphism represented a risk factor for this condition. No association was found between the other SNPs and ISR.

Discussion

Vascular injury sustained during PCI and bare-metal stent implantation results in a complex inflammatory

Table 3 Distribution of polymorphism genotypes in groups with and without ISR, minor alele frequencies (MAF) and logistic regression analysis, separately for each parameter with adjustment for diabetes mellitus

Gene, polymorphism	Distribution of polymorphism genotypes			MAF in general CZ population, ISR and non-ISR groups; statistics			Logistic regression analysis, compared to the wild type allele with adjustment for diabetes mellitus		
	ISR group No of pts (%)	Non-ISR group No of pts (%)	p	Czech GP	ISR vs. GP p	Non-ISR vs GP p	OR	95 % CI for OR	p
BCHE, rs1803274									0.016
No of pts (n)	160	158							
GG	102 (63.8 %)	122 (77.2 %)							
GA	50 (31.2 %)	35 (22.2 %)					1.715	1.034 - 2.846	0.037
AA	8 (5 %)	1 (0.6 %)	*0.008*[a]				*9.703*[a]	*1.191 - 79.05*[a]	*0.034*[a]
GA + AA	58 (36.2 %)	36 (22.8 %)	0.009				1.934	1.181 -3.166	0.009
MAF	0.21	0.12	0.007	0.18	0.280	0.367			
ROS1, rs529038									0.280
No of pts (n)	160	160							
GG	75 (46.9 %)	78 (48.8 %)							
GA	75 (46.9 %)	65 (40.6 %)					1.200	0.758 - 1.899	0.436
AA	10 (6.2 %)	17 (10.6 %)	0.269				0.612	0.263 - 1.421	0.253
GA + AA	86 (53.8 %)	82 (51.2 %)	0.823				1.078	0.695 - 1.672	0.737
MAF	0.3	0.31	1	0.3	1	1			
UPC3, rs1800849									0.982
No of pts (n)	149	160							
CC	86 (57.8 %)	90 (56.2 %)							
CT	51 (34.2 %)	63 (39.4 %)					0.847	0.527 - 1.361	0.492
TT	12 (8.1 %)	7 (4.8 %)	0.323				1.792	0.670 - 4.793	0.245
CT + TT	63 (42.3 %)	70 (43.8 %)	0.795				0.939	0.597–1.477	0.785
MAF	0,25	0,24	1	0,28	1	0,696			
GPX1, rs1050450									0.981
No of pts (n)	157	160							
CC	72 (46 %)	76 (47.5 %)							
CT	74 (47.1 %)	71 (44.5 %)					1.085	0.687 - 1.715	0.726
TT	10 (6.4 %)	13 (8.1 %)	0.788				0.801	0.331 - 1.941	0.623
CT + TT	84 (53.5 %)	84 (52.5 %)	0.811				1.041	0.670 - 1.619	0.857
MAF	0.3	0.3	1	0.23	0.101	0.094			

Table 3 Distribution of polymorphism genotypes in groups with and without ISR, minor alele frequencies (MAF) and logistic regression analysis, separately for each parameter with adjustment for diabetes mellitus *(Continued)*

ALOX5AP, rs17216473									1.000
No of pts (n)	149	160							
GG	113 (75.8 %)	120 (75 %)							
GA	36 (24.2 %)	38 (23.8 %)					1.007	0.597 - 1.699	0.980
AA	0	2 (1.2 %)	0.642				-	-	0.999
GA + AA	36 (24.2 %)	40 (25 %)	0.895				0.956	0.569 - 1.605	0.865
MAF	0.12	0.13	1	0.09	0.738	1			
APOE, rs7412, rs429358									0.995
No of pts (n)	154	160							
*2/*2	1 (0.6 %)	0					-	-	1.000
2.3	12 (7.8 %)	15 (9.4 %)					0.814	0.363 - 1.826	0.618
2.4	2 (1.3 %)	2 (1.2 %)					1.019	0.141 - 7.369	0.985
*2/*2; *2/*3; *2/*4	15 (9.7 %)	17 (10.6 %)	0.975				0.899	0.427 - 1.896	0.781
3/3 (wild)	106 (68.8 %)	108 (67.5 %)	0.952						
3.4	31 (20.1 %)	32 (20 %)					0.987	0.563 - 1.732	0.964
4.4	2 (1.3 %)	3 (1.9 %)					0.680	0.111 - 4.152	0.676
3/4;4/4	33 (21.4 %)	35 (21.9 %)					0.960	0.556 - 1.658	0.885
MAF *2	0.05	0.05	1	0.08	0.343	0.383			
MAF *4	0.11	0.12	1	0.14	0.831	1			
GC, rs7041									0.722
No of pts (n)	154	160							
TT	17 (11 %)	19 (11.9 %)							
TG	83 (53.9 %)	79 (49.4 %)					1.176	0.570 - 2.424	0.661
GG	54 (35.1 %)	62 (38.8 %)	0.741				0.974	0.460 - 2.060	0.945
TG + GG	137 (89 %)	141 (88.1 %)	0.861				1.086	0.542 - 2.178	0.815
MAF	0.38	0.37	1	0.43	0.374	1			
GC, rs4588									0.803
No of pts (n)	149	160							
CC	73 (49 %)	82 (51.2 %)							
CA	64 (43 %)	68 (42.5 %)					1.059	0.665 - 1.686	0.810
AA	12 (8.1 %)	10 (6.2 %)	0.821				1.350	0.551 - 3.311	0.512
CA + AA	76 (51.0 %)	78 (48.8 %)	0.733				1.096	0.701–1.713	0.688

Table 3 Distribution of polymorphism genotypes in groups with and without ISR, minor alele frequencies (MAF) and logistic regression analysis, separately for each parameter with adjustment for diabetes mellitus *(Continued)*

MAF	0.29	0.28	1	0.31	1	1			
VDR, rs2228570									0.913
No of pts (n)	149	160							
TT	30 (20.1 %)	32 (20 %)							
TC	70 (47 %)	79 (49.4 %)					0.945	0.552 - 1.544	0.760
CC	49 (32.9 %)	49 (30.6 %)	0.9				1.065	0.169 - 3.577	0.747
TC + CC	119 (79.9 %)	128 (80 %)	1				0.991	0.553 - 1.498	0.711
MAF	0.43	0.45	1	0.43	1	1			
LRP1, rs1799986									0.913
No of pts (n)	149	160							
CC	109 (73.2 %)	114 (71.2 %)							
CT	37 (24.8 %)	42 (26.2 %)					0.923	0.552 - 1.544	0.760
TT	3 (2.0 %)	4 (2.5 %)	0.941				0.778	0.169 - 3.577	0.747
CT + TT	40 (26.8 %)	46 (28.8 %)	0.8				0.910	0.553 - 1.498	0.711
MAF	0.14	0.15	1	0.16	1	1			
LDLR, rs2228671									0.716
No of pts (n)	149	160							
CC	124 (83.2 %)	130 (81.2 %)							
CT	22 (14.8 %)	28 (17.5 %)					0.824	0.447 - 1.516	0.533
TT	3 (2 %)	2 (1.2 %)	0.679				1.579	0.259 - 9.617	0.620
CT + TT	25 (16.9 %)	30 (18.8 %)	0.659				0.874	0.487 - 1.569	0.651
MAF	0.09	0.1	1	0.1	1	1			

p = chi-square test
GP general population, *CZ* Czech
[a]the confidence interval - for rs1803274 homozygotes AA vs. GG is too wide. Therefore the data were analyzed only in the setting of a dominant model

and reparative process. The acute vascular reaction is characterized by early deposition of platelets and fibrin. Activated platelets attach to circulating leukocytes (neutrophils and monocytes) at the injured surface. Over weeks, acute inflammatory cells are replaced by chronic inflammatory cells (macrophages and giant cells). In addition to this inflammatory response, platelet- and leukocyte-related growth factors drive further VSMC proliferation and migration from the media to the nascent neointima and subsequent extracellular matrix formation.

Two weeks following bare-metal stent implantation, a complete neointimal layer, composed of VSMCs and a proteoglycan-rich extracellular matrix, can be observed above stent struts. Excessive VSMC proliferation and extracellular matrix formation lead to neointimal hyperplasia, which represents the major pathophysiologic mechanism of ISR. Peak of BMS restenosis is observed at 3–6 months and remains relatively stable beyond 1 year [13].

In our study, the ISR and the control groups of patients did not differ significantly in the main demographic, clinical, angiografic and biochemical parameters, with the exception of total and LDL cholesterol levels, that were significantly higher in the control group. However, we do not consider this difference important in the context of the study results, as BCHE is not involved in cholesterol metabolism and no differences were detected in *LDLR* and *LRP1* SNPs between the groups.

Oguri et al. reported that the rs1803274 polymorphism of *BCHE*, rs529038 polymorphism of *ROS1*, and rs1050450 polymorphism of *GPX1* were significantly associated ($p < 0.05$) with ISR and that the rs1800849 polymorphism of *UCP3* was associated with recurrent ISR ($p = 0.0006$) in the Japanese population [3, 4].

Our results show that the rs1803274 (1699G>A, p.Ala567Thr) polymorphism of BCHE was also significantly associated with ISR in the Central European population and that the A allele represents a risk factor for this condition.

We analyzed this association only in the setting of a dominant model, i.e. minor allele homozygotes plus heterozygotes (AA and GA) versus major allele homozygotes (GG), as the confidence interval for rs1803274 homozygotes AA versus GG is too wide, probably due to the low number of AA homozygotes.

A significant difference was also found for rs1803274 minor allele frequencies between the ISR and non ISR groups. However, such a difference was not proved for either the ISR or non ISR groups compared to general Czech population. This may be due to a relatively small sample size.

Butyrylcholinesterase (BCHE) is a secretion enzyme produced by liver cells and released into the bloodstream. In plasma, it contributes to cholinesterase activity, but its endogenous substrate is not known. Cholinesterase synthesis and its activity in plasma are decreased after liver parenchyma damage or in the case of insufficient protein intake in the diet. Previous studies have reported a significant association between serum BCHE activity and metabolic syndrome risk variables, such as high body mass index, plasma concentrations of triglycerides and HDL cholesterol, and blood pressure [14]. BCH E co-participates in the hydrolysis of aspirin and thus could affect its bioavailability and ability to inhibit platelet aggregation [15]. The rs1803274 (the so-called K-variant) SNP could be associated with type 2 diabetes mellitus; on the other hand, results are conflicting on the association between this SNP and early onset of coronary artery disease [16, 17]. The underlying mechanism of the association between the rs1803274 polymorphism of *BCHE* and ISR remains to be elucidated.

Although the rs1050450 polymorphism of the *GPX1* gene has also been associated with an increased risk of ISR in Russian individuals [18] and in the Gender study [19], we found no relationships between the polymorphisms of *ROS1*, *GPX1*, and *UCP3* and ISR in the Central European population.

Arachidonate 5-lipoxygenase-activating protein (ALOX5AP) has an important role in the initial steps of the biosynthesis of leukotrienes, which in turn have a variety of proinflammatory effects [20]. Shah et al. found a significant association between the occurrence of ISR and rs17216473 in a North American population [5]. In contrast to their results, however, we could not confirm the association between rs17216473 and the risk of ISR in a Central European population.

In addition to the above genes, we focused on a group of genes affecting metabolic processes including *APOE, VDR, GC, LRP1* and *LDLR*. The corresponding proteins may be involved not only in atherosclerosis but also in inflammation and may influence proliferation and migration of SMCs, key players in ISR development [6–11].

Apolipoprotein E (APOE) plays an important role not only in the metabolism of cholesterol and triglycerides but also in inhibiting growth factor–induced SMC migration and proliferation and limiting neointimal hyperplasia after arterial injury [6, 7, 21]. APOE deficiency has been associated with increased neointima formation after vessel wall injury [22]. In an apoE-knockout mouse model, the in-stent neointimal area was greater compared with wild-type mice [22]. Although the level of APOE could play a protective role against various forms of vascular disease, including atherosclerosis and injury-induced restenosis, we did not observe a significant correlation between the *APOE*2*, **3*, and **4* polymorphisms and the risk of ISR. Koch et al. made a similar

observation, concluding that some *APOE* polymorphisms, i.e., *APOE* –219G>T, 113G>C, 334T>C (*APOE*4*), and 472C>T (*APOE*2*) either alone or in combination do not represent genetic markers of the risk of ISR or stent thrombosis in German patients with coronary artery disease [21].

Vitamin D is involved not only in bone metabolism but also in modulating immune responses and cell proliferation. The active form of vitamin D achieves its biological effects by binding to the VDR, which is expressed in most tissues and cells, including cardiac myocytes, VSMCs and endothelial cells [8, 9]. In vivo and in vitro studies have shown that down-regulation of VDR in SMCs of post-interventional arteries could be involved in the uncontrolled growth of SMCs, leading to neointimal hyperplasia and restenosis [10]. We have studied the rs2228570 polymorphism of the *VDR* gene (known as a Fok I variant according to the restriction enzyme used to detect it previously) and the rs7041 and rs4588 polymorphisms of the *GC* gene encoding vitamin D binding protein (DBP) and found that none of these polymorphisms was associated with the risk of ISR in this population. The findings regarding the rs2228570 in *VDR* gene correspond to the results of the study by Monraats et al. Although some substitutions (the -1012A>G, –25C>A and 464G>T) of the *VDR* gene increased the risk of clinical restenosis in their study, such an association was not proved for rs2228570 [23].

The members of the low-density lipoprotein receptor family (the LRs) such as low-density lipoprotein receptor (LDLR), low-density lipoprotein receptor-related protein-1 (LRP1), and others play a key role not only in lipoprotein metabolism but also in the catabolism of many membrane-associated proteins [11]. LRs can influence the migration and proliferation of SMCs through urokinase-type plasminogen activator receptor (uPA) and the platelet-derived growth factor (PDGF) receptor. Neither the rs1799986 polymorphism of *LRP1* nor the rs2228671 polymorphism of *LDLR* were significantly associated with the risk of ISR in our study.

Limitations

Several limitations of our study need to be mentioned. This study could be limited by its observational nature and a relatively small sample size. Nevertheless, we believe that selection bias did not play a major role, because both patient cohorts did not differ with respect to main baseline parameters. As non-invasive MS-CT coronarography was used in control group to confirm the stent patency, it is not possible to avoid completely potential false negatives findings. However, in previous studies, MS-CT coronarography revealed sufficient accuracy for ISR detection [24, 25].

Conclusion

Our results show that the rs1803274 polymorphism of *BCHE* was significantly associated with ISR in our Central European patients after PCI with bare-metal stent implantation. The A allele of this polymorphism represents a risk factor for this condition. The underlying molecular mechanism of the association between this polymorphism and ISR remains to be elucidated. No association was found with the other studied SNPs, including rs529038 (*ROS1*), rs1050450 (*GPX1*), rs1800849 (*UCP3*), rs17216473 (*ALOX5AP*), rs7412, rs429358 (*APOE*), rs2228570 (*VDR*), rs7041, rs4588 (*GC*), rs1799986 (*LRP1*), and rs2228671 (*LDLR*).

Availability of supporting data

The data sets supporting the results of this article are available in the LabArchives repository [http://dx.doi.org/10.6070/H4TB14XG].

Competing interests

The authors declare that they have no competing interests.

Authors' contributions

LP: study design; PP, LF, PK, SH: literature search; LP, PK: data collection; PK, PP, LF, SH: data analysis; JZ: statistical analysis; LP: data interpretation; All authors: manuscript revision. All authors read and approved the final manuscript.

Financial disclosure

This article was co-supported by the project of European Social Fund and the State Budget of the Czech Republic, registration number CZ.1.07/2.3.00/20.0040 and by Ministry of Health, Czech Republic - conceptual development of research organizations - FNOs/2013.

Author details

[1]Department of Clinical Studies, Medical Faculty, University of Ostrava, Syllabova 19, Ostrava, Zabreh 703 00, Czech Republic. [2]Department of Cardiovascular Diseases, University Hospital Ostrava, Ostrava, Czech Republic. [3]Department of Biomedical Sciencies, Medical Faculty, University of Ostrava, Ostrava, Czech Republic. [4]Blood Center, University Hospital of Ostrava, Ostrava, Czech Republic. [5]Department of Medical Genetics, University Hospital Ostrava, Ostrava, Czech Republic. [6]Department of Medical Biophysics, Palacky University, Olomouc, Czech Republic. [7]Department of Laboratory Medicine, University Hospital Ostrava, Ostrava, Czech Republic.

Received: 16 May 2015 Accepted: 16 October 2015
Published online: 24 October 2015

References

1. Kim MS, Dean LS. In-Stent Restenosis. Cardiovasc Ther. 2011;29:190–8.
2. Ryan TJ, Faxon DP, Gunnar RM, Kennedy JW, King III SB, Loop FD, et al. Guidelines for percutaneous transluminal coronary angioplasty: A report of the American College of Cardiology/American Heart Association Task Force on the Assesment of Diagnostic and Therapeutic Cardiovascular Procedures. Circulation. 1988;78(2):486–502.
3. Oguri M, Kato K, Hibino T, Yokoi K, Segawa T, Matsuo H, et al. Genetic risk for restenosis after coronary stenting. Atherosclerosis. 2007;194:e172–8.
4. Oguri M, Kato K, Hibino T, Yokoi K, Segawa T, Matsuo H, et al. Identification of a polymorphism of *UCP3* associated with recurrent in-stent restenosis of coronary arteries. Int J Mol Med. 2007;20:533–8.
5. Shah SH, Hauser ER, Crosslin D, Wang L, Haynes C, Connelly J. ALOX5AP variants are associated with in-stent restenosis after percutaneous coronary intervention. Atherosclerosis. 2008;201:148–54.
6. Xu H, Li H, Liu J, Zhu D, Wang Z, Chen A. Meta-Analysis of Apolipoprotein E Gene Polymorphism and Susceptibility of Myocardial Infarction. PLoS One. 2014;9(8):e104608.

7. Bennet AM, Angelantonio E, Ye Z, Wensley F, Dahlin A, Ahlbom A. Association of Apolipoprotein E Genotypes With Lipid Levels and Coronary Risk. JAMA. 2007;298(11):1300–11.
8. Chen S, Law CS, Gardner DG. Vitamin D-dependent suppression of endothelin-induced vascular smooth muscle cell proliferation through inhibition of CDK2 activity. J Steroid Biochem Mol Biol. 2010;118:135–41.
9. Holick MF. Vitamin D, deficiency. N Engl J Med. 2007;357:266–81.
10. Gupta GK, Agrawal T, Del Core MG, Hunter WJ, Agrawal DK. Decreased Expression of Vitamin D Receptors in Neointimal Lesions following Coronary Artery Angioplasty in Atherosclerotic Swine. PLoS One. 2012;7(8):e42789.
11. Bujo H, Saito Y. Lipoprotein Receptor Family Modulation of Smooth Muscle Cell Migration by Members of the Low-Density Lipoprotein Receptor Family. Arterioscler Thromb Vasc Biol. 2006;26:1246–52.
12. Dunnen JT, Antonarakis SE. Mutation Nomenclature Extensions and Suggestions to Describe Complex Mutations: A Discussion. Hum Mutat. 2000;15:7–12.
13. Byrne RA, Joner M, Massberg S, Kastrati A. Restenosis in bare metal and drug-eluting stents. In: Escaned J, Serruys PW, editors. Coronary stenosis, imaging, structure and physiology. 1st ed. Toulouse, France: Europa Edition; 2010. p. 475–96.
14. Valle A, O'Connor DT, Taylor PW, Zhu G, Montgomery GW, Slagboom PE, et al. Pseudocholinesterase: association with the metabolic syndrome and identification of 2 gene loci affecting activity. Clin Chem. 2006;52:1014–20.
15. Zhou G, Marathe GK, Hartiala J, Hazen SL, Allayee H, Tang WWH. Aspirin Hydrolysis in Plasma Is a Variable Function of Butyrylcholinesterase and Platelet-activating Factor Acetylhydrolase 1b2 (PAFAH1b2). J Biol Chem. 2013;288(17):11940–8.
16. Nassar BA, Rockwood K, Kirkland SA, Ransom TP, Darvesh S. Improved prediction of early-onset coronary artery disease using APOE epsilon 4, BChE-K, PPAR gamma2 Pro12 and *ENOS T-786C* in a polygenic model. Clin Biochem. 2006;39:109–14.
17. Scacchi R, Ruggeri M, Corbo MR. Variation of the butyrylcholinesterase (BChE) and acetylcholinesterase (AChE) genes in coronary artery disease. Clin Chim Acta. 2011;412:1341–4.
18. Shuvalova YA, Kaminnyi AI, Meshkov AN, Shirokov RO, Samko AN. Association between polymorphisms of eNOS and GPx-1 genes, activity of free-radical processes and in-stent restenosis. Mol Cell Biochem. 2012;370:241–9.
19. Verschuren JJ, Trompet S, Postmus I, Sampietro ML, Heijmans BT. Systematic Testing of Literature Reported Genetic Variation Associated with Coronary Restenosis: Results of the GENDER Study. PLoS One. 2012;7(8):e42401.
20. Girelli D, Martinelli N, Trabetti E, Olivieri O, Cavallari U, Malerba G, et al. ALOX5AP gene variants and risk of coronary artery disease: an angiography-based study. Eur J Hum Genet. 2007;15:959–66.
21. Koch W, Mehilli J, Pfeufer A, Schömig A, Kastrati A. Apolipoprotein E gene polymorphisms and thrombosis and restenosis after coronary artery stenting. J Lipid Res. 2004;45:2221–6.
22. Ali ZA, Alp NJ, Lupton H, Arnold N, Bannister T, Hu Y, et al. Increased In-Stent Stenosis in *ApoE* Knockout Mice. Insights from a Novel Mouse Model of Balloon Angioplasty and Stenting. Arterioscler Thromb Vasc Biol. 2007;27:833–40.
23. Monraats PS, Fang Y, Pons D, Pires NMM, Pols HAP, Zwinderman AH. Vitamin D receptor: A new risk marker for clinical restenosis after percutaneous coronary intervention. Expert Opin Ther Tar. 2010;14(3):243–51.
24. Sun Z, Marzouq A, Almutairi D. Diagnostic accuracy of 64 multislice CT angiography in the assessment of coronary in-stent restenosis: A meta-analysis. Eur J Radiol. 2010;73:266–73.
25. Kumbhani DJ, Ingelmo CP, Schoenhagen P, Curtin RJ, Flamm SD, Desai MY. Meta-analysis of diagnostic efficacy of 64-slice Computed Tomography in the evaluation of coronary in-stent restenosis. Am J Cardiol. 2009;103:1675–81.

15. Comparison of three methods used in the diagnosis of extraesophageal reflux in children with chronic otitis media with effusion

Formánek M, Komínek P, Matoušek P, Tomanová R, Urban O, Zeleník K

Originally published in Gastroenterology Research and Practice, [online], 2015, vol. 2015, no. Article ID 547959, p. 1-5.

Hindawi Publishing Corporation
Gastroenterology Research and Practice
Volume 2015, Article ID 547959, 5 pages
http://dx.doi.org/10.1155/2015/547959

Clinical Study

Comparison of Three Methods Used in the Diagnosis of Extraesophageal Reflux in Children with Chronic Otitis Media with Effusion

Martin Formánek,[1,2] Pavel Komínek,[1,2] Petr Matoušek,[1,2] Radoslava Tomanova,[3] Ondřej Urban,[2,4] and Karol Zeleník[1,2]

[1]*Department of Otorhinolaryngology, University Hospital Ostrava, 17 Listopadu 1790, 708 52 Ostrava, Czech Republic*
[2]*Faculty of Medicine, University of Ostrava, Syllabova 19, 703 00 Ostrava, Czech Republic*
[3]*Department of Pathology, University Hospital Ostrava, 17 Listopadu 1790, 708 52 Ostrava, Czech Republic*
[4]*Gastroenterology Department, Vitkovicka Hospital, Zalužanského 1192/15, 703 84 Ostrava, Czech Republic*

Correspondence should be addressed to Karol Zeleník; karol.zelenik@fno.cz

Received 16 October 2014; Accepted 23 April 2015

Academic Editor: Greger Lindberg

Objectives. Detection of extraesophageal reflux (EER) in children with chronic otitis media with effusion (OME) using three different diagnostic methods. *Methods*. Children between 1 and 7 years with OME who underwent adenoidectomy and myringotomy with insertion of a ventilation tube were included in this prospective study. EER was detected using three methods: oropharyngeal pH was monitored for 24 hours using the Restech system; detection of pepsin in middle ear fluid obtained during myringotomy was done using Peptest, and detection of pepsin in an adenoid specimen was done immunohistochemically. *Results*. Altogether 21 children were included in the study. Pathological oropharyngeal pH was confirmed in 13/21 (61.9%) children. Pepsin in the middle ear fluid was present in 5/21 (23.8%) children; these 5 patients were diagnosed with the most severe EER established through monitoring of oropharyngeal pH. No specimen of adenoids tested was positive for pepsin upon immunohistochemical examination. *Conclusions*. Diagnosis of EER in patients with OME using Restech is sensitive but less specific when compared to the detection of pepsin in middle ear fluid using Peptest. Pepsin in the middle ear was consistently present in patients with RYAN score above 200, and these patients in particular could potentially profit from antireflux therapy.

1. Introduction

Acute otitis media (AOM) and chronic otitis media with effusion (OME) are among the most frequent causes for visits to the doctor in children 1–3 years old. Despite of the fact that there was an overall downward trend in the United States during the pneumococcal conjugated vaccine era, AOM and OME remain major health and socioeconomic issue [1]. It is estimated that up to 60% of children have experienced at least one episode of AOM by age 7 [2, 3]. There are several well-known conditions that cause or facilitate the development of middle ear infection. The most important are upper respiratory infections, allergies, and enlarged adenoids [4]. Despite adequate treatment of these conditions, AOM and OME remain common issues [5, 6]. In consequence, there is an effort to identify other possible risk factors and thereby reduce the number of ear infections and their consequences.

Extraesophageal reflux (EER) is considered one among several possible risk factors of AOM and OME [5–9]. Until recently, more accurate exploration of the relationship between ear infection and EER has been very complicated due to limitations in diagnostic methods. However, in recent years superior pharyngeal pH monitoring devices and new techniques which can measure pepsin in tissues and fluids have been developed and EER can be diagnosed quite precisely [10, 11]. The problem is that it is not yet known how to select patients with OME who would respond to antireflux therapy. The reason for this is that a diagnosis of pathological

EER based on the given thresholds does not mean that the patient will respond to antireflux therapy [12]. And because of likely side effects, it is not possible to put all patients with OME on proton pump inhibitors.

The aim of the study was detection of EER in children with OME using three different diagnostic methods (oropharyngeal pH monitoring, detection of pepsin in the middle ear fluid, and immunohistochemical detection of pepsin in a biopic specimen of adenoids) and selection of the group of patients with the most severe EER who could potentially benefit from antireflux therapy (diet, behaviour, and proton pump inhibitors).

2. Materials and Methods

The prospective study was approved by the Ethics Committee of the University Hospital and was performed in accordance with the Declaration of Helsinki, good clinical practice, and applicable regulatory requirements. Written informed consent was obtained from both parents before initiating any procedure.

Children aged between 1 and 7 years diagnosed with bilateral or unilateral OME who underwent adenoidectomy and myringotomy with insertion of a ventilation tube were included in the prospective study from June 2012 to March 2014. OME was defined as effusion in the middle ear behind an intact eardrum for longer than 3 months. Diagnosis was made on the basis of otomicroscopic findings, pneumatic otoscopy, type B tympanometry, and audiometry (in cooperative older children). Children with no fluid in the middle ear during myringotomy were rediagnosed as having tympanosclerosis and were excluded from the study. Children with craniofacial abnormalities (Down syndrome, Treacher Collins syndrome, clefts, etc.) were excluded from the study as well. Demographic data (including tobacco exposure) and symptoms of EER disease were provided by parents, who were also specifically questioned regarding the presence of hoarseness, recurrent lower respiratory infection (e.g., bronchitis and pneumonia), and bronchial asthma in their child.

24-hour monitoring of oropharyngeal pH using the Restech system (Respiratory Technology Corporation, San Diego, CA, USA) was performed before surgery. Parents were instructed to record the time their child spent eating and drinking and in a horizontal position directly to the device and manually to the diary. If there was any discrepancy, periods logged in the device were modified according to the diary. A standardized RYAN composite score was calculated automatically using the software supplied. Patients with pathological RYAN composite scores in the vertical (higher than 9.4) and/or horizontal (higher than 6.8) position were classified as having pathological EER. Severe EER was diagnosed when the RYAN composite score in the vertical or horizontal position was higher than 200.

Myringotomy under magnification was performed in the anterior inferior part of the tympanic membrane. The type of middle ear effusion (i.e., fluid or mucous) was noted. Middle ear fluid was collected with a Tympanocentesis Collector 1419020 (Medtronic, Minneapolis, MN, USA), and a ventilation tube was inserted in the tympanic membrane. In cases of bilateral OME, bilateral ventilation tube insertion was performed simultaneously and the effusion was collected and analyzed separately. Analyses were performed on the day of surgery. First, 0.1 mL of 10% citric acid was added. Afterwards, the specimen was centrifuged at 4,000 rpm for 5 min. If a clear supernatant layer was not visible, the sample was centrifuged again. An 80 μL sample was drawn from the clear supernatant layer, added to a screw top microtube containing 240 μL of migration buffer, and mixed with a vortexer for 10 s. Afterwards, the specimen was assayed with Peptest (RD Biomed Limited, Hull, UK), which contains monoclonal antibodies targeted to pepsin. The results were collected after 15 min. Peptest results are specified as positive (two lines), negative (one line), or invalid (no line).

Then, adenoidectomy using a cold instrument was performed. A specimen of adenoids (5 × 5 × 5 mm) from the area close to the torus tubarius was fixed in formaldehyde and immunohistochemically analysed at the Department of Pathology. Antibody P3635Rb-h (Uscn Life, USA, concentration 1 : 100) was used as the primary antibody. Antibody N-Histofine Simple Stain MAX PO (Nichirei Biosciences Inc., USA) was used as the secondary antibody. Statistical analysis was done using MS Excel. There was no missing data.

3. Results

In total, 24 children were included in the study. Three children with no middle ear fluid during myringotomy were rediagnosed as having tympanosclerosis and were excluded from the study. Thus 21 children, 11 boys (52.4%) and 10 girls (47.6%), with an average age of 4.2 years, were analysed. 2/21 (9.5%) children were hoarse and were diagnosed with vocal cord nodules, 3/21 (14.3%) suffered from recurrent pneumonias (3 or more pneumonias during the previous two years), and 5/21 (23.8%) children suffered from bronchial asthma. None of the children took medications for gastroesophageal reflux disease.

Pathological EER was diagnosed by oropharyngeal pH monitoring (Restech) in 13/21 (61.9%) children. The average RYAN composite score of patients diagnosed with EER was 106.05 in the vertical position and 6.69 in the horizontal position. In 5/21 (23.8) children, the RYAN composite score in the vertical position was higher than 200 (severe EER).

Bilateral myringotomy was performed in 12/21 (57.1%) children and unilateral myringotomy in 9/21 (42.9%) children. Altogether, 33 middle ear fluid specimens were examined. Pepsin in the middle ear was detected in 5/21 (23.8%) children. In three children with bilateral OME, pepsin was detected in the middle ear fluid in both ears. Pepsin was detected in the middle ear fluid in two patients with unilateral OME as well. Thus pepsin was detected in 8/33 (24.2%) middle ear specimens. No invalid result was noted. Serous samples were positive to pepsin in 5/17 (29.4%) cases, while mucous samples were positive in 3/16 (18.8%) cases. Pepsin in the middle ear fluid was present only in 5 children with severe EER (RYAN composite score higher than 200), as established by monitoring the oropharyngeal pH. In the remaining 8 children with less serious EER ascertained by

means of oropharyngeal pH monitoring, pepsin in the middle ear fluid was not diagnosed. Pepsin in the middle ear was detected in 2/5 children (40.0%) with bronchial asthma.

Immunohistochemical detection of pepsin in biopic specimens of adenoids was negative in 21/21 (100%) samples. Antibodies used for control in the main cells of the gastric mucosa were strongly positive.

4. Discussion

It is supposed that EER is an etiological factor or cofactor in many lower and upper respiratory diseases, such as laryngitis, cough, globus pharyngeus, bronchial asthma, papillomatosis, and rhinosinusitis, and in middle ear inflammations, as well [13, 14]. Many studies investigated that contact between the refluxed content and mucous of the nasopharynx, Eustachian tube, or middle ear causes local inflammation and oedema; thus it facilitates the development of middle ear inflammation [5–9, 15]. This is why EER is nowadays included among other well-known predisposing factors for developing middle ear inflammation [5–9, 15].

Diagnosis of EER in patients with OME is not easy. Many reflux questionnaires have been developed in the recent past, even for infants and small children. They summarize complaints potentially caused by reflux (frequent awakening at night, regurgitation of food, hoarseness, cough, lower respiratory infections, etc.) [16, 17]. However, evaluation of reflux, and particularly EER in children using questionnaires, seems to be inadequate and inaccurate, because symptoms are very common and too heterogeneous [16]. Another problem is that the questionnaire is filled in by parents, who could interpret symptoms incorrectly. For children older than 12 years, the Reflux Symptom Index can be used to evaluate patient problems [16].

Many novel methods have become available recently for making the diagnosis of pathological EER and quantifying it. Diagnosis of EER by 24-hour esophageal pH-metry or impedance is relatively invasive and not always well tolerated, especially by children. Therefore it is advantageous to use new, less invasive diagnostic methods, such as 24-hour monitoring of oropharyngeal pH by the Restech system, detection of pepsin in middle ear fluid using Peptest, and immunohistochemical detection of pepsin in tissues.

Currently, one of the widely used methods for measuring EER is 24-hour monitoring of pH in the esophagus. It has been shown that there is a 10 times higher risk of development of recurrent AOM or OME in children in whom EER is detected by means of double-probe esophageal pH monitoring [9]. However, double probe esophageal pH monitoring is not very well tolerated by children, especially children aged two to seven years. This is one of the reasons why oropharyngeal pH monitoring, which is less invasive and much better tolerated by children, was developed and implemented in clinical practice [11]. However, there are some disadvantages of this method as well. In particular, the absence of a distal sensor, which means that it is necessary to rely on data about meal periods and the position of the patient as entered by the parent. Nevertheless, the majority of studies comparing esophageal and oropharyngeal pH-metry (simultaneous monitoring in one patient) have established good reciprocal correlation between these two methods [10, 18].

There is no pepsin in the middle ear in normal physiologic conditions [5]. The presence of pepsin in the middle ear is therefore considered indirect confirmation of previous episodes of reflux into the middle ear [5, 6]. In the study by O'Reilly et al. pepsin in middle ear effusions in patients with recurrent AOM or OME was detected in 20.2% of cases, in comparison with the control group of patients who underwent cochlear implantation (only 1.5% cases) [7]. Other studies that examined pepsin in the middle ear secretions of children with OME refer to the presence of pepsin in 1/3 cases [8]. This suggests that EER is likely one of the etiological factors behind OME in as many as 1/3 children. Similar results were obtained in our study, as pepsin was detected by Peptest in 5/21 (23.8%) children, more frequently in serous samples (29.4%) than in mucous samples (18.8%). Previous studies use accurate but time consuming and expensive methods of detecting pepsin, which are too complicated to be used on a daily basis. Peptest, on the other hand, seems to be suitable for frequent daily use as an easy, cheap, and quick diagnostic method.

It is possible to detect pepsin in tissues using immunohistochemical analysis as well [15]. In the study by Jiang et al., immunohistochemical detection of pepsin in interarytenoid biopsy specimens in patients with pathological EER (detected by esophageal impedance) was performed. In their study, pepsin was evidenced both in patients with acid (6 of 7 patients) and with weak acid reflux (6 of 8) [15]. Pepsin was evidenced in 3/21 patients in the control group who had negative results for esophageal impedance. This can be explained by the higher sensitivity of an immunohistochemical examination due to the protracted collection of pepsin in tissues, compared to pH monitoring that lasts only 24 hours. It is possible to detect pepsin in tissues even though there may have been no reflux over several days [15]. In theory, the diagnosis of pepsin in adenoids could be another way to diagnose EER in children with OME so as to get a wider view of the severity of reflux in the nasopharynx. Interestingly, in our study, all 21 specimens of adenoids were found to be pepsin negative using immunohistochemical detection. The authors cannot explain this fact but only speculate that the amount of pepsin in the nasopharynx was too low to be detected (in comparison with the interarytenoid region). Our results are consistent with the results of Harris et al., where pepsin was not detected in specimens of adenoids, and the authors conclude that this method is not suitable for the diagnosis of EER in the nasopharynx [19].

All in all, using 24-hour monitoring of oropharyngeal pH (Restech) and detection of pepsin in the middle ear fluid (Peptest), diagnosis of EER in patients with OME and its quantifying can be accomplished quite precisely nowadays. But there is still one big question remaining to be answered: which patients would respond to antireflux therapy? The problem is that AOM/OME, as well as EER, are very common diseases, and diagnosis of pathological EER according to the given thresholds does not guarantee that the patient will respond to antireflux therapy. Last systemic

review of Miura et al. concludes that the prevalence of gastroesophageal reflux disease in children with chronic otitis media with effusion/recurrent acute otitis media may be higher than the overall prevalence for children. However, presence of pepsin/pepsinogen in the middle ear could be related to physiologic reflux. A cause-effect relationship between pepsin/pepsinogen in the middle ear and otitis media is unclear and therefore antireflux therapy for otitis media cannot be endorsed based on existing research [20]. And because it is not possible to put all patients with OME on proton pump inhibitors, particularly because of possible side effects, it is very important to quantify EER. It has been proved that the stricter the criteria for the diagnosis of EER, the more the patients that would respond to antireflux therapy [12]. The results of our study demonstrated that pepsin in the middle ear fluid was present in five children with the most severe EER (RYAN score above 200) established by monitoring of oropharyngeal pH. On the contrary, eight children with mild pathological EER had no pepsin in their middle ear fluid. In order to select patients with severe EER, who would potentially benefit from antireflux therapy, this information seems to be very important. It can be assumed that patients with a RYAN composite score above 200 and patients with a positive Peptest would be the best candidates for antireflux therapy. Whatever the case, it is very important to pursue research in this area with better designed controlled studies with more patients involved.

5. Conclusions

EER can cause inflammatory changes in the Eustachian tube and middle ear, with consequential development of middle ear inflammation. On the basis of previous studies, as well as ours, we may conclude that EER is likely coresponsible for as many as 1/3 of OME. 24-hour monitoring of oropharyngeal pH and detection of pepsin in the middle ear fluid are suitable methods for detecting EER in children with OME. Patients with a positive Peptest and patients with a RYAN composite score above 200 have most severe EER and could be possibly the best candidates for antireflux treatment.

Conflict of Interests

The authors declare that there is no actual or potential conflict of interests in relation to this paper. No benefits in any form have been received or will be received from a commercial party related directly or indirectly to the subject of this paper.

Acknowledgment

This research was supported by the Ministry of Health, Czech Republic, Conceptual Development of Research Organization (FNOs/2013).

References

[1] J. F. Lubianca Neto, L. Hemb, and D. Brunelli E Silva, "Systematic literature review of modifiable risk factors for recurrent acute otitis media in childhood," *Jornal de Pediatria*, vol. 82, no. 2, pp. 87–96, 2006.

[2] E. A. MacIntyre, C. J. Karr, M. Koehoorn et al., "Otitis media incidence and risk factors in a population-based birth cohort," *Paediatrics and Child Health*, vol. 15, no. 7, pp. 437–442, 2010.

[3] T. Todberg, A. Koch, M. Andersson et al., "Incidence of otitis media in a contemporary Danish National Birth Cohort," *PLoS ONE*, vol. 9, no. 12, Article ID e111732, 2014.

[4] C. D. Bluestone, "Studies in otitis media: Children's Hospital of Pittsburgh-University of Pittsburgh Progress Report-2004," *Laryngoscope*, vol. 114, no. 11, pp. 1–26, 2004.

[5] Z. He, R. C. O'Reilly, and D. Mehta, "Gastric pepsin in middle ear fluid of children with otitis media: clinical implications," *Current Allergy and Asthma Reports*, vol. 8, no. 6, pp. 513–518, 2008.

[6] M. Crapko, J. E. Kerschner, M. Syring, and N. Johnston, "Role of extra-esophageal reflux in chronic otitis media with effusion," *Laryngoscope*, vol. 117, no. 8, pp. 1419–1423, 2007.

[7] R. C. O'Reilly, Z. He, E. Bloedon et al., "The role of extraesophageal reflux in otitis media in infants and children," *The Laryngoscope*, vol. 118, no. 7, pp. 1–9, 2008.

[8] J. E. C. Lieu, P. G. Muthappan, and R. Uppaluri, "Association of reflux with otitis media in children," *Otolaryngology—Head and Neck Surgery*, vol. 133, no. 3, pp. 357–361, 2005.

[9] V. Rožmanic, M. Velepic, V. Ahel, D. Bonifacic, and M. Velepic, "Prolonged esophageal pH monitoring in the evaluation of gastroesophageal reflux in children with chronic tubotympanal disorders," *Journal of Pediatric Gastroenterology and Nutrition*, vol. 34, no. 3, pp. 278–280, 2002.

[10] S. Ayazi, J. C. Lipham, J. A. Hagen et al., "A new technique for measurement of pharyngeal pH: normal values and discriminating pH threshold," *Journal of Gastrointestinal Surgery*, vol. 13, no. 8, pp. 1422–1429, 2009.

[11] G. J. Wiener, R. Tsukashima, C. Kelly et al., "Oropharyngeal pH monitoring for the detection of liquid and aerosolised supraesophageal gastric reflux," *Journal of Voice*, vol. 23, pp. 498–504, 2009.

[12] K. Zelenik, P. Matousek, M. Tedla, J. Syrovatka, and P. Kominek, "Extraesophageal reflux: what is the best parameter for pH-monitoring data analysis from the perspective of patient response to proton pump inhibitors?" *Gastroenterology Research and Practice*, vol. 2013, Article ID 736486, 5 pages, 2013.

[13] J. M. DelGaudio, "Direct nasopharyngeal reflux of gastric acid is a contributing factor in refractory chronic rhinosinusitis," *Laryngoscope*, vol. 115, no. 6, pp. 946–957, 2005.

[14] K. Zeleník, P. Matoušek, O. Urban, P. Schwarz, I. Stárek, and P. Komínek, "Globus pharyngeus and extraesophageal reflux: simultaneous pH <4.0 and pH <5.0 analysis," *Laryngoscope*, vol. 120, no. 11, pp. 2160–2164, 2010.

[15] A. Jiang, M. Liang, Z. Su et al., "Immunohistochemical detection of pepsin in laryngeal mucosa for diagnosing laryngopharyngeal reflux," *The Laryngoscope*, vol. 121, no. 7, pp. 1426–1430, 2011.

[16] L. Deal, B. D. Gold, D. A. Gremse et al., "Age-specific questionnaires distinguish GERD symptom frequency and severity in infants and young children: development and initial validation," *Journal of Pediatric Gastroenterology and Nutrition*, vol. 41, no. 2, pp. 178–185, 2005.

[17] L. Kleinman, S. Nelson, S. Kothari-Talwar et al., "Development and psychometric evaluation of 2 age-stratified versions of the

pediatric GERD symptom and quality of life questionnaire," *Journal of Pediatric Gastroenterology and Nutrition*, vol. 52, no. 5, pp. 514–522, 2011.

[18] N. N. Chheda, M. W. Seybt, R. R. Schade, and G. N. Postma, "Normal values for pharyngeal pH monitoring," *Annals of Otology, Rhinology and Laryngology*, vol. 118, no. 3, pp. 166–171, 2009.

[19] P. K. Harris, D. J. Hussey, D. I. Watson et al., "Reflux changes in adenoidal hyperplasia: a controlled prospective study to investigate its aetiology," *Clinical Otolaryngology*, vol. 34, no. 2, pp. 120–126, 2009.

[20] M. S. Miura, M. Mascaro, and R. M. Rosenfeld, "Association between otitis media and gastroesophageal reflux: a systematic review," *Otolaryngology—Head and Neck Surgery*, vol. 146, no. 3, pp. 345–352, 2012.

16. Semi-spherical radiofrequency bipolar device - a new technique for liver resection: experimental in vivo study on the porcine model

Vávra P, Penhaker M, Jurčíková J, Škrobánková M, Crha M, Ostruszka P, Ihnát P, Grepl J, Delongová P, Dvořáčková J, Procházka V, Šalounová D, Škořič M, Rauser P, Habib N, Zonča P

Originally published in Technology in Cancer Research & Treatment, 2015, vol. 14, no. 5, p. 573-582.

Technology in Cancer Research and Treatment
ISSN 1533-0346
2014 June 5. Epub ahead of print.

Semi-spherical Radiofrequency Bipolar Device – A New Technique for Liver Resection: Experimental *In Vivo* Study on the Porcine Model

www.tcrt.org
DOI: 10.7785/tcrt.2012.500432

The incidence of colorectal carcinoma is still growing in the Czech Republic and also all around the world. With success of oncological treatment is also growing a number of potential patients with liver metastases, who can profit from surgical therapy. The aim of this study was to confirm on porcine models that this method by using new surgical device is effective and safe for patients who have to undergo liver resection. The primary hypothesis of the study was to evaluate whether this new device is able to consistently produce homogeneous and predictable areas of coagulation necrosis without the Pringle maneuver of vascular inflow occlusion. The secondary hypothesis of the study was to compare the standard linear radiofrequency device and a new semi-spherical bipolar device for liver ablation and resection in a hepatic porcine model. Twelve pigs were randomly divided into two groups. Each pig underwent liver resection from both liver lobes in the marginal, thinner part of liver parenchyma. The pigs in first group were operated with standard using device and in the second group we used new developed semi-spherical device. We followed blood count in 0th, 14th and 30th day from operation. 14th day from resection pigs underwent diagnostic laparoscopy to evaluate of their state, and 30th day after operation were all pigs euthanized and subjected to histopathological examination. Histopathological evaluation of thermal changes at the resection margin showed strong thermal alteration in both groups. Statistical analysis of collected dates did not prove any significant ($p < 0.05$) differences between standard using device and our new surgical tool. We proved safety of new designed semi-spherical surgical. This device can offer the possibility of shortening the ablation time and operating time, which is benefit for patients undergoing the liver resection.

Key words: Liver resection; Porcine model; Radiofrequency energy; Surgical device.

Vavra, P., M.D., Ph.D.[1-3,11]*
Penhaker, M., MSc., Ph.D.[2]
Jurcikova, J., D.V.M., Ph.D.[4]
Skrobankova, M.[3]
Crha, M., D.V.M., Ph.D.[5]
Ostruszka, P., M.D.[1]
Ihnat, P., M.D., Ph.D.[1,3]
Grepl, J., Ing.[6]
Delongova, P., M.D.[7]
Dvorackova, J., M.D., Ph.D.[7]
Prochazka, V., M.Sc., M.D., Ph.D.[4]
Salounova, D. RNDr., Ph.D.[8]
Skoric, M., D.V.M.[9]
Rauser, P., D.V.M., Ph.D.[10]
Habib, N., M.D., Ph.D.[11]
Zonca, P., M.D., Ph.D., FRCS[1,3]

[1]Department of Surgery, University Hospital Ostrava, the Czech Republic
[2]Department of Cybernetics and Biomedical Engineering, Faculty of Electrical Engineering and Computer Science, VŠB–Technical University of Ostrava, the Czech Republic
[3]Department of Surgery, Medical Faculty, Ostrava University, the Czech Republic
[4]Department of Vice-President for Science and Research, University Hospital Ostrava, the Czech Republic
[5]CEITEC VFU, University of Veterinary and Pharmaceutical Sciences Brno, the Czech Republic
[6]Faculty of Mechanical Engineering VŠB–Technical University of Ostrava, the Czech Republic
[7]Institute of Pathology, Ostrava Medical Faculty and University Hospital Ostrava, the Czech Republic
[8]Department of Mathematical Methods in Economy, Faculty of Economics, VŠB–Technical University of Ostrava, the Czech Republic
[9]Department of Pathological Morphology and Parasitology, Faculty of Veterinary Medicine, University of Veterinary and Pharmaceutical Sciences Brno, the Czech Republic
[10]Department of Surgery and Orthopaedics, Small Animal Clinic, Faculty of Veterinary Medicine, University of Veterinary and Pharmaceutical Sciences Brno, the Czech Republic
[11]Liver and Pancreas Surgery, Hammersmith Hospital, Imperial College London, United Kingdom

*Coressponding author:
Vavra, P., M.D., Ph.D.
Phone: +420 737 550 050
E-mail: petrvavra@yahoo.co.uk

Abbreviations: AM: Amplitude Modification; CEITEC: Central European Institute of Technology; DaPZ: Dilatation and Proliferation of Bile Ducts; DisPZ: Dispersion Proliferation of Bile Ducts; IP: Institutional Substitution; KC: Lymphocytes Accumulation; KCT: Kaolin Test; MZ: Department of Health; PDS: Polydioxanon; PZ: Proliferation of Bile Ducts; RF: Radiofrequency; RFA: Radiofrequency Ablation; RONJA: Semi-spherical Bipolar Radiofrequency Device; TACR: Technological Agency of Czech Republic; TKX: Tiletamin–zolazepam; VSB–TUO: Technical University in Ostrava; ZC: Thickening of the Arteries.

Introduction

Radiofrequency (RF) energy is commonly used at present in the treatment of numerous medical disorders. Radiofrequency is high-frequency alternating electrical current which creates the desired clinical effect by passing through the tissue. As the current passes through, it heats the tissue around the active electrodes. Radiofrequency alternating electrical current has a frequency in the range from 300 KHz to 3 MHz (1, 2).

Radiofrequency energy has been used in medicine for more than a hundred years. First, French physicist D'Arsonval described the effects of alternating current at a frequency of 250 KHz on biological tissue in Paris in 1891 (3).

Primary and secondary liver tumours present a challenging problem in clinical oncology because of their very high morbidity and mortality. Patients with unresectable tumours (because of tumour extent or localization, inadequate hepatic reserve or high patient co-morbidity) may be candidates for local ablative techniques, chemoembolization, systemic or local chemotherapy (4-9). Of the available local ablative techniques, RF thermal ablation (RFA) has become the most frequently used and widespread (5). Multiple trials have evaluated RFA for the treatment of unresectable primary and secondary liver tumours and proved that RFA can control hepatic malignancies with few associated complications (4, 6-9).

In 1990, McGahan and Rossi, two independent authors, published experiments on animal models using radiofrequency currents for the ablation of primary and metastatic liver tumours. These experiments in animal models proved the safety and efficiency of percutaneous RFA (10, 11).

The role of RF energy in liver surgery has expanded in recent years from simple tumour ablation to its use in the technique of RF-assisted liver resection. In 2002, Habib's team used a specially modified bipolar RFA probe to manage a patient with gallbladder cancer who refused to have a blood transfusion (12). This method can be used in open or minimally invasive surgery. The pioneer in using RF energy for liver resection is Professor Nagy Habib, which is why it's also called Habib's resection surgery (13-21). The RF-assisted resection technique has been reported to be associated with minimal blood loss, low blood transfusion requirement, no need for intraoperative hepatic inflow occlusion techniques (such as Pringle's manoeuvre, dissection and clamping of the hepatic pedicle) and reasonable postoperative morbidity and mortality (16, 18-21). The most widely used instruments used for RF-assisted liver resection at present are the Habib™ 4X and Laparoscopic Habib™ 4X. Radiofrequency-induced coagulative necrosis offers very effective haemostasis and biliostasis of liver parenchyma (20, 22).

Based on data compiled by the National Center for Health Statistics between 1960 and 2004, the mortality rate due to liver cancer has been steadily increasing over the past two decades (23). Hepatic resection is currently the standard treatment for liver cancer. Radiofrequency energy in the form of RFA or RF-assisted resection has become one of the standard methods for the treatment of primary and secondary liver malignancies in the last 10-15 years.

The present study assessed the feasibility and safety of liver resection a new semi-spherical bipolar radiofrequency device (RONJA). The primary hypothesis of the study was to evaluate whether this new device (Figures 1 and 2) is able to consistently produce homogeneous and predictable areas of coagulation necrosis without the Pringle maneuver of vascular inflow occlusion. The secondary hypothesis of the study

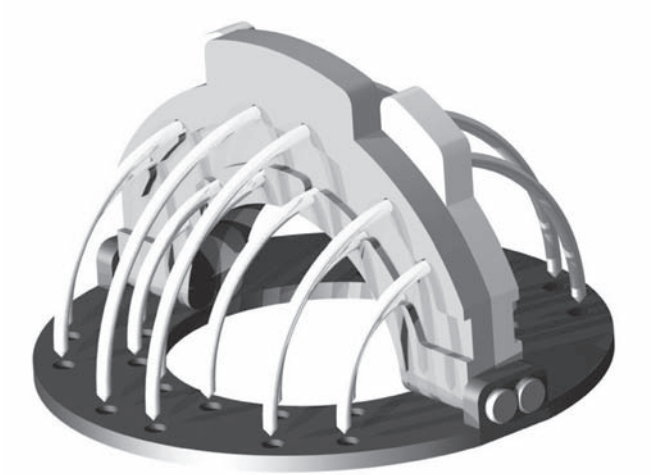

Figure 1: RONJA (semi-spherical bipolar radiofrequency device). Three dimensional model of new surgical device – view of the organization of electrode needles.

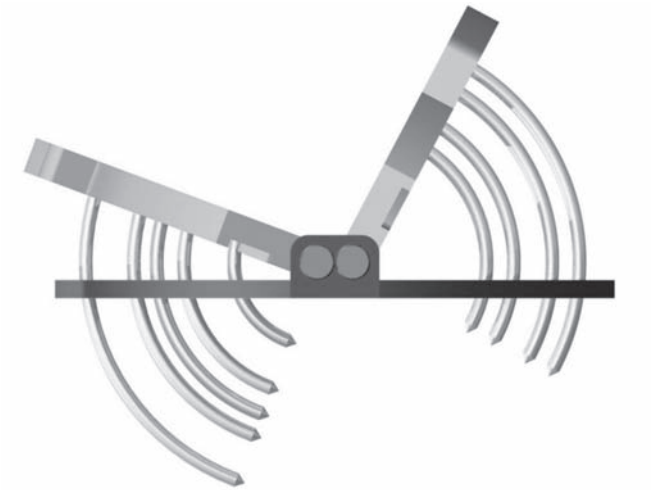

Figure 2: RONJA – Three dimensional model of new surgical device–the side view.

was to compare the standard linear radiofrequency device and a new semi-spherical bipolar device for liver ablation and resection in a hepatic porcine model. We aim to confirm that this new method is effective and safe.

New Device

Our new proposed surgical device is specific with his arrangement, where the tool is formed by annular base plates with holes for guiding the electrode needles and two wings attached to the electrode assemblies and two lead wires for each electrode wing (Figures 3 and 4). Electrode needles are arranged in a square array, which are located on both sides of the edges of a regular 16-square radius. The shape and length of the electrode needles must be such that, after introduction into the tissue it forms a spherical shape in this tissue. Bipolar electrode needles are driven electrode in each wing separately and between the inner and outer semi-circle, with one pole ablation tools consist of one semicircle of needles. It may also other combinations excitation electrode needles of wings so that it always been sufficiently coagulated tissue for subsequent incision performed by surgeon.

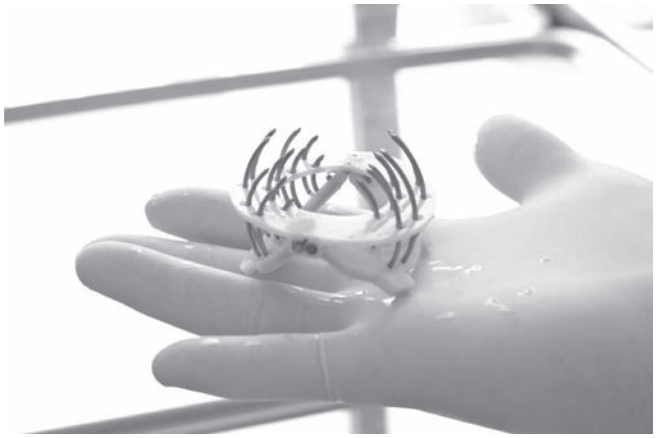

Figure 3: RONJA – prototype of radiofrequency surgery tool–upper side view.

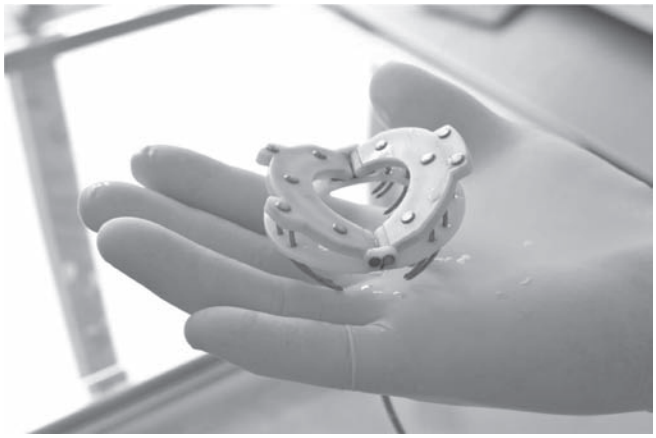

Figure 4: RONJA – prototype of radiofrequency surgery tool–top side view.

Materials and Methods

In vivo testing was conducted on a set of 12 pigs (*Sus scrofa domestica*) randomly divided into two groups of 6 pigs. The whole experiment was made up of three parts. Before each phase all animals were weighed and underwent blood sampling for haematological and biochemical tests. During the first part the animals in both groups underwent middle laparotomy and radiofrequency-assisted liver resection under general anaesthesia. Pigs in group A underwent liver resection using the new testing tool RONJA and in the control B group pigs were operated on with a commonly used surgical multiple needles tool for radiofrequency liver ablation. The second part of the study followed 14 days after intervention and was focused on control laparoscopy. In the last part, after 30 days after the operation, all the pigs were euthanized and samples were pathologically evaluated.

Pigs aged one year were provided by the Research Institute of Animal Production (Uhrineves, Department of Pig Breeding, Kostelec, address: Komenskeho 1240, 51741, the Czech Republic, accreditation number: 444/2011-MZE-17214, valid until April 6, 2016).

Our experimental project (no. 65/2012) was approved by the expert committee on animal welfare of the Veterinary and Pharmaceutical University Brno according to the law on the protection of animals against cruelty, as amended by §18, paragraph 6b), Act No. 246/1992 Coll. Then our experiment was approved by the Ministry of Education, Youth and Sport of the Czech Republic and was granted permission to carry out the experiment on September 7, 2012.

Phases of Testing

All phases of this experiment took place in the research operating theatre of the Faculty of Veterinary medicine of the Veterinary and Pharmaceutical University Brno. All surgical terms were performed in aseptic conditions according to a predetermined schedule and protocol. The surgical team was formed of pairs of surgeons from the surgical department of the University Hospital Ostrava as well as veterinary surgeons from the Veterinary and Pharmaceutical University Brno.

The First Phase

The surgical field and its surroundings were shaved before each surgical performance. The surgical field was made antiseptic by washing with iodopovidon (Betadine soap, Egis Pharmaceutical, Hungary, Europe), and chorhexidine (Nolvasan, Cymedica s.r.o., the Czech Republic, Europe)

was applied to the surgical field. Anaesthesia was induced by intravenously given propofol (Norofol, Norbrook Lab. Ltd., North Ireland) (0.5-1 mg/kg) then anaesthesia was maintained by constant rate infusion of propofol (0.1 mg/kg/min). During the operation hartmann solution (B. Braun, Germany) (10 ml/kg/h) was served to animals intravenously through a cannulated auricular vein. The operating field was protected by a drape, a single Foliodrape system for laparotomy–HARTMAN. Instrumentation AESCULAP B. Braun Medical was used to performing laparotomy. After preparing the surgical field it was penetrated into the abdominal cavity through upper middle laparotomy in the position of the animal on his back. Monopolar electrocoagulation electrosurgery EMED ES 350 with an output of 255 W was used to this performance. Laparotomy retractor was applied and surgeons performed the revision of the abdominal cavity 3.

Resection Procedure

For each animal two liver resections were always executed–one from the right lateral lobe and one resection of the left lateral liver lobe. All resections were performed in thinner part of the liver. A commonly used device was employed as the radiofrequency power generator. Liver resection was always executed in the following mode–after mobilization of the liver lobe, first it was planned by a resection line marked on the liver surface using electrocoagulation. The semi-spherical device was applied on the liver parenchyma afterwards. We have implemented the first wing of the RF device and have proceeded by inserting the second wing, which together created a spherical pattern in liver parenchyma. The time measurement of ablation was associated with supply of radiofrequency energy.

The liver resection was carried out by radiofrequency-assisted resection technique without liver blood flow occlusion (Figure 5). The main principle of this technique (radiofrequency ablation) is coagulation in the liver resection margin estimated using radiofrequency instruments with subsequent liver transection using a scalpel or surgical scissors (Figures 6 and 7). Possibly bleeding from the resection line was treated with the radiofrequency instrument or electrocoagulation. Resected samples were fixed in 10% formalin solution, so that they could later be histopathologically examined for depth of necrosis of liver parenchyma. After checking and drying of the surgical field, the entire abdominal laparotomy was closed in layers–peritoneum and fascia technique "en masse" with 0 PDS continuous monofilament suture, subcutaneous tissue vicryls individual sutures and skin with non-absorbable monofilament fiber Ethilon 2/0

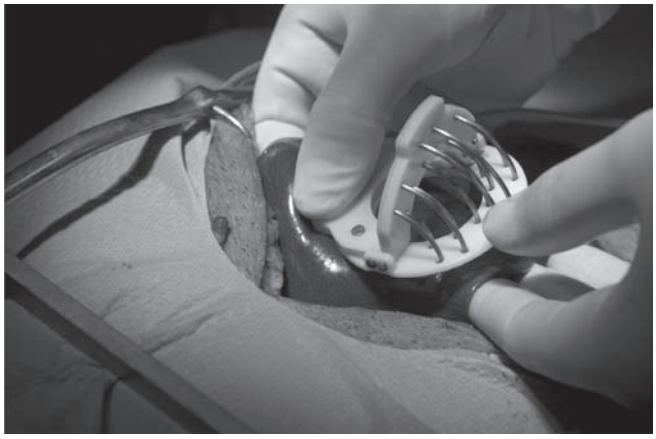

Figure 5: *In vivo* study – functional prototype – example of application on pig's liver.

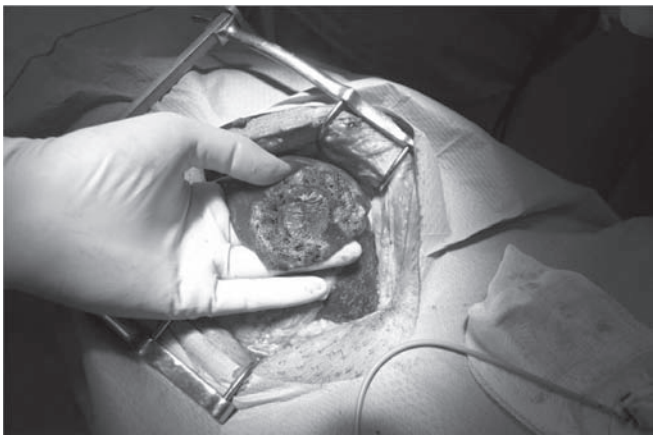

Figure 6: *In vivo* study – view on liver tissue after radiofrequency coagulation with new surgical semi-spherical device.

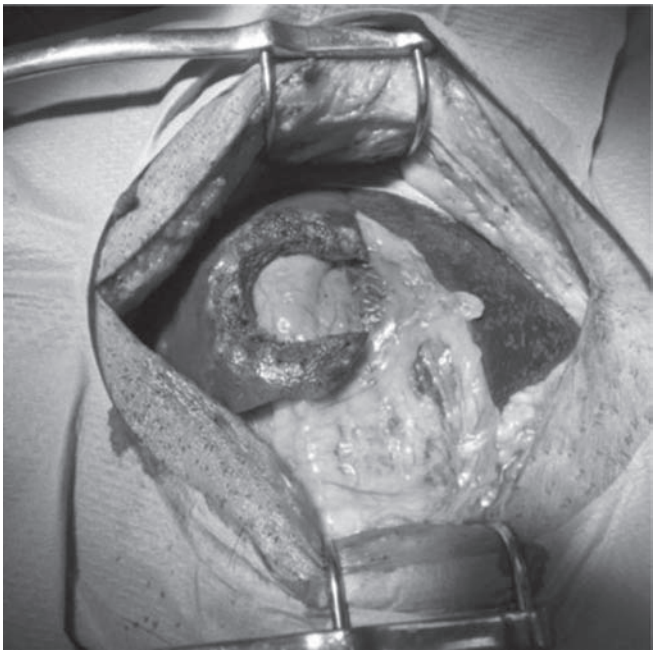

Figure 7: *In vivo* study – view in operation field and condition of liver tissue after excision.

(Ethicon–Johnson & Johnson company, USA). Special antiseptic spray–Silver Aluminium Aerosol–bandage protection against contamination (Henry Schein, Inc., Germany) was applied on the surgical wound. Subsequently, the animals, under the control of the veterinary anaesthesiologist, were escorted from general anaesthesia and housed in standard breeding boxes with conventional terms and were also placed under veterinary supervision. Postoperatively, the animals were given intramuscularly amoxicillin (Betamox, Norbrook, Northern Ireland) (15 mg/kg) and meloxicam (Metacam, Boehringer Ingelheim, Germany) (0.4 mg/kg).

During the liver resection surgery of each animal the value of the total operating time and ablation time of lobes were measured and compared in both groups.

The Second Phase

Fourteen days after liver resection the second phase was executed. The main aim of the second phase of this experimental study was to determine the status of healing or postoperative complications in the abdominal cavity of each animal. For this purpose, a diagnostic laparoscopy of each pig was performed to assess the postoperative findings. AESCULAP (B. Braun Medical, s.r.o., the Czech Republic) laparoscopy instrumentation was used for surgery–humane version of the endoscopic video unit TELE PACK X and laparoscopic optic HOPKINS with an outer diameter of 5 mm and a length of 290 mm (KARL STORZ Endoscopy, Germany) insufflations device Smith & Nephew, laparoscopic set with Veres FlexTray needle and trocars, harmonic scalpel, harmonic pliers HARMONIC ACE (Ethicon Endo-Surgery, LLC and Johnson & Johnson company, USA). Overall, 12 diagnostic laparoscopies were performed. As expected, many adhesions were found in the abdominal cavity between resected part of liver and omentum, or abdominal wall, respectively.

There were no liver abscesses, biliary leak, subhepatic abscess, hematoma or signs of peritonitis in any animal of both groups.

The Third Phase

The last part of the testing was performed 30 days after the first operation. In this phase of our experimental study, autopsies of the 12 pigs were performed by a veterinary pathologist from the Institute of Pathological Morphology and Parasitology of the Veterinary and Pharmaceutical University Brno in the presence of a pathologist from the University Hospital Ostrava. Slaughtering was done by the protocol, *lege artis*. The animal carcasses were disposed of through a rendering service.

Nutritional status of the animals were described as good to very good according to body weight, clinical veterinary status and examination of blood sampling. In the *linea alba* they had a well healed suture without secretion. Only one pig, which had been injured in the transverse colon in the second phase, had in the subcutaneous space an abscess without caving into the abdominal cavity.

All animals were opened in the abdominal cavity then in the thoracic cavity, and then followed removal of the organs. In the abdominal cavity fibrous synechia was detected in parts of the resected liver lobes with peritoneum, some adhesions were found between the liver lobes and stomach, omentum or loops of jejunum. Resection margins in the liver lobes were mostly covered with fibrous tissue at the adhesions. Four female pigs had in their abdominal cavity a less serous effusion. The thoracic cavity in four pigs was without adhesions and effusions. The lungs of five pigs had pathological findings consisting of atelectatic bearings – acute inflammatory or chronic bronchopneumonia. Fibrinoid purulent pericardial effusion was observed in one of these pigs. Samples of the right and left hepatic lobe were collected in all pigs for histological examination. The tissue was fixed in 10% formalin solution.

For comparison and statistical evaluation data were collected including results of blood samples, the values recorded during surgery and postoperatively and also the histopathological evaluation. Throughout the experiment the weight of individual animals was recorded. Examination of blood sampling was carried out at the Department of Haematology at the Clinic of Immunology and cytology laboratories for small animals at the Veterinary and Pharmaceutical University Brno.

Results

The overall blood analysis showed no marked differences in the observed values before resection, on the 14th day after surgery or the 30th day.

The average total operating time (time from start of operation–intubation until the last stitch) in the groups of pigs operated on with the newly designed instrument, was 57.5 min, in contrast to the control group, where the average time was 69 min. Average ablation time (time was measured from the first burning liver resection until removal) was as follows: left lobe ablation time for the testing group was 8.83 min, 7.33 min right lobe. Left lobe ablation time in control group B was 11.67 min and the right lobe ablation time was 8.5 min. As seen from the average time the tested instrument RONJA has shorten ablation time in left lobe 2.84 min and 1.17 min in right lobe than generally using device. With newly designed instrument was also shorten operating time 11.5 min than with using standard device (see Table I). Statistical analysis using the median test (p-value was computed

Table I
Obtained data.

Rank	ID	Group	Weight 4.10 (kg)	Total operating time (min)	Ablation time of left lobe (min)	Ablation time of right lobe (min)	Supplied power (W)	Weight 18.10 (kg)	Total laparoscopy time (min)	Actual time of laparoscopy (min)	Weight	Total weight increment compared to original state 4.10 (kg)	Liver weight 5.11 (kg)
1	189	B	65	80	20	11	90	65	46	28	69	4	1.7
2	196	B	44	74	13	7	90	47.5	26	14	51	7	1.45
3	195	B	44	83	12	11	90	42	21	14	46.6	2.6	1.15
4	225	B	51	81	10	9	90	48	32	20	61	10	1.5
10	216	B	44	47	11	7	90	51	15	4	–	–	–
11	161	B	57	49	4	6	90	64	12	3	66.5	9.5	1.9
Av.			**50.83**	**69**	**11.67**	**8.5**	**90**	**52.92**	**25.33**	**13.83**	**58.82**	**6.62**	**1.54**
5	200	A	34	68	14	7	90	39	21	9	41	7	1.3
6	167	A	58	71	11	11	80	64	19	10	64.8	6.8	1.9
7	232	A	46	53	8	8	80	49	48	5	50.75	4.75	1.4
8	193	A	65	46	7	6	80	62	25	5	71.5	6.5	1.6
9	177	A	53	53	7	5	80	53	32	4	55	2	1.1
12	191	A	62	54	6	7	80	64	18	3	69.95	7.95	1.55
Av.			**53**	**57.5**	**8.83**	**7.33**	**82**	**55.17**	**27.17**	**6**	**58.83**	**5.83**	**1.48**

by Fisher's exact test) failed to demonstrate any significant differences between the two groups.

Blood losses during the liver resections were less than 20 ml.

The power delivery of the radiofrequency energy generator was optimized during the surgical procedure. To gain more effective coagulation of liver tissue using new device the supply power was reduced to 80 W compared with the standard used device with the need to output of 90 W. In the postoperative period all animals had a weight gain. In the tested group A the weight gain was on average 5.83 kg and in the control group B 6.62 kg (Table I).

Complications

During the liver ablation only one complication occurred. A spleen was deserozated in a pig in the tested group A. In this animal serous effusion of 250 ml was observed during pathomorphological evaluation.

The control laparoscopy showed postoperative adhesions in all 12 animals. No serious postoperative complications occurred. Only one adverse event appeared during an inspection laparoscopy. Transverse colon of one pig in experimental A group was injured when establishing capnoperitoneum. It was treated with a suture thread of monofilamentosis PDS 3/0 PDS and 4/0 (Ethicon Endo-Surgery, LLC and Johnson & Johnson company, USA).

The death of one pig in the control B group occurred in the postoperative period after laparoscopy performance. An autopsy was executed by a veterinarian from the Institute of Pathological Morphology and the Parasitology Faculty of Veterinary Medicine and an acute catarrhal-purulent bronchopneumonia, tonsillitis and rhinitis were detected.

The cause of death was determined as animal circulatory failure due to respiratory insufficiency in the postoperative period in connection with probable mycoplasmal infections. The abdominal cavity after surgery was examined without pathological findings. Resected samples of the liver were loaded into 10% formalin solution and secured for further histological examination.

Histopathology

Histopathological evaluation was performed by pathologists from the Institute of Pathological Anatomy of the University Hospital Ostrava. Examination of thermal changes at the resection margin showed strong thermal alteration in both groups (Figure 8). The depth of thermal damage from the resection margin of resected samples exceeded 10 mm in all cases, with a median of 14 mm damage in the group of the newly designed instrument. The results are shown in Table II. With this method in areas without significant thermal alteration congested liver tissue dominates. In this tissue coagulated blood was rarely present in the central vein and also occasionally along the wall thermal alteration of the bile ducts, in one case with mild inflammatory cellulization.

The thermal alteration in samples of the control group B was mostly up to 10 mm. Similarly, thermal alteration of the bile duct was up to 10 mm, in only one case was thermal

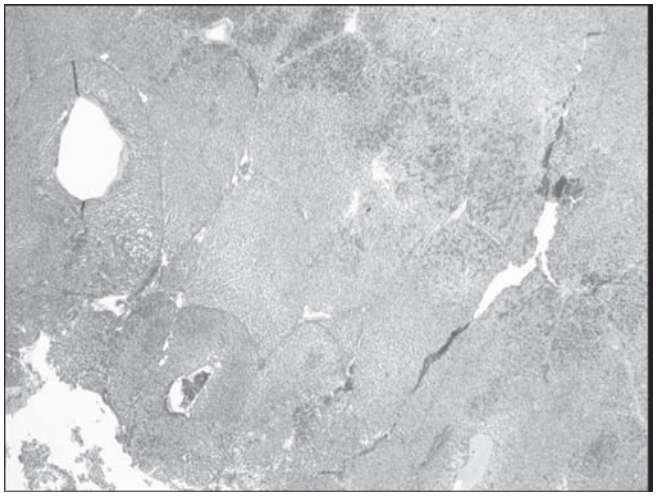

Figure 8: Microscopic section of liver biopsy, blood congestion bordered thermal alteration of liver tissue. Stained in Hematoxylin and eosin.

Table II
Maximum depth of thermal alteration from excised liver tissue.

RONJA device, sample no.	Lobe 1 = dx, 2 = sin	Weight of resected particle (g)	Size of resected particle (cm)	Maximum depth of thermal alteration (cm)
5/ V 200	1	16.1	7.0×4.0×1.6	1.3
	2	12.9	3.7×4.2×1.5	1.7
6/V 167	1	19.4	4.3×4.3×2.2	1.4
	2	16.7	5.8×4.2×1.7	1.4
7/V 232	1	25.7	8.0×4.0×1.9	1.5
	2	18.5	6.5×4.0×1.7	1.4
8/V 193	1	9.2	5.5×4.0×1.4	1.4
	2	12.5	2.8×4.0×2.2	1.5
9/V 177	1	12.7	5.0×4.0×1.6	1.7
	2	15.6	5.3×4.0×1.9	1.5
12/V 191	1	8.9	4.0×4.0×1.9	1.2
	2	12.3	4.3×5.0×2.2	1.2
Standard device, sample no.	**Lobe 1 = dx, 2 = sin**	**Weight of resected particle (g)**	**Size of resected particle (cm)**	**Maximum depth of thermal alteration (cm)**
1/V 189	1	4.8	4.5×2.5×1.0	Up to 1
	2	10.7	4.0×4.0×1.3	1.2
2/V 196	1	7	4.5×3.0×1.7	1.5
	2	10.6	5.0×3.7×1.5	1
3/V 195	1	12.6	7.0×3.3×1.7	Up to 1
	2	15.5	5.0×4.0×1.9	1.3
4/V 225	1	12.5	6.0×4.3×1.5	Up to 1
	2	11.9	4.0×4.8×1.6	1
10/V 216	1	8.2	6.0×2.8×1.4	Up to 1
	2	6.9	4.4×3.5×1.3	Up to 1
11/V 161	1	12.2	6.5×3.5×2.5	Up to1
	2	14.9	6.0×4.0×1.6	Up to 1

alteration of bile ducts in intact tissue observed. In preserved liver tissue significant congestion and periductal round cell infiltration was detected. To summarize, the depth of the thermal alteration was on average 4 mm larger in the cases of the newly tested instrument, dispersion of values was 12-17 mm. In the method of the control group the thermal alteration was up to 10 mm, also in intact tissue congestion, but to a lesser degree, and mild round cell cellulization periductal and perivasal. The autopsy material from the tested A group was formed by the depth of necrosis with a median of 14 mm and 13.5 mm. Furthermore we encountered a proliferation of bile ducts and vascular thickening in healthy hepatic tissue. The results are shown in Tables III and IV. In samples of the control B group disability necrosis was confirmed with a median depth of 13 mm and 14 mm in healthy tissue and also expansion and proliferation of bile ducts. Statistical analysis using the median test (p-value was computed by Fisher's exact test) did not show any significant differences between the groups (Table III).

Statistical Analysis

Data are presented as mean ± standard error of mean (S.E.M.) and median for continuous variables and as counts and

Table III
Material processing – autopsy samples – RONJA device. In all samples, fibrosis around necrosis, hyperaemia of healthy liver tissue, deposits of iron and KCT (kaolin test) responses around necrosis were confirmed.

	Maximum depth of necrosis from resection line (mm)		
Sample no.	Piece of right lobe	Piece of left lobe	Other
1	20	9	DisPZ
2	15	9	PZ
3	12	14	DaPZ
4	8	14	DaPZ
10	13	14	PZ, KC
11	13	22	PZ
Σ	13	14	–
Ø	11.8	13.6	–

Table IV
Material processing – autopsy samples – standard device. In all samples, fibrosis around necrosis, hyperaemia of healthy liver tissue, deposits of iron and KCT responses around necrosis were confirmed.

	Maximum depth of necrosis from resection line (mm)		
Sample no.	Piece of right lobe	Piece of left lobe	Other
5	15	14	ZC, PZ
6	13	11	ZC, PZ
7	10	13	ZC, PZ
8	11	18	ZC, PZ
9	15	13	ZC, PZ, KC
12	25	15	ZC, PZ
Σ	14	13.5	–
Ø	14.8	14	–

Table V
Operating data.

	Standard device	RONJA	
	mean ± S.E.M. (median)	mean ± S.E.M. (median)	*p*-value
Weight 1 (kg)	50.83 ± 3.55 (47.50)	53.00 ± 4.69 (55.50)	0.567
Total operating time (min)	69.00 ± 6.76 (77.00)	57.50 ± 3.99 (53.50)	0.567
Ablation time of left lobe (min)	11.67 ± 2.11 (11.50)	8.83 ± 1.25 (7.50)	0.567
Ablation time of right lobe (min)	8.50 ± 0.89 (8.00)	7.33 ± 0.84 (7.00)	1
Supplied power (W)	90.00 (unchanging)	81.67 ± 1.67 (80.00)	0.005*
Weight 2 (kg)	52.92 ± 3.85 (49.50)	55.17 ± 4.11 (57.50)	0.567
Laparoscopic total time (min)	25.33 ± 5.08 (23.50)	27.17 ± 4.66 (23.00)	1
Actual time of laparoscopy (min)	13.83 ± 3.89 (14.00)	6.00 ± 1.16 (5.00)	0.567
Weight 3 (kg)	58.82 ± 4.35 (61.00)	58.83 ± 4.89 (59.90)	1
Total weight increment (kg)	6.62 ± 1.46 (7.00)	5.83 ± 0.88 (6.65)	0.567
Liver weight (kg)	1.54 ± 0.13 (1.50)	1.48 ± 0.11 (1.48)	1

*There was a significant difference ($p = 0.005$) in supplied power between the groups.

percentages for categorical variables (complications). Data between the standard device group and RONJA group were compared using the median test for continuous variables and Fisher's exact test for categorical variables. Statistical analyses were performed with IBM SPSS software version 18.0. A two-sided value of $p < 0.05$ was considered statistically significant for all analyses (Tables V-VII).

The statistical analysis definitely showed that there were not any differences between tested group A and standard group B. Thus, after statistical confirmation we can claim that we have suggested a new liver ablation device for resectable tumours in liver tissue which is comparable as far as its parameters with the standard device. In detected data we can see, that ablation and operation time was shorter with new device RONJA unlike the standard using device, but because there were small number of pigs in our experiment file, it was not confirmed by statistical analysis.

Table VI
Data concerning complications. There was no significant differences between the groups.

	Standard device (*n*) (%)	RONJA (*n*) (%)	*p*-value
Complications during surgery	0 (0)	1 (16.7)	1
Post-operative complications	1 (16.7)	0 (0)	1
Complications during laparoscopy	0 (0)	4 (66.7)	0.061
Post-operative adhesions (liver)	6 (100)	6 (100)	–
Post-operative adhesions (spleen)	2 (33.3)	2 (33.3)	1
Pathological findings – ascites	1 (16.7)	2 (33.3)	1
Pathological findings – abscess	0 (0)	1 (16.7)	1
Pathological findings in lungs	4 (66.7)	2 (33.3)	0.567

Table VII
Data concerning histopathological findings of thermal alteration. There was no significant differences between the groups.

	Standard device	RONJA	
	mean ± S.E.M. (median)	mean ± S.E.M. (median)	*p*-value
Thermal alteration at the resection margin (%) – right lobe	98.33 ± 1.67 (100.00)	98.33 ± 1.67 (100.00)	–
Thermal alteration at the resection margin (%) – left lobe	100.00 (unchanging)	95.00 ± 3.42 (100.00)	–
Maximum depth of necrosis (mm) – right lobe	13.00 ± 1.61 (13.00)	14.83 ± 2.20 (14.00)	1.00
Maximum depth of necrosis (mm) – left lobe	13.67 ± 1.94 (14.00)	14.00 ± 0.97 (13.50)	1.00
Weight of resected particle (g) – right lobe	9.55 ± 1.37 (10.20)	15.33 ± 2.65 (14.40)	0.567
Weight of resected particle (g) – left lobe	11.75 ± 1.29 (11.30)	14.75 ± 1.05 (14.25)	0.567
Maximum depth of thermal alteration (cm) – right lobe	1.08 ± 0.08 (1.00)	1.42 ± 0.07 (1.40)	0.08
Maximum depth of thermal alteration (cm) – left lobe	1.08 ± 0.05 (1.00)	1.45 ± 0.07 (1.45)	0.08

Discussion

This experimental study proved the feasibility and safety of the newly developed semi-spherical bipolar device for liver ablation and resection. No statistically significant differences were observed between the new tested device compared to the generally used device. The overall blood analysis showed no marked differences in the observed values before resection, on the 14th day after surgery or the 30th day. By our point of view, the ablation and operating time was shorter when using the RONJA device but the difference was not statistically significant. The reason may be due to the low number of

pigs used in the study. A spherical area of coagulated necrosis was produced in all livers that marked the line for surgical resection of liver parenchyma.

Many authors have used a porcine model in feasibility and safety studies of devices for radiofrequency ablation. Varadarajulu *et al.* (2009) performed RFA of pig liver using the retractable umbrella-shaped electrode array with effective coagulation necrosis of large areas (24). Burdío *et al.* (2008) compared a new radiofrequency (RF)-assisted device specifically designed for tissue thermocoagulation and division of the liver with a state-of-the-art saline-linked device. The tested RF-assisted device was shown to address parenchymal division and hemostasis simultaneously, with lower blood loss and faster transection time than saline-linked technology in that pig model (25). Solazzo *et al.* (2007) used a porcine model with the aim of prospectively maximizing the extent of created tissue coagulation by using a high-power (1000 W, 4000 mA) RF generator to optimize pulsing algorithms (26).

We have found out that the advantage of our new designed tool is in shortening operating time as well as saving healthy liver parenchyma in comparison with commonly used multiple needles linear devices. This linear device has four long needles ordered to form a rectangle, which destroys tissue in depth. The semi-spherical conformation of the device allows removal of necessary liver tissue only apart from common used linear tools. Time shortening is the consequence of reducing number of steps of coagulation, because new designed device coagulates in both wings. It means that if the deposit is up to 20 mm, there are only a few steps necessary to coagulate the whole deposit apart from the linear device. This device was designed to be compatible with generally used power generators, so it does not increase the need of additional technical equipment. We should also mention disadvantages, in comparison with commonly used linear tools, arising from the specific layout of needles. The device is designated only for the surface and subsurface liver tumours or metastases with the size up to 20 mm, which limits practical application.

Conclusion

We have developed a new semi-spherical bipolar radiofrequency device that adequately coagulates the hepatic resection plane in a porcine model. Our prototype system was able to coagulate the semi-spherical contour of liver parenchyma in the thinner part with successful coagulation of all blood vessels. This device shows promise in the effort to reduce healthy tissue liver parenchyma resection during liver surgery in a porcine model. Performing resection of liver parenchyma using the new semi-spherical device we confirmed this new method is effective and safe.

Future animal and clinical studies will need to evaluate semi-spherical liver RF resection with respect to the local recurrence of hepatic tumours.

Practical Application

The method described in this study could be used in open liver surgery without inflow occlusion for the treatment of small liver malignancies in a single application with the aim to save normal liver parenchyma. Further experimental studies are needed to confirm these results before clinical application of the method in the treatment of human liver malignancies.

Conflict of Interest

The authors report no conflicts of interest in this *in vivo* study.

Acknowledgements

This work was supported by IP MZ CR 1 RVO-FNOs/2012, IP MZ CR c.2 RVO-FNOs/2013, SGS VSB-TUO Grant No. SP2013/116 and by the project "CEITEC–Central European Institute of Technology" (CZ.1.05/1.1.00/02.0068) from European Regional Development Fund. The work and the contributions were supported by the project SP2013/35 "Biomedical engineering systems IX" and TACR TA01010632 "SCADA system for control and measurement of process in real time". The paper has been elaborated in the framework of the IT4 Innovations Centre of Excellence project, reg. no. CZ.1.05/1.1.00/02.0070 supported by Operational Programme 'Research and Development for Innovations' funded by Structural Funds of the European Union and state budget of the Czech Republic.

References

1. Pearce, J. A. Electrosurgery. New York: John Wiley (1986).
2. Pearce, J. A. Electrosurgical Unit. In: Encyclopedia of Medical Devices and Instrumentation, Webster, J. G. (Ed.), 2nd Edition, New York, NY: John Wiley, pp. 156-177 (2006).
3. D'Arsonval, M. A. Action physiologique des courants alternatifs. *C R Soc Biol 43*, 283-286 (1891).
4. Lencioni, R., Cioni, D. Percutaneous Methods for Ablation of Hepatic Neoplasms. In: Surgery of the Liver, Biliary Tract, and Pancreas, Blumgart, L. H. (Ed.), 4th Edition, Philadelphia, PA: Saunders, pp. 1269-1277 (2007).
5. Friedman, M., Mikityansky, I., Kam, A., Libutti, S. K., Walther, M. M., Neeman, Z., Locklin, J. K., Wood, B. J. Radiofrequency ablation of cancer. *Cardiovasc Intervent Radiol 27*, 427-434 (2004). DOI: 10.1007/s00270-004-0062-0
6. Pereira, P. L. Actual role of radiofrequency ablation of liver metastases. *Eur Radiol 17*, 2062-2070 (2007). DOI: 10.1007/s00330-007-0587-0
7. Hao, C. Y., Ji, J. F. Surgical treatment of liver metastases of colorectal cancer: stragegies and controversies. *Eur J Surg Oncol 32*, 473-483 (2006). DOI: 10.1016/j.ejso.2006.02.016
8. Lencioni, R., Crocetti, L., Cioni, D., Della Pina, C., Bartolozzi, C. Percutaneous radiofrequency ablation of hepatic colorectal

metastases: technique, indications, results, and new promises. *Invest Radiol39*,689-697(2004).DOI:10.1097/00004424-200411000-00007
9. Strasberg, S. M., Linehan, D. Radiofrequency ablation of liver tumors. *Curr Prob Surg 40*, 451-498 (2003). DOI: 10.1016/S0011-3840(03)00050-9
10. Rossi, S., Fornari, F., Pathies, C., Buscarini, L. Thermal lesions induced by 480 KHz localized current field in guinea pig and pig liver. *Tumori 76*, 54-57 (1990).
11. McGahan, J. P., Browning, P. D., Brock, J. M., Tesluk, H. Hepatic ablation using radiofrequency electrocautery. *Invest Radiol 25*, 267-270 (1990). DOI: 10.1097/00004424-199003000-00011
12. Navarra, G., Jiao, J. C., Weber, J. P., Nicholls, J. P., Jensen, S. L., Habib, N. A. A novel approach to gallbladder cancer in a Jehovah's Witness. *Surg Endosc 16*, 1109-1110 (2002). DOI: 10.1007/s00464-001-4245-3
13. Ayav, B. P., Habib, N. A., Pellicci, R., Tierris, J., Milicevic, M., Jiao, L. R. Impact of radiofrequency assisted hepatectomy for reduction of transfusion requirements. *Am J Surg 193*, 143-148 (2007). DOI: 10.1016/j.amjsurg.2006.04.008
14. Weber, J. C., Navarra, G., Jiao, L. R., Nicholls, J. P., Jensen, S. L., Habib, N. A. New technique for liver resection using heat coagulative necrosis. *Ann Surg 236*, 560-563 (2002). DOI: 10.1097/01.SLA.0000032952.65498.C2
15. Milicevic, M., Bulajic, P., Zuvela, M., Dervenic, C., Basaric, D., Galun, D. A radiofrequency-assisted minimal blood loss liver parenchyma dissection technique. *Dig Surg 24*, 306-313 (2007). DOI: 10.1159/000103663
16. Pai, M., Jiao, L. R., Khorsandi, S., Canelo, R., Spalding, D., Habib, N. A. Liver resection with bipolar radiofrequency device: Habib™ 4x. *HPB (Oxford) 10*, 256-260 (2008). DOI: 10.1080/13651820802167136
17. Yao, P., Morris, D. L. Radiofrequency ablation-assisted liver resection: review of the literature and our experience. *HPB (Oxford) 8*, 248-254 (2006). DOI: 10.1080/13651820600703272
18. Vavra, P., Ihnat, P., Vavrova, M., Martinek, L., Dostalik, J., Habib, N. Hand-assisted laparoscopic liver resection using Habib's technique: early experience. *Wideochir Inne Tech Malo Inwazyjne 7*, 8-12 (2012). DOI: 10.5114/wiitm.2011.25739
19. Ihnat, P., Vavra, P., Rudinska, L., Ostruszka, P., Dostalik, J. Radiofrequency-assisted liver resection: short-term results in a single institution. *Bratisl Lek Listy 114*, 19-22 (2013). DOI: 10.4149/BLL_2013_005
20. Ayav, B. P., Jiao, L., Dickinson, R., Nicholls, J., Milicevic, M., Pellicci, R., Bachellier, P., Habib, N. A. Liver resection with a new multiprobe bipolar radiofrequency device. *Arch Surg 43*, 396-401 (2008). DOI: 10.1001/archsurg.143.4.396
21. Vavra, P., El Gendi, A., Papaevangelou, A., Vavrova, M., Martinek, L., Ihnat, P., Dostalik, J. New treatment approach in liver metastases: hand-assisted laparoscopic radiofrequency liver resection. *Rozhl Chir 86*, 554-557 (2007).
22. Pai, M., Frampton, A. E., Mikhail, S., Resende, V., Kornasiewicz, O., Spalding, D. R., Jiao, L. R., Habib, N. A. Radiofrequency assisted liver resection: analysis of 604 consecutive cases. *EJSO 38*, 274-280 (2012). DOI: 10.1016/j.ejso.2011.12.006
23. Jemal, A., Siegel, R., Ward, E., Hao, Y., Xu, J., Murray, T., Thun, M. J. Cancer statistics, 2008. *Ca Cancer J Clin 58*, 71-96 (2008). DOI: 10.3322/CA.2007.0010
24. Varadarajulu, S., Jhala, N. C., Drelichman, E. R. EUS-guided radiofrequency ablation with a prototype electrode array system in an animal model (with video). *Gastrointest Endosc 70*, 372-376 (2009). DOI: 10.1016/j.gie.2009.03.008
25. Burdío, F., Navarro, A., Berjano, E., Sousa, R., Burdío, J. M., Güemes, A., Subiró, J., Gonzalez, A., Cruz, I., Castiella, T., Tejero, E., Lozano, R., Grande, L., de Gregorio, M. A. A radiofrequency-assisted device for bloodless rapid transection of the liver: a comparative study in a pig liver model. *Eur J Surg Oncol 34*, 599-605 (2008). DOI: 10.1016/j.ejso.2007.05.008
26. Solazzo, S. A., Ahmed, M., Liu, Z., Hines-Peralta, A. U., Goldberg, S. N. High-power generator for radiofrequency ablation: larger electrodes and pulsing algorithms in bovine ex vivo and porcine in vivo settings. *Radiology 242*, 743-750 (2007). DOI: 10.1148/radiol.2423052039

Received: October 8, 2013; Revised: January 25, 2014;
Accepted: February 26, 2014

17. Micro- and nanosized particles in nasal mucosa: a pilot study

Čábalová L, Čabanová K, Bielniková H, Kukutschová J, Dvořáčková J, Dědková K, Zeleník K, Komínek P

Originally published in BioMed Research International, [online], 2015, vol. 2015, no. Article ID 505986, p. 1-6.

Hindawi Publishing Corporation
BioMed Research International
Volume 2015, Article ID 505986, 6 pages
http://dx.doi.org/10.1155/2015/505986

Clinical Study

Micro- and Nanosized Particles in Nasal Mucosa: A Pilot Study

Lenka Čábalová,[1,2,3] Kristina Čabanová,[4] Hana Bielniková,[5] Jana Kukutschová,[4] Jana Dvořáčková,[3,5] Kateřina Dědková,[4] Karol Zeleník,[1,3] and Pavel Komínek[1,3]

[1]*Department of Otorhinolaryngology, Head and Neck Surgery, University Hospital Ostrava, 17. Listopadu 1790, 708 52 Ostrava, Czech Republic*
[2]*Centre of Endoscopic Skull Base Surgery, University Hospital Ostrava, 17. Listopadu 1790, 708 52 Ostrava, Czech Republic*
[3]*Faculty of Medicine, University of Ostrava, Syllabova 19, 703 00 Ostrava, Czech Republic*
[4]*Nanotechnology Centre, VŠB-Technical University of Ostrava, 17. Listopadu 15/2172, 708 33 Ostrava, Czech Republic*
[5]*Institute of Pathology, University Hospital Ostrava, 17. Listopadu 1790, 708 52 Ostrava, Czech Republic*

Correspondence should be addressed to Karol Zeleník; karol.zelenik@fno.cz

Received 27 October 2014; Revised 17 December 2014; Accepted 31 December 2014

Academic Editor: Il Je Yu

Objective. The aim of this prospective study is to evaluate presence and quantity of micro- and nanosized particles (NPs) and interindividual differences in their distribution and composition in nasal mucosa. *Methods*. Six samples of nasal mucosa obtained by mucotomy from patients with chronic hypertrophic rhinosinusitis were examined. Samples divided into 4 parts according to the distance from the nostrils were analyzed by scanning electron microscopy and Raman microspectroscopy to detect solid particles and characterize their morphology and composition. A novel method of quantification of the particles was designed and used to evaluate interindividual differences in distribution of the particles. The findings were compared with patients' employment history. *Results*. In all the samples, NPs of different elemental composition were found (iron, barium, copper, titanium, etc.), predominantly in the parts most distant from nostrils, in various depths from the surface of the mucosa and interindividual differences in their quantity and composition were found, possibly in relation to professional exposition. *Conclusions*. This study has proven the possibility of quantification of distribution of micro- and nanosized particles in tissue samples and that the NPs may deposit in deeper layers of mucosa and their elemental composition may be related to professional exposition to the sources of NPs.

1. Introduction

Nanosized particles (NPs), having submicron size from 10 nm to several hundred nanometers, are ubiquitous in environment [1]. They are composed of carbon (e.g., soot) or metal oxides (iron, chrome, nickel, aluminium, copper, zinc, titanium, etc.) and they are mostly antropogenous (fossil fuel combustion, smoking, welding, road traffic, etc.) [2]. Due to their very small size, they possess different properties from the microparticles of the same material (chemical and physical reactivity and interaction with living cells and organisms) [1].

The main routes of entrance of the NPs into the organism, aside from skin and digestive tract, are airways and lungs. They penetrate tissues, redistribute in organism, accumulate in organs, and induce pathological changes in tissues, while their lysosomal degradation in cells is limited [1, 3]. They induce oxidative stress in cells and, thus, changes in their organelles and genetic information and can also enter the cell nucleus and interact with DNA directly [1, 3–9].

So far, the studies have proven pathological effect of NPs on living cells in vitro or in lungs and digestive tract of rodents in terms of induction of acute and chronic inflammatory changes, while the same material of identical chemical composition but micrometer size was not found to be harmful [4, 7, 10–12]. Other studies focused on presence, distribution, and accumulation of NPs in different levels of airways; this was studied on rodents, as well as on computed models. The computed models show assumed distribution of inhaled NPs in the tissues of airways. It is assumed that their behavior when inhaled is different from that of the larger particles. Ghalali's computed model shows that the most of NPs deposit in the nasal cavity on the anterior-most parts of turbinates as well as microparticles, but the second location of the most

abundant deposition differs; the NPs tend to deposit in pharynx, whereas the microparticles deposit in larynx [13, 14].

Although the pathological influence of fine and ultrafine particles including elemental metal particles on lungs is well-known (e.g., occupational pneumoconiosis due to exposure to rare metals) [15], only few clinical studies on nanotoxicology and nanopathology in airways have been conducted so far; for example, Zeleník et al. studied presence and elemental compositions of nanoparticles in human palatine tonsils [16].

One of the main challenges of clinical research focusing on nanotoxicology and nanopathology has been only a limited possibility to quantify and determine the concentration of NPs in the examined tissues, because the principle of their detection in tissues is vastly different from that of larger particles [16]. Mapping of the tissues and statistical analysis of the presence of NPs becomes difficult due to the enormously small scale of the "nanoworld." The main aim of this prospective study was to design and test a novel method of quantification of micro- and nanosized particles in tissue samples.

Since the nasal cavity and its turbinates are the first barrier filtering the inhaled air, it is probable that the airborne nano- and microparticles would deposit in the mucosa of the nasal cavity, enter its deeper layers, and play a role in chronic inflammatory changes. Since the pathophysiological mechanisms of inflammatory changes in chronic rhinosinusitis are not yet completely clear [17], this study also aims to provide first information on deposition, distribution, and elemental composition of nano- and microparticles in the nasal mucosa and future prospects in further research concerning their possible role in inflammatory changes of the mucosa of upper airways.

2. Material and Methods

This prospective study was conducted from September 2013 to March 2014. It was approved by the Institutional Ethics Committee (identifier FNO-ENT-Nanoparticles, 2 RVO-FNOs/2013) and registered at ClincialTrials.gov (identifier NCT02270125). The study was performed in accordance with the Declaration of Helsinki, good clinical practice, and applicable regulatory requirements. Informed consent was obtained from all participants before initiation of any procedure.

Patients aged from 19 to 74 (mean 44) with chronic hypertrophic rhinosinusitis nonresponsive to conservative therapy indicated for endoscopic mucotomy were enrolled in the study. Demographic data and occupational histories were obtained from the patients (Table 1). The tissue samples were processed at the Institute of Pathology and examined by scanning electron microscopy (SEM) and Raman microspectroscopy (RMS) at the Nanotechnology Center.

2.1. Biopsy and Sample Preparation. The tissue samples, mucosa of the inferior nasal turbinates, were obtained by endoscopic "cold-steel" mucotomy under general anesthesia. The samples were attached to paraffin tablets by sterile surgical needles; the orientation of the mucosa was marked on the tablet (anterior and posterior sides) and sent to the Institute of Pathology under sterile conditions for further processing. The samples were immersed in 10% formalin and vertically divided into four parts according to the distance from the nostrils: part 1, closest to the nostrils; parts 2 and 3, in the middle; and part 4, closest to choanae (Figure 1). After alcohol-xylene dehydratation and automated paraffin embedding, 2–4 μm thin sections were cut and mounted on glass microscope slides, before staining with hematoxylin/eosin for routine pathological examination. Thin sections were also cut for further chemical analysis (SEM and RMS) and mounted as above. These sections were deparaffinized in xylene and alcohol and were not stained.

Table 1: Summary of sex, age, and occupation history of patients.

Sample	Sex	Age	Occupation
A	M	74	Retired, former welder
B	M	34	Programmer
C	M	34	Locksmith/welder
D	M	61	Security guard
E	F	19	Student
F	F	40	Industrial worker

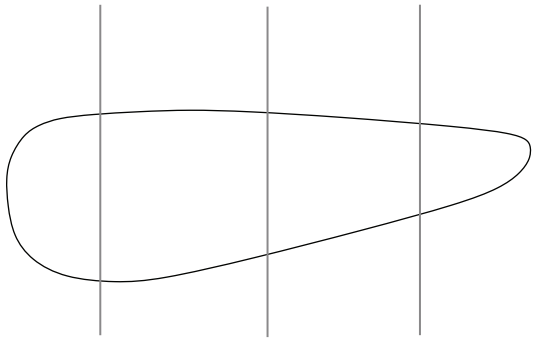

Figure 1: Scheme of a tissue sample obtained by mucotomy; vertical lines indicate division of the sample into four parts according to the distance from the nostrils.

2.2. Analytical Methods Utilized for Detection and Characterization of Particles. SEM (Quanta FEG 450, FEI) with X-ray microanalysis APOLLO X (EDAX) and SEM Philips XL 30 operating at 30 keV were utilized for morphology characterization and elemental composition of the particles found in single tissue samples. Samples were evaluated in the BSE (back-scattered electrons) mode allowing for visual detection of changes in elemental composition. For example, metallic particles scattering electrons appear as light spots compared to the tissue absorbing electrons and therefore have a dark colour in the BSE mode. Thus, the entire area of each section was inspected and the light spots were analyzed.

Raman spectra allowing for phase characterization of particles in the human tissue were obtained using a Smart Raman Microscopy System XploRA (HORIBA Jobin Yvon,

Table 2: Elements revealed in a single sections of the nasal tissue samples by SEM-EDX elemental analysis of the visually detected spots (part 1, anterior part, closest to the the nostrils; parts 2 and 3 in the middle; and part 4, posterior part, closest to choanae).

Element	Samples																								
	A				B				C				D				E				F				
	1	2	3	4	1	2	3	4	1	2	3	4	1	2	3	4	1	2	3	4	1	2	3	4	
Ba	x	x				x	x		x	x	x	x		x						x					
Cd												x													
Cu				x			x	x	x	x	x	x													
Cr				x						x	x														
Fe	x	x	x	x	x	x		x	x	x	x	x		x	x	x	x	x	x	x	x	x	x	x	
Mn			x								x														
Mo	x																								
Ni				x						x	x	x													
Pb									x																
Ti								x	x	x	x	x		x	x										
Zn		x		x				x		x		x													

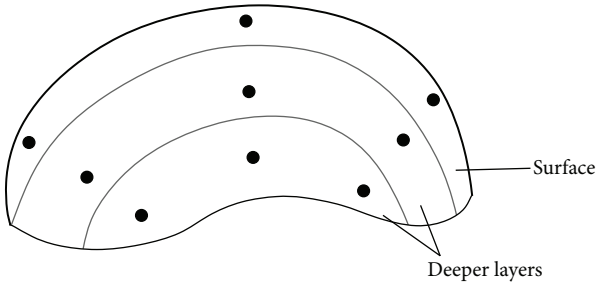

Figure 2: Scheme of cross sections with marked points of Raman microanalysis within superficial and deep layers of the mucosa.

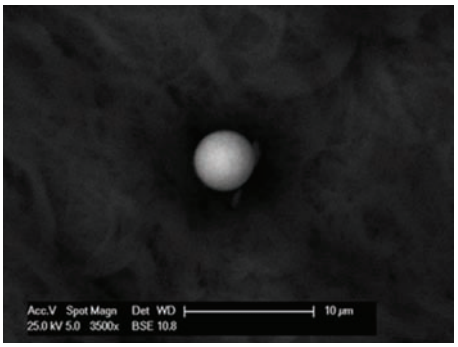

Figure 3: Scanning electron microscope image of a spherical Fe containing particle in the sample A (magnification 3,500x).

France), using the 532 nm excitation laser source, 100x objective, and 1200 gr./mm grating in the range from 80 to 2000 cm^{-1}. The laser beam with diameter approximately of 0.5 μm allows for point phase analysis of microsized particles. Raman microspectroscopic analysis was performed in each of the tissue sample sections obtained from single sample. To quantify the distribution of particles, a field consisting of 9 points with similar distances from each other and covering the entire sample area was selected in each section (Figure 2, scheme of the cross section). The points of analysis were selected to include the area directly below the nasal mucosa (denoted as superficial layer, approximate thickness of 1 mm) but also areas located in deeper epithelium layers (deep layers, over 2 mm from the surface). Raman spectrum in each selected point was obtained and interpreted.

3. Results

In this pilot study, a total of six nasal mucosa samples obtained from six patients with chronic hypertrophic rhinosinusitis were examined. In all the samples, micro- and nanosized particles of different elemental composition were found. Elements detected in individual tissue samples and in their sections according to the distance from the nostrils are listed in Table 2. The most abundant element was iron (also barium, copper, titanium, and zinc).

The particles detected by SEM ranged from approximately 10 μm to submicron sizes and most often in form of aggregates/agglomerates and their morphologies varied from spherical to polygonal (Figures 3 and 4). A representative example of a spherical particle composed of metal (Fe) was found in the tissue of a welder (sample A) (Figure 3).

Interindividual differences in elemental composition of particles were found (Table 2). The greatest variety of the detected metals was observed in the tissues of the patients occupationally exposed to welding emissions (samples A and C). Iron in the tissue samples of the welders was present in all sections analyzed.

The samples were analyzed in terms of distribution and quantity of the particles by RMS. Our analysis of the geometry of particle distribution is based on the system of 9-point coordinates as described above. The specific compounds detected by the analysis of 9 points in each tissue section using RMS are listed in Table 3. The highest incidence of the particles in all samples was found in areas further from

Table 3: Compounds detected in various sections of the tissue samples by the Raman microspectroscopy. The particles were found in both superficial (S) and deeper (D) layers of the tissue samples, with interindividual differences.

Compound	Samples																							
	A				B				C				D				E				F			
	1	2	3	4	1	2	3	4	1	2	3	4	1	2	3	4	1	2	3	4	1	2	3	4
Anatase	D	D				S				S				S		S								
Rutile								D																
Calcite		D			D	S																		
Magnetite								S			S													
Barite																								
Siderite				D												S	S				S			
Graphite		D										S*		S		S	D				S			S
Amorphous carbon	D	D	S											S	D									S

* Detected twice.

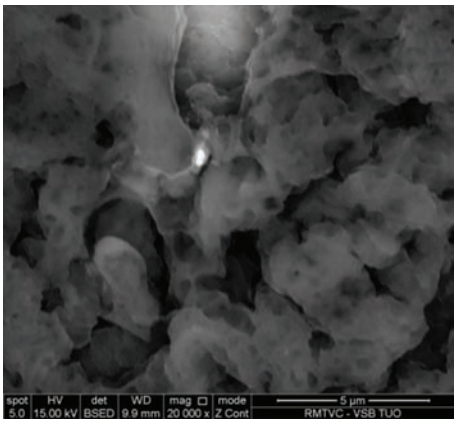

Figure 4: Scanning electron microscope image of an aggregate based on Ba detected in the sample C (magnification 20,000x).

the nostrils (parts 2–4), while lower numbers of particles were detected in the proximal area, part 1.

Different areas according to their depth from the surface of the mucosa were also assessed by RMS (Table 3). Interindividual differences were also found: in sample A (retired welder), there was a higher number of particles in deeper layers of the tissue than in the superficial layer, whereas in samples C, D, and F (C, welder/locksmith; D, security guard; F, industrial worker), the particles were found predominantly in the superficial layer. In samples B and E (B, programmer and E, student), there was approximately the same number of particles detected in the superficial and deeper layers of the mucosa.

4. Discussion

It has been proven that inhaled NPs of various elemental composition cause acute and chronic inflammatory changes in lower levels of respiratory tract and may also induce malignant transformation of cells, but the role in pathologic changes in the mucosa of the upper airways has not been sufficiently studied yet [1, 2, 4, 10, 12, 18, 19]. So far only a few clinical studies have been conducted; for example, Zeleník et al. studied presence and elemental composition in tissues of palatine tonsils [16]. The behavior of NPs in human tissues and immunologic reaction of the organism is still unclear; further understanding of the role of NPs in inflammation induction may contribute to better understanding of the pathophysiological mechanisms of inflammatory changes in the nasal mucosa in chronic hypertrophic rhinosinusitis.

This pilot study was focused on detection of micro- and nanosized particles in the nasal mucosa, their elemental composition, distribution throughout the tissue samples, and comparison of differences in NPs' quantity in different patients. We did not assess histological changes in the mucosa, which is an objective of a subsequent ongoing study conducted in our department. The possibility of quantification of NPs has been only limited so far as the principle of their detection in tissues is vastly different than in larger particles due to the enormously small scale of the "nanoworld" [16]. In our study we present a novel method of quantification of the nano- and microparticles in the nasal mucosa.

The greatest variety of the detected metals was observed in the tissues of the patients occupationally exposed to welding emissions (samples A and C), mostly iron, which was found in all the sections of the samples. This fact is not surprising as the welding fumes contain mostly iron and manganese [20, 21]. Anyway, welders may be exposed to similar airborne pollutants as the general population (road traffic, industrial pollution, and smoking). Also, we have to consider if using stainless steel instruments during surgery may cause artificial contamination of the tissue samples, as all the examined samples contained iron particles. However, artificial contamination would cause presence of the particles only on the surface or in the superficial-most layers of mucosa and cannot explain presence of the particles in the deep layers of the samples.

The morphology of the detected particles was studied by SEM. The particles varied from spherical to polygonal. Spherical iron particles were found in sample A (welder). These are often produced by high-temperature processes and

were described as the most abundant particulate emission in welding fumes [21] (Figure 3).

The highest incidence of the particles in all samples was found in areas distant from the nostrils, while lower numbers of particles were detected in the anterior-most parts of the samples. There is no clear explanation for this finding, but the distribution of the airflow in the nasal cavity, the state of the mucosa, and other factors are likely determinants of the deposition of the inhaled particles. This is in contrast with the results of Ghalati et al. (2012), who assumed that most NPs would deposit on the anterior-most parts of the turbinates based on computed modeling [13]. This difference in results could possibly be explained by deposition and redistribution of the particles in the mucosa. Since our cohort is too small to make any conclusions about the NPs distribution, further research in this area is needed.

There is no clear explanation of the interindividual differences in distribution of NPs in areas of the tissue according to their depth from the surface (Table 3). Further research in this area with larger cohorts of patients and also thorough histopathological examination of the tissues is needed.

Although this pilot study has shown some interesting results, we are aware that the examined cohort is too small to make definitive conclusions concerning the NPs composition, distribution, and interindividual differences and to give any possible explanations of our findings. The study was not meant to provide statistical or quantitative evidence as to the prevalence of particles in nasal mucosa, their types, sources, and the health hazard (if any) they may pose. Our main objective was to design and test a novel work flow platform, which could be used to conduct a more comprehensive analysis.

In the future, the aim of our subsequent ongoing study is to analyze more tissue samples including thorough histopathological examination and to compare the findings in the patients with chronic rhinosinusitis with healthy mucosa samples obtained from cadavers.

5. Conclusions

This pilot study has proven the possibility of quantification of distribution of micro- and nanosized particles in tissue samples, which had previously been one of the main challenges of the clinical research in nanopathology. It has also shown that these particles may deposit in deeper layers of nasal mucosa and that their elemental composition may be related to professional exposition to their sources (welding fumes). Since the cohort examined in our study is too small, further research in this area is needed to confirm our findings.

Conflict of Interests

The authors declare that there is no conflict of interests regarding the publication of this paper.

Acknowledgments

This study was supported by the Institutional Support of the Ministry of Health of the Czech Republic no. 2 RVOs/2013 and Institutional Developmental Plan of University of Ostrava, project Pedagogical Work Support of Academic Staff in the Form of Professional Upskilling, Foreign Traineeship, no. IRP201423. The paper has been elaborated in the framework of the "Regional Materials Science and Technology Centre" project registration no. CZ.1.05/2.1.00/01.0040 supported by the operational programme "Research and Development for Innovations" and financed by the Structural Funds and from the state budget of the Czech Republic.

References

[1] N. A. Monteiro-Riviere and C. L. Tran, *Nanotoxicology: Characterization, Dosing and Health Effects*, Informa Healthcare, New York, NY, USA, 2007.

[2] K. Donaldson, V. Stone, C. L. Tran, W. Kreyling, and P. J. A. Borm, "Nanotoxicology," *Occupational and Environmental Medicine*, vol. 61, no. 9, pp. 727–728, 2004.

[3] M. C. Garnett and P. Kallinteri, "Nanomedicines and nanotoxicology: some physiological principles," *Occupational Medicine*, vol. 56, no. 5, pp. 307–311, 2006.

[4] A. Srinivas, P. J. Rao, G. Selvam, P. B. Murthy, and P. N. Reddy, "Acute inhalation toxicity of cerium oxide nanoparticles in rats," *Toxicology Letters*, vol. 205, no. 2, pp. 105–115, 2011.

[5] R. Foldbjerg, D. A. Dang, and H. Autrup, "Cytotoxicity and genotoxicity of silver nanoparticles in the human lung cancer cell line, A549," *Archives of Toxicology*, vol. 85, no. 7, pp. 743–750, 2011.

[6] H. Gehrke, J. Pelka, C. G. Hartinger et al., "Platinum nanoparticles and their cellular uptake and DNA platination at non-cytotoxic concentrations," *Archives of Toxicology*, vol. 85, no. 7, pp. 799–812, 2011.

[7] S. Hackenberg, A. Scherzed, A. Technau et al., "Cytotoxic, genotoxic and pro-inflammatory effects of zinc oxide nanoparticles in human nasal mucosa cells in vitro," *Toxicology in Vitro*, vol. 25, no. 3, pp. 657–663, 2011.

[8] J. Xu, W. Dai, Z. Wang, B. Chen, Z. Li, and X. Fan, "Intranasal vaccination with chitosan-DNA nanoparticles expressing pneumococcal surface antigen A protects mice against nasopharyngeal colonization by *Streptococcus pneumoniae*," *Clinical and Vaccine Immunology*, vol. 18, no. 1, pp. 75–81, 2011.

[9] A. Kumar and A. Dhawan, "Genotoxic and carcinogenic potential of engineered nanoparticles: an update," *Archives of Toxicology*, vol. 87, no. 11, pp. 1883–1900, 2013.

[10] S. Singh and H. S. Nalwa, "Nanotechnology and health safety—toxicity and risk assessments of nanostructured materials on human health," *Journal of Nanoscience and Nanotechnology*, vol. 7, no. 9, pp. 3048–3070, 2007.

[11] M. B. Genter, N. C. Newman, H. G. Shertzer, S. F. Ali, and B. Bolon, "Distribution and systemic effects of intranasally administered 25 nm silver nanoparticles in adult mice," *Toxicologic Pathology*, vol. 40, no. 7, pp. 1004–1013, 2012.

[12] G. Oberdörster, Z. Sharp, V. Atudorei et al., "Extrapulmonary translocation of ultrafine carbon particles following whole-body inhalation exposure of rats," *Journal of Toxicology and Environmental Health, Part A: Current Issues*, vol. 65, no. 20, pp. 1531–1543, 2002.

[13] P. F. Ghalati, E. Keshavarzian, O. Abouali, A. Faramarzi, J. Tu, and A. Shakibafard, "Numerical analysis of micro- and nanoparticle deposition in a realistic human upper airway," *Computers in Biology and Medicine*, vol. 42, no. 1, pp. 39–49, 2012.

[14] P. Zamankhan, G. Ahmadi, Z. Wang et al., "Airflow and deposition of nano-particles in a human nasal cavity," *Aerosol Science and Technology*, vol. 40, no. 6, pp. 463–476, 2006.

[15] K. T. Rim, K. H. Koo, and J. S. Park, "Toxicological evaluations of rare earths and their health impacts to workers: a literature review," *Safety and Health at Work*, vol. 4, no. 1, pp. 12–26, 2013.

[16] K. Zeleník, J. Kukutschová, J. Dvořáčková et al., "Possible role of nano-sized particles in chronic tonsillitis and tonsillar carcinoma: a pilot study," *European Archives of Oto-Rhino-Laryngology*, vol. 270, no. 2, pp. 705–709, 2013.

[17] W. J. Fokkens, V. J. Lund, J. Mullol et al., "European position paper on rhinosinusitis and nasal polyps 2012," *Rhinology*, vol. 50, supplement 23, pp. 1–298, 2012.

[18] G. Oberdörster, E. Oberdörster, and J. Oberdörster, "Nanotoxicology: an emerging discipline evolving from studies of ultrafine particles," *Environmental Health Perspectives*, vol. 113, no. 7, pp. 823–839, 2005.

[19] HSE, *Health Effects of Particles Produced for Nanotechnologies*, EH75/6, HSE Books, 2004.

[20] J. D. Richman, K. J. T. Livi, and A. S. Geyh, "A scanning transmission electron microscopy method for determination of manganese composition in welding fume as a function of primary particle size," *Journal of Aerosol Science*, vol. 42, no. 6, pp. 408–418, 2011.

[21] M. Oprya, S. Kiro, A. Worobiec et al., "Size distribution and chemical properties of welding fumes of inhalable particles," *Journal of Aerosol Science*, vol. 45, pp. 50–57, 2012.

18. Evaluation of biochemical markers and bone mineral density in patients with chronic kidney disease stage 5D at the start of hemodialysis treatment

Valkovský I, Olšanská R, Tvrdík J, Martínek A, Švagera Z, Pernicová M, Dědochová J, Čermáková Z

Originally published in Biomedical Papers, 2015, vol. 159, no. 1, p. 93-99.

Evaluation of biochemical markers and bone mineral density in patients with chronic kidney disease stage 5D at the start of hemodialysis treatment

Ivo Valkovsky[a,e], Renata Olsanska[a], Josef Tvrdik[f], Arnost Martinek[a,e], Zdenek Svagera[b,e], Marketa Pernicova[c], Jarmila Dedochova[a], Zuzana Cermakova[d,e]

Background. Patients with chronic kidney disease (CKD) have significant disorders of bone and mineral metabolism. In addition, they can also develop other bone disorders including osteoporosis. This study evaluated the bone mineral density (BMD) of patients at the start of hemodialysis treatment as well as the relationship between BMD and possible risk factors or biochemical markers.
Methods. The study was performed in 82 patients (28 females, 54 males). BMD was measured by dual-energy X-ray absorptiometry (DXA) at the lumbar spine and the proximal femur.
Results. We found a high prevalence of 25-hydroxyvitamin D deficiency (96%; mean levels 30.0 ± 17.7 nmol/L) and a reduction of BMD in comparison with gender- and age-matched normal population values at the total hip (*Z*-score = -0.31 ± 1.11) and the femoral neck (*Z*-score = -0.48 ± 1.16), but not at the lumbar spine (*Z*-score = 0.68 ± 1.81). The prevalence of *T*-scores ≤ -2.5 SD in the group of patients over 50 years was 52.0% in females and 33.3% in males. BMD positively correlated: with male gender and calcium levels at all measured sites, with age at the lumbar spine and with weight or BMI at the proximal femur.
Conclusion. CKD patients at the start of hemodialysis treatment had a high prevalence of low *T*-score values, corresponding to values for osteoporosis in the general population. BMD at the proximal femur was below the expected average for age and gender, but at the lumbar spine, BMD in hemodialysis patients was above average in persons without known CKD.

Key words: bone mineral density, DXA, chronic kidney disease, hemodialysis, osteoporosis

Received: May 17, 2013; Accepted with revision: November 18, 2013; Available online: November 29, 2013
http://dx.doi.org/10.5507/bp.2013.087

[a]Clinic of Internal Medicine, University Hospital Ostrava, Ostrava, Czech Republic
[b]Institute of Laboratory Diagnostics, University Hospital Ostrava, Ostrava
[c]Institute of Radiodiagnostic, University Hospital Ostrava, Ostrava
[d]Blood Centre, University Hospital Ostrava, Ostrava
[e]Department of Biomedical Sciences, Faculty of Medicine, University of Ostrava, Ostrava
[f]Department of Informatics and Computers, Faculty of Science, University of Ostrava, Ostrava
Corresponding author: Ivo Valkovsky, e-mail: ivo.valkovsky@fno.cz

INTRODUCTION

Skeletal changes are initiated at the early stage of chronic renal failure, as estimated from reduced bone mineral density (BMD) (ref.[1]). Men and women with impaired kidney function are at increased risk of bone loss, even with minimal reduction in kidney function[2]. It is reasonable to assume that many patients with chronic kidney disease (CKD) have other disorders of bone that contribute to the final picture of renal osteodystrophy. Osteoporosis is the most prevalent bone disorder in the general population, but relatively little attention has been paid to its possible contribution to the bone alterations observed in patients with CKD, particularly in the increasing population of middle and older age groups that account for more than half of the patients on dialysis[3]. There is no reason why osteoporosis cannot accompany the derangements in bone metabolism that characterize chronic kidney disease. In fact, osteoporosis could and should be included in the broad characterization of chronic kidney disease-mineral and bone disorder (CKD-MBD), as recently proposed by the "Kidney Disease: Improving Global Outcomes" (KDIGO) working group. The pathophysiology leading to osteoporosis or CKD-MBD shares many common, yet distinctly different pathways. Both pathways may lead to the impairment of bone strength and the occurrence of low-trauma fractures[4].

Osteoporosis is generally defined as a skeletal disorder characterized by compromised bone strength predisposing to an increased risk of fracture[5]. In the general population, osteoporosis can be clinically diagnosed by the presence of a low trauma (fragility) fracture or by measuring BMD (ref.[6]). Osteoporosis may be diagnosed if the *T*-score of the lumbar spine, total hip, or femoral neck is -2.5 SD or less[7].The challenge in clinical practice is how to discriminate between osteoporosis and CKD-MBD. The diagnostic tools used to identify osteoporosis in the general population are not suitable for detecting the complex bone and metabolic changes that occur with chronic kidney disease. The interpretation of BMD in CKD patients is still a subject of controversy[5].

Almost all studies of BMD in patients with CKD stage 5D have investigated patients on long term hemodialysis treatment. The present study was designed to determine BMD in patients at the beginning of hemodialysis treatment and to assess the relationship between BMD and age, gender, diabetes mellitus, body mass index, residual renal function and biochemical markers (serum levels of 25-hydroxyvitamin D, parathyroid hormone, estradiol, calcium, phosphate, calcium-phosphate product and blood pH).

MATERIALS AND METHODS

Study subjects

Eighty-two CKD stage 5D patients from our dialysis unit were investigated. All patients had been undergoing hemodialysis treatment for less than 3 months, were clinically stable and their estimated glomerular filtration rate (eGFR) before the first dialysis treatment was < 0.25 mL/s/1.73 m^2. Exclusion criteria included the following: previous kidney transplantation, corticosteroid treatment and hormone replacement therapy. All patients were Caucasian. None of the patients had a history of osteoporotic fracture. The study was approved by the local ethics committee and all patients gave written informed consent.

The etiology of renal failure was diabetic nephropathy in 22 patients (27%), renal vascular disease in 20 (24%), glomerulonephritis in 14 (17%), tubulointerstitial nephritis in 11 (13%), adult cystic kidney disease in 5 (6%), other renal disease in 7 (9%), and unknown in 3 (4%). Diabetic nephropathy was the cause of renal failure in 63% of diabetic patients in this study, whereas among the other diabetics, the cause was different, mostly renal vascular disease (17%). All diabetic patients suffered from type 2 diabetes.

Biochemical measurements

Blood samples were collected after an overnight fast, before hemodialysis treatment, into plastic collection tubes containing lithium heparinate as an anticoagulant. Plasma was separated by centrifugation at 2000 × *g* for 15 min at 4 °C. Concentrations of the following substances were assayed: calcium, creatinine and phosphate, analyzed photometrically (AU 5420, Beckman Coulter, Inc., Brea, CA), and total 25-hydroxyvitamin D (DiaSorin, Inc., Stillwater, MN) and estradiol by RIA (Orion Diagnostica, Espoo, Finland). The concentration of intact parathyroid hormone (iPTH: parathyroid hormone 1-84 with 44.8% cross reactivity of fragment 7-84) was measured by Immulite 2000 (Siemens Medical Solutions Diagnostics, New York, NY) and blood pH by Radiometer ABL 835 FLEX (Radiometer Medical ApS, Brønshøj, Denmark). The analysis of calcium, creatinine, and phosphate showed inter-assay coefficients of variation between 2 and 5%. The analysis of 25-hydroxyvitamin D, estradiol, and parathyroid hormone showed inter-assay coefficients of variation of 8.3%, 12.3% and 8.7%, respectively. All biochemical markers were measured repeatedly once a month within a 3-month period before measurement of BMD. The mean value of 3 assays was taken for further assessment. Estimated glomerular filtration rate was calculated using the abbreviated MDRD (Modification of Diet in Renal Disease) formula.

Bone mineral density measurements

Determination of BMD was performed in each patient within three months of the start of hemodialysis treatment. Measurements were performed on a QRD 2000 bone densitometer (Hologic Inc.), using dual-energy X-ray absorptiometry (DXA). The results are expressed as *T*-scores and *Z*-scores and in absolute values (g/cm^2). *T*-scores and *Z*-scores reflect the number of standard deviations by which a patient value differs from the sex-matched young adult reference mean or from the sex- and age-matched mean, respectively. These scores are also expressed as a percentage. The reference database was created by the manufacturer, based on 1000 measurements of the lumbar spine (650 females, 350 males) and over 1400 measurements of the hip (750 females, 730 males) in healthy volunteers. BMD was assessed in two areas of the central skeleton, at the lumbar spine (L1 through L4) and at the site of the left proximal femur (at the femoral neck and the total hip).

Statistical analysis

Group characteristics are shown as mean ± SD. Potential differences between the groups were assessed by the Wilcoxon two-sample test. Differences between the groups in the prevalence of osteoporosis and osteopenia were tested by the Chi-Square test. Stepwise multiple regression analysis was applied to investigate relationships between BMD and risk factors or biochemical markers. Statistical analysis was performed using NCSS (Hintze J. (2001) NCSS and PASS, Number Cruncher Statistical System, Kaysville, UT, WWW.NCSS.COM).

RESULTS

Demographic and biochemical data

Patient data and statistical comparisons between the groups of females and males, non-diabetics and diabetics are presented in Table 1. Nine patients (11%) were under the age of 50 years, 41 patients (50%) between 50 and 70 years and 32 patients (39%) over the age of 70 years. Patients were predominantly male (66%). Diabetics accounted for 43% of the patients and were older and had a higher body mass index (BMI). Males had significantly higher values of eGFR, 25-hydroxyvitamin D (25(OH) D) and estradiol than females (89% of the female patients were post-menopausal). Higher eGFR values but lower 25(OH)D and iPTH levels were measured in the group of diabetic patients than in non-diabetics and these differences were statistically significant. Severe deficiency of 25-hydroxyvitamin D (below 12.5 nmol/L) was found in 17% of hemodialysis patients, mild deficiency (from 12.5 to 40 nmol/L) in 60%, and insufficiency (from 40

Table 1. Demographic and biochemical data.

Variable	All subjects (*N* = 82)	Females (*N* = 28)	Males (*N* = 54)	*P**	Non-diabetics (*N* = 47)	Diabetics (*N* = 35)	*P***
Age (years)	65.2 ± 14.0	66.9 ± 15.5	64.4 ± 13.2	NS	61.9 ± 14.5	69.7 ± 12.0	< 0.01
Weight (kg)	75.2 ± 14.7	68.1 ± 13.3	78.8 ± 14.2	< 0.01	73.4 ± 13.9	77.6 ± 15.6	NS
Height (cm)	169.7 ± 9.5	160.6 ± 5.9	174.5 ± 7.3	< 0.0001	171.2 ± 10.2	167.8 ± 8.2	NS
BMI (kg/m²)	26.1 ± 4.5	26.4 ± 4.9	25.9 ± 4.3	NS	24.9 ± 3.5	27.6 ± 5.2	< 0.05
eGFR (mL/s/1.73m²)	0.16 ± 0.05	0.14 ± 0.05	0.17 ± 0.05	< 0.01	0.14 ± 0.05	0.18 ± 0.06	< 0.05
25(OH)D (nmol/L)	30.0 ± 17.7	23.7 ± 10.2	33.2 ± 20.0	< 0.05	35.7 ± 20.2	22.7 ± 10.0	< 0.01
iPTH (pmol/L)	34.9 ± 31.9	36.9 ± 45.9	33.9 ± 21.8	NS	42.1 ± 39.3	25.3 ± 12.5	< 0.01
Estradiol (nmol/L)	0.062 ± 0.052	0.052 ± 0.077	0.067 ± 0.032	< 0.0001	0.065 ± 0.066	0.058 ± 0.027	NS
Calcium (mmol/L)	2.22 ± 0.17	2.26 ± 0.16	2.20 ± 0.17	NS	2.21 ± 0.16	2.23 ± 0.17	NS
Phosphate (mmol/L)	1.88 ± 0.45	1.87 ± 0.45	1.88 ± 0.44	NS	1.95 ± 0.51	1.79 ± 0.33	NS
Ca x P (mmol²/L²)	4.18 ± 1.03	4.22 ± 1.01	4.15 ± 1.05	NS	4.31 ± 1.16	3.99 ± 0.80	NS
blood pH	7.35 ± 0.04	7.34 ± 0.04	7.36 ± 0.04	NS	7.35 ± 0.04	7.37 ± 0.04	NS

Notes: BMI, body mass index; eGFR, estimated glomerular filtration rate; 25(OH)D, 25-hydroxyvitamin D; iPTH, intact parathyroid hormone; Ca x P, calcium phosphate product. Data are presented as means ± SD; *P**, comparison between females and males; *P****, comparison between non-diabetics and diabetics; NS, not significant.

Table 2. Bone densitometric data for all subjects and for subgroups of females, males, non-diabetics and diabetics.

	All subjects (*N* = 82)	Females (*N* = 28)	Males (*N* = 54)	*P**	Non-diabetics (*N* = 47)	Diabetics (*N* = 35)	*P***
LUMBAR SPINE							
g/cm²	1.080 ± 0.231	1.000 ± 0.137	1.120 ± 0.258	< 0.01	1.068 ± 0.270	1.096 ± 0.170	NS
T-score (SD)	-0.31 ± 1.69	-0.79 ± 1.29	-0.06 ± 1.82	NS	-0.49 ± 1.81	-0.07 ± 1.51	NS
T-score (%)	96.8 ± 17.0	91.7 ± 13.5	99.3 ± 18.2	NS	95.0 ± 18.2	99.2 ± 15.2	NS
Z-score (SD)	0.68 ± 1.81	0.85 ± 1.76	0.59 ± 1.84	NS	0.43 ± 1.97	1.01 ± 1.54	NS
Z-score (%)	108.5 ± 21.1	112.8 ± 23.5	106.5 ± 19.7	NS	105.8 ± 22.9	112.2 ± 18.2	NS
NECK							
g/cm²	0.742 ± 0.146	0.669 ± 0.098	0.779 ± 0.152	< 0.001	0.740 ± 0.135	0.745 ± 0.161	NS
T-score (SD)	-2.13 ± 1.12	-2.39 ± 0.96	-2.00 ± 1.19	NS	-2.20 ± 1.03	-2.04 ± 1.25	NS
T-score (%)	75.2 ± 13.3	71.5 ± 11.5	77.0 ± 13.8	NS	74.3 ± 12.1	76.3 ± 14.8	NS
Z-score (SD)	-0.48 ± 1.16	-0.40 ± 1.27	-0.52 ± 1.12	NS	-0.67 ± 1.06	-0.24 ± 1.26	NS
Z-score (%)	92.1 ± 19.3	90.5 ± 26.3	92.9 ± 15.1	NS	88.6 ± 20.1	96.8 ± 17.4	NS
TOTAL HIP							
g/cm²	0.872 ± 0.158	0.762 ± 0.106	0.927 ± 0.152	< 0.0001	0.857 ± 0.143	0.891 ± 0.177	NS
T-score (SD)	-1.37 ± 1.07	-1.83 ± 0.89	-1.15 ± 1.09	< 0.05	-1.50 ± 0.95	-1.20 ± 1.21	NS
T-score (%)	82.1 ± 16.3	74.5 ± 18.5	85.8 ± 13.8	< 0.01	79.6 ± 16.9	85.3 ± 15.1	NS
Z-score (SD)	-0.31 ± 1.11	-0.34 ± 1.18	-0.29 ± 1.08	NS	-0.50 ± 0.96	-0.05 ± 1.25	NS
Z-score (%)	94.6 ± 19.1	92.0 ± 25.9	95.9 ± 14.8	NS	90.9 ± 19.4	99.6 ± 17.6	< 0.05

Notes: Data are presented as means ± SD; P*, comparison between females and males; P**, comparison between non-diabetics and diabetics; NS, not significant.

to 75 nmol/L) in 19%. Normal levels of 25(OH)D above 75 nmol/L were found in only 4% of patients (3 males, non-diabetics). Low levels of intact parathyroid hormone (below 16.5 pmol/L) were measured in 22% of patients, the mean (from 16.5 to 33.0 pmol/L) in 41%, and high levels (above 33.0 pmol/L) in 37% of the patient population. Classification of degrees of 25(OH)D deficiency and iPTH levels was based on K/DOQI guidelines[8].

Bone mineral density

Bone densitometric data are shown in Table 2. The lowest values of BMD expressed in g/cm² among all patient groups were found at the femoral neck, while the highest were found at the lumbar spine, where BMD values expressed as *Z*-scores were above the age- and sex-matched mean. Female patients had significantly lower BMD (in g/cm²) at all measured sites as compared with males and furthermore, BMD values expressed as *T*-scores

Table 3. Prevalence of *T*-score values corresponding to osteoporosis and osteopenia for all subjects and for subgroups of females, males, non-diabetics and diabetics.

	All subjects (*N* = 82)	Females (*N* = 28)	Males (*N* = 54)	*P**	Non-diabetics (*N* = 47)	Diabetics (*N* = 35)	*P***
LUMBAR SPINE				NS			NS
T-score ≤ -2.5 SD	6.2%	7.4%	5.6%		8.7%	2.9%	
T-score -1.0 to -2.49 SD	33.3%	44.4%	27.8%		37.0%	28.6%	
Normal BMD	60.5%	48.1%	66.7%		54.3%	68.6%	
NECK				NS			NS
T-score ≤ -2.5 SD	35.8%	48.1%	29.6%		39.1%	31.4%	
T-score -1.0 to -2.49 SD	53.1%	40.7%	59.3%		50.0%	57.1%	
Normal BMD	11.1%	11.1%	11.1%		10.9%	11.4%	
TOTAL HIP				< 0,05			NS
T-score ≤ -2.5 SD	17.3%	33.3%	9.3%		15.2%	20.0%	
T-score -1.0 to -2.49 SD	45.7%	44.4%	46.3%		54.3%	34.3%	
Normal BMD	37.0%	22.2%	44.4%		30.4%	45.7%	

Notes: In the general population *T*-score ≤ -2.5 SD = Osteoporosis, *T*-score -1.0 to -2.49 SD = Osteopenia; *P**, comparison between females and males; *P***, comparison between non-diabetics and diabetics; NS, not significant.

Table 4. Prevalence of *T*-score ≤ -2.5 SD in the area of the proximal femur and/or at the lumbar spine in the age group over 50 years.

BOTH GENDER			FEMALES			MALES		
All > 50 y (*N* = 73)	> 50 - 70 y (*N* = 41)	> 70 y (*N* = 32)	All > 50 y (*N* = 25)	> 50 - 70 y (*N* = 12)	> 70 y (*N* = 13)	All > 50 y (*N* = 48)	> 50 - 70 y (*N* = 29)	> 70 y (*N* = 19)
39.7%	41.5% *	37.5% **	52.0%	50.0% *	53.8% **	33.3%	37.9% *	26.3% **

Notes: y, years; there was no statistically significant difference between groups * and **.

were significantly lower at the total hip. There were no statistically significant differences in BMD values between non-diabetic and diabetic patients, except for BMD expressed as *Z*-score % at the total hip.

The prevalence of *T*-scores in the ranges corresponding to values for osteoporosis and osteopenia in the general population are shown in Table 3. *T*-scores ≤ -2.5 SD were found most frequently at the femoral neck and this applies to all patient groups. Females had low values of *T*-scores significantly more frequently than males at the total hip. The differences in *T*-scores ≤ -2.5 SD between non-diabetic and diabetic patients were not significant.

Table 4 shows *T*-scores ≤ -2.5 SD in the area of the proximal femur and/or at the lumbar spine in the group of patients aged over 50 years. *T*-scores ≤ -2.5 SD were found most often in female patients over the age of 70 years, but the differences between the age groups from 50 to 70 years and over 70 years were not statistically significant. There were 9 patients (6 males and 3 females) in the age group up to 50 years (not listed in Table 4) and only one female had a *T*-score < -2.5 SD.

Significant factors influencing BMD findings selected by stepwise multiple linear regression are presented in Table 5. The selection was carried out among the factors listed in Table 1, including gender and diabetes mellitus.

DISCUSSION

The study found a high prevalence of 25-hydroxyvitamin D deficiency in our group of CKD stage 5D patients at the start of hemodialysis treatment. This condition is known to be common in hemodialysis patients[9,10]. We found significantly lower levels of 25(OH)D in females and diabetics than in males and non-diabetics, which is in agreement with findings of other studies[9-11]. A high prevalence of vitamin D deficiency suggests the possibility of a significant number of patients with osteomalacia in our study.

Measured values of iPTH were lower in diabetic than in non-diabetic subjects. It is known that diabetic hemodialysis patients are often characterized by a relative hypoparathyroidism and reduced bone remodeling[12,13].

Table 5. Independent variables reaching significance from stepwise linear multiple regression analyses using lumbar spine, femoral neck and total hip BMD as dependent variables (all subjects).

	LUMBAR SPINE (R^2 = 0.16)			NECK (R^2 = 0.32)			TOTAL HIP (R^2 = 0.44)		
	Regression Coefficient	Standardized Coefficient	*P*	Regression Coefficient	Standardized Coefficient	*P*	Regression Coefficient	Standardized Coefficient	*P*
Calcium	0.3213	0.23	< 0.05	0.1897	0.22	< 0.05	0.3023	0.32	< 0.001
Male gender	0.1473	0.30	< 0.01	0.0839	0.27	< 0.01	0.1867	0.56	< 0.0001
Age	0.0044	0.27	< 0.05	-	-		-	-	
Weight	-	-		0.0036	0.36	< 0.001	-	-	
BMI	-	-		-	-		0.0084	0.24	< 0.01

Poor glycaemic control in diabetic hemodialysis patients is associated with lower PTH values compared to diabetic hemodialysis patients with good control[14].

We identified significant differences in values of residual renal function between female and male patients, as well as between non-diabetic and diabetic patients. Jamal et al. did not find that bone loss increased with deteriorating kidney function[2]. Linear regression analysis in our study also showed no association between eGFR and BMD. Therefore, we believe that bone mineral density findings cannot be explained by the relatively small differences in the measured eGFR.

This study found a reduction in BMD, especially at the femoral neck and to a lesser extent, also at the total hip. In contrast, the mean value of *T*-scores at the lumbar spine was within the normal range and the mean value of *Z*-scores was actually above the average value expected for age- and sex-matched controls. Meta-analysis of densitometric studies published in KDIGO guidelines showed, that in areas with a greater proportion of cortical bone (proximal femur, forearm, total body), *Z*-scores for patients with CKD stage 5D were approximately -0.5 to -1 standard deviation; but at the lumbar spine, *Z*-scores were closer to the average in persons without known CKD (ref.[15]). These differences in BMD findings could arise for several reasons. The effects of increased parathyroid hormone may be different on cortical and trabecular bone and be dependent on the severity of hyperparathyroidism[16]. Since the proximal femur contains more cortical bone than the vertebral body, hyperparathyroidism may have a different effect on DXA findings at the lumbar spine and in the area of the proximal femur. In addition, artefacts can cause inaccuracies in DXA measurements in the lumbar spine. Any calcium in the path of the X-ray beam will contribute to the BMD measurement (degenerative disc disease, osteophytes, osteoarthritis with hyperostosis, aortic calcifications, etc.) and cause false elevation[3,16-18].

Lower BMD and higher prevalence of *T*-score values corresponding to osteoporosis in females in this study are consistent with data in the general population[19,20]. Female sex negatively correlated with BMD at all measured skeletal sites. Several studies of dialysis patients have reported the same findings[21-24]. On the other hand, some other studies have found no correlation between gender and BMD (ref.[25-27]).

In our study, no statistically significant differences were found either in BMD values (expressed as g/cm^2 and *T*-score) or in the prevalence of *T*-scores ≤ -2.5 SD between non-diabetic and diabetic patients. Only at the total hip, *Z*-score (expressed as %) was significantly higher in diabetics. The results of studies dealing with bone mineral density in patients with diabetes in the general population are inconsistent. However, a recent meta-analysis of 15 studies involving 3,437 diabetics and 19,139 non-diabetics, showed that BMD in type 2 diabetics was significantly higher in the area of the proximal femur and at the spine[28]. Studies in dialysis patients reported different conclusions: lower BMD in diabetics[21,29-31], no difference between non-diabetics and diabetics[32], or no difference at the spine but higher BMD at the forearm[33].

In the present study, a high prevalence of low *T*-score values (corresponding to values for osteoporosis) was found in the patients aged over 50 years. Studies in the general population of this age reported a lower prevalence of osteoporosis. The estimated prevalence of osteoporosis in Germany in 2003 was 39% in females and 9.7% in males[34], while data from Sweden showed the prevalence to be 21.2% and 6.3%, respectively[35]. According to a Canadian survey from 2009, 19% of females and 3% of males aged 50 or older reported having been diagnosed with osteoporosis[19]. The prevalence of low BMD is increased among patients with end-stage renal disease. Patients with later stages of CKD share similar risk factors with the general population for osteoporosis and are also affected by bone disease associated with CKD (ref.[3,26,36,37]). It should be noted that the bone disease associated with CKD is complex and multifactorial and BMD measurements alone may not be adequate to characterize the bone disorder[3].

Calcium levels positively correlated with BMD at all measured sites. Several studies in CKD patients have not previously reported this association[25,38-40]. It should be noted that calcium levels in our study were measured only during the three months before the determination of BMD and therefore do not reflect the long-term impact of calcium levels on BMD.

Positive association between age and BMD at the

lumbar spine can be explained by age-related changes. Artefacts in DXA measurements at this site are most common in the elderly population[3,37].

The results of our study demonstrate a positive correlation between BMD at the regions of the proximal femur and weight or body mass index. Low body weight is known to be a risk factor for low BMD in the general population and several studies in CKD patients observed the same relationship[40-43].

In conclusion, this study confirmed a high prevalence of 25-hydroxyvitamin D deficiency in hemodialysis patients, especially in women and diabetics. A significant reduction of BMD was found in the area of the proximal femur, but not at the lumbar spine. This difference may result from the different effects of parathyroid hormone on cortical and trabecular bone as well as the frequent false elevation of BMD in the lumbar spine in the elderly hemodialysis population. Compared to data obtained from the general population, the present study showed a higher prevalence of low *T*-score values (corresponding to values for osteoporosis) in patients over 50 years. Male gender and calcium levels were positively correlated with BMD at all measured sites. Age was positively correlated with BMD only at the lumbar spine, whereas weight and BMI correlated only in the area of the proximal femur.

ACKNOWLEDGEMENT

Authorship contributions: IV: literature search; IV, ZS, MP, ZC: manuscript writing; IV, JT: study design; IV, RO, JD: data collection; IV, AM, ZS, MP: data analysis; IV: data interpretation; JT: statistical analysis, figures; IV: final approval.

Conflict of interest statement: None declared.

REFERENCES

1. Rix M, Andreassen H, Eskildsen P, Langdahl B, Olgaard K. Bone mineral density and biochemical markers of bone turnover in patients with predialysis chronic renal failure. Kidney Int 1999;56:1084-93.
2. Jamal SA, Swan VJ, Brown JP, Hanley DA, Prior JC, Papaioannou A, Langsetmo L, Josse RG. Kidney function and rate of bone loss at the hip and spine: the Canadian Multicentre Osteoporosis Study. Am J Kidney Dis 2010;55:291-9.
3. Bellorin-Font E, Adams J, Cunningham J. Osteopenia in uremia. In: Olgaard K, Salutsky IB, Silver J, editors. The Spectrum of Mineral and Bone Disorders in Chronic Kidney Disease. New York, NY: Oxford University Press; 2010. p. 235-251.
4. Miller PD. Diagnosis and treatment of osteoporosis in chronic renal disease. Semin Nephrol 2009;29:144-55.
5. Gal-Moscovici A, Sprague SM. Osteoporosis and chronic kidney disease. Semin Dial 2007;5:423-30.
6. Sprague SM. Is bone mineral density measurement of any value in a dialysis patient? Semin Dial 2011;24:433-4.
7. ISCD Official Positions. Available at: http://www.iscd.org/Visitors/pdfs/ISCD2007OfficialPositions-Adult.pdf (accessed November 15, 2012).
8. National Kidney Foundation. K/DOQI clinical practice guidelines for bone metabolism and disease in chronic kidney disease. Am J Kidney Dis 2003;42:1-201.
9. Jean G, Charra B, Chazot C. Vitamin D deficiency and associated factors in hemodialysis patients. J Ren Nutr 2008;5:395-9.
10. Del Valle E, Negri AL, Aguirre C, Fradinger E, Zanchetta JR. Prevalence of 25(OH) vitamin D insufficiency and deficiency in chronic kidney disease stage 5 patients on hemodialysis. Hemodial Int 2007;3:315-21.
11. Hutchinson MS, Figenschau Y, Almás B, Njølstad I, Jorde R. Serum 25-hydroxyvitamin D levels in subjects with reduced glukose tolerance and type 2 diabetes - The Tromsø OGTT-Study. Int J Vitam Nutr Res 2011;81:317-27.
12. Pei Y, Hercz G, Greenwood C, Segre G, Manuel A, Saiphoo C, Fenton S, Sherrard D. Renal osteodystrophy in diabetic patiens. Kidney Int 1993;44:159-64.
13. Felsenfeld AJ, Torres A. Bone histomorphometry in renal osteodystrophy. In: Olgaard K, Salutsky IB, Silver J, editors. The Spectrum of Mineral and Bone Disorders in Chronic Kidney Disease. New York, NY: Oxford University Press; 2010. p.160-161.
14. Murakami R, Murakami S, Tsushima R, Ueda C, Mikami K, Ebina T, Kumasaka R, Nakamura N, Okumura K. Glycaemic control and serum intact parathyroid hormone levels in diabetic patients on haemodialysis therapy. Nephrol Dial Transplant 2008;23:315-20.
15. KDIGO Clinical Practice Guideline for the Diagnosis, Evaluation, Prevention, and Treatment of Chronic Kidney Disease-Mineral and Bone Disorder (CKD-MBD). Kidney Int 2009;76(Suppl.13):32-49.
16. Leonard MB. A structural approach to skeletal fragility in chronic kidney disease. Semin Nephrol 2009;29:133-43.
17. Cunningham J, Sprague SM, Cannata-Andia J, Coco M, Cohen-Solal M, Fitzpatrick L, Goltzmann D, Lafage-Proust MH, Leonard M, Ott S, Rodriguez M, Stehman-Breen C, Stern P, Weisinger J; Osteoporosis Work Group. Osteoporosis in chronic kidney disease. Am J Kidney 2004;3:566-71.
18. Ott SM. Rewiev article: Bone density in patients with chronic kidney disease stages 4-5. Nephrology 2009;14:395-403.
19. Garriguet D. Bone health: osteoporosis, calcium and vitamin D. Health Rep 2011;3:1-8.
20. Vestergaard P, Rejnmark L, Mosekilde L. Osteoporosis is markedly underdiagnosed: a nationwide study from Denmark. Osteoporos Int 2005;16:134-41.
21. Taal MW, Masud T, Green D, Cassidy MJD. Risk factors for reduced bone density in haemodialysis patients. Nephrol Dial Transplant 1999;14:1922-8.
22. Orlic L, Crncevic Z, Pavlovic D, Zaputovic L. Bone mineral densitometry in patients on hemodialysis: difference between genders and what to measure. Renal Failure 2010;32:300-8.
23. Foldes AJ, Arnon E, Popovtzer MM. Reduced speed of sound in tibial bone of haemodialysed patients: association with serum PTH level. Nephrol Dial Transplant 1996;11:1318-21.
24. Nakai T, Masuhara K, Kato K, Kanbara N. Longitudinal measurement of bone mineral density at the radius in hemodialysis patients using dual-energy X-ray absorptiometry. J Muscoloskel Neuron Interact 2001;2:163-5.
25. Binici DN, Gunes N. Risk factors leading to reduce bone mineral density in hemodialysis patients with metabolic syndrome. Renal Failure 2010;32:469-74.
26. Pecovnik Balon B, Hojs R, Zavratnik A, Kos M. Bone mineral density in patients beginning hemodialysis treatment. Am J Nephrol 2002;22:14-7.
27. Rickers H, Christensen M, Rødbro P. Bone mineral content in patients on prolonged maintenance hemodialysis: a three year follow-up study. Clin Nephrol 1983;20:302-7.
28. Ma L, Oei L, Jiang L, Estrada K, Chen H, Wang Z, Yu Q, Zillikens MC, Gao X, Rivadeneira F. Association between bone mineral density and type 2 diabetes mellitus: a meta-analysis of observational studies. Eur J Epidemiol 2012;27:319-32.
29. Zayour D, Daouk M, Medawar W, Salamoun M, El-Hajj Fuleihan G. Predictors of Bone Mineral Density in Patients on Hemodialysis. Transplant Proc 2004;36:1297-301.
30. Elder GJ, Mackun K. 25-hydroxyvitamin D deficiency and diabetes predict reduced BMD in patients with chronic kidney disease. J Bone Miner Res 2006;21:1778-84.
31. Nishitani H, Miki T, Morii H, Nishizawa Y, Ishimura E, Hagiwara S, Nakatsuka K, Yamakawa M. Decreased bone mineral density in diabetic patients on hemodialysis. Contrib Nephrol 1991;90:223-7.
32. Kaji H, Hattori S, Sekita K, Sugimoto T, Chihara K. Factors affecting bone mineral density in hemodialysis patients with diabetic nephropathy. Endocrin J 2003;50:127-33.

33. Inaba M, Okuno S, Kumeda Y, Yamakawa T, Ishimura E, Nishizawa Y. Increased incidence of vertebral fracture in older female hemodialyzed patients with type 2 diabetes mellitus. Calcif Tissue Int 2005;76:256-60.
34. Häussler B, Gothe H, Göl D, Glaeske G, Pientka L, Felsenberg. Epidemiology, treatment and cost of osteoporosis in Germany - the BoneEVA study. Osteoporos Int 2007;18:77-84.
35. Kanis JA, Johnell O, Oden A, Jonsson B, De Laet C, Dawson A. Risk of hip fracture according to the World Health Organization criteria for osteopenia and osteoporosis. Bone 2000;27:585-90.
36. Stehman-Breen C. Bone Mineral Density Measurements in Dialysis Patients. Semin Dial 2001;14:228-9.
37. Jamal SA, West SL, Miller PD. Fracture risk assesment in patients with chronic kidney diesase. Osteoporos Int 2012;23:1191-8.
38. Toussaint ND, Lau KK, Strauss BJ, Polkinghorne KR, Kerr PG. Associations between vascular calcification, arterial stiffness and bone mineral density in chronic kidney disease. Nephrol Dial Transplant 2008;23:586-93.
39. Toussaint ND, Lau KK, Strauss BJ, Polkinghorne KR, Kerr PG. Associations between vascular calcification, arterial stiffness and bone mineral density in a cross-sectional study of prevalent Australian haemodialysis patients. Nephrology 2009;14:105-12.
40. Tomida K, Hamano T, Mikami S, Fujii N, Okada N, Matsui I, Nagasawa Y, Moriyama T, Ito T, Imai E, Isaka Y, Rakugi H. Serum 25-hydroxyvitamin D as an independent determinant of 1-84 PTH and bone mineral density in non-diabetic predialysis CKD patients. Bone 2009;44:678-83.
41. Waugh EJ, Lam MA, Hawker GA, McGowan J, Papaioannou A, Cheung AM, Hodsman AB, Leslie WD, Siminoski K, Jamal SA. Risk factors for low bone mass in healthy 40-60 year old women: a systematic review of the literature. Osteoporos Int 2009;1:1-21.
42. Papaioannou A, Kennedy CC, Cranney A, Hawker G, Brown JP, Kaiser SM, Leslie WD, O'Brien CJ, Sawka AM, Khan A, Siminoski K, Tarulli G, Webster D, McGowan J,Adachi JD. Risk factors for low BMD in healthy men age 50 years or older: a systematic review. Osteoporos Int 2009;4:507-18.
43. Ersoy FF. Osteoporosis in the elderly with chronic kidney disease. Int Urol Nephrol 2007;39:321-31.

19. Oligoclonal free light chains in cerebrospinal fluid as markers of intrathecal inflammation. Comparison with oligoclonal IgG

Zeman D, Hradílek P, Kušnierová P, Píža R, Reguliová K, Woznicová I, Zapletalová O

Originally published in Biomedical Papers, 2015, vol. 159, no. 1, p. 104-113.

Oligoclonal free light chains in cerebrospinal fluid as markers of intrathecal inflammation. Comparison with oligoclonal IgG

David Zeman[a,b,c], Pavel Hradilek[b], Pavlina Kusnierova[a,c], Radim Piza[b], Katarina Reguliova[b], Ivana Woznicova[b], Olga Zapletalova[b]

Aims. To compare the sensitivity and specificity of CSF-restricted oligoclonal IgG and free light chains as markers of multiple sclerosis and other inflammatory neurological diseases.
Methods. 196 paired CSF and serum samples were examined for oligoclonal IgG and oligoclonal free light chains. The sensitivity and specificity of the tests were calculated and optimal cut-offs for the number of CSF-restricted oligoclonal bands were then determined by analysis of receiver operating characteristic curves.
Results. Optimal cut-off values were ≥5 IgG bands for multiple sclerosis, ≥4 IgG bands for inflammatory neurological disease, ≥6 free κ, and ≥2 free λ bands for both purposes. Using these cut-off values, sensitivities and specificities for multiple sclerosis were 83.8% and 91.3% for IgG, 83.8% and 81.0% for free κ, and 67.6% and 75.4% for free λ. For inflammatory neurological disease, sensitivities and specificities were 60.8% and 95.7% for IgG, 69.6% and 92.6% for free κ, and 64.8% and 86.2% for free λ.
Conclusions. Although exact cut-off values may vary according to method, reporting borderline results as positive, may compromise the specificity of the test and should be avoided.. The detection of intrathecal free light chain synthesis may be of value especially when the oligoclonal IgG test is negative or borderline, even though its specificity is slightly lower.

Key words: cerebrospinal fluid, oligoclonal free light chains, oligoclonal IgG

Received: May 29, 2014; Accepted: November 6, 2014; Available online: December 5, 2014
http://dx.doi.org/10.5507/bp.2014.058

[a]Department of Biomedical Sciences, Faculty of Medicine, University of Ostrava, Czech Republic
[b]Clinic of Neurology, University Hospital Ostrava
[c]Department of Clinical Biochemistry, Institute of Laboratory Medicine, University Hospital Ostrava
Corresponding author: David Zeman, e-mail: david.zeman@osu.cz

INTRODUCTION

Intrathecal synthesis of IgG as well as free light chains (fLC) are detectable in the majority of patients with multiple sclerosis (MS) and less frequently in other, mostly inflammatory, nervous system diseases[1,2]. Little information is available however that compares these tests and the existing results are somewhat conflicting.

In their seminal paper on oligoclonal free light chains (o-fLC), Sindic and Laterre reported a method of affinity-mediated immunoblotting (AIB) after isoelectric focusing (IEF) and they found that CSF-restricted free κ light chains can occur even in the absence of oligoclonal IgG (o-IgG) in MS (ref.[3]). This was later confirmed by the same group, showing o-free κ bands in 18 out of 33 o-IgG negative patients who presented isolated symptoms suggestive of MS (ref.[4]). Lamers et al. reported o-free κ in most samples with CSF-restricted o-IgG and only rarely in those without[5]. Similar results were reported by Krakauer et al.[6] using classical passive blotting but prolonged incubation (overnight) with anti-fLC antisera. These authors found o-free λ to be both less sensitive and less specific for MS than o-free κ which was at variance with the earlier reports of Bracco et al.[7] and Gallo et al.[8,9] of o-free λ being more frequent than o-free κ both in MS (ref.[7,8]) and human imunodeficiency virus type 1-infected patients[9]. Lolli et al. studied o-fLC by means of the classical blotting technique; they found o-fLC less frequently than o-IgG (ref.[10]). Vakaet and Thompson used polyacrylamide gel electrophoresis followed by immunoblotting and also found o-fLC less frequently than o-IgG in MS (ref.[11]) and other inflammatory nervous system diseases[12].

Positivity criteria for the o-fLC test are not well established. Usually, ≥2 cerebrospinal fluid (CSF)-restricted oligoclonal bands (OCB) are required for o-IgG (ref.[1,2,13]). However, some authors use different criteria for o-IgG positivity. Mayringer et al.[14] reported 3 bands, which were found to be an optimum cut-off in the context of MS diagnosis in a recent large study[15]. Wurster reported 2 or 3 bands to be a "borderline" finding and used 4 bands as a cut-off value for definitely positive samples[16]. On the other hand, only 1 CSF-restricted band was considered sufficient for o-IgG positivity in another recent study[17].

We therefore decided to analyze o-IgG as well as o-fLC in various disease groups and to compare the sensitivity and specificity of individual tests for MS and inflammatory nervous system diseases (IND) diagnosis in general.

MATERIALS AND METHODS

The study was approved by Ostrava University Hospital Ethics Committee (reference number 615/2011). All patients underwent lumbar puncture (LP) for diagnostic purposes; o-IgG test was always requested by the clinician. All gave written informed consent for the use of the surplus of biological material for research purposes. We examined a total of 196 paired CSF and serum samples for o-IgG and o-fLC. Subsequently, neurologists were asked to provide a diagnosis and samples were then divided into the following groups:

Group I – Multiple sclerosis (MS) at the time of lumbar puncture (n=28): mainly patients with relapsing-remitting MS (n=21); only 5 patients had primary progressive MS and 2 patients secondary progressive MS;

Group II – Clinically isolated syndrome (CIS) (n=42): we simplified the classification of Miller et al.[18] and grouped patients with at least one asymptomatic MRI lesion versus those without;

Group III – CNS infectious diseases (n=13): neuroborreliosis (n=3), varicella zoster virus (VZV) infection (n=2), aseptic meningitis/meningoencephalitis of unknown aetiology (n=4), and 1 case each of sepsis complicated by meningitis, enteroviral meningitis, herpes simplex encephalitis, and tick-borne encephalitis;

Group IV – Other inflammatory CNS diseases (n=9): CNS vasculitis (n=2), idiopathic recurrent myelitis (n=2), and 1 case each of neuromyelitis optica, paraneoplastic cerebellitis, limbic encephalitis, Tolosa-Hunt syndrome, and chorioretinitis;

Group V – Immune-mediated neuropathies (IMN) (n=10): 4 cases of acute and 4 cases of chronic inflammatory demyelinating polyneuropathy, 1 case of acute motor axonal neuropathy and 1 case of polyneuropathy associated with trace amounts of IgM kappa paraprotein and anti-ganglioside IgM reactivity;

Group VI – Non-inflammatory nervous system diseases (NIND) (n=79): included a very wide and heterogeneous spectrum of diagnoses; more frequent were non-inflammatory (mostly diabetic) polyneuropathy (n=9), discarthrosis, spinal canal stenosis and/or radiculopathy (n=6), CNS tumors (n=5), vertigo (n=5), ischaemic stroke (n=4), idiopathic facial nerve palsy (n=3), motor neuron disease (n=3), dementia (n=3), and migraine (n=3);

Group VII – No evidence of organic neurological disorder (control group, n=15): these patients presented mainly with mild mood disorders and/or psychosomatic problems.

For the analysis of the diagnostic value of CSF-restricted OCB tests, an MS group was created of patients fulfilling criteria for definite MS at the time of lumbar puncture (n=28) plus patients presenting CIS who developed definite MS during the follow-up (n=9). The non-MS group consisted of patients in groups III, IV, V, VI and VII. Groups I, II, III, IV and V were considered inflammatory neurological diseases (IND), whereas groups VI and VII were considered "non-inflammatory".

Most patients were not treated by any immunomodulatory agents. However, we identified 30 patients who had received such treatment either at the time of the LP or less than six months prior to it: 7 patients in group I, 9 patients in group II, 2 patients in group III, 4 patients in group IV, 7 patients in group VI and 1 patient in group VII. One patient in the MS group was treated with natalizumab. Five patients were treated with intravenous methylprednisolone (IVMP) at the time of LP (first infusion at least one day before LP) and another five patients received IVMP 2-4 months prior to LP (two of them were still given low-dose oral steroids at the time of the LP). Another three patients were on low-dose oral steroids (in one case in combination with oral azathioprine). These treatments were given for MS or CIS-related symptoms. Another MS patient, suffering from type 1 diabetes with organ complications, received mycophenolate mofetil after previous renal/pancreas transplant, and one CIS patient received infliximab because of psoriasis. One patient with neuroborreliosis had been treated with intravenous dexamethasone several days prior to LP because of radicular syndrome, and a patient with VZV-infection had received oral steroids for facial palsy. A patient with neuromyelitis optica had been treated with oral methylprednisolone and azathioprine and had received a series of plasma exchanges one month prior to LP. One patient with idiopathic recurrent myelitis received IVMP and both patients with CNS vasculitis received low-dose oral steroids. In the NIND group, two patients had been treated with interferon alfa-2a because of polycythaemia vera (one had received intravenous dexamethasone two weeks prior to the LP); two patients with suspected optic neuritis were treated with IVMP (final diagnoses were nasopharyngeal carcinoma with propagation into the orbit in one case and acute hypertonic neuroretinopathy in the other case), one patient received intravenous dexamethasone for radicular syndrome and two patients received low dose oral methylprednisolone in combination with sulfasalazine for rheumatoid arthritis and unspecified arthralgias, respectively. One patient in the control group too, had been treated with oral methylprednisolone because of suspected central limb monoparesis and minimal non-specific MRI changes (the final diagnosis was somatoform disorder).

In the exceptional cases of repeated lumbar punctures, the results of the first sample were used. Heavily blood-contaminated CSFs were not used for the purpose of this study. Microscopic blood contamination was allowed, since no false positive results of the qualitative tests were expected.

CSF and sera were kept at 2-8 °C for up to one week for o-IgG test, and up to three weeks for o-fLC test. Repeated analyses of several samples showed consistent results during this time period. Samples were not frozen before OCB analysis.

o-IgG was detected by means of IEF followed by immunofixation using a commercial kit on Hydrasys instrument (Sebia, Évry Cedex, France, Cat. No. 4355). Standard amounts of IgG were applied. o-fLC were ana-

lyzed in undiluted CSFs and paired sera diluted 1/100 by IEF focusing followed by AIB as originally described by Sindic and Laterre[3] and slightly modified by us[19]. This method combines the advantages of the previously described techniques of AIB (ref.[20]), glutaraldehyde fixation[21], biotin-(strept)avidin amplification[22] and alkaline phosphatase detection[23] to obtain maximum sensitivity. The only difference to our previous report consisted in the prolongation of the incubation time with biotinylated antibodies against free κ and free λ light chains to 105 min, which improved the detection limit for free λ up to 0.75 ng of monoclonal free λ protein. o-IgGκ and o-IgGλ bands were analyzed as described[19], but the amount of applied IgG was reduced to 12 ng. For logistic reasons and/or due to the shortage of antibodies, only 79 samples could be analyzed for the o-IgGκ/IgGλ pattern. The patient group described in this study included none of samples reported in our previous paper.

The results were classified as negative or positive based on the conventional criterion of ≥2 CSF-restricted OCB for positivity. Classification into types 1-5 according to the international consensus for o-IgG (ref.[24,25]) was also performed but for the sake of simplicity is not reported in this paper. CSF-restricted bands were counted and if faint bands only were observed, this was noted. Analysis of receiver operating characteristic (ROC) curves was undertaken to find optimal cut-off values for the number of CSF-restricted OCB.

The predominance of free κ or λ bands was assessed on the basis of visual comparison of the blots, taking into account both the number and intensity of CSF restricted bands. However, at least twice as many bands of one type, compared to the other, were required for judging the predominance of one light chain type.

Statistical analysis was performed using MedCalc software version 11.4.4 (Frank Schoonjans, Belgium). Binomial exact confidence intervals were calculated for individual areas under the curve and the method of DeLong et al.[26] was used to calculate the difference between two areas under the curve. Chi squared tests were used for categorical data.

RESULTS

Table 1 shows the proportions of samples positive for o-IgG, o-free κ and o-free λ in groups I-VII, using conventional criterion of at least 2 CSF-restricted OCB. The presence of o-IgG correlated with the presence of o-free κ as well as o-free λ (chi-square test, $P<0.0001$). Also, the presence of both o-fLC correlated with each other (chi-square test, $P<0.0001$).

Subdividing CIS patients according to Miller et al.[18] showed that the intrathecal humoral immune response strongly correlated with the MRI findings (chi-square test, $P=0.0081$ for o-IgG, $P<0.0001$ for o-free κ and $P=0.0002$ for o-free λ). Only 2/6 patients without at least one asymptomatic MRI lesion displayed CSF-restricted o-IgG (only two bands in both cases), and none displayed CSF-restricted o-fLC bands. In contrast, 32/36 patients with at least one asymptomatic MRI lesion displayed CSF-restricted o-IgG, 33 o-free κ, and 30 o-free λ light chain bands. Nine CIS patients progressed to definite MS during the study. All of these patients had multiple MRI lesions, in 8 cases, CSF-restricted o-IgG as well as o-fLC (both o-free κ and o-free λ in 7 cases and o-free κ only in the remaining case) and 1 patient was OCB-negative in all tests. In CNS infectious diseases, o-fLC were positive

Table 1. Proportion of patients positive for o-IgG, o-free κ and o-free λ in individual disease groups, using conventional criterion of ≥2 CSF-restricted bands.

Group	o-IgG	o-free κ	o-free λ	At least 1 out of the 3 tests	At least 1 of both fLC tests	Both fLC	All tests positive
I (MS; n=28)	23 (82.1%)	24 (85.7%)	18 (64.3%)	25 (89.3%)	24 (85.7%)	18 (64.3%)	17 (60.7%)
II (CIS; n=42)	34 (81.0%)	33 (78.6%)	30 (71.4%)	36 (85.7%)	34 (81.0%)	29 (69.0%)	28 (66.7%)
III (CNS infections; n=13)	4 (30.7%)	11 (84.6%)	9 (69.2%)	12 (92.3%)	12 (92.3%)	8 (61.5%)	3 (23.1%)
IV (OIND; n=9)	5 (55.6%)	7 (77.8%)	6 (66.7%)	7 (77.8%)	7 (77.8%)	8 (88.9%)	5 (55.6%)
V (IMN; n=10)	1 (10.0%)	5 (50.0%)	3 (30.0%)	6 (60.0%)	5 (50.0%)	3 (30.0%)	0 (0%)
VI (NIND; n=79)	10 (12.7%)	18 (22.8%)	13 (16.5%)	23 (29.1%)	21 (26.6%)	10 (12.7%)	5 (6.3%)
VII (control group; n=15)	1 (6.7%)	3 (20.0%)	0 (0%)	3 (20.0%)	3 (20.0%)	0 (0%)	0 (0%)
Total (n=196)	78 (39.8%)	101 (51.5%)	79 (40.3%)	112 (57.1%)	106 (54.1%)	76 (38.7%)	58 (29.6%)

MS, multiple sclerosis; CIS, clinically isolated syndrome; OIND, other inflammatory CNS diseases; IMN, immune-mediated neuropathies; NIND, non-inflammatory nervous system diseases

more frequently than o-IgG. The only o-fLC negative case of a patient with VZV ganglionitis was also negative for o-IgG, but pleocytosis and elevated anti-VZV antibody index were found.

For group IV, all OCB tests were negative in both patients with idiopatic myelitis. One case of CNS vasculitis was borderline positive for o-free κ, while other OCB tests were negative. In the other case of CNS vasculitis, all three OCB tests were positive, as in patients with paraneoplastic cerebellitis, neuromyelitis optica, Tolosa-Hunt syndrome, and chorioretinitis. In the case of limbic encephalitis, both o-fLC tests were positive but the o-IgG test was negative. 9 out of 10 cases of immune-mediated neuropathy (group V) were negative for CSF-restricted IgG bands, whereas 2 CSF-restricted IgG bands were found in the remaining case. Nevertheless, 5 cases were positive for CSF-restricted o-free κ and 3 cases also for o-free λ bands.

Within the NIND group, findings in 5 patients with CNS tumors are worth mentioning in detail. In 3/5 cases, CSF cytology was positive for atypical/malignant cells (highly atypical lymphocytes in 2 cases of the B-CLL and unspecified malignant cells in the case of malignant meningeal infiltration of unknown primary source), whereas only mild lymphocytic pleocytosis was present in the other 2 cases (1 case each of primary CNS lymphoma and glioblastoma). 3 cases were positive for o-IgG and all cases were positive for o-free κ and 3 for o-free λ. An example of OCB findings in one patient of this group is shown in Fig. 1. Other positive cases in the NIND group comprised a wide range of other diagnoses: ischaemic stroke and vestibular syndrome in two cases each and epilepsy, dementia, idiopathic facial palsy, ocular myositis, myasthenia gravis, vertigo, cervicocranial syndrome, cervical myelopathy, spinal stenosis, intervertebral disc herniation with radiculopathy, ischaemic mononeuropathy, toxic/diabetic polyneuropathy, fibromyalgias, headache in patient with monoclonal gammopathy of undetermined significance, tetany, mood disorder and somatoform disorder in one case each). Those cases without proven etiological diagnosis (i.e. with only symptom-related diagnoses) had features atypical for CIS, normal brain CT and/or MRI and no evidence of an infectious cause.

Analysis of samples positive for CSF-restricted o-fLC showed κ fLC predominance in more than half of the cases (62 out of 106 o-fLC positive cases, i.e. 58.5%), whereas free λ predominance was rarely found (9 out of 106 cases, i.e. 8.5%). Free κ/λ light chain predominance correlated well with the predominance of κ/λ light chains in IgG (chi-square test, $P<0.0001$), although IgGκ predominance was found somewhat less frequently than that of free κ (13 out of 32 positive cases, i.e. 40.6%).

Although there were similar frequencies of o-IgG and o-free κ positivity in groups I and II, o-free κ were positive more frequently than o-IgG not only in the other "inflammatory" groups III, IV and V, but also in the "non-inflammatory" groups VI and VII. This finding led us to search for an optimal criterion for positivity of individual tests.

Fig. 2 shows fewer CSF-restricted bands in patients in NIND and control groups than in IND patients. We there-

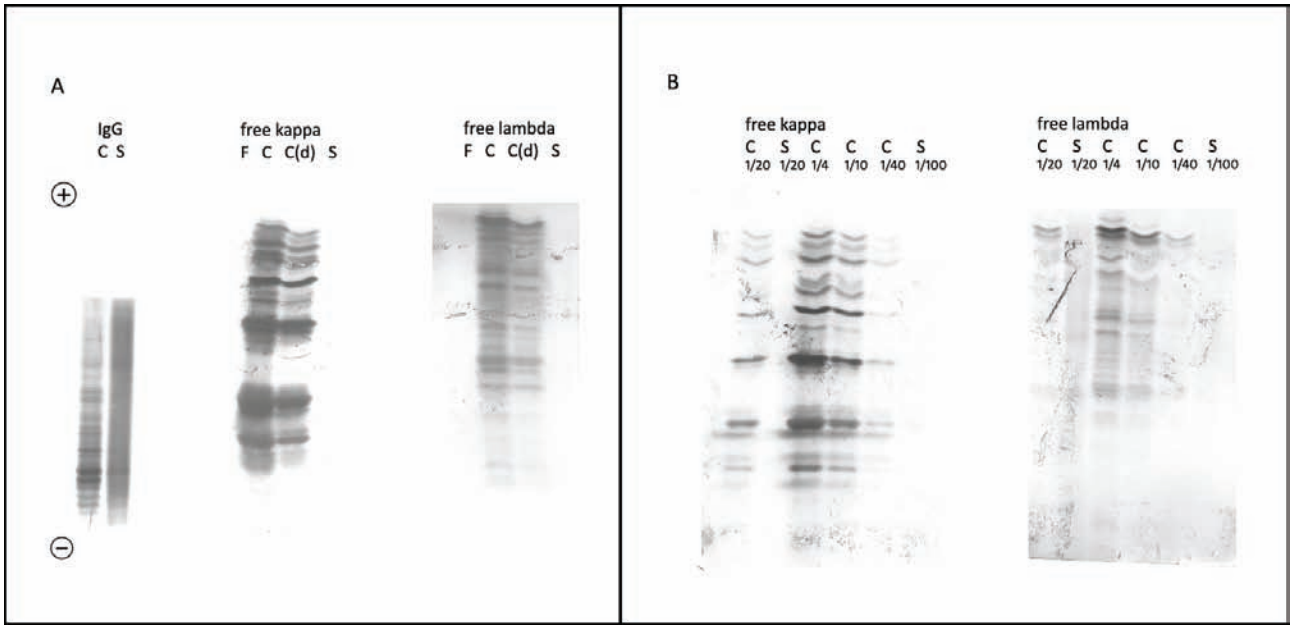

Fig. 1. Pronounced intrathecal IgG and fLC synthesis in the case of malignant meningeal infiltration.
C, cerebrospinal fluid; S, serum; F, Flebogamma (intravenous IgG preparation – negative control); (d), diluted 1/4. (A) CSF-restricted oligoclonal IgG, free κ and free λ bands. For fLC analysis, CSF sample was examined neat as well as diluted 1/4. (B) Dilution experiments showing CSF-restricted o-fLC bands even when CSF and serum were equally diluted (1/20). Higher concentration of CSF fLC than in serum can be assumed. Indeed, using Freelite kit on the SPA Analyzer (The Binding Site, Birmingham, United Kingdom), we measured CSF free κ and free λ 80.5 mg/L and 32.2 mg/L, respectively, whereas serum free κ and free λ concentrations were 14.5 mg/L and 12.1 mg/L, respectively.

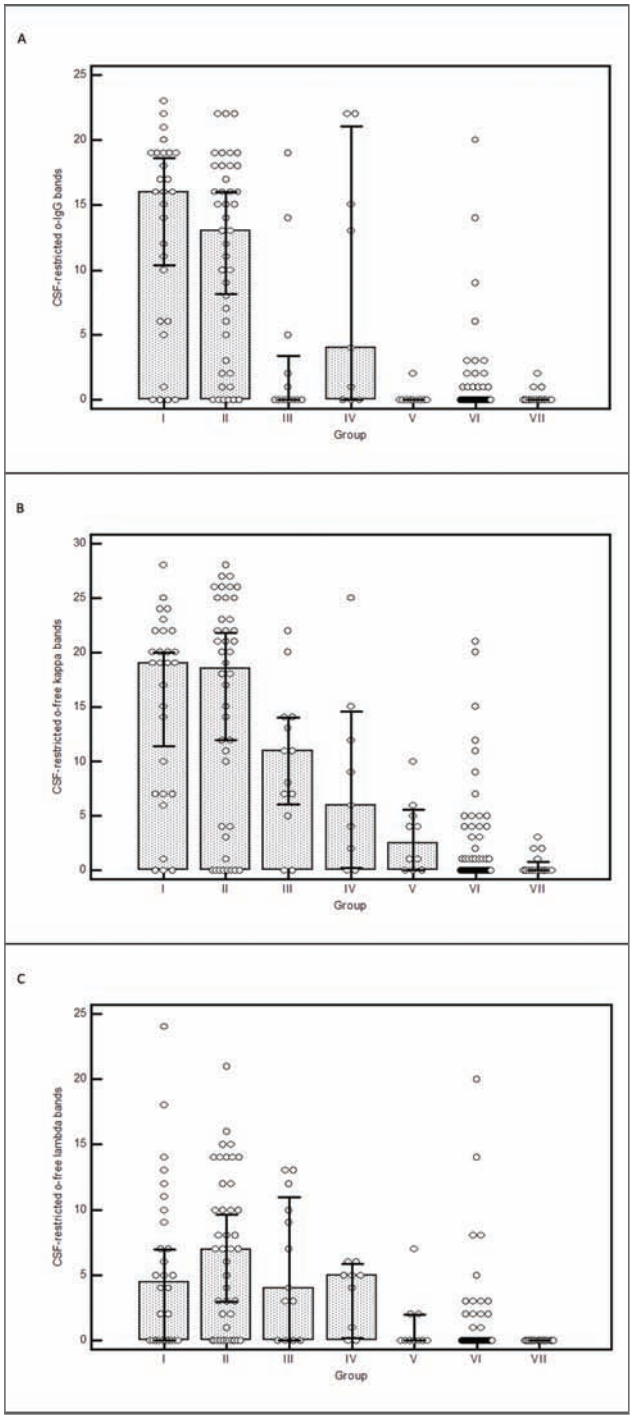

Fig. 2. Numbers of CSF-restricted oligoclonal bands in the individual disease groups. Bars for medians; error bars: 95% confidence intervals for medians
I = multiple sclerosis, II = clinically isolated syndrome, III = CNS infectious diseases, IV = other inflammatory CNS diseases, V = immune-mediated neuropathies, VI = non-inflammatory neurologic diseases, VII = control group. (A) oligoclonal IgG, (B) oligoclonal free κ, (C) oligoclonal free λ.

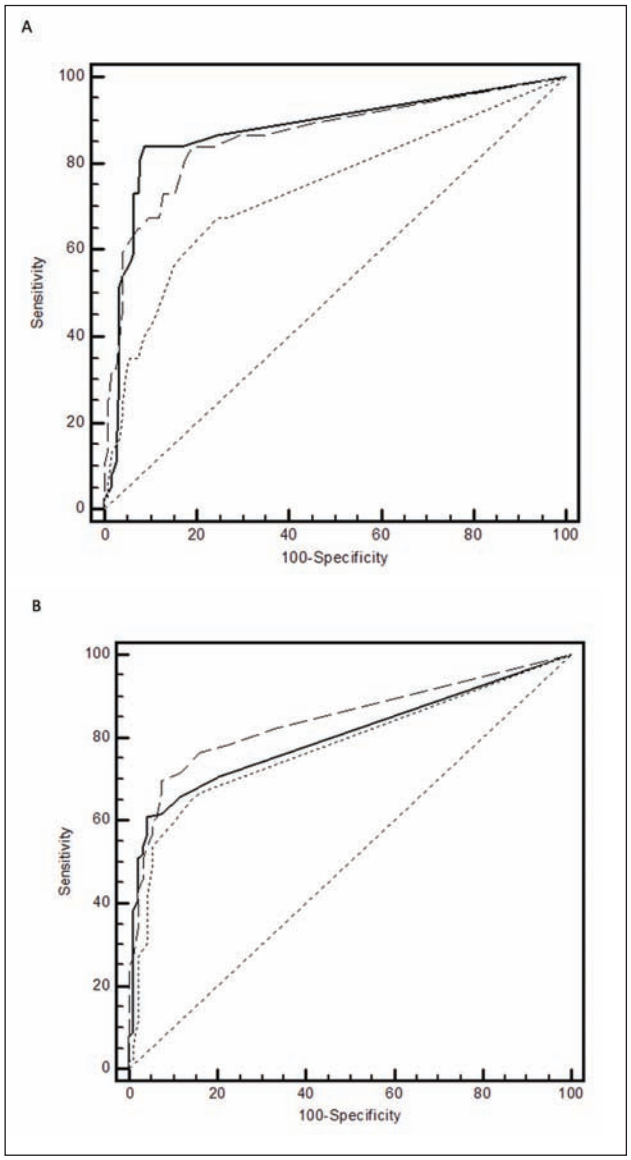

Fig. 3. Comparison of ROC curves for o-IgG (solid line), o-free κ (dashed line) and o-free λ (dotted line).
(A) For the diagnosis of multiple sclerosis. (B) For the diagnosis of inflammatory nervous system disease. For MS diagnosis, AUC values were 0.876 (95% CI: 0.816-0.923), 0.862 (95% CI: 0.800-0.911), and 0.739 (95% CI: 0.664-0.804); for IND diagnosis, AUC values were 0.802 (95% CI: 0.739-0.855), 0.843 (95% CI: 0.784-0.891) and 0.777 (95% CI: 0.712-0.833), for o-IgG, o-free κ and o-free λ respectively (P<0.0001 in all cases). Differences between areas were significant for o-IgG versus o-free λ (P=0.0008) and o-free κ versus o-free λ (P=0.0026) in A, and between o-free κ versus o-free λ (P=0.0059) in B.

Table 2. Sensitivity and specificity of CSF-restricted OCB for the diagnosis of MS or inflammatory neurologic disorder (IND) in general, using different cut-off values.

		MS		IND	
		Sensitivity (95% CI)	Specificity (95% CI)	Sensitivity (95% CI)	Specificity (95% CI)
o-IgG	**≥5 for MS, ≥4 for IND**	**83.8** (68.0-93.8)	**91.3** (84.9-95.6)	**60.8** (50.6-70.3)	**95.8** (89.5-98.8)
	≥2	83.8 (68.0-93.8)	83.3 (75.7-89.4)	65.7 (55.6-74.8)	88.3 (80.0-94.0)
	At least 1	86.5 (71.2-95.5)	75.4 (66.9-82.6)	70.6 (60.7-79.2)	79.8 (70.2-87.4)
o-free kappa	**≥6**	**83.8** (68.0-93.8)	**81.0** (73.0-87.4)	**69.6** (59.7-78.3)	**92.6** (85.3-97.0)
	≥2	86.5 (71.2-95.5)	65.1 (56.1-73.4)	78.4 (69.2-86.0)	77.7 (67.9-85.6)
	At least 1	89.2 (74.6-97.0)	55.6 (46.4-64.4)	82.4 (73.6-89.2)	67.0 (56.6-76.4)
o-free lambda	**≥2**	**67.6** (50.2-82.0)	**75.4** (66.9-82.6)	**64.7** (54.6-73.9)	**86.2** (77.5-92.4)
	At least 1	67.6 (50.2-82.0)	73.0 (64.4-80.5)	66.7 (56.6-75.7)	84.0 (75.0-90.8)

CI, confidence interval
Please note that MS group in Tables 3 and 4 is not identical with group I but comprises patients of group I (n=28) plus those patients presenting with CIS who developed definite MS during follow-up (n=9). The IND group consists of patient groups I-V. Sensitivity is defined as the percentage of patients having MS or IND positive for CSF-restricted OCB; specificity for MS is defined as percentage of patients from groups III-VII without CSF-restricted OCB; specificity for IND is defined as percentage of patients from groups VI and VII without CSF-restricted OCB.
Calculated optimal cut-off values and appropriate sensitivities and specificities are indicated in bold.

Table 3. Sensitivity and specificity of CSF-restricted OCB combined tests for the diagnosis of MS or inflammatory neurologic disorder in general, using different cut-off values.

Combined test	Positivity criteria	MS		IND	
		Sensitivity	Specificity	Sensitivity	Specificity
At least 1 OCB test +	Conventional (≥2 CSF-restricted bands)	89.2	59.5	84.3	72.3
	Excluding weak bands	86.5	65.1	77.5	74.5
	Using optimal cut-off values	**89.2**	**69.8**	**77.5**	**80.9**
At least 1 fLC OCB test +	Conventional (≥2 CSF-restricted bands)	86.5	61.9	80.4	74.5
	Excluding weak bands	83.8	66.7	74.5	75.5
	Using optimal cut-off values	**86.5**	**70.6**	**76.5**	**81.9**
Both fLC OCB tests +	Conventional (≥2 CSF-restricted bands)	67.6	77.0	64.7	89.4
	Excluding weak bands	62.2	84.9	53.9	94.7
	Using optimal cut-off values	**67.6**	**85.7**	**57.8**	**96.8**
All OCB tests +	Conventional (≥2 CSF-restricted bands)	64.9	89.7	52.0	94.7
	Excluding weak bands	59.5	92.1	43.1	96.8
	Using optimal cut-off values	**64.9**	**92.9**	**48.0**	**97.9**

Optimal cut-off values for the number of CSF-restricted bands: ≥4 for o-IgG; ≥6 for free κ and ≥2 for free λ. For the sake of simplicity, minor difference in optimal cut-off values for o-IgG bands (≥5 for MS and ≥4 for IND) was not taken into account and the criterion of ≥4 o-IgG bands was used for both groups. Sensitivities and specificities using optimal cut-off values are shown in bold. See also legend to Table 2 for details.

fore compared and analyzed ROC curves to determine the optimal cut-off values of the number of CSF-restricted bands, for the MS and IND diagnoses (Fig. 3).

An optimal cut-off for positivity was estimated to be ≥5 IgG bands for MS and ≥4 IgG bands for IND; for fLC bands, optimal cut-off values were the same for both purposes, namely ≥6 for free κ and ≥2 for free λ.

The specificity and sensitivity of the tests using calculated optimal cut-off values or a conventional cut-off value of ≥2 bands or at least 1 CSF-restricted band were compared (Tables 2 and 3).

We tested whether specificity could be increased if weak bands were ignored. This, however, decreased the sensitivity and failed to help increase the specificity (Table 3). In contrast, using optimal cut-off values helped

CSF analysis (except for primary progressive MS fulfilling only 1 of 2 MRI criteria) (ref.[13]), most neurologists still recommend CSF examination as an important tool to exclude alternative diagnosis in CIS patients as well as to increase the predictive value for conversion to clinically definite MS (ref.[36]). It has been demonstrated that the presence of OCB considerably increases the risk of suffering a second attack even in MRI-negative patients[37] and, in contrast, that as many as 50% of MRI-positive but OCB-negative CIS patients were finally diagnosed as having diseases other than MS during the follow-up[38].

Different properties of fLC monomers and dimers have been reported, as well as a more specific CSF fLC profile for MS using sodium dodecyl sulfate-polyacrylamide gel electrophoresis (SDS-PAGE) separation[40,41]. Interestingly, we also found two types of CSF-restricted oligoclonal patterns in MS patients: one with a predominance of κ light chains and the other with both CSF-restricted κ as well as λ light chains (Fig. 4). These two types may correspond to patients with the elevation of free κ monomers and free λ dimers in CSF in the study of Kaplan et al.[41] On the other hand, free λ predominance was rare in our study. It would be interesting to demonstrate whether κ light chain predominance is associated with more or less aggressive course of the disease compared to balanced κ and λ light chain intrathecal production. The value of elevated CSF free κ concentrations for predicting disability progression has already been reported[41,42], but no ratio of CSF free κ to CSF free λ concentrations has been sought for. Further studies on similar relationships are warranted. Although the value of quantitative analysis prior to IEF is questioned by some authors[43,44], it would be interesting to apply standardized amounts of fLC in both CSF and serum for IEF analysis. This would, however, require precise fLC quantification in both fluids that is difficult to achieve for the low concentrations that occur in normal CSFs (ref.[45]). Up to now, there is no commercially available method explicitly designated for fLC measurement in the CSF, and absolute values obtained by various ELISAs or nephelometric assays modified for fLC measurement in the CSF are quite discrepant[5,33,46-50]. Also, greater dilution of samples would require more sensitive, e.g. luminescent, detection of o-fLC on the membranes. We are not aware of any study using such an approach for o-fLC. Recently, quantitation of CSF free κ light chains has been compared with o-IgG test in MS and CIS patients with encouraging results[51-53]. We believe that CSF fLC concentrations should be compared with the o-fLC test as well. It is known that qualitative analysis of o-IgG is more sensitive for the demonstration of intrathecal IgG synthesis than quantitative tests. However, this might not be true for fLC; indeed, correlation between quantitative and qualitative tests is much better than for IgG, and no or only marginal increase in sensitivity has been achieved with the qualitative test compared to fLC quantitation in two studies[3,5].

Unlike Kaplan et al.[39,40], the specificity of our o-fLC test was lower than that of the o-IgG test. This might point to a more important role of fLC dimerization status (on which no information is available using IEF) than that of free κ/λ proportion in the pathophysiology of MS, as it has been shown recently that fLC monomers and dimers are differentially secreted by plasma cells and functionally distinct[54]. Methods yielding combined information on both molecular weight and isoelectric point were described for fLC (ref.[55]), but these are technically more demanding and hardly applicable in routine clinical laboratories.

The antigen specificity of fLC (ref.[3,54]) should also be addressed in future studies. Only one study demonstrating antigen-specific fLC in the CSF was found[56]. These authors failed to demonstrate *Toxoplasma gondii*-specific fLC in AIDS patients with *T. gondii* encephalitis using IEF/AIB:although o-fLC were found in all patients; antigen-specific fLC were demonstrated by ELISA instead. The way Villar et al. described CSF-restricted lipid-specific oligoclonal IgM bands[57], we can speculate whether CSF-restricted fLC could have the same specificity.

The main limitation of this study was patient selection. Although we attempted to investigate all consecutive samples sent for routine immunochemical CSF analyses, for logistic reasons this was not possible. Instead, after the publication of our previous study, we were frequently asked for o-fLC tests by clinicians. The neurologists were hence not blind to the results. However, it is rather unlikely that this could lead to misdiagnosis of MS since current MS diagnostic criteria[13] do not usually rely on CSF findings. Inclusion of patients treated with immunomodulatory agents may also be considered problematic. Changes in o-IgG patterns after such therapies have been described by some authors[58-60] but not others[61,62]. It should be noted, however, that the only natalizumab-treated patient in our study had numerous CSF-restricted o-IgG (o-IgGκ only) as well as o-free κ (but no o-free λ) bands, and that we found no significant difference either in the numbers of CSF-restricted o-IgG or o-fLC bands or in the proportions of positive samples in treated and untreated MS patients (data not shown). However, the study was not aimed at looking for these differences. Collection of larger data sets and analysis of paired pre- and post-treatment samples are clearly warranted to analyze the effect of treatment on o-IgG and o-fLC profile in detail.

There are two other concerns that might complicate the interpretation of the results. First, the inclusion of CIS patients who did not progress to definite MS in inflammatory neurological disease group remains speculative; it cannot be excluded that some of these patients suffered from a non-inflammatory condition.

Second, an optimal cut-off for the decision between negative or positive can vary for different OCB detection techniques.

One may argue that using sensitive IEF/AIB method for both o-IgG as well as for o-fLC detection would be more appropriate than comparison with routine o-IgG detection method. However, evaluation of an in-house method requires comparison with a widely used routine method rather than with another in-house method. In addition, we found no clinically significant difference between routine IEF with immunofixation (Sebia) and in-house IEF/AIB method for o-IgG detection[27].

CONCLUSIONS

For MS diagnosis, the CSF-restricted o-fLC test has similar sensitivity to the oligoclonal IgG test but lower specificity. For other inflammatory nervous system diseases, o-fLCs are more frequent than oligoclonal IgG. Detection of intrathecal fLC synthesis for routine clinical purposes is meaningful only when the o-IgG test is negative or borderline. Reporting borderline OCB results as positive, compromises the specificity of the test both for MS and IND and thus should be avoided. While we tried to assess the utility of the test for IND in general and to discuss unexpected findings in non-MS cases in more detail, further studies directed more specifically to the CIS and MS patients are warranted.

ACKNOWLEDGEMENT

The authors are indebted to Assoc. Prof. Kristian Safarcik, Head of the Dept. of Biomedical Sciences, University of Ostrava, and Dr. Zdenek Svagera, Head of the Dept. of Clinical Biochemistry, University Hospital Ostrava for their continuous support; to Ilona Faruzelova, Lenka Fürstova, Renata Maleckova, and Olga Michnova for performing routine o-IgG analyses; to Monika Hradecka for language corrections; to Frantisek Vsiansky for his advice on reporting the results of statistical analysis; and to Filip Chadzijski for his help in preparing figures for the manuscript.

Authorship contributions: DZ, PH, PK, OZ: study design; DZ, PK: evaluation of o-IgG and o-fLC tests; DZ, PH, RP, KR, IW, OZ: clinical data collection and management; DZ, PK, PH, RP, KR, IW, OZ: data analysis; DZ, PH, PK, OZ: manuscript drafting; DZ, PH, PK, RP, KR, IW, OZ: final approval.

Conflict of interest statement: The authors state that there are no conflicts of interest regarding the publication of this article.

REFERENCES

1. Sindic CJ, Van Antwerpen MP, Goffette S. The intrathecal humoral immune response: laboratory analysis and clinical relevance. Clin Chem Lab Med 2001;39:333-40.
2. Link H, Huang YM. Oligoclonal bands in multiple sclerosis cerebrospinal fluid: An update on methodology and clinical usefulness. J Neuroimmunol 2006;180:17-28.
3. Sindic CJ, Laterre EC. Oligoclonal free kappa and lambda bands in the cerebrospinal fluid of patients with multiple sclerosis and other neurological diseases. An immunoaffinity-mediated capillary blot study. J Neuroimmunol 1991;33:63-72.
4. Goffette S, Schluep M, Henry H, Duprez T, Sindic CJ. Detection of oligoclonal free kappa chains in the absence of oligoclonal IgG in the CSF of patients with suspected multiple sclerosis. J Neurol Neurosurg Psychiatry 2004;75:308-10.
5. Lamers KJ, de Jong JG, Jongen PJ, Kock-Jansen MJ, Teunesen MA, Prudon-Rosmulder EM. Cerebrospinal fluid free kappa light chains versus IgG findings in neurological disorders: qualitative and quantitative measurements. J Neuroimmunol 1995;62:19-25.
6. Krakauer M, Schaldemose Nielsen H, Jensen J, Sellebjerg F. Intrathecal synthesis of free immunoglobulin light chains in multiple sclerosis. Acta Neurol Scand 1998;98:161-5.
7. Bracco F, Gallo P, Menna R, Battistin L, Tavolato B. Free light chains in the CSF in multiple sclerosis. J Neurol 1987;234:303-7.
8. Gallo P, Tavolato B, Bergenbrant S, Sidén Å. Immunoglobulin light chain patterns in the cerebrospinal fluid. A study with special reference to the occurrence of free light chains in cerebrospinal fluid with and without oligoclonal immunoglobulin G. J Neurol Sci 1989;94:241-53.
9. Gallo P, Piccinno MG, De Rossi A, Pagni S, Amadori A, Chieco-Bianchi L, Tavolato B. Free light chains of immunoglobulins in the cerebrospinal fluid of human immunodeficiency virus type 1-infected patients. J Neuroimmunol 1990;26:229-38.
10. Lolli F, Siracusa G, Amato MP, Fratiglioni L, Dal Pozzo G, Galli E, Amaducci L. Intrathecal synthesis of free immunoglobulin light chains and IgM in initial multiple sclerosis. Acta Neurol Scand 1991;83:239-43.
11. Vakaet A, Thompson EJ. Free light chains in the cerebrospinal fluid: an indicator of recent immunological stimulation. J Neurol Neurosurg Psychiatry 1985;48:995-8.
12. McLean BN, Miller D, Thompson EJ. Oligoclonal banding of IgG in CSF, blood-brain barrier function, and MRI findings in patients with sarcoidosis, systemic lupus erythematosus, and Behçet's disease involving the nervous system. J Neurol Neurosurg Psychiatry 1995;58:548-54.
13. Polman CH, Reingold SC, Banwell B, Clanet M, Cohen JA, Filippi M, Fujihara K, Havrdova E, Hutchinson M, Kappos L, Lublin FD, Montalban X, O'Connor P, Sandberg-Wollheim M, Thompson AJ, Waubant E, Weinshenker B, Wolinsky JS. Diagnostic criteria for multiple sclerosis: 2010 revisions to the McDonald criteria. Ann Neurol 2011;69:292-302.
14. Mayringer I, Timeltaler B, Deisenhammer F. Correlation between the IgG index, oligoclonal bands in CSF, and the diagnosis of demyelinating diseases. Eur J Neurol 2005;12:527-30.
15. Bourahoui A, de Seze J, Guttierez R, Onraed B, Hennache B, Ferriby D, Stojkovic T, Vermersch P. CSF isoelectrofocusing in a large cohort of MS and other neurological diseases. Eur J Neurol 2004;11:525-9.
16. Wurster U. The clinical significance of an intrathecal monoclonal immunoglobulin band: A follow up study. Letter to the Editor. Neurology 2004;62:1237.
17. Lourenco P, Shirani A, Saeedi J, Oger J, Schreiber WE, Tremlett H. Oligoclonal bands and cerebrospinal fluid markers in multiple sclerosis: associations with disease course and progression. Mult Scler 2012;19:577-84.
18. Miller DH, Weinshenker BG, Filippi M, Banvell BL, Cohen JA, Freedman MS, Galetta SL, Hutchinson M, Johnson RT, Kappos L, Kira J, Lublin FD, McFarland HF, Montalban X, Panitch H, Richert JR, Reingold SC, Polman CH. Differential diagnosis of suspected multiple sclerosis: a consensus approach. Mult Scler 2008;14:1157-74.
19. Zeman D, Hradílek P, Švagera Z, Mojžíšková E, Woznicová I, Zapletalová O.. Detection of oligoclonal IgG kappa and IgG lambda using Hevylite antibodies. Comparison with oligoclonal free light chain pattern. Fluids Barriers CNS 2012;9:5.
20. Knisley KA, Rodkey LS. Affinity immunoblotting. High resolution isoelectric focusing analysis of antibody clonotype distribution. J Immunol Methods 1986;95:79-87.
21. Ikegati N, Kennet RH. Glutaraldehyde fixation of the primary antibody-antigen complex on nitrocelulose paper increases the overall sensitivity of immunoblot assay. J Immunol Methods 1989;124:205-10.
22. Olsson T, Kostulas V, Link H. Improved detection of oligoclonal IgG in cerebrospinal fluid by isoelectric focusing in agarose, double-antibody peroxidase labeling, and avidin-biotin amplification. Clin Chem 1984;30:1246-9.
23. Sádaba MC, González-Porqué P, Masjuan J, Álvarez-Cermeño JC, Bootello A, Villar LM. An ultrasensitive method for the detection of oligoclonal IgG bands. J Immunol Methods 2004;284:141-5.
24. Andersson M, Alvarez-Cermeño J, Bernardi G, Cogato I, Fredman P, Frederiksen J, Fredrikson S, Gallo P, Grimaldi LM, Grønning M, Keir G, Lamers K, Link H, Magalhães A, Massaro AR, Öhman S, Reiber H, Rönnbäck L, Schluep M, Schuller E, Sindic CJ, Thompson EJ, Trojano M, Wurster U. Cerebrospinal fluid in the diagnosis of multiple sclerosis: a consensus report. J Neurol Neurosurg Psychiatry 1994;57:897-902.
25. Freedman MS, Thompson EJ, Deisenhammer F, Giovannoni G, Grimsley G, Keir G, Öhman S, Racke MK, Sharief M, Sindic CJ,

Sellebjerg F, Tourtellotte WW. Recommended standard of cerebrospinal fluid analysis in the diagnosis of multiple sclerosis. Arch Neurol 2005;62:865-70.
26. DeLong ER, DeLong DM, Clarke-Pearson DL. Comparing the areas under two or more correlated receiver operating characteristic curves: a non-parametric approach. Biometrics 1988;44:837-45.
27. Novackova L, Zeman D. Detection of oligoclonal IgG bands in cerebrospinal fluid and serum: comparison between commercial immunofixation method and home-made affinity immunoblotting method and evaluation of interobserver agreement. Klin Biochem Metab 2011;19:229-33.
28. Lin MW, Suan D, Lenton K, Henniker T, Burke T, Vucic S, Fulcher DA. Differentiating patterns of oligoclonal banding in the cerebrospinal fluid improves diagnostic utility for multiple sclerosis. Pathology 2012;44:248-50.
29. Davies G, Keir G, Thompson EJ, Giovannoni G. The clinical significance of an intrathecal monoclonal immunoglobulin band: a follow-up study. Neurology 2003;60:1163-6.
30. Franciotta D, Bergamaschi R, Amato MP, Zardini E, Persico A, Portaccio E, Lolli F. Clinical correlations of CSF single IgG bands. J Neurol 2005;252:1274-5.
31. Absalom S, Shah S. Differentiating patterns of oligoclonal banding in the cerebrospinal fluid and the diagnosis of multiple sclerosis. Pathology 2013;45:441-2.
32. Dobson R, Ramagopalan S, Davis A, Giovannoni G. Cerebrospinal fluid oligoclonal bands in multiple sclerosis and clinically isolated syndromes: a meta-analysis of prevalence, prognosis and effect of latitude. J Neurol Neurosurg Psychiatry 2013;84:909-14.
33. Arneth B, Birklein F. High sensitivity of free lambda and free kappa light chains for detection of intrathecal immunoglobulin synthesis in cerebrospinal fluid. Acta Neurol Scand 2009;119:39-44.
34. Reiber H. Free light chains in CSF – pushing a method with biased interpretations. Letter to the editor. Acta Neurol Scand 2009;120:445-6.
35. Arneth B. Author's response to professor Reiber's second letter concerning our article: High sensitivity of free lambda and free kappa light chains for the detection of intrathecal immunoglobulin synthesis in cerebrospinal fluid. Acta Neurol Scand 2009; 120:451-2.
36. Tumani H, Deisenhammer F, Giovannoni G, Gold R, Hartung HP, Hemmer B, Hohlfeld R, Otto M, Stangel M, Wildemann B, Zettl UK. Revised McDonald kriteria: the persisting importance of cerebrospinal fluid analysis. Letter to the Editor. Ann Neurol 2011;70:520.
37. Tintoré M, Rovira A, Río J, Tur C, Pelayo R, Nos C, Téllez N, Perkal H, Comabella M, Sastre-Garriga J, Montalban X. Do oligoclonal bands add information to MRI in first attacks of multiple sclerosis? Neurology 2008;70:1079-83.
38. Zipoli V, Hakiki B, Portaccio E, Lolli F, Siracusa G, Giannini M, Pantoni L, Pescini F, Sorbi S, Amato MP. The contribution of cerebrospinal fluid oligoclonal bands to the early diagnosis of multiple sclerosis. Mult Scler 2009;15:472-8.
39. Kaplan B, Aizenbud BM, Golderman S,Yaskariev R, Sela BA. Free light chain monomers in the diagnosis of multiple sclerosis. J Neuroimmunol 2010;229:263-71.
40. Kaplan B, Golderman S, Yahalom G, Yeskaraev R, Ziv T, Aizenbud BM, Sela BA, Livneh A. Free light chain monomer-dimer patterns in the diagnosis of multiple sclerosis. J Immunol Methods 2013;390:74-80.
41. Rudick RA, Medendorp SV, Namey M, Boyle S, Fischer J. Multiple sclerosis progression in a natural history study: Predictive value of cerebrospinal fluid free kappa light chains. Mult Scler 1995;1:150-5.
42. Rinker JR, Trinkaus K, Cross AH. Elevated CSF free kappa light chains correlate with disability prognosis in multiple sclerosis. Neurology 2006;67:1288-90.
43. Thompson EJ. Quality versus quantity: Which is better for cerebrospinal fluid IgG? Clin Chem 2004;50:1721-2.
44. Keir G, Barrio S, Thompson EJ. Discrepancies between qualitative and quantitative analysis of cerebrospinal fluid IgG: densitometric comparison of nephelometry-silver versus immuno-enzymes. Ann Clin Biochem 2008;45:404-8.
45. Nakano T, Miyazaki S, Takahashi H, Matsumori A, Maruyama T, Komoda T, Nagata A. Immunochemical quantification of free immunoglobulin light chains from an analytical perspective. Clin Chem Lab Med 2006;44:522-32.
46. Fagnart OC, Sindic CJM, Laterre C. Free kappa and lambda light chain levels in the cerebrospinal fluid of patients with multiple sclerosis and other neurological diseases. J Neuroimmunol 1988;19:119-32.
47. Lolli F, Amaducci L. Measurement of free kappa immunoglobulin light chains in the cerebrospinal fluid by a competitive avidin-biotin ELISA. Clin Chim Acta 1989;182:229-34.
48. Fischer C, Arneth B, Koehler J, Lotz J, Lackner KJ. Kappa free light chains in cerebrospinal fluid as markers of intrathecal immunoglobulin synthesis. Clin Chem 2004;50:1809-13.
49. Desplat-Jégo S, Feuillet L, Pelletier J, Bernard D, Chériff AA, Boucraut J. Quantification of immunoglobulin free light chains in cerebrospinal fluid by nephelometry. J Clin Immunol 2005;25:338-45.
50. Presslauer S, Milosavljevic D, Brücke T, Bayer P, Hübl W. Elevated levels of kappa free light chains in CSF support the diagnosis of multiple sclerosis. J Neurol 2008;255:1508-14.
51. Villar LM, Espiño M, Costa-Frossard L, Muriel A, Jiménez J, Álvarez-Cermeño JC. High levels of cerebrospinal fluid free kappa chains predict conversion to multiple sclerosis. Clin Chim Acta 2012;413:1813-6.
52. Presslauer S, Milosavljevic D, Huebl W, Parigger S, Schneider-Koch G, Bruecke T. Kappa free light chains: diagnostic and prognostic relevance in MS and CIS. PLoS One 2014;9(2):e89945.
53. Senel M, Tumani H, Lauda C, Presslauer S, Mojib-Yezdani R, Otto M, Brettschneider J. Cerebrospinal fluid immunoglobulin kappa light chain in clinically isolated syndrome and multiple sclerosis. PLoS One 2014;9(4):e88680.
54. Groot Kormelink T, Blokhuis BR, Kil L, Hendriks R, Redegeld FA. Immunoglobulin free light chain monomers and dimers are differentially secreted by plasma cells and are functionally distinct. In: Groot Kormelink T. Immunoglobulin free light chains in inflammatory diseases. New findings on FLCs fitted into current concepts of immune regulation. Thesis. GVO/Ponson & Looijen B.V., Ede, The Netherlands 2012:187-203.
55. Kaplan B, Ramirez-Alvarado M, Dispenzieri A, Zeldenrust SR, Leung N, Livneh A, Gallo G. Isolation and biochemical characterization of plasma monoclonal free light chains in amyloidosis and multiple myeloma: a pilot study of intact and truncated forms of light chains and their charge properties. Clin Chem Lab Med 2008;46:335-41.
56. Contini C, Gainardi E, Cultrera R, Seraceni S, Castellazi M, Peyron F, Granieri E. Evidence of cerebrospinal fluid free kappa light chains in AIDS patients with Toxoplasma gondii encephalitis. J Neuroimmunol 2000;108:221-6.
57. Villar LM, Sádaba MC, Roldán E, Masjuan J, González-Porqué P, Villarrubia N, Espiño M, García-Trujillo JA, Bootello A, Alvarez-Cermeño JC. Intrathecal synthesis of oligoclonal IgM against myelin lipids predicts an aggressive disease course in MS. J Clin Invest 2005;115:187-94.
58. Anderson TJ, Donaldson IM, Sheat JM, George PM. Methylprednisolone in multiple sclerosis exacerbation: changes in CSF parameters. Aust N Z J Med 1990;20:794-7.
59. Mares J, Muchova B, Herzig R, Urbanek K. Changes in the pattern of oligoclonal bands in the cerebrospinal fluid of patients with multiple sclerosis during therapy with beta interferons, and glatiramer acetate respectively. Pilot study. Ces a Slov Neurol Neurochir 2003;66/99:118-20.
60. Von Glehn F, Farias AS, de Oliveira AC, Damasceno A, Longhini AL, Oliveira EC, Damasceno BP, Santos LM, Brandao CO. Disappearance of cerebrospinal fluid oligoclonal bands after natalizumab treatment of multiple sclerosis patients. Mult Scler 2012;18:1038-41.
61. Tourtellotte WW. The cerebrospinal fluid in multiple sclerosis. In: Vinken JP, Bruyn GW, Klawans HL, Koetsier JC, editors. Handbook of Clinical Neurology Vol. 47. Demyelinating diseases. Rev. ser. 3. Amsterdam: Elsevier; 1985. p. 79-130.
62. Rudick RA, Cookfair DL, Simonian NA, Ransohoff RM, Richert JR, Jacobs LD, Herndon RM, Salazar AM, Fischer JS, Granger CV, Goodkin DE, Simon JH, Bartoszak DM, Bourdette DN, Braiman J, Brownscheidle CM, Coats ME, Cohan SL, Dougherty DS, Kinkel RP, Mass MK, Munchsauer FE, O'Reilly K, Priore RL, Pullicino PM, Scherokman BJ, Wende K, Weinstock-Guttman B, Whitham RH, The Multiple Sclerosis Collaborative Research Group. Cerebrospinal fluid abnormalities in a phase III trial of Avonex (IFN-beta 1a) for relapsing multiple sclerosis. J Neuroimmunol 1999;93:8-14.

20. A new modified technique for the treatment of high-risk prethreshold ROP under the direct visual control of RetCam 3

Timkovič J, Němčanský, Cholevík D, Mašek P, Autrata R, Krejčířová I

Originally published in Biomedical Papers, 2015, vol. 159, no. 3, p. 413-416.

A new modified technique for the treatment of high-risk prethreshold ROP under the direct visual control of RetCam 3

Juraj Timkovic[a,b,c], Jan Nemcansky[a,c], Dalibor Cholevik[a,b,c], Petr Masek[a], Rudolf Autrata[b], Inka Krejcirova[b]

Purpose. To describe a new modified technique in the treatment of ROP (retinopathy of prematurity) using the RetCam 3 digital imaging system - Camera-Assisted Laser photocoagulation and Cryotherapy of the Retina (CALCR).
Methods. From Nov 2011 to Oct 2013, 113 infants were diagnosed with ROP. The average post-conceptual age (PCA) at the time of diagnosis was the 35th week of PCA; the average birth weight was 1,041 g. According to the ETROP study, the avascular part of the retina of infants with high-risk prethreshold ROP was treated with a trans-scleral diode laser or with cryotherapy within 48-72 h after the diagnosis. The intervention was performed under general anaesthesia under the direct visual control of the RetCam 3.
Results. The CALCR technique was used in all 23 infants (46 eyes) diagnosed with high-risk prethreshold ROP. The average age of these infants at the time of the intervention was the 38th week of PCA. None of the infants had any serious complications during the CALCR procedure. In contrast to the traditional technique, CALCR offers many benefits: the image of the retina is real, magnified and not inverted, it shows details of the retina in a high resolution, photo and video documentation is available. Therefore the preoperative, intraoperative and postoperative condition of the retina can be precisely evaluated and compared on a fully standardized basis.
Conclusions. The CALCR procedure represents a new technique providing greater accuracy when targeting the avascular part of the retina, enables better visualisation and more precise treatment, and reduces the risk of unintended damage to healthy retinal tissue.

Key words: retinopathy of prematurity, laser photocoagulation, cryotherapy, RetCam photography

Received: January 14, 2015; Accepted with revision: May 15, 2015; Available online: July 3, 2015
http://dx.doi.org/10.5507/bp.2015.027

[a]Clinic of Ophthalmology, University Hospital Ostrava, Czech Republic
[b]Department of Pediatric Ophthalmology, Faculty of Medicine, Masaryk University, Brno and Faculty Hospital Brno
[c]Department of Craniofacial Surgery, Faculty of Medicine, University of Ostrava
Corresponding author: Juraj Timkovic, e-mail: timkovic.j@bluepoint.sk

INTRODUCTION

Retinopathy of prematurity (ROP) was first described in 1942 by Terry as greyish - white opaque retrolental membranes (retrolental fibroplasia). He assumed that the cause was a proliferation of the embryonic hyaloid system[1]. The term "retinopathy of prematurity" was first used by Health in 1953, who described three histopathological stages of this disease: primary retinal disease, secondary retinal disease from vitreous organization, and ocular atrophy as a result of reparative processes[2].

According to the current concept, retinopathy of prematurity (ROP) is considered to be a vasoproliferative disease that mainly affects prematurely-born infants with a birth-weight below 1500 g and born before the 32nd week of gestation. ROP is the most common cause of blindness in children in developed countries[3,4]. According to the ETROP study, cryotherapy and laser therapy of the peripheral avascular part of the retina are recommended as a standard treatment for Type 1 ROP. When the early stages of ROP with high risks are diagnosed, prompt treatment within 48-72 h is indicated. Laser therapy of the avascular part of the retina over a 360-degree range or cryotherapy under the direct visual control of an indirect ophthalmoscope are recommended as up-to-date techniques[5-7]. The efficacy of laser photocoagulation or the combination of cryotherapy and photocoagulation is about 80% in terms of anatomical success and about 75% in terms of functional success[5,6,8].

Indirect ophthalmoscopy is considered to be the standard method for examining prematurely-born infants during ROP screening. The RetCam 3 digital imaging system is a modern alternative for the screening and diagnostics of retinal disorders in children. The possibility of taking photographs or recording a video during the examination, and having a wider view of the retina are the main benefits of this method of examination. This has been confirmed in many studies, which have demonstrated the higher sensitivity of using the RetCam 3 digital system in comparison to the conventional technique of indirect ophthalmoscopy[9-11].

The aim of this paper is to describe a new modified technique for treating children with high-risk prethreshold ROP using the RetCam 3 digital imaging system – Camera-Assisted Laser photocoagulation and Cryotherapy of the Retina (CALCR).

METHODS

From 1st November 2011 to 31th October 2013, a total of 380 prematurely-born infants (206 boys, 174 girls) were screened for ROP by an ophthalmologist. Their average gestational age at birth was 29.3 weeks (median: 30 weeks, SD ± 2.15, range 24-32 weeks) and their average birth weight was 1,331 g (median: 1,350 g, SD ± 417.61, range 460 - 2,645 g). All the ophthalmological examinations were performed through a dilated pupil (phenylephrine hydrochloride 2.5% eye drops + tropicamide 0.5% eye drops) and using an eyelid retractor (K1-5401 / K1-5677, Katen Products Inc., Denville, NJ, USA) with the use of local anaesthesia (oxybuprocaine hydrochloride 0.4% eye drops). The posterior segment of the eye was examined with the RetCam 3 digital imaging system (Clarity Medical Systems Inc., Pleasanton, CA, USA). According to the results and recommendations of the ETROP study, the avascular part of the retina of infants with a high-risk prethreshold stage of ROP was treated with a trans-scleral diode laser (IQ 810, Iridex, Mountain View, CA, USA) or with cryotherapy (Cryomatic Cryo, Keeler Instruments Inc., Broomall, PA, USA) within 48-72 hours of the diagnosis being made. The intervention was targeted to the avascular parts of the retina; direct treatment of the ridge and extraretinal fibrovascular proliferations were not performed. During the laser therapy, the technique of near confluent laser photocoagulation of the retina was used. The trans-scleral laser photocoagulation and cryotherapy were performed through the conjunctiva, a conjuctival incision was not necessary. The therapeutic intervention was performed in all prematurely-born infants under general anesthesia, through a dilated pupil (phenylephrini hydrochlordium 2.5% eye drops + tropicamidum 0.5% eye drops), using an eyelid retractor (K1-5401 / K1-5677 / K1-5340, Katena Products Inc., Denville, NJ, USA), under the direct visual control of the RetCam 3 digital imaging system (Clarity Medical Systems Inc, Pleasanton, CA, USA).

RESULTS

113 (29.7%) prematurely-born infants were diagnosed with ROP; all the cases were classified as stage 1 when the diagnosis was made. The average post conceptual age (PCA) of these infants at the time of diagnosis was the 35th week of PCA (median: 34th week of PCA, SD ± 2.17, range 30th - 40th week of PCA); the average birth weight was 1,041 g (median: 990 g, SD ± 337.26, range 460 - 2,645 g). The intervention (cryotherapy - 14 eyes / laser photocoagulation of the retina - 32 eyes) under the direct visual control of RetCam 3 was indicated and performed by an ophthalmologist in all 23 infants (20.4%, 46 eyes) with high-risk prethreshold ROP (Fig. 1, 2). The average age of these infants at the time of the intervention was the 38th week of PCA (median: 38th week of PCA, SD ± 2.58, range 34th - 44th week of PCA).; the average birth weight was 827 g (median: 850 g, SD ± 171.58, range 550 - 1,250 g). The extent of the treatment corresponded with the standards and recommendations of the ETROP study in all children. The average number of laser spots that were used during the CALCR procedure was 260 spots per eye, the range of time per spot was 800 - 1,500 ms, the range of power used per spot was 900 - 1,500 mW. The average number of cryo spots during the cryotherapy was 12, the temperature at the tip of the cryoprobe was -112 °F (-80 °C), the range of time was 4-5 s per spot. A mild conjunctival injection with chemosis and retinal / vitreous haemorrhages were relatively common but not serious complications. The retinal and vitreous haemorrhages resolved spontaneously within four weeks after the CALCR procedure (Fig. 3a, b). None of the infants had any intraoperative complications during the intervention under the direct visual control of RetCam3; therefore a switch to the conventional technique of treatment under the direct visual control of an indirect ophthalmoscope

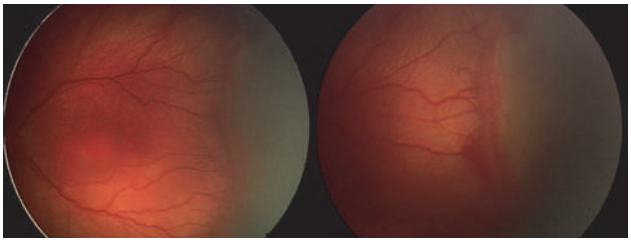

Fig. 1. Preoperative clinical findings of prematurely-born infant born in 25th week of gestation, with a birth weight of 850 grams. Retinopathy of prematurity stage 3, zone II-III, plus disease. Images were taken in the 36th week of PCA with the RetCam 3 digital imaging system.

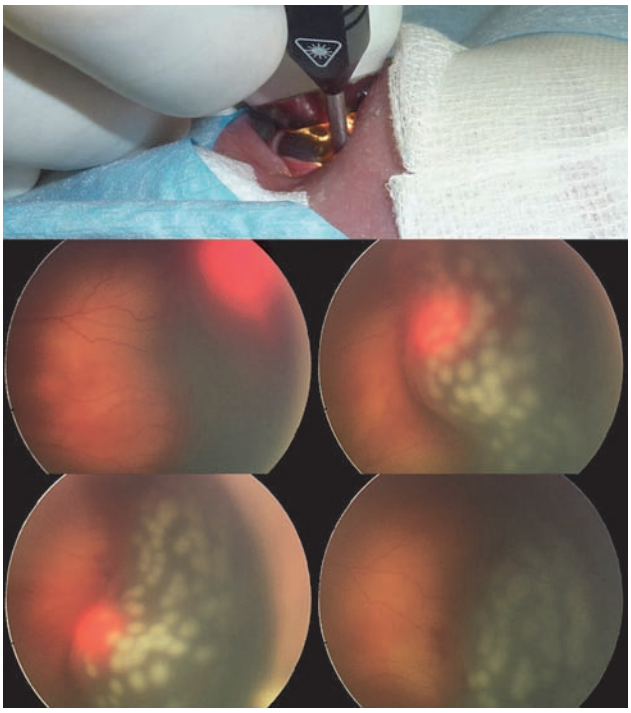

Fig. 2. CALCR treatment technique . Detailed images of the retina during the CALCR procedure.

was not necessary. A minor difficulty of this new treatment technique was with the approach to the middle periphery of the retina with a cryo or laser probe at the points where the extraocular muscles attach and pass. We did not observe any other complications during the CALCR procedure. Unlike the traditional technique, which is performed under the direct control of an indirect ophthalmoscope, The CALCR procedure offers many benefits: the image of the retina during the intervention is real, magnified and not inverted, it shows details of the retina in highresolution, the possibility of scleral indentation and there is also a possibility of taking photographs or recording a video during the intervention. These benefits enable precise comparison of the preoperative, intraoperative and postoperative retinal findings.

DISCUSSION

The development and improvement of intensive neonatal care of premature infants requires enhanced ophthalmological care and its continuous improvement, following current trends that undoubtedly include the RetCam 3 digital imaging system. The system enables taking photographs and recording a video during the examination, comparing the images over time, monitoring the progress of the disease or the effects of the treatment. In addition to this, it enables connecting to a computer network, sharing and consulting relatively rare retinal findings with other pediatric ophthalmologists. Last but not least, it provides credible and defensible medical and legal documentation. Since November 2011, we have been also using this device for therapeutic interventions (the CALCR procedure). We have not found any similar usage of this system in the literature yet.

Using the CALCR procedure, we treated the avascular part of the retina outside the ridge and extraretinal fibrovascular tissue. There are different views on the direct treatment of the ridge between the vascular and avascular parts of the retina[8,12,12-20]. Near confluent laser photocoagulation, which was used in the CALCR procedure, seems to be more effective than the usage of individual laser spots. None of the infants treated with the CALCR procedure required further intervention. A larger study involving more prematurely born infants with high-risk prethreshold ROP treated with both laser photocoagulation methods would be required for a more precise comparison. Studies confirm the current trend of using more dense forms of photocoagulation in the treatment of ROP (ref.[14-16,21-23]). When comparing the methods of single spots and near confluent photocoagulation, the method of dense laser photocoagulation seems to be more effective and safer[23-25].

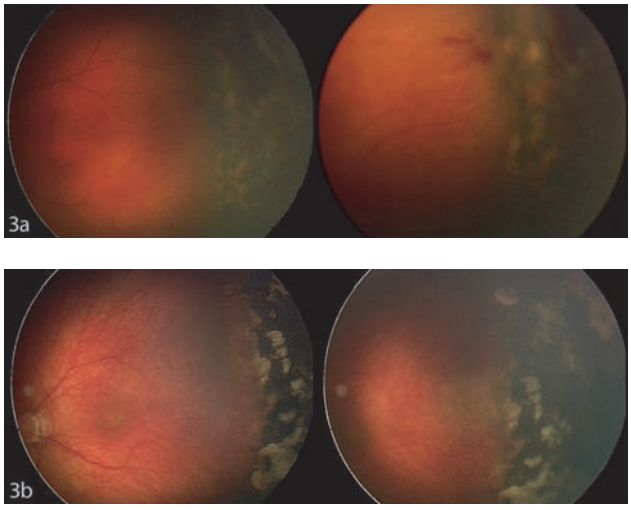

Fig. 3. Postoperative clinical findings two weeks (fig. 3a) and four weeks (fig. 3b) after the CALCR procedure. Images were taken with the RetCam 3 digital imaging system.

The complications of the CALCR procedure do not vary in principle from the complications that are described in standard methods of treatment with laser and cryocoagulation under the visual control of an indirect ophthalmoscope[12-16,19,20,22]. In particular, we encountered a various extent of retinal and vitreous haemorrhages in all infants in our study group. None of the complications were serious, and they did not require any further intervention or treatment. The retinal and vitreous haemorrhages resolved spontaneously within four weeks after the CALCR procedure. None of the infants had any intraoperative complications during the intervention under the direct visual control of RetCam 3; therefore a switch to the conventional technique of treatment under the direct visual control of an indirect ophthalmoscope was not necessary.

A disadvantage of the CALCR technique is the more difficult approach to the posterior pole of the globe. This is caused by the anatomy of the eye. One possible solution for this relative complication is performing a conjunctival incision that enables us to reach the central parts of the retina with the laser probe. This problem occurs especially in the treatment of prematurely born infants with an aggressive or atypical form of ROP and with diagnosed retinal changes in zone I or at the border of zone I and II. A low therapeutical effect of the laser photocoagulation of the peripheral avascular parts of the retina was described in these forms of ROP. A relatively new method of intravitreal application of anti-VEGF appears to be a more promising treatment for infants with these types of aggressive and atypical forms of ROP (ref.[26-27]). We assume that this type of treatment will gradually replace the technique of the laser photocoagulation and will become the first-choice method for the treatment of these forms of ROP. Photocoagulation will probably remain the first-choice method for the treatment of infants with ROP with changes in the anterior part of zone II. As we mentioned above, this area can be easily reached with the CALCR treatment technique without the need for conjunctival incision.

CONCLUSION

The laser photocoagulation and cryotherapy of the peripheral avascular part of the retina under the direct visual control of the RetCam 3 digital imaging system

(CALCR) in prematurely-born infants with high-risk pre-threshold ROP is a safe and effective technique in the treatment of ROP. This new modified technique for the treatment introduces greater accuracy when targeting the laser and cryo spots to the avascular part of retina, enables greater visualisation and treatment precision and reduces the risk of unintended damage to surrounding healthy retinal tissue. The possibility of taking a high-resolution photo-documentation of the retina enables the preoperative, intraoperative and postoperative condition of the retina to be precisely evaluated and compared on a fully standardized basis.

ACKNOWLEDGEMENT

Author contributions: JT, JN, DC, IK: literature search; JT, RA, IK: data collection; JT, JN, DC, RA, IK: data analysis and interpretation; JT, RA: statistical analysis; JT, RA, JN: conception and manuscript writing; JT, DC, RA, PM: final approval.

Conflict of interest statement: The authors state that there are no conflicts of interest regarding the publication of this article.

REFERENCES

1. Terry TL. Extreme Prematurity and Fibroblastic Overgrowth of Persistent Vascular Shealth Behind Each Crystalline lens. I. Preliminary report. Am J Ophthalmol 1942;25:203-4.
2. Health P. Pathology of retinopathy of prematurity, RLF. Am J Ophthalmol 1953;34:1249-59.
3. Gilbert C. Retinopathy of prematurity: A global perspective of the epidemics, population of babies at risk and implications for control. Early Hum Dev 2008;84:77-82.
4. Steinkuller PG, Du L, Gilbert C, Foster A, Collins ML, Coats DK. Childhood blindness. J Am Assoc Pediatr Ophthalmol Strabismus 1999;3:26-32.
5. The Early Treatment for Retinopathy of Prematurity Cooperative Group. The Incidence and Course of Retinopathy of Prematurity: Findings From the Early Treatment for Retinopathy of Prematurity Study. Pediatrics 2005;116:15-23.
6. The Early Treatment for Retinopathy of Prematurity Cooperative Group. The Early Treatment for Retinopathy Of Prematurity Study: structural findings at age 2 years. Br J Ophthalmol 2006;90:1378-82.
7. Elsas FJ, Collins M, Jones J, et al. Multicenter Trial of Cryotherapy for Retinopathy of Prematurity: Ophthalmological Outcomes at 10 Years. Arch Ophthalmol 2001;119:1110-8.
8. Autrata R, Senkova K, Holousova M, Helmanova I, Pyrochtova S. Combined treatment with laser photocoagulation and cryotherapy for threshold retinopathy of prematurity. Eur J Ophthalmol 2008;18:112-7.
9. Balasubramanian M, Capone A Jr, Hartnett ME, Pignatto S, Trese MT. The Photographic Screening for Retinopathy of Prematurity Study (Photo-ROP): study design and baseline characteristics of enrolled patients. Retina Phila Pa 2006;26:S4-S10.
10. Capone A, Ells A, Balasubramanian M. The photographic screening for retinopathy of prematurity study (photo-ROP) - Primary outcomes. Retina- J Retin Vitr Dis 2008;28:S47-S54.
11. Salcone EM, Johnston S, VanderVeen D. Review of the use of digital imaging in retinopathy of prematurity screening. Semin Ophthalmol 2010;25:214-7.
12. Coats D, Miller A, McCreery K, Holz E, Paysse E. Involution of threshold retinopathy of prematurity after diode laser photocoagulation. Ophtalmology 2004;111:1894-8.
13. Harrell SN, Brandon DH. Retinopathy of prematurity: the disease process, classifications, screening, treatment, and outcomes. Neonatal Netw NN 2007;26:371-8.
14. Hubbard GB. Surgical management of retinopathy of prematurity. Curr Opin Ophthalmol 2008;19:384-90.
15. Arvas S, Sarici AM, Akar S. Diode laser photocoagulation posterior to the ridge in severe stage 3+threshold retinopathy of prematurity. Cutan Ocul Toxicol 2014;33:197-200.
16. Uparkar M, Sen P, Rawal A, Agarwal S, Khan B, Gopal L. Laser photocoagulation (810 nm diode) for threshold retinopathy of prematurity: a prospective randomized pilot study of treatment to ridge and avascular retina versus avascular retina alone. Int Ophthalmol 2011;31:3-8.
17. Ells A, Gole G, Hildebrand P, Ingram A, Wilson C, Williams R. Posterior to the ridge laser treatment for severe stage 3 retinopathy of prematurity. Eye 2013;27:525-30.
18. Gunn DJ, Cartwright DW, Gole GA. Prevalence and outcomes of laser treatment of aggressive posterior retinopathy of prematurity. Clin Experiment Ophthalmol 2014;42:459-65.
19. Jalali S, Azad R, Trehan HS, Dogra MR, Gopal L, Narendran V. Technical aspects of laser treatment for acute retinopathy of prematurity undertopical anesthesia. Indian J Ophthalmol 2010;58:509-15.
20. Parvaresh MM, Ghasemi Falavarjani K, Modarres M, Nazari H, Saiepour N. Transscleral diode laser photocoagulation for type 1 prethreshold retinopathy of prematurity. J Ophthalmic Vis Res 2013;8:298-302.
21. Banach MJ, Ferrone PJ, Trese MT. A comparison of dense versus less dense diode laser photocoagulation patterns for threshold retinopathy of prematurity. Ophthalmology 2000;107:324-7.
22. Gonzalez VH, Giuliari GP, Banda RM, Guel DA, Wingard M. Confluent laser photocoagulation for the treatment of retinopathy of prematurity. J Pediatr Ophthalmol Strabismus 2010;47:81-5.
23. Paysse E, Hussein M, Miller A, McCreery K, Coats D. Pulsed mode versus near-continuous mode delivery of diode laser photocoagulation for high-risk retinopathy of prematurity. J AAPOS 2007;11:388-92.
24. Tomcikova D, Prepiakova Z, Kostolna B, Gerinec A. Benefit of paint diode laser coagulation in the treatment of ROP. Cesk Slov Oftalmol 2011;67(4):115-8.
25. Prepiakova Z, Tomcikova D, Kostolna B, Gerinec A. Confluent diode laser coagulation: The gold standard of therapy for retinopathy of prematurity. J Pediatr Ophthalmol Strabismus 2015;52(1):43-51.
26. Autrata R, Senkova K, Holousova M, Krejcirova I, Dolezel Z, Borek I. Effects of intravitreal pegaptanib or bevacizumab and laser in treatment of threshold retinopathy of prematurity in zone I and posterior zone II – four years results. Cesk Slov Oftalmol 2012;68(1):29-36.
27. Autrata R, Krejcirova I, Senkova K, Holousova M, Dolezel Z, Borek I. Intravitreal pegaptanib combined with diode laser therapy for stage 3+ retinopathy of prematurity in zone I and posterior zone II. Eur J Ophthalmol 2012;22(5):687-94.

Č.	Autor	Název	Časopis	IF
1.	Kuliha Martin	Randomized clinical trial comparing neurological outcomes after carotid endarterectomy or stenting	British Journal of Surgery	5.542
2.	Češková Eva	Gender differences in the treatment of first-episode schizophrenia: Results from the European First Episode Schizophrenia Trial	Schizophrenia Research	3.923
3.	Zonča Pavel	Retroperitoneoscopic adrenalectomy in obese patients: is it suitable?	Obesity Surgery	3.747
4.	Ihnát Peter	The impact of standard protocol implementation on the quality of colorectal cancer pathology reporting	World Journal of Surgery	2.642
5.	Štětinský Jiří	The time factor in the LDI (Laser Doppler Imaging) diagnosis of burns	Lasers in Surgery and Medicine	2.619
6.	Šilhán Petr	Transcranial sonography of brainstem structures in panic disorder	Psychiatry Research: Neuroimaging	2.424
7.	Krhut Jan	Comparison between uroflowmetry and sonouroflowmetry in recording of urinary flow in healthy men	International Journal of Urology	2.409
8.	Ihnát Peter	Treatment strategies for colorectal carcinoma with synchronous liver metastases: Which way to go?	World Journal of Gastroenterology	2.369
9.	Bojková Martina	Immunoglobulin G4, autoimmune pancreatitis and pancreatic cancer	Digestive Diseases: Clinical Reviews	2.181
10.	Zeleník Karol	Patients with chronic rhinosinusitis and simultaneous bronchial asthma suffer from significant extraesophageal reflux	International Forum of Allergy & Rhinology	2.082
11.	Jelínek Tomáš	Plasma cell leukemia: from biology to treatment	European Journal of Haematology	2.066
12.	Beránková Dagmar	Addenbrooke´s cognitive examination and individual domain cut-off scores for discriminating between different cognitive subtypes of Parkinson´s disease	Parkinson´s Disease	2.010
13.	Kušnierová Pavlína	Reference intervals of plasma matrix metalloproteinases 2, 3, and 9 and serum asymmetric dimethylarginine levels	Scandinavian journal of clinical & laboratory investigation	1.899
14	Pleva Leoš	The rs1803274 polymorphism of the BCHE gene is associated with an increased risk of coronary in-stent restenosis	BMC Cardiovascular disorders	1.878
15.	Formánek Martin	Comparison of three methods used in the diagnosis of extraesophageal reflux in children with chronic otitis media with effusion	Gastroenterology Research and Practice	1.749
16.	Vávra Petr	Semi-spherical radiofrequency bipolar device - a new technique for liver resection: experimental in vivo study on the porcine model	Technology in Cancer Research & Treatment	1.730
17.	Čábalová Lenka	Micro- and nanosized particles in nasal mucosa: a pilot study	BioMed Research International	1.579
18.	Valkovský Ivo	Evaluation of biochemical markers and bone mineral density in patients with chronic kidney disease stage 5D at the start of hemodialysis treatment	Biomedical Papers	1.200
19.	Zeman David	Oligoclonal free light chains in cerebrospinal fluid as markers of intrathecal inflammation. Comparison with oligoclonal IgG	Biomedical Papers	1.200
20.	Timkovič Juraj	A new modified technique for the treatment of high-risk prethreshold ROP under the direct visual control of RetCam 3	Biomedical Papers	1.200

Poznámky / Notes:

www.fno.cz

ISBN 978-80-906002-9-4 (print)
ISBN 978-80-88159-00-1 (on-line)